

Synthesis of Heterocyclic Aromatic Compounds
by Intramolecular Cyclization

March 2021

Yuji Kurimoto

Graduate School of Natural Science and Technology

(Doctor's Course)

OKAYAMA UNIVERSITY

Preface

The studies presented in this thesis have been carried out under the direction of Professor Seiji Suga at the Division of Applied Chemistry, Graduate School of Natural Science and Technology, Okayama University during 2016–2021.

The author would like to express my sincerest gratitude to Professor Seiji Suga for his kind guidance and valuable discussions throughout this work. The author greatly appreciates to Associate Professor Koichi Mitsudo for this constant advice and valuable discussions during the course of this work. The author also thanks to Assistant Professor Hiroki Mandai and Eisuke Sato for his helpful advice.

The author would like to express sincere thanks to Professor Yasujiro Murata and Professor Atsushi Wakamiya of Institute for Chemical Research of Kyoto University for the measurement of quantum yield of fluorescence. The author deeply appreciates to Professor Yasushi Nishihara and Assistant Professor Hiroki Mori (Division of Molecular Sciences, Graduate School of Natural Science and Technology, Okayama University) for the measurement of the carrier mobility.

The author would like to express our sincere thanks and appreciation to Professor Siegfried R. Waldvogel for his kind guidance and encouragement for the work at Mainz University. The author greatly appreciate to Dr. Michael Berger, John D. Herszman and all other members of Laboratory of Professor Siegfried R. Waldvogel for their kindness.

The author must express special appreciate to Mr. Jun Yamashita for their great assistance for this work.

The author also thanks to Mr. Satoki Ishii, Mr. Toki Yonezawa, Mr. Takuya Asada, Mr. Yoshiaki Kobashi, Mr. Kazuki Yoshioka, Mr. Arata Yamasaki, Mr. Seiichi Tanaka, Mr. Ryota Isobuchi, Mr. Tomohiro Inada and Mrs. Ayako Shioya for their active collaborations and kindness.

Finally, the author would like to express my deepest appreciation to my parents Mr. Isao Kurimoto, Mrs. Harumi Kurimoto for their constant assistance and encouragement.

Yuji Kurimoto
Division of Applied Chemistry
Graduate School of Natural Science and Technology

Okayama University

2021

Contents

Chapter 1. General Introduction	1
Chapter 2. Synthesis of Heteroring-Fused Fluoreneol via Selective Intramolecular C–H Functionalization	23
Chapter 3. Synthesis of Benzodithienofuran (BDTF) via Construction of Oxygen-Bridged Bithiophenes Using 3-Bromobenzo[<i>b</i>]thiophene 1,1-Dioxide as a Key Compound	51
Chapter 4. Synthesis of Benzodithienothiophene (BDTT) via Construction of Sulfur-Bridged Bithiophenes Using 3-Bromobenzo[<i>b</i>]thiophene 1,1-Dioxide as a Key Compound	79
Chapter 5. Physical Properties of BDTF, BDTT and Their Derivatives	93
Chapter 6. Synthesis of Diarylphosphole Oxide via Electrochemical Cyclization	131
Chapter 7. Grand Summary	155
List of Publications	159

Chapter 1. General Introduction

1-1.	Polycyclic Aromatic Compounds	2
1-1-1.	PAHs (Polycyclic Aromatic Hydrocarbons)	2
1-1-2.	Polycyclic Heteroaromatic Compounds	2
1-2.	Synthesis of Polycyclic Aromatic Compounds by Intramolecular Cyclization	4
1-2-1.	Transition Metal-Catalyzed Intramolecular Cyclization	5
1-2-2.	Transition Metal-Free Intramolecular Cyclization	15
1-3.	The Purposes	17
1-3-1.	Synthesis of Heteroring-Fused Fluorenol by Intramolecular Cyclization	17
1-3-2.	Synthesis of Thienoacenes by Intramolecular Cyclization	18
1-3-3.	Synthesis of Diarylphosphole Oxide by Intramolecular Cyclization	18
	Reference	19

1-1. Polycyclic Aromatic Compounds

Aromatic compounds are an important class not only in basic chemistry such as structural chemistry and reaction chemistry, but also in applied chemistry such as synthetic organic chemistry, biochemistry, medicinal chemistry, and material chemistry.¹ To date, various skeletal aromatic compounds have been discovered or synthesized. In particular, polycyclic aromatic compounds having a plurality of aromatic rings in the structure are also used in material science.² In this section, the author will focus on polycyclic aromatics and introduce representative compounds.

Polycyclic aromatic compounds can be divided into two main groups: polycyclic aromatic hydrocarbons (PAHs) and heterocyclic aromatic compounds.

1-1-1. PAHs (Polycyclic Aromatic Hydrocarbons)

PAHs are generally known to contain many compounds with excellent in absorption and emission properties of long-wavelength light. It is also known that these properties are directly related to their chemical structure. For example, acene type PAHs such as pentacene are known to become unstable as the number of condensing rings increases. Therefore, acenes having a condensed ring number of hexacene or more can be handled only in an inert gas or matrix.³ On the other hand, phenacene type PAHs such as picene are chemically stable and can be handled in the atmosphere even if the number of condensed rings is higher than that of [6]phenacene.⁴ Applying these unique properties of PAHs to electronic materials have been studied all over the world. Polyfluorene, one of the PAHs, is currently the mainstream of polymer EL materials because it is thermally and chemically stable and shows a high fluorescence quantum yield (Figure 1).⁵

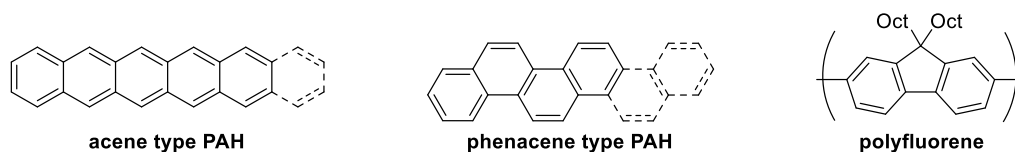


Figure 1. Representative PAHs

1-1-2. Polycyclic Heteroaromatic Compounds

PAHs are known to have various excellent properties, but most of them have extremely low solubility in organic solvents, and some compounds have low atmospheric stability. One of the typical methods for modifying the physical properties of PAHs is introducing heteroatoms in the aromatic ring.⁶ Heteroatom-introduced PAH is called polycyclic heteroaromatic compounds and is known to exhibit physical and electronic properties which are different from conventional PAHs, and many compounds with excellent solubility and atmospheric stability have been reported. For instance, dibenzo[*d,d'*]thieno[3,2-*b*;4,5-*b'*]dithiophene (DBTDT) synthesized by Zhu and co-workers, is

known to have higher charge mobility than all-carbon parent congener (Figure 2).⁷ The manifestation of these interesting properties is due to intermolecular interactions based on the polarization structure of the heterocycle and large change of sulfur atoms.

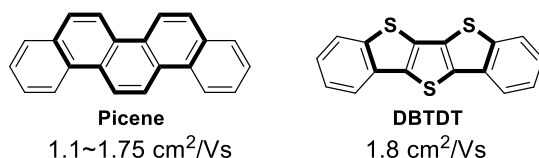


Figure 2. Comparison of PAH and Polycyclic Heteroaromatic Compounds

These properties make polycyclic heteroaromatic compounds promising candidates for electronic materials. Indeed, one of the polycyclic heteroaromatic compounds, heteroacenes, is used as an active material for organic thin-film transistor (Figure 3).⁸ A typical example is 2,9-decyl-dinaphtho[2,3-*b*:2',3'-*f*]thieno[3,2-*b*]thiophene (C₁₀-DNNT) reported by Takimiya and co-workers.⁹ Not only does C₁₀-DNNT have excellent solubility and semiconductor properties (7.9 cm²/Vs), it also has high atmospheric stability (*more than 100 days under the ambient lab conditions). Nakamura and co-workers reported 3,7-bis[4-(*N*-carbazolyl)phenyl]benzo[1,2-*b*:4,5-*b'*]difuran (CZBDF), which shows well-balanced ambipolar semiconductor properties (carrier mobilities for both holes and electrons (>10⁻³ cm²/Vs)).¹⁰ Therefore, it has become possible to produce efficient *p-i-n* homozygous devices that emit light across the full visible color range and perform at a level similar to state-of-the-art heterojunction devices.

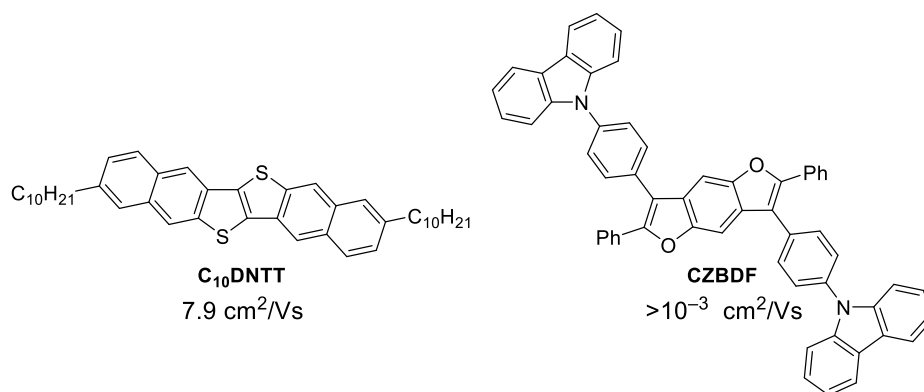


Figure 3. Representative polycyclic heteroaromatic compounds with semiconductor properties

Polycyclic heteroaromatic compounds with a wide π -conjugated system have a narrow bandgap and exhibit absorption / fluorescence in the visible light region. Furthermore, polycyclic heteroaromatic compound may exhibit high fluorescence properties in the absence of deactivation paths such as non-radiative decay (Figure 4). For example, Thomas and co-workers reported 5,11-bis[(4-methoxyphenyl)ethynyl]-2,8-dimethylantra-[2,3-*b*:6,7-*b'*]dithiophene (DE-ADT) which shows a high fluorescence quantum yield ($\Phi_{em} = 0.92$).¹¹ Recently, polycyclic heteroaromatic compound, which contains phosphole oxide in the skeleton, have also been attracting attention as a

compound with excellent fluorescence properties. Yamaguchi and co-workers reported C-Naphox which shows a high fluorescence quantum yield ($\Phi_{em} = 0.93$).¹² Furthermore, C-Naphox is also highly photoresistance and is also used for repeated STED imaging of HeLa cells.

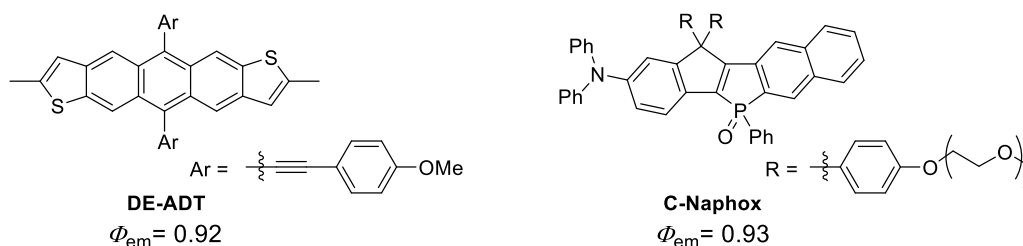


Figure 4. Representative polycyclic heteroaromatic compounds with fluorescence properties

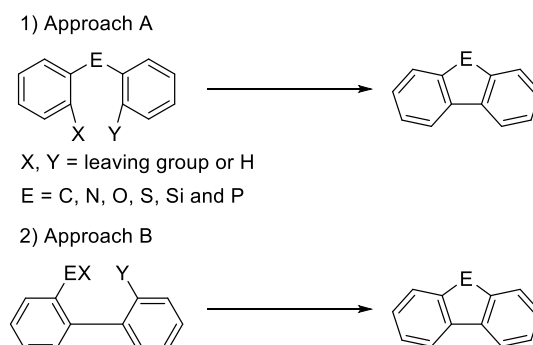
1-2. Synthesis of Polycyclic Aromatic Compounds by Intramolecular Cyclization

As methods for synthesizing polycyclic aromatic compounds, a variety of reactions have been reported.¹³ Among them, intramolecular reactions tend to be less likely to cause side reactions than intermolecular reactions. In addition, desired reactions tend to proceed efficiently because the reaction sites are likely to be close each other. Meanwhile, fluorenes and heteroacenes are very useful compounds among polycyclic aromatic compounds. Therefore, the author will focus on these compounds and introduce synthetic methods of these compounds by intramolecular cyclization.

Synthetic Strategies

As far as synthetic strategies toward fluorenes or heteroacenes scaffold are concerned, two synthetic approaches can be envisioned (Scheme 1). Intramolecular cyclization of the corresponding E (C, N, O, S, Si and P atoms) atom bridged biaryl precursors via C–X and C–Y formation (Approach A) or E–X containing 2-biphenyl precursors via E–C and C–Y formation (Approach B) are ideal approaches to produce target compound. In general, these approaches are versatile and allows us for syntheses of a wider range of potential structures containing E. Although other approaches have emerged in the last decade, approaches A and B are still most commonly used methods for fluorenes or heteroacenes synthesis.

Scheme 1. Synthetic strategies of fluorenes or heteroacenes by intramolecular cyclization



1-2-1. Transition Metal-Catalyzed Intramolecular Cyclization

In this section, the author will focus on representative transition metal-catalyzed intramolecular cyclizations.

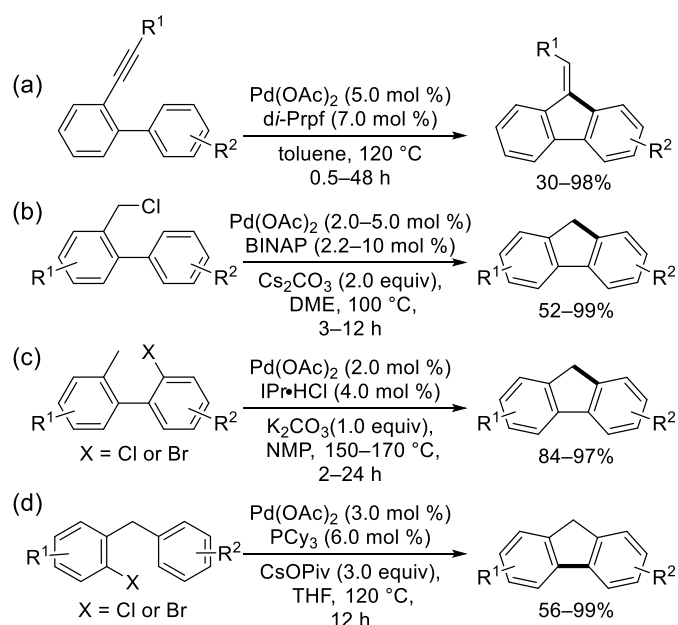
Synthesis of Fluorene Analogues

Among various synthetic approaches to compounds bearing a fluorene scaffold, syntheses based on the use of transition metal-catalyzed methodology have emerged and been developed during the last two decades. Indeed, these processes are now one of the most powerful tools for C–C bond formation within the class of fluorene analogues.

Palladium-Catalyzed Intramolecular Cyclization

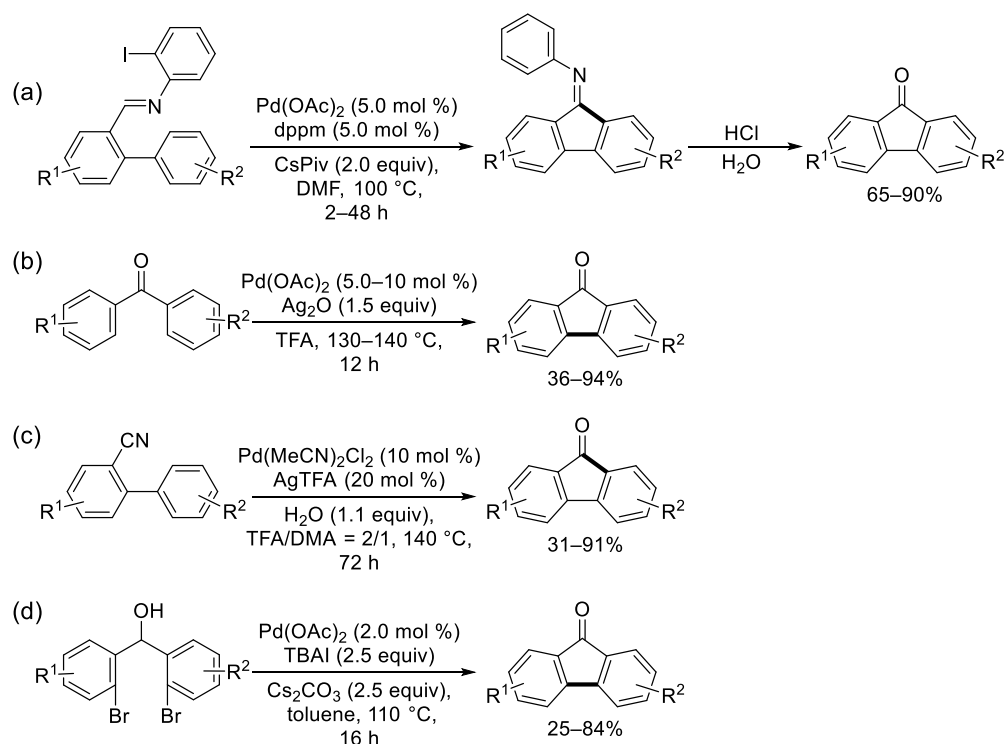
Palladium catalysts are one of the most widely used transition metal-catalysts and have a wide range of applications in the synthesis of fluorenes. In 2008, Gevorgyan and co-workers reported the first example of Pd-catalyzed 5-*exo*-dig hydroarylation to give monosubstituted 9-alkylidene fluorenes (Scheme 2a).¹⁴ In 2009, Chen and co-workers reported an intramolecular cyclization of arylbenzyl chlorides which has excellent functional group tolerance and enables to access various fluorenes (Scheme 2b).¹⁵ In 2010, Wu and co-workers developed a synthetic method of fluorenes by C(sp³)–H functionalization which has also various functional group tolerance, but the 2'-functional group was limited to methyl group (Scheme 2c).¹⁶ In 2016, Liu and co-workers discovered a new route to give fluorenes using a substituted diarylmethanes as a substrate (Scheme 2d).¹⁷

Scheme 2. Representative Pd-catalyzed intramolecular cyclizations



In 2007, Larock and co-workers reported the synthesis of fluorenone by the process of an aryl to imidoyl palladium migration (Scheme 3a).¹⁸ In this reaction, almost quantitative yields of fluorenones have been obtained for both electron-rich and electron-poor functionally substituted substrates. The only exception was the reaction employing the substrate with a 2-chloro group, possibly due to competing oxidative addition of the aryl chloride or perhaps hindered reaction of the aromatic ring or simply reduction in the number of ortho positions available for reaction. In 2012, almost simultaneous, independent reports by Cheng^{19a} and Shi^{19b} disclosed a novel methodology of dehydrogenative cyclization which has enabled simpler and more efficient synthesis of fluorenone (Scheme 3b). Furthermore, many similar approach have been discovered since the above method was reported.^{19c-e} In 2013, Hsieh and co-workers discovered a novel synthetic method of fluorenone using 2-phenylbenzotrile as a substrate (Scheme 3c).²⁰ In 2018, Xu and co-workers developed synthesis of fluorenone from bis(2-bromophenyl)methanols via oxidation of alcohol/reductive coupling of the C–Br bond sequence (Scheme 3d).²¹

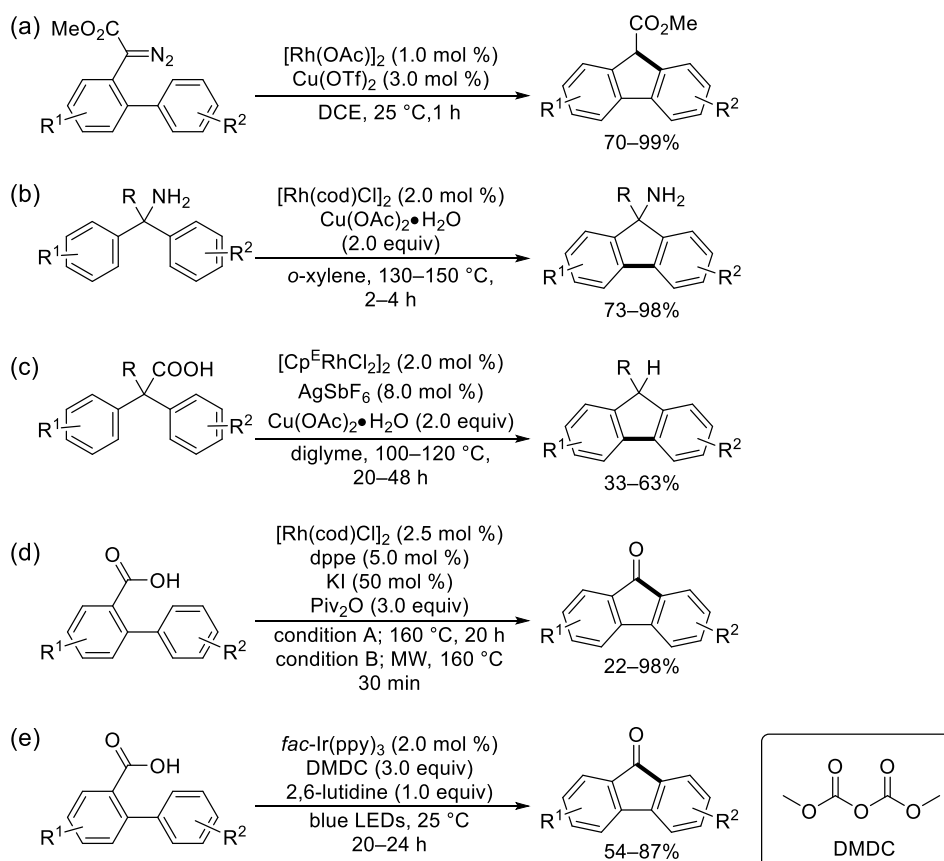
Scheme 3. Representative synthesis of fluorenone by Pd-catalyzed intramolecular cyclizations



Rhodium or Iridium-Catalyzed Intramolecular Cyclization

Rhodium and Iridium catalysts have also been explored to produce fluorenes. In 2011, Chang and co-workers developed a novel synthetic method of fluorene carboxylates via Rh-catalyzed intramolecular carbenoid insertion into aryl C(sp²)–H (Scheme 4a).²² A Cu catalyst is also applicable for this reaction, however less effective when compared to the Rh catalyst. In 2012, Miura and co-workers developed a straightforward synthesis of 9-amino fluorenes through Rh-catalyzed dehydrogenative cyclization (Scheme 4b).²³ In subsequent work by the same group, they enabled to access fluorene from 2,2-diarylkanoic acids by Rh-catalyzed cyclization (Scheme 4c).²⁴ In 2014, Ryu and co-workers reported the synthesis of fluorenones through Rh-catalyzed intramolecular acylation of biarylcarboxylic acids (Scheme 4d).^{25a} In this reaction, microwave irradiation shortened the reaction time significantly (condition B). In 2017, Zhu and co-workers discovered an Ir-photocatalyzed deoxygenative radical cyclization of biarylcarboxylic acids to fluorenones which proceeds under mild conditions (Scheme 4e).^{25b}

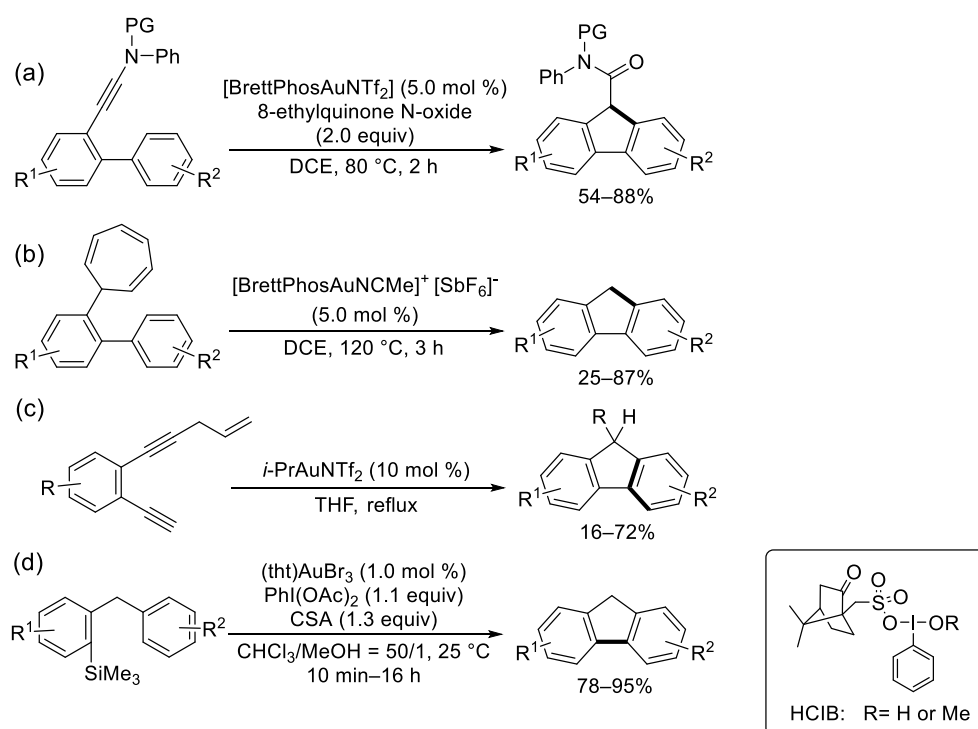
Scheme 4. Representative synthesis of fluorenes by Rh or Ir-catalyzed intramolecular cyclizations



Gold-Catalyzed Intramolecular Cyclization

In the past decade, homogeneous gold catalysts have emerged as a powerful tool for organic synthesis. Therefore, variety of synthetic methods on this study have been reported for the construction of fluorenes. In 2014, Ye and co-workers discovered a novel Au-catalyzed oxidative cyclization of *o*-alkynylbiaryls to give fluorenes (Scheme 5a).²⁶ However, no reactivity was observed on the electron-deficient substrate in this reaction. Echavarren and co-workers reported a novel synthetic route to fluorenes using 2-cycloheptatrienyl biphenyls and a gold catalyst in the same year, which involves the formation of a gold(I)-carbene that underwent cyclization by a Friedel–Crafts-type methylenation (Scheme 5b).²⁷ In 2017, a novel Au-catalyzed annulation to access fluorene was published by Hashmi and co-workers (Scheme 5c).²⁸ In this reaction, the yield of the corresponding product turned out to be rather low depending on the thermal stability of the substrate. In the same year, Lloyd–Jones and co-workers developed a straightforward synthesis of (trimethylsilyl)diarylmethanes furnishing fluorenes (Scheme 5d).²⁹ The HCIB generated in situ by the reaction of CSA and $\text{PhI}(\text{OAc})_2$ functions as an oxidant.

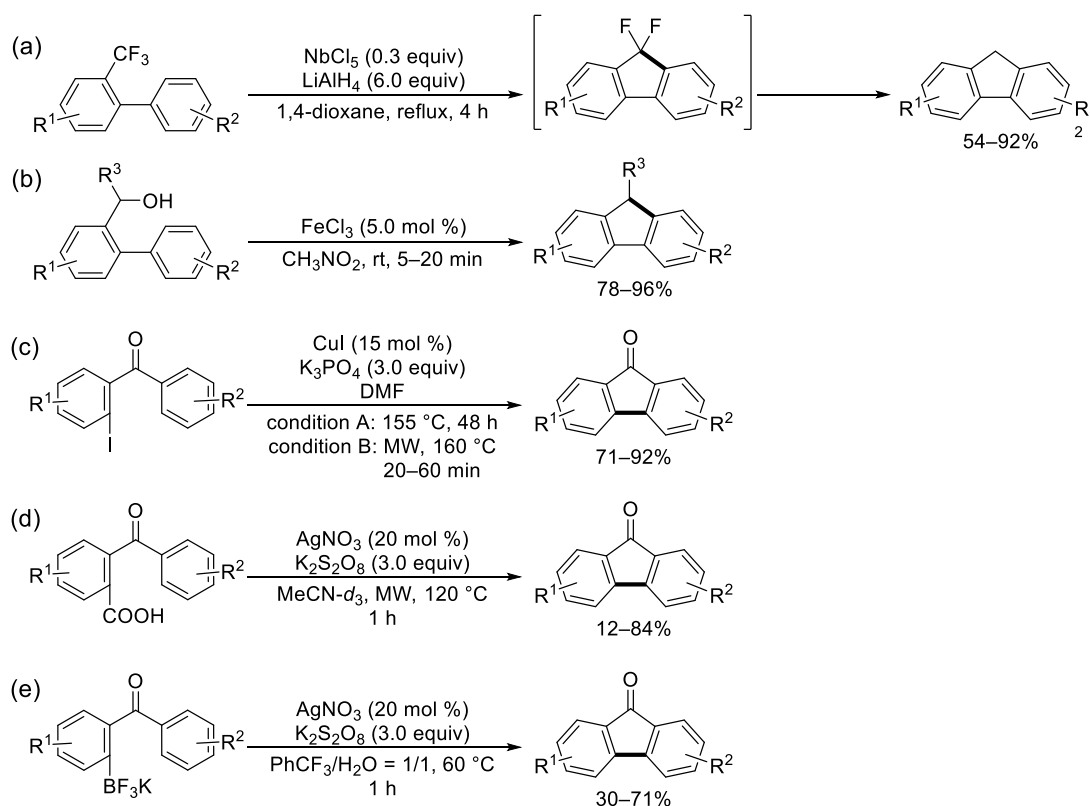
Scheme 5. Representative synthesis of fluorenes by Au-catalyzed intramolecular cyclizations



Other Transition Metal-Catalyzed Intramolecular Cyclization

In 2006, Akiyama and co-workers reported a pioneering work for the synthesis of fluorenes from *o*-arylated α, α, α -trifluorotoluene via low-valent niobium-mediated double activation of C–H/C–F (Scheme 6a).³⁰ This reaction proceeds via intramolecular dehydrofluorination to form 9,9-difluorofluorene, which is then reduced by excess LiAlH₄ to give fluorene. In 2012, an Fe-catalyzed Friedel–Crafts type cyclization for the conversion of biaryl methanols into the fluorenes was reported by Jana and co-workers, which proceeds under mild conditions and has a wide range of functional group tolerance (Scheme 6b).³¹ In 2013, Haggam and co-workers discovered a practical methodology involving intramolecular Cu-catalyzed cyclization of 2-iodobenzophenones under thermal and microwave (MW) conditions for the synthesis of fluorenone (Scheme 6c).³² In this reaction, microwave irradiation shortened the reaction time significantly. In 2012, Ag-catalyzed decarboxylative radical cyclization has been developed for the conversion of fluorenone by Greaney and co-workers (Scheme 6d).^{33a} This reaction has the limitation that expensive MeCN-*d*₃ is required as a solvent. Baran and co-workers also reported a similar reaction which does not require the use of MeCN-*d*₃ as a solvent (Scheme 6e).^{33b}

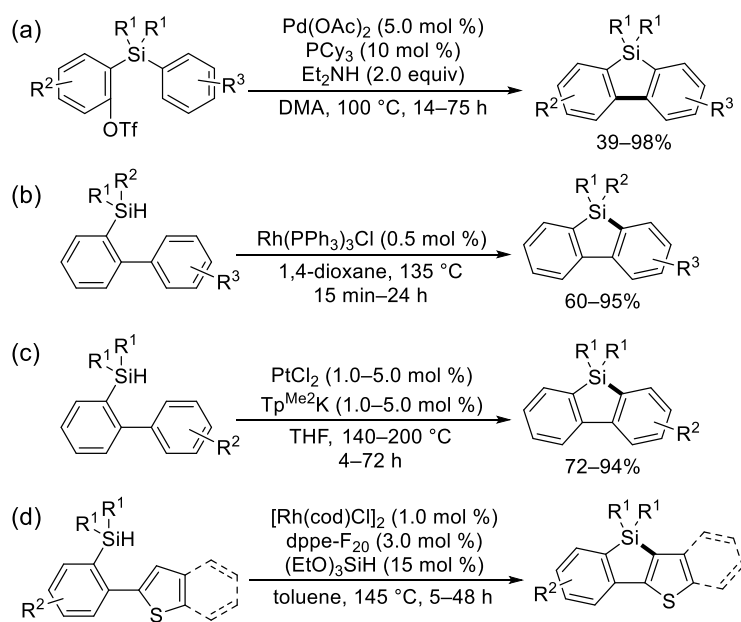
Scheme 6. Representative synthesis of fluorenes by other transition metal-catalyzed intramolecular cyclizations



Synthesis of Silafluorenes

Recently, compounds in which biphenyl is crosslinked with silicon (silafluorene) have attracted attention in the field of the organic light emitting diode (OLED). In 2008, Shimizu and co-workers developed a synthesis of silafluorenes via Pd-catalyzed intramolecular direct arylation of 2-(arylsilyl)aryl triflates (Scheme 7a).³⁴ However, it is necessary to introduce a bulky substituents on silicon to proceed this reaction efficiently. In 2010, Takai and co-workers reported a Rh-catalyzed synthesis of silafluorenes from biphenylhydrosilanes, which does not require oxidants, such as O₂ (Scheme 7b).^{35a} In 2016, Watanabe and co-workers discovered to give silafluorenes via a similar reaction pathway using Pt catalyst (Scheme 7c).^{35b} In our laboratory, we reported Rh-catalyzed reaction of thiophene-fused silafluorenes (Scheme 7d).^{35c} In this reaction, Rh(dppe-F₂₀)H is considered to be active catalytic species.

Scheme 7. Representative synthesis of silafluorenes by transition metal-catalyzed intramolecular cyclizations

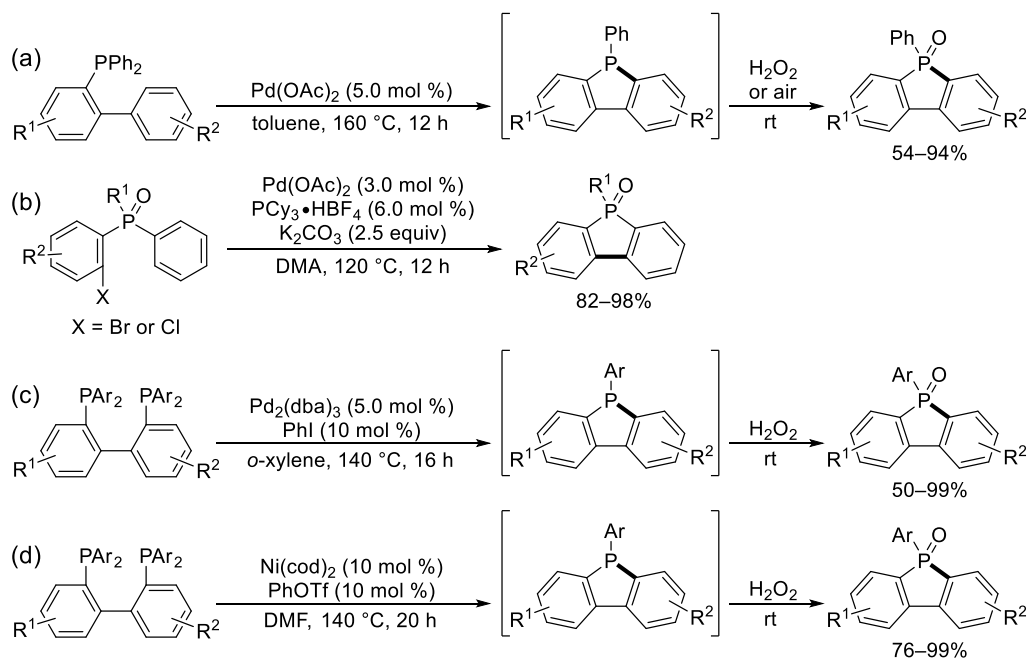


Synthesis of Diarylphosphole oxides

In this section, the author describes synthetic methods of diarylphosphole oxide (DPO) using substrates other than diarylphosphine oxide. (The author will describe them in the Chapter 6.) In 2013, Chatani and co-workers discovered Pd-catalyzed direct synthesis of DPOs from triarylphosphines (Scheme 8a).^{36a} However, this method still needs considerable improvement in terms of instability of a triarylphosphine group. In 2014, Jiang and co-workers discovered the synthesis of DPOs via Pd-catalyzed direct arylation of *o*-halodiarylphosphine oxides, which features simplicity, high yield and excellent functional group compatibility (Scheme 8b).^{36b} In 2017, Morandi and co-workers developed cyclization of bisphosphines to DPOs via the cleavage of two C–P by Pd catalyst (Scheme 8c).^{36c} In this reaction, because phospholes are sensitive to oxygen, the product was quantified as the air stable DPOs after an oxidative workup with H₂O₂. In 2019, a Ni-catalyzed similar reaction was reported by Tobisu and co-workers (Scheme 8d).^{36d}

These phosphole oxides can be easily reduced to phosphines by treatment with HSiCl₃ and further functionalization (sulfration, borylation, methylation, metalation, etc.) can be carried out following established procedures.³⁷

Scheme 8. Representative synthesis of DPOs by transition metal-catalyzed intramolecular cyclizations

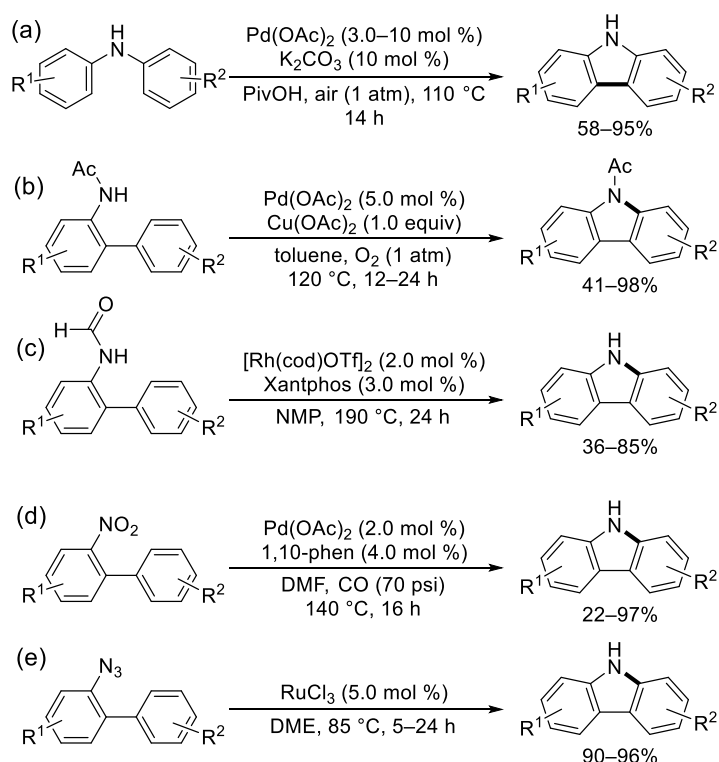


Synthesis of Carbazoles

The study of Åkermark pioneered in the field of carbazole synthesis by transition metal-catalyzed intramolecular cyclization.^{38a} Various researchers have reported methods for synthesis of carbazoles to date.^{38b,c}

In 2008, Fagnou and co-workers reported a straightforward synthesis of carbazoles through Pd-catalyzed dehydrogenative cyclization (Scheme 9a).^{38d} The reaction mechanism is similar to that reported by Åkermark. In 2005, Buchwald and co-workers developed the first example of accessing carbazole through oxidative C–H amination (Scheme 9b).^{38e} Shortly after this report, a Pt-catalyzed similar reaction was reported by Matsubara and co-workers.^{38f} In 2015, Rh-catalyzed decarbonylative synthesis of carbazoles was reported by Feng and co-workers, which tolerates a broad range of functional group (Scheme 9c).^{38g} In 2003, Davies and co-workers discovered Pd-catalyzed synthesis of carbazoles from 2-nitrobiaryls (Scheme 9d).^{38h} CO is used as a stoichiometric reductant in this reaction. In 2009, Jia and co-workers reported Ru-catalyzed synthesis of carbazoles via intramolecular C–H amination (Scheme 9e).³⁸ⁱ This reaction is unaffected by halogen substituents such as iodine and bromine.

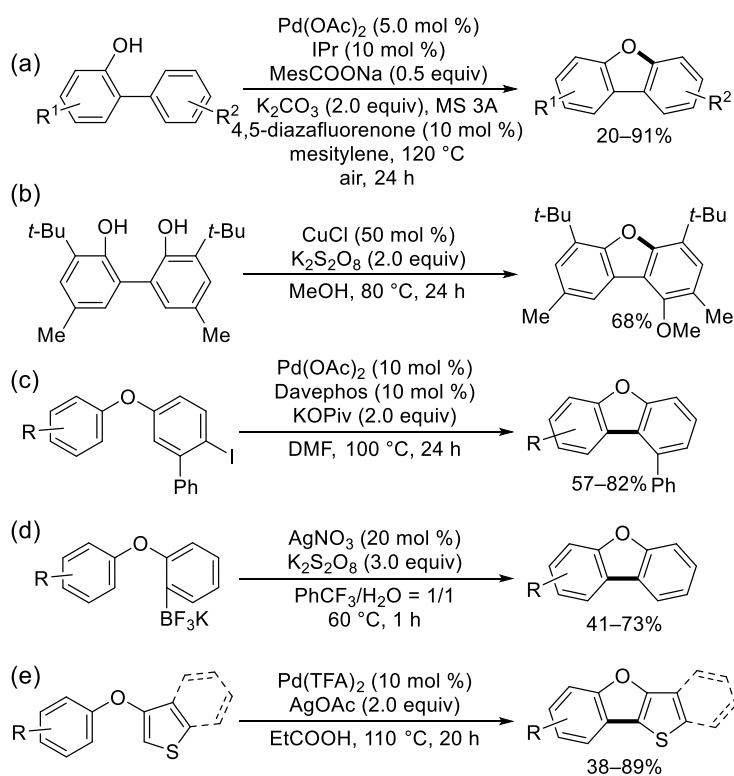
Scheme 9. Representative synthesis of carbazoles by transition metal-catalyzed intramolecular cyclizations



Synthesis of Diarylfurans

In 2011, Liu and co-workers reported a straightforward synthesis of dibenzofurans through Pd-catalyzed dehydrogenative cyclization which features without the use of strong oxidants such as $\text{PhI}(\text{OAc})_2$ (Scheme 10a).^{39a} In 2015, You and co-workers discovered Cu-catalyzed dehydrative cyclization for the synthesis of dibenzofurans from biphenyl diol (Scheme 10b).^{39b} In 2019, Lin and co-workers developed the synthesis of dibenzofurans via intramolecular remote C–H functionalization via sequential 1,4-palladium migration which provides an efficient route to construct diverse polycyclic frameworks (Scheme 10c).^{39c} In 2011, Ag-catalyzed radical cyclization for the conversion of trifluoroborates into the benzofurans was reported by Baran and co-workers, which proceeds under mild conditions as compared with a general transition metal-catalyzed condition (Scheme 10d).^{39d} In 2015, Miura and co-workers developed Pd-catalyzed synthesis of thienobenzofurans from 3-aryloxythiophenes (Scheme 10e).^{39e} This reaction can be applied not only to the synthesis of benzothienofurans but also to the synthesis of dithienothiophene.

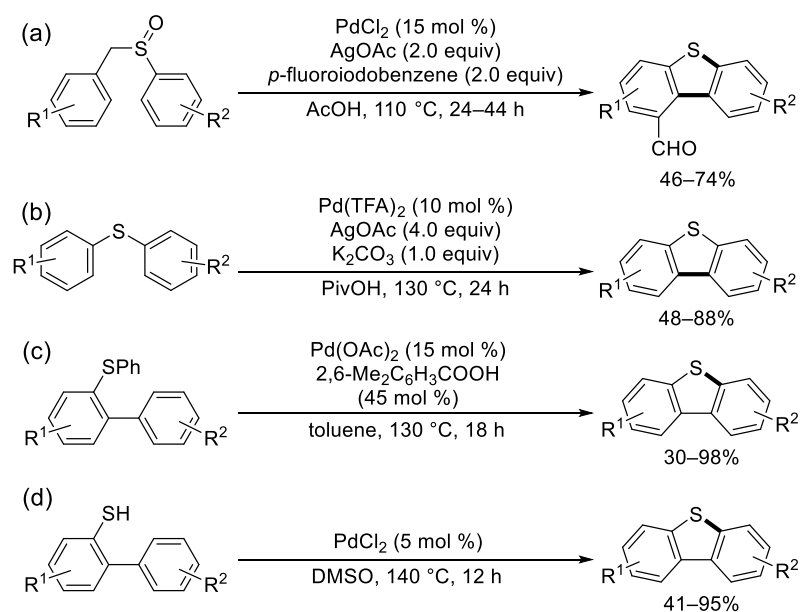
Scheme 10. Representative synthesis of diarylfurans by transition metal-catalyzed intramolecular cyclizations



Synthesis of Diarylthiophenes

In 2011, Antonchick and co-workers reported a Pd-catalyzed sulfoxide-directed synthesis of dibenzothiophenes bearing a formyl group (Scheme 11a).^{40a} In 2014, Zhou and co-workers developed to produce dibenzothiophenes from diaryl sulfides by a Pd-catalyzed dehydrogenative cyclization which afforded various dibenzothiophenes in moderate to good yields with tolerance of a wide variety of substrates (Scheme 11b).^{40b} In 2016, Chatani and co-workers discovered a Pd-catalyzed synthesis of dibenzothiophenes via cleavage of C–S bond (Scheme 11c).^{40c} This reaction can be applied not only to the synthesis of dibenzothiophenes but also to the synthesis of dibenzoselenophene. In 2018, a Pd-catalyzed cyclization of 2-biphenylthiols to dibenzothiophenes was reported by Xu and co-workers (Scheme 11d).^{40d} The utility of the reaction was demonstrated by the facile synthesis of helical dinaphthothiophene.

Scheme 11. Representative synthesis of diarylthiophenes by transition metal-catalyzed intramolecular



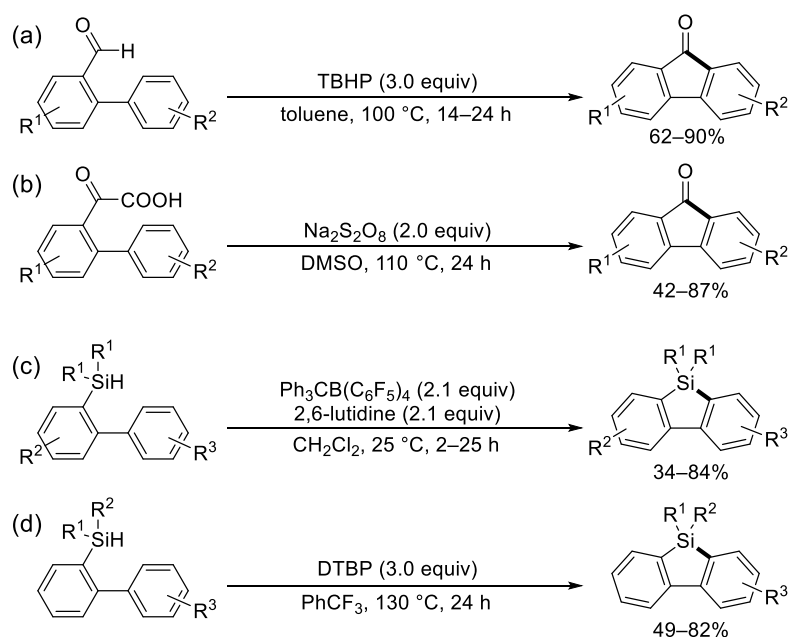
1-2-2. Transition Metal-Free Intramolecular Cyclization

Recently, transition metal-free reaction has been attracting attention. Because most transition metal catalysts are expensive, sometimes require harsh reaction conditions and are unstable under ambient conditions. As a consequence, the development of a transition metal-free and environmentally benign synthetic methodology is highly desirable. In this section, the author will focus on transition metal-free intramolecular cyclizations under relatively mild conditions

Synthesis of Fluorene and Silafluorene Analogues

In 2016, Singh and co-workers reported a synthesis of fluorenones via TBHP-promoted radical dehydrogenative cyclization which is initiated by the *t*-BuO radical generated by the O–O homolytic bond dissociation of TBHP (Scheme 12a).^{41a} In 2017, a decarboxylative radical cyclization for the conversion of α -oxocarboxylic acids leading to the fluorenones was reported by Jethava and co-workers (Scheme 12b).^{41b} The initiator of this reaction is the SO₄ radical anion produced by K₂S₂O₈ undergoing O–O bond splitting by heating. In 2009, Kawashima and co-workers developed a Sila-Friedel–Crafts reaction and its application to the synthesis of dibenzosiloles from biphenylhydrosilanes (Scheme 12c).^{42a} Initially, the reaction of biphenylhydrosilanes with a trityl cation produces a silicenium ion, which spontaneously forms arene complexes. The dibenzosiloles were obtained by deprotonation from the species. In 2015, Li and co-workers reported DTBP-promoted radical dehydrogenative cyclization for the synthesis of dibenzosiloles (Scheme 12d).^{42b}

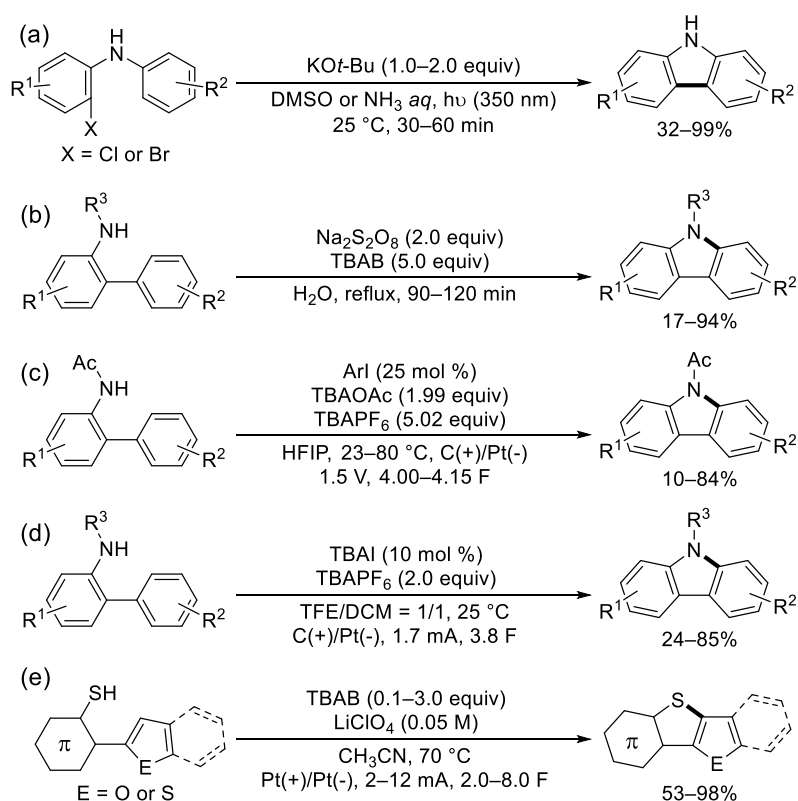
Scheme 12. Representative synthesis of fluorenes and silafluorenes by transition metal-free intramolecular



Synthesis of Heteroacenes

In 2009, Rossi and co-workers reported the synthesis of carbazoles by the photostimulated $S_{RN}1$ substitution reaction (Scheme 13a).^{43a} By using this methodology, 3,3'-bi(9*H*-carbazole) was also obtained via a double $S_{RN}1$ reaction with benzidines. In 2017, oxidative radical cyclization for the conversion of 2-aminobiaryls into the carbazoles was reported by Chuskit and co-workers (Scheme 13b).^{43b} The SO_4 radical anion produced by $Na_2S_2O_8$ is used as the radical initiator in this reaction. In 2020, Powers and co-workers discovered electrochemical synthesis of carbazoles (Scheme 13c).^{43c} In this reaction, anodically generated hypervalent iodine intermediates acts as an electrocatalysis. In 2020, Chen and co-workers was reported electrochemical dehydrogenative amination of 2-amidobiphenyls enable carbazoles synthesis with the assistance of iodine generated by anodic oxidation of TBAI (Scheme 13d).^{43d} In 2020, the electrochemical dehydrogenative cyclization for the synthesis of thienoacenes was reported Suga and co-workers (Scheme 13e).⁴⁴ In this reaction, TBAB promoted the reaction as a mediator.

Scheme 13. Representative synthesis of heteroacenes by transition metal-free intramolecular cyclizations



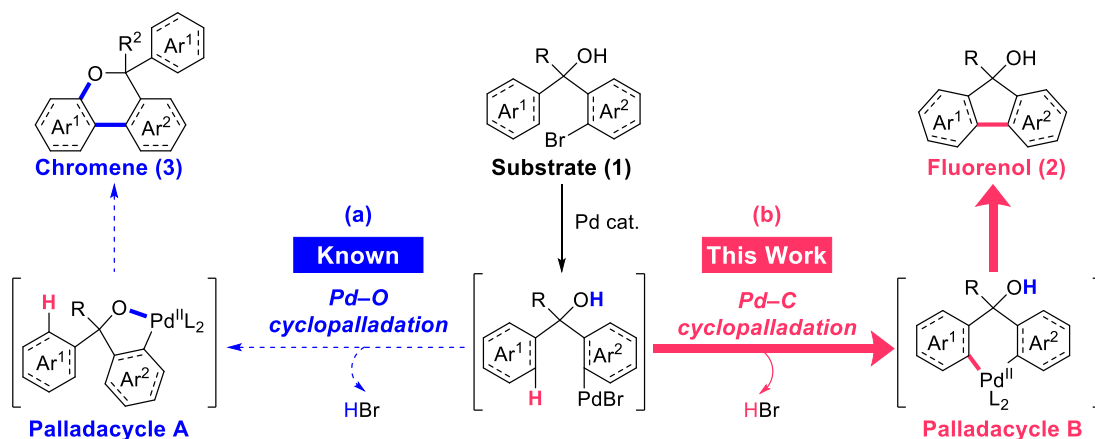
1-3. The Purposes

Up to the previous page, the author has introduced the synthesis of polycyclic aromatic compounds by various intramolecular cyclizations. However, there are few reports on the synthesis of multiple heteroring-fused polycyclic aromatic compounds (MHPAs). In this study, the author focus on heteroring-fused fluorenes and heteroacenes among MHPAs and aims to develop an efficient synthetic method with intramolecular cyclization as the key reaction.

1-3-1. Synthesis of Heteroring-Fused Fluorenol by Intramolecular Cyclization

As shown in section 1-2-1 and 1-2-2, among fluorenes, there are few reports on the straightforward synthesis of fluorenols by intramolecular cyclization. In particular, there are no reports applied to the synthesis of heteroring-fused fluorenol by transition metal-catalyzed intramolecular cyclization. One reason for this is that the heteroaryl C–H differs significantly from the benzene C–H in terms of acidity, electronic state, and steric state. Heteroring-fused fluorenols should be potential candidates for bioactive compounds and precursors for functional materials. The author aimed to develop efficient methods for the synthesis of fluorenols and heteroring-fused analogues by transition metal-catalyzed intramolecular cyclization. The author envisioned the synthetic strategy as shown in Scheme 14b. Fluorenols **2** could be converted from the substrate **1** in the presence of a transition metal-catalyst via the elimination of HBr. Designed transformation includes selective activation of the aromatic C–H. However, it is already known that **1** was selectively converted to a chromene **3** under Pd-catalyzed C–H functionalization conditions and **2** was not obtained at all (Scheme 14a).⁴⁵ The reason for the chemoselectivity would be that the Pd catalyst activates the highly reactive O–H to form the palladacycle A. In contrast, to convert **1** to **2**, it is necessary to activate the aryl C–H having lower reactivity than the O–H to form the palladacycle B. The author devised that the desired selectivity could be achieved by adjusting the steric and electronic states of the Pd catalyst. In Chapter 2, the details of the results are described.

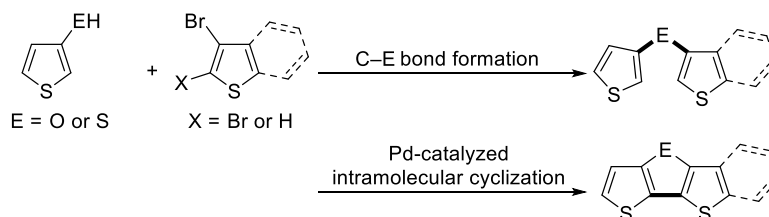
Scheme 14. Selective synthesis of fluorenols by Pd-catalyzed intramolecular cyclization



1-3-2. Synthesis of Thienoacenes by Intramolecular Cyclization

The author aimed to develop an efficient method to access chalcogen-bridged bithiophene derivatives. Chalcogen-bridged bithiophenes has been attracting interest due to their role in organic thin-film transistor.⁸ Among them, *Oxygen-bridged* bithiophenes are expected to be applied to the active material of organic light emitting transistors due to the high probability of exhibiting excellent fluorescent properties. However, there have been only two reports on the synthesis of oxygen-bridged bithiophenes. Furthermore, the total yield was very low and the substrate scope was narrow. The author envisioned the synthetic strategy as shown in Scheme 15. The authors designed that oxygen-bridged bithiophenes could be converted by Pd-catalyzed intramolecular cyclization following C–O bond formation. In Chapter 3, the details of the results are described. The author also achieved the synthesis of *Sulfur-bridged* bithiophenes by this synthetic approach. In Chapter 4, the details of these results are described. Furthermore, the detailed physical properties of Oxygen and Sulfur-bridged bithiophenes were elucidated. In Chapter 5, the details of the results are described.

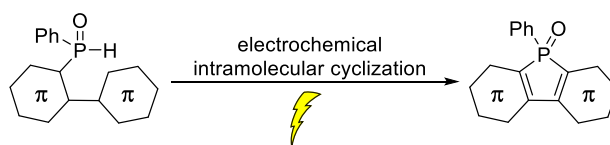
Scheme 15. Synthesis of thienoacenes via C–E bond formation and subsequent intramolecular cyclization



1-3-3. Synthesis of Diarylphosphole Oxide by Intramolecular Cyclization

The author also developed a method for the synthesis of diarylphosphole oxides by intramolecular cyclization. As a method for synthesizing diarylphosphole oxides, an approach derived from diarylphosphine oxide is known.⁴⁶ However, previously reported methods required harsh reaction conditions, transition-metal catalysts, and excess amount of acids. Meanwhile, the electrochemical approach has attracted attention in recent years. Organic electrochemistry offers many advantages over traditional, reagent-based reactions, because usual reagents are often highly toxic, expensive and often generate a lot of reagent waste. The electrochemical approach allows the use of electrical current as a renewable, inexpensive and inherently safe reagent. Therefore, the author envisioned the synthesis of diarylphosphole oxides by an electrochemical approach (Scheme 16). In Chapter 6, the details of the results are described.

Scheme 16. Synthesis of diarylphosphole oxides by an electrochemical intramolecular cyclization



References

- (1) (a) Taylor, R. D.; MacCoss, M.; Lawson, A. D. G. *J. Med. Chem.* **2014**, *57*, 5845–5859. (b) Anthony, J. E. *Chem. Rev.* **2006**, *106*, 5028–5048.
- (2) (a) Venuti, E.; Valle, R. G. D.; Bilotti, I.; Brillante, A.; Cavallini, M.; Calo, A.; Geerts, Y. H. *J. Phys. Chem. C* **2011**, *115*, 12150–12157. (b) Pal, S. K.; Setia, S.; Avinash, B. S.; Kumar, S. *Liq. Cryst.* **2013**, *40*, 1769–1816. (c) Piot, L.; Marie, C.; Feng, X.; Müllen, K.; Fichou, D. *Adv. Mater.* **2008**, *20*, 3854–3858. (d) Alam, M. A.; Motoyanagi, J.; Yamamoto, Y.; Fukushima, T.; Kim, J.; Kato, K.; Takata, M.; Saeki, A.; Seki, S.; Tagawa, S.; Aida, T. *J. Am. Chem. Soc.* **2009**, *121*, 17722–17725.
- (3) (a) Payne, M. M.; Parkin, S. R.; Anthony, J. E. *J. Am. Chem. Soc.* **2005**, *127*, 8028–8029. (b) Mondal, R.; Adhikari, R. M.; Shah, B. K.; Neckers, D. C. *Org. Lett.* **2007**, *9*, 2505–2508.
- (4) (a) Eguchi, R.; He, X.; Hamao, S.; Goto, H.; Okamoto, H.; Gohda, S.; Sato, K.; Kubozono, Y. *Phys. Chem. Chem. Phys.* **2013**, *15*, 20611–20617. (b) He, X.; Eguhci, R.; Goto, H.; Uesugi, E.; Hamao, S.; Takabayashi, Y.; Kubozono, Y. *Org. Electron.* **2013**, *14*, 1673–1682. (c) Okamoto, H.; Eguchi, R.; Hamao, S.; Goto, H.; Gotoh, K.; Sakai, Y.; Izumi, M.; Takaguchi, Y.; Gohda, S.; Kubozono, Y. *Sci. Rep.* **2014**, *4*, 5330. (d) Okamoto, H.; Hamao, S.; Eguchi, R.; Goto, H.; Takabayashi, Y.; Yen, P. Y.; Liang, L. U.; Chou, C.; Hoffmann, G.; Gohda, S.; Sugino, H.; Liao, Y.; Ishii, H.; Kubozono, Y. *Sci. Rep.* **2019**, *9*, 4009. (e) Chen, S.; Sang, I.; Okamoto, H.; Hoffmann, G. *J. Phys. Chem. C* **2017**, *121*, 11390–11398.
- (5) (a) Fukuda, M.; Sawada, K.; Yoshino, K. *J. Polym. Sci., Part A: Polym. Chem.* **1993**, *31*, 2465–2471. (b) Pei, Q.; Yang, Y. *J. Am. Chem. Soc.* **1996**, *118*, 7416–7417. (c) Grice, A. W.; Bradley, D. D. C.; Bernius, M. T.; Inbasekaran, M.; Wu, W. W.; Woo, E. P. *Appl. Phys. Lett.* **1998**, *73*, 629–631. (d) Inbasekaran, M.; Woo, E.; Wu, W. S.; Bernius, M.; Wujkowski, L. *Synth. Met.* **2000**, *111*, 397–401. (e) Bernius, M. T.; Inbasekaran, M.; Woo, E.; Wu, W.; Wujkowski, L. *J. Mater. Sci.: Mater. Electron.* **2000**, *11*, 111–116.
- (6) Fukazawa, A.; Yamaguchi, S. *Chem. Asian J.* **2009**, *4*, 1386–1400.
- (7) (a) Okamoto, H.; Kawasaki, N.; Kaji, Y.; Kubozono, Y.; Fujiwara, A.; Yamaji, M. *J. Am. Chem. Soc.* **2008**, *130*, 10470–10471. (b) Mitsuhashi, R.; Suzuki, Y.; Yamanari, Y.; Mitamura, H.; Kambe, T.; Ikeda, N.; Okamoto, H.; Fujiwara, A.; Yamaji, M.; Kawasaki, N.; Maniwa, Y.; Kubozono, Y. *Nature* **2010**, *464*, 76–79. (c) Gao, J.; Li, R.; Li, L.; Meng, Q.; Jiang, H.; Li, H.; Hu, W. *Adv. Mater.* **2007**, *19*, 3008–3011. (d) Li, R.; Jiang, L.; Meng, Q.; Gao, J.; Li, H.; Tang, Q.; He, M.; Hu, W.; Liu, Y.; Zhu, D. *Adv. Mater.* **2009**, *21*, 4492–4495.
- (8) (a) Cinar, M. E.; Ozturk, T.; *Chem. Rev.* **2015**, *115*, 3036–3140. (b) Li, B. *Chin. J. Org. Chem.* **2015**, *35*, 2487–2506. (c) Takimiya, K.; Shinamura, S.; Osaka, I.; Miyazaki, E. *Adv. Mater.* **2011**, *23*, 4347–4370.
- (9) (a) Kang, M. J.; Doi, I.; Mori, H.; Miyazaki, E.; Takimiya, K.; Ikeda, M.; Kuwabara, H. *Adv.*

- Mater.* **2011**, *23*, 1222–1225. (b) Nakayama, K.; Hirose, Y.; Soeda, J.; Yoshizumi, M.; Uemura, T.; Uno, M.; Li, W.; Kang, M. J.; Yamagishi, M.; Okada, Y.; Miyazaki, E.; Nakazawa, Y.; Nakao, A.; Takimiya, K.; Takeya, J. *Adv. Mater.* **2011**, *23*, 1626–1629.
- (10) Tsuji, H.; Mitsui, C.; Sato, Y.; Nakamura, E. *Adv. Mater.* **2009**, *21*, 3776–3779.
- (11) Zhang, J.; Smith, Z. C.; Thomas III, S. W. *J. Org. Chem.* **2014**, *79*, 10081–10093.
- (12) Wang, C.; Fukazawa, A.; Taki, M.; Sato, Y.; Higashiyama, T.; Yamaguchi, S. *Angew. Chem., Int. Ed.* **2015**, *54*, 15213–15217.
- (13) (a) Bamann, G. A.; Cowen, B. J. *Molecules* **2016**, *21*, 986. (b) Kandimalla, S. R.; Parvathaneni, S. P.; Sabitha, G.; Reddy, B. V. S. *Eur. J. Org. Chem.* **2019**, 1687–1714. (c) Sharma, R.; Kour, P.; Kumar, A. *J. Chem. Sci.* **2018**, *130*, 73. (d) Ferretti, F.; Ramadan, D. R.; Ragaini, F. *ChemCatChem*, **2019**, *11*, 4450–4488. (e) Pawlowski, R.; Stanek, F.; Stodulski, M. *Molecules* **2019**, *24*, 1533. (f) Zuo, L.; Liu, T.; Chang, X.; Guo, W. *Molecules* **2019**, *24*, 3930. (g) Hsieh, J. C.; Su, H. L. *Synthesis* **2020**, *52*, 819–833. (h) Choury, M.; Lopes, A. B.; Blond, G.; Gulea, M. *Molecules* **2020**, *25*, 3147.
- (14) Chernyak, N.; Gevorgyan, V. *J. Am. Chem. Soc.* **2008**, *130*, 5636–5637.
- (15) Hwang, S. J.; Kim, H. J.; Chang, S. *Org. Lett.* **2009**, *11*, 4588–4591.
- (16) Hsiao, C.; Lin, Y.; Liu, C.; Wu, T.; Wu, Y. *Adv. Synth. Catal.* **2010**, *352*, 3267–3274.
- (17) Song, J.; Li, Y.; Sun, W.; Yi, C.; Wu, H.; Wang, H.; Ding, K.; Xiao, K.; Liu, C. *New J. Chem.* **2016**, *40*, 9030–9033.
- (18) Zhao, J.; Yue, D.; Campo, M. A.; Larock, R. C. *J. Am. Chem. Soc.* **2007**, *129*, 5288–5295.
- (19) (a) Gandeepan, P.; Hung, C.; Cheng, C. *Chem. Commun.* **2012**, *48*, 9379–9381. (b) Li, H.; Zhu, R.; Shi, W.; He, K.; Shi, Z. *Org. Lett.* **2012**, *14*, 4850–4853. (c) Kishore, R.; Priya, S.; Sudhakar, M.; Venu, B.; Venugopal, A.; Yadav, J.; Kantam, M. L. *Catal. Sci. Technol.* **2015**, *5*, 3363–3367. (d) Silveira, C.; Larghi, E.; Mendes, S.; Bracca, A.; Rinaldi, F.; Kaufman, T. *Eur. J. Org. Chem.* **2009**, 4637–4645. (e) Wu, R.; Silks, L. A.; Olivault-Shiflett, M.; Williams, R. F.; Ortiz, E. G.; Stotter, P.; Kimball, D. B.; Martinez, R. A. *J. Label Compd. Radiopharm.* **2013**, *56*, 581–586.
- (20) Wan, J.; Huang, J.; Jhan, Y.; Hsieh, J. *Org. Lett.* **2013**, *15*, 2742–2745.
- (21) Gao, Q.; Xu, S. *Org. Biomol. Chem.* **2018**, *16*, 208–212.
- (22) Kim, J.; Ohk, Y.; Park, S. H.; Jung, Y.; Chang, S. *Chem. Asian J.* **2011**, *6*, 2040–2047.
- (23) Morimoto, K.; Itoh, M.; Hirano, K.; Satoh, T.; Shibata, Y.; Tanaka, K.; Miura, M. *Angew. Chem., Int. Ed.* **2012**, *51*, 5359–5362.
- (24) Itoh, M.; Hirano, K.; Satoh, T.; Shibata, Y.; Tanaka, K.; Miura, M. *J. Org. Chem.* **2013**, *78*, 1365–1370.
- (25) (a) Fukuyama, T.; Maetani, S.; Miyagawa, K.; Ryu, I. *Org. Lett.* **2014**, *16*, 3216–3219. (b) Ruzi R.; Zhang, M.; Ablajan, K.; Zhu, C. *J. Org. Chem.*, **2017**, *82*, 12834–12839.
- (26) Pan, F.; Liu, S.; Shu, C.; Lin, R.; Yu, Y.; Zhou, J.; Ye, L. *Chem. Commun.* **2014**, *50*, 10726–

10729.

- (27) Wang, P.; McGonigal, P. R.; Herlé, B.; Besora, M.; Echavarren, A. M. *J. Am. Chem. Soc.* **2014**, *136*, 801–809.
- (28) Bucher, J.; Wurm, T.; Taschinski, S.; Sachs, E.; Ascough, D.; Rudolph, M.; Rominger, F.; Hashmi, A.S. *Adv. Synth. Catal.* **2017**, *359*, 225–233.
- (29) Corrie, T. J. A.; Ball, L. T.; Russell, C. A.; Lloyd-Jones, G. C. *J. Am. Chem. Soc.* **2017**, *139*, 245–254.
- (30) Fuchibe, K.; Akiyama, T. *J. Am. Chem. Soc.* **2006**, *128*, 1434–1435.
- (31) Sarkar, S.; Maiti, S.; Bera, K.; Jalal, S.; Jana, U. *Tetrahedron Lett.* **2012**, *53*, 5544–5547.
- (32) Haggam, R. A. *Tetrahedron* **2013**, *69*, 6488–6494.
- (33) (a) Seo, S.; Slater, M.; Greaney, M. F. *Org. Lett.* **2012**, *14*, 2650–2653. (b) Lockner, J. W.; Dixon, D. D.; Risgaard, R.; Baran, P. S. *Org. Lett.* **2011**, *13*, 5628–5631.
- (34) Shimizu, M.; Mochida, K.; Hiyama, T. *Angew. Chem., Int. Ed.* **2008**, *47*, 9760–9764.
- (35) (a) Ureshino, T.; Yoshida, T.; Kuninobu, Y.; Takai, K. *J. Am. Chem. Soc.* **2010**, *132*, 14324–14326. (b) Murata, M.; Talizawa, M.; Sasaki, H.; Kohari, Y.; Sakagami, H.; Namikoshi, T.; Watanabe, S. *Chem. Lett.* **2016**, *45*, 857–859. (c) Mitsudo, K.; Tanaka, S.; Isobuchi, R.; Inada, T.; Mandai, H.; Korenaga, T.; Wakamiya, A.; Murata, Y.; Suga, S. *Org. Lett.* **2017**, *19*, 2564–2567.
- (36) (a) Baba, K.; Tobisu, M.; Chatani, N. *Angew. Chem., Int. Ed.* **2013**, *52*, 11892–11895. (b) Cui, Y.; Fu, L.; Cao, J.; Deng, Y.; Jiang, J. *Adv. Synth. Catal.* **2014**, *356*, 1217–1222. (c) Lian, Z.; Bhawal, B. N.; Yu, P.; Morandi, B. *Science* **2017**, *356*, 1059–1063. (d) Fujimoto, H.; Kusano, M.; Kodama, T.; Tobisu, M. *Org. Lett.* **2019**, *21*, 4177–4181.
- (37) Baumgartner, T.; Neumann, T.; Wirges, B. *Angew. Chem., Int. Ed.* **2004**, *43*, 6197–6201.
- (38) (a) Åkermark, B.; Ebersson, L.; Jonsson, E.; Pettersson, E. *J. Org. Chem.* **1975**, *40*, 1365–1367. (b) Xubin, F.; Lei, F.; Shaohua, G. *Chin. J. Org. Chem.* **2012**, *32*, 1217–1231. (c) Yoshikai, N.; Wei, Y. *Asian. J. Org. Chem.* **2013**, *2*, 466–478. (d) Liegault, B.; Lee, D.; Huestis, M. P.; Stuart, D. R.; Fagnou, K. *J. Org. Chem.* **2008**, *73*, 5022–5028. (e) Tsang, W. C. P.; Zheng, N.; Buchwald, S. L. *J. Am. Chem. Soc.* **2005**, *127*, 14560–14561. (f) Yamamoto, M.; Matsubara, S. *Chem. Lett.* **2007**, *36*, 172–173. (g) Fan, W.; Jiang, S.; Feng, B. *Tetrahedron* **2015**, *71*, 4035–4038. (h) Smitrovich, J. H.; Davies, L. W. *Org. Lett.* **2004**, *6*, 533–555. (i) Shou, W. G.; Li, J.; Guo, T.; Lin, Z.; Jia, G. *Organometallics* **2009**, *28*, 6847–6854.
- (39) (a) Xiao, B.; Gong, T.; Liu, Z.; Liu, J.; Luo, D. Xu, J.; Liu, L. *J. Am. Chem. Soc.* **2011**, *133*, 9250–9253. (b) Li, W.; Song, F.; You, J. *Chem. Eur. J.* **2015**, *21*, 13913–13918. (c) Li, P.; Li, Q.; Weng, H.; Diao, J.; Yao, H.; Lin, A. *Org. Lett.* **2019**, *21*, 6765–6769. (d) Lockner, J. W.; Dixon, D. D.; Risgaard, R.; Baran, P. S. *Org. Lett.* **2011**, *13*, 5628–5631. (e) Kaida, H.; Satoh, T.; Hirano, K.; Miura, M. *Chem. Lett.* **2015**, *44*, 1125–1127.

- (40) (a) Samanta, R.; Antonchick, A. P. *Angew. Chem., Int. Ed.* **2011**, *50*, 5217–5220. (b) Che, R.; Wu, Z.; Li, Z.; Xiang, H.; Zhou, X. *Chem. Eur. J.* **2014**, *20*, 7258–7261. (c) Tobisu, M.; Masuya, Y.; Baba, K.; Chatani, N. *Chem. Sci.* **2016**, *7*, 2587–2591. (d) Zhang, T.; Deng, G.; Li, H.; Liu, B.; Tan, Q.; Xu, B. *Org. Lett.* **2018**, *20*, 5439–5443.
- (41) (a) Mishra, K.; Pandey, A. K.; Singh, J. B.; Singh, R. M. *Org. Biomol. Chem.* **2016**, *14*, 6328–6336. (b) Laha, J. K.; Patel, K. V.; Dubey, G.; Jethava, K. P. *Org. Biomol. Chem.* **2017**, *15*, 2199–2210.
- (42) (a) Furukawa, S.; Kobayashi, J.; Kawashima, T. *J. Am. Chem. Soc.* **2009**, *131*, 14192–14193. (b) Xu, L.; Zhang, S.; Li, P. *Org. Chem. Front.* **2015**, *2*, 459–463.
- (43) (a) Budén, M. E.; Vaillard, V. A.; Martin, S. E.; Rossi, R. A. *J. Org. Chem.* **2009**, *74*, 4490–4498. (b) Natarajan, P.; Chuskit, Priya and D. *Green Chem.* **2017**, *19*, 5854–5861. (c) Maity, A.; Frey, B. L.; Hoskinson, N. D.; Powers, D. C. *J. Am. Chem. Soc.* **2020**, *142*, 4990–4995. (d) Zhang, P.; Li, B.; Niu, L.; Wang, L.; Zhang, G.; Jia, X.; Zhang, G.; Liu, S.; Ma, L.; Gao, W.; Qin, D.; Che, J. *Adv. Synth. Catal.* **2020**, *362*, 2342–2347.
- (44) Mitsudo, K.; Matsuo, R.; Yonezawa, T.; Inoue, H.; Mandai, H.; Suga, S. *Angew. Chem., Int. Ed.* **2020**, *59*, 7803–7807.
- (45) Ma-hendar, L.; Satyanarayana, G. *J. Org. Chem.* **2014**, *79*, 2059–2074.
- (46) (a) Kuninobu, Y.; Yoshida, T.; Takai, K. *J. Org. Chem.* **2011**, *76*, 7370–7376. (b) Furukawa, S.; Haga, S.; Kobayashi, J.; Kawashima, T. *Org. Lett.* **2014**, *16*, 3228–3231. (c) Nishimura, K.; Hirano, K.; Miura, M. *Org. Lett.* **2019**, *21*, 1467–1470.

Chapter 2. Synthesis of Heteroring-Fused Fluorenol via Selective Intramolecular C–H Functionalization

2-1.	Abstract	24
2-2.	Introduction	24
2-3.	Optimization for the Selective Synthesis of Fluorenols	26
2-4.	Substrate Scope	30
2-5.	Plausible Reaction Mechanism	32
2-6.	Application	33
2-7.	Conclusion	34
2-8.	Experimental Section and Analytical Data	35
	References	48

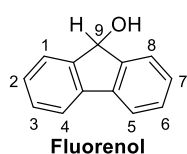
2-1. Abstract

The author developed an efficient synthetic method of 9-substituted fluoreneols (FOLs) by suppressing intermolecular cyclization and promoting intramolecular C–H functionalization. This method was also applied to the synthesis of heteroring-fused FOLs. Further, the obtained FOLs were converted to fulvenes by dehydration.

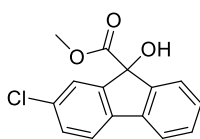
2-2. Introduction

Fluorenes and related compounds have long been widely used as bioactive compounds and active materials for functional materials.¹ Among them, 9-hydroxyfluorenes (fluoreneols) are useful molecules that are found in physiologically active compounds and synthetic intermediates of compounds for organic materials. Example compounds include the wakefulness-enhancing agent fluoreneol,^{2a} the auxin polar transport inhibitors morphactin IT 3456^{2b} and HFCA,^{2c} and a synthetic intermediate of 3,8-bis[bis(4-methoxyphenyl)amino]fluoranthene-4,5-dicarbonitrile (BTF)^{2d} (Figure 1A and 1B). The heteroring-fused analogues have also attracted attention. For instance, pyridine-fused analogues are known to have antimycobacterial activity against *Mycobacterium tuberculosis* H37Rv and antiprotozoal activity against *Trypanosoma spp.*, *Leishmania* and *T. cruzi*.^{3a-d} A thiophene-fused analogue also acts as a 5-HT_{2B} receptor antagonist^{3e} (Figure 1C).

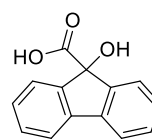
A. Bioactive compounds



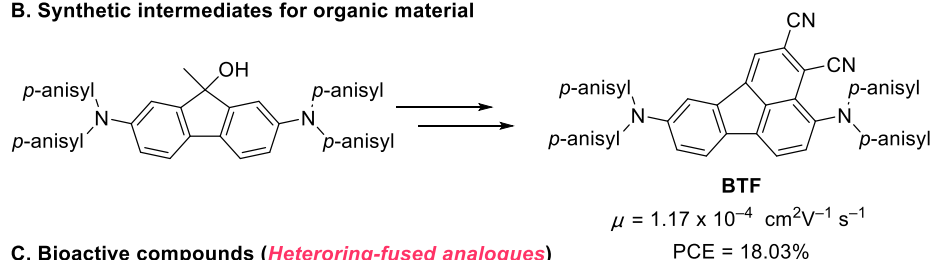
wakefulness enhancing agents



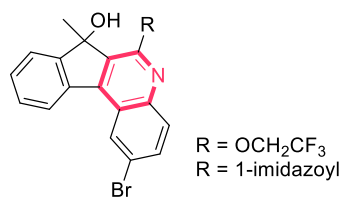
auxin polar transport inhibitors



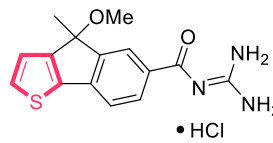
B. Synthetic intermediates for organic material



C. Bioactive compounds (Heteroring-fused analogues)



Antimycobacterial activity or antiprotozoal activity



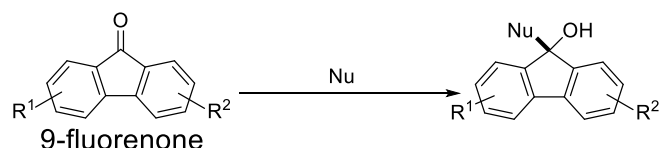
5-HT_{2B} receptor antagonists

Figure 1. Representative FOLs

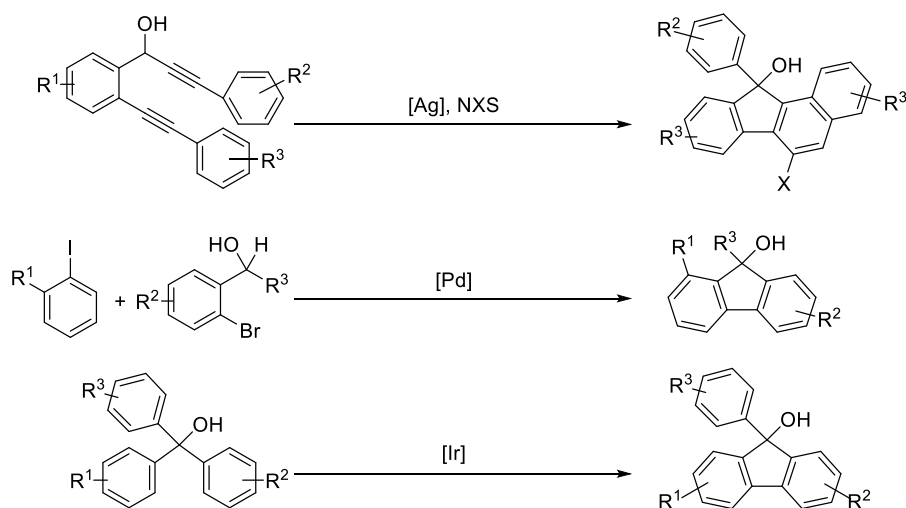
Among fluorenols, 9-substituted fluorenols (FOLs) are generally synthesized by the reaction of 9-fluorenone with a nucleophile such as a Grignard reagent (Scheme 1A).⁴ For this method, the corresponding 9-fluorenone should be prepared as a precursor, and the efficiency of the reaction depends on the reactivity of the 9-fluorenone and the nucleophile. As a method for the direct synthesis of FOLs, transition metal-catalyzed cyclization has also received attention. The synthesis of FOLs has been achieved by catalytic reactions using a transition metal catalyst, such as Ag, Au, Pd or Ir (Scheme 1B).⁵ Although these methods enable easy access to various FOLs, the synthesis of heteroring-fused analogues has not been achieved. One reason for this is that the heteroaryl C–H differs significantly from the benzene C–H in terms of acidity, electronic state, and steric state. Heteroring-fused FOLs should be potential candidates for bioactive compounds and precursors for functional materials. Therefore, the author aimed to develop a straightforward method for the synthesis of FOLs and heteroring-fused analogues by transition metal-catalyzed cyclization.

Scheme 1. Representative synthetic methods of FOLs

A. General Method: 9-fluorenone with a nucleophile



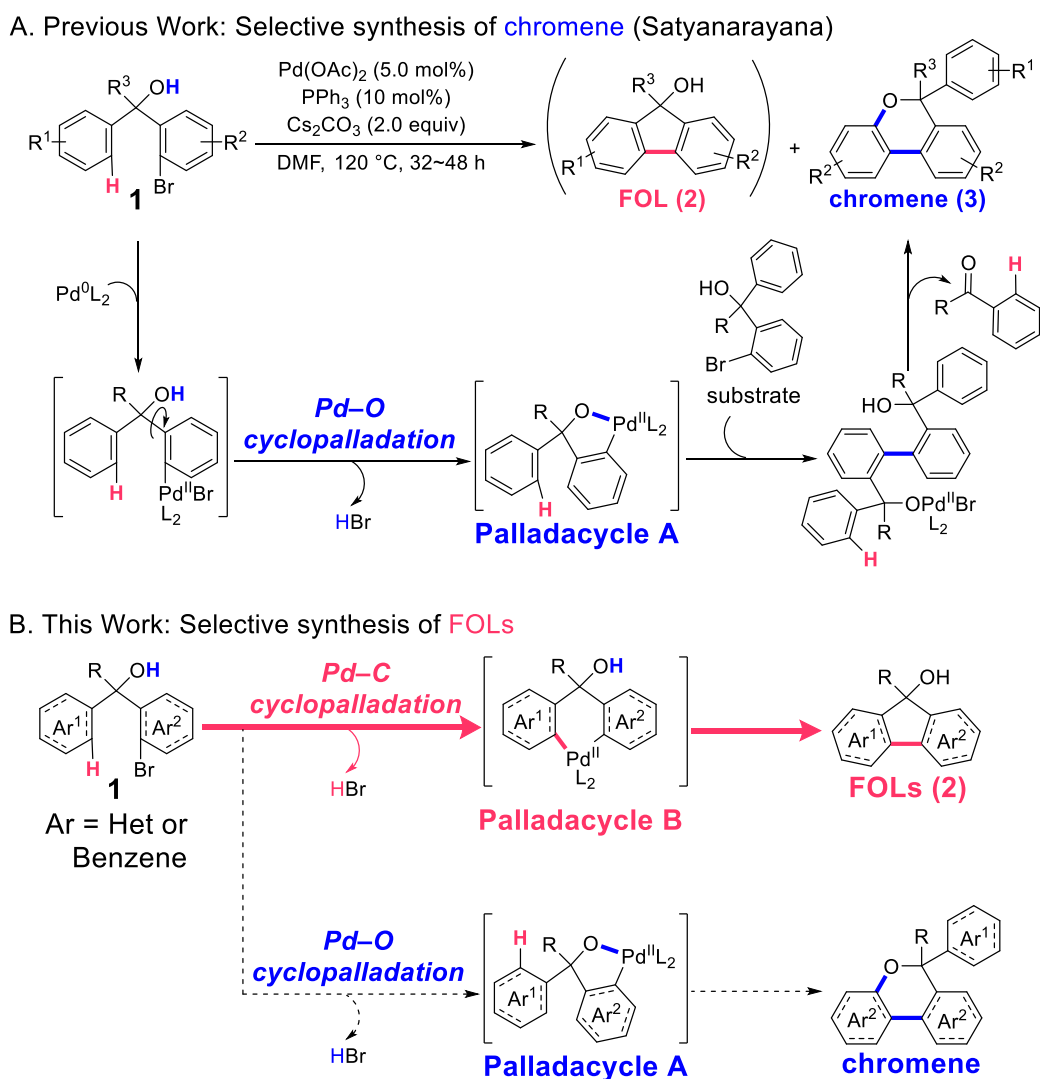
B. Representative Reported Methods: Transition metal-catalyzed cyclization



The approach for synthesizing FOLs **2** is envisioned in Scheme 2B. The author considered that **2** could be synthesized from the tertiary alcohols **1** via the elimination of HBr. The author's designed transformation includes selective activation of the aromatic C–H bond. However, Satyanarayana and co-workers reported that **1** was selectively converted to a chromene **3** under Pd-catalyzed C–H functionalization conditions and **2** was not obtained at all (Scheme 2A).⁶ The reason for the

chemoselectivity would be that the Pd catalyst activates the highly reactive O–H to form the palladacycle A. In contrast, to convert **1** to **2**, it is necessary to activate the aryl C–H having lower reactivity than the O–H to form the palladacycle B (Scheme 2B). Thus, the selective conversion of **1** to **2** is challenging, but the author devised that the desired selectivity could be achieved by adjusting the steric and electronic states of the Pd catalyst.

Scheme 2. Previous and this work

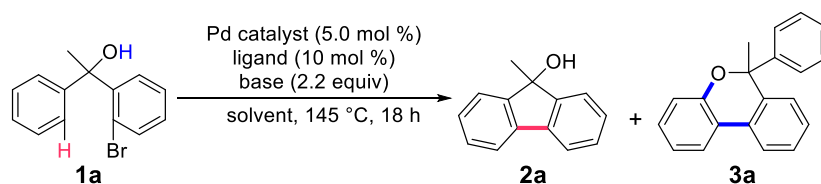


2-3. Optimization for the Selective Synthesis of Fluorenols

Initially, by heating tertiary alcohol **1a** in the presence of palladium acetate (Pd(OAc)₂, 5.0 mol %), Cs₂CO₃ (2.2 equiv) in DMA at 145 °C for 18 h, chromene **3a** was selectively obtained in 52% yield, the desired FOLs could not be obtained at all (Table 1, entry 1). The use of CsOAc instead of Cs₂CO₃ completely changed the selectivity of this reaction, and the target product **2a** was obtained in 34% yield along with a trace amount of chromene **3a** (entry 2). Base plays a key role in the selectivity. The addition of the PPh₃ as a ligand improved the yield of **2a** to 43%, and the selectivity of the reaction

was completely controlled (entry 3). The author next investigated various solvents (entries 3–6). Consequently, DMA was found to be the optimum solvent for this reaction. Next, the effects of Pd-catalysts were examined (entries 3, 7 and 8). Using Pd(OPiv)₂, which has a bulky counter anion, **2a** was obtained in 58% yield. Further studies of reaction temperature and amount of base did not provide additional insights.

Table 1. Optimization for the selective synthesis of FOLs^a

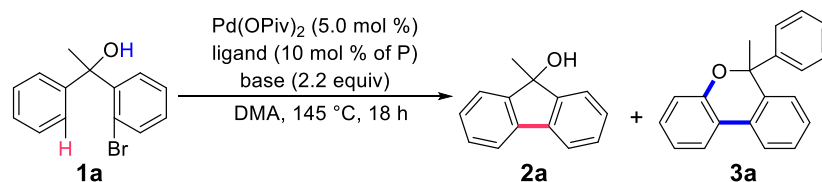


entry	Pd	ligand	base	solvent	2a (%)	3a (%)
1	Pd(OAc) ₂	–	Cs ₂ CO ₃	DMA	N.D. ^b	52
2	Pd(OAc) ₂	–	CsOAc	DMA	34	trace
3	Pd(OAc) ₂	PPh ₃	CsOAc	DMA	43	N.D.
4	Pd(OAc) ₂	PPh ₃	CsOAc	DMF	11	N.D.
5	Pd(OAc) ₂	PPh ₃	CsOAc	toluene	17	N.D.
6	Pd(OAc) ₂	PPh ₃	CsOAc	1,4-dioxane	32	N.D.
7	Pd(TFA) ₂	PPh ₃	CsOAc	DMA	56	N.D.
8	Pd(OPiv) ₂	PPh ₃	CsOAc	DMA	58	N.D.
9 ^c	Pd(OPiv) ₂	PPh ₃	CsOAc	DMA	58	N.D.
10 ^d	Pd(OPiv) ₂	PPh ₃	CsOAc	DMA	N.D.	N.D.
11	Pd(OPiv) ₂	PPh ₃	CsOAc ^e	DMA	37	N.D.
12	Pd(OPiv) ₂	PPh ₃	CsOAc ^f	DMA	54	N.D.

^a Reaction conditions: **1a** (0.20 mmol), Pd catalyst (5.0 mol %), ligand (10 mol %), base (2.2 equiv), solvent (0.4 mL) at 145 °C, 18 h. Yield was determined by ¹H NMR analysis using 1,1,2,2-tetrachloroethane as an internal standard. ^b N.D. = Not Detected. ^c Performed at 175 °C. ^d Performed at 100 °C. ^e 5.0 equiv. ^f 1.0 equiv.

The author continued to screen various acetate bases and ligands with optimal catalyst Pd(OPiv)₂ to explore the optimal conditions (Table 2). However, no improvement in yield was observed when bases other than CsOPiv were used (entries 1–4). Among the ligands examined, the electron-rich ligand such as dppf gave the best results (entries 5–12).

Table 2. The effect of bases and ligand ^a



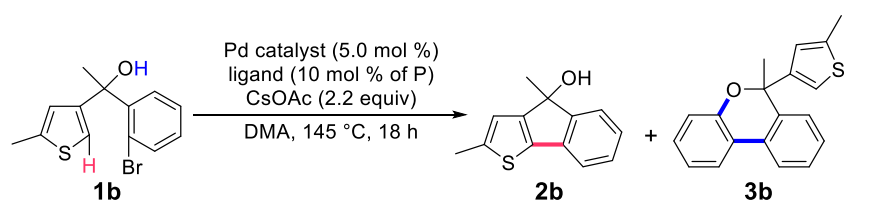
entry	ligand	base	2a (%)	3a (%)
1	PPh ₃	CsOPiv	58	N.D. ^b
2	PPh ₃	CsTFA	complex mixture	
3	PPh ₃	KOAc	43	N.D.
4	PPh ₃	NaOAc	37	N.D.
5	PCy ₃	CsOPiv	59	N.D.
6	P(<i>o</i> -tol) ₃	CsOPiv	50	N.D.
7	OPPh ₃	CsOPiv	12	N.D.
8	XPhos	CsOPiv	43	N.D.
9	XantPhos	CsOPiv	55	N.D.
10	QPhos	CsOPiv	64	N.D.
11	dppf	CsOPiv	69	N.D.
12	IPr	CsOPiv	48	N.D.

^a Reaction conditions: **1a** (0.20 mmol), Pd(OPiv)₂ (5.0 mol %), ligand (10 mol %), base (2.2 equiv), DMA (0.4 mL) at 145 °C, 18 h. Yield was determined by ¹H NMR analysis using 1,1,2,2-tetrachloroethane as an internal standard. ^b

N.D. = Not Detected.

Next, the author examined the synthesis of a heteroring-fused FOL, which has never been synthesized by transition metal-catalyzed reactions. In the case of a tertiary alcohol **1b** bearing a 2-methylthiophene, the corresponding **2b** was obtained in 67% yield with complete chemoselectivity, and chromene **3b** was not obtained at all (Table 3, entry 1). The use of PPh₃ as a ligand gave **2b** in a similar yield to that of dppf (entry 2). The optimal Pd catalyst was found to be Pd(OAc)₂ for this substrate (entries 2–4). With the use of Pd(OAc)₂ as a catalyst and dppf as a ligand, the yield of **2b** decreased to 59% (entry 5). The choice of an appropriate catalyst and ligand should be important in this reaction, probably because both the steric and electronic states of the substrate strongly affect the efficiency of the reactions.

Table 3. Optimization for the selective synthesis of heteroring-fused FOLs ^a



entry	Pd	ligand	2b (%)	3b (%)
1	Pd(OPiv) ₂	dppf	67	N.D. ^b
2	Pd(OPiv) ₂	PPh ₃	67	N.D.
3	Pd(TFA) ₂	PPh ₃	63	N.D.
4	Pd(OAc) ₂	PPh ₃	72	N.D.
5	Pd(OAc) ₂	dppf	59	N.D.

^a Reaction conditions: **1a** (0.20 mmol), Pd catalyst (5.0 mol %), ligand (10 mol %), CsOAc (2.2 equiv), DMA (0.4 mL) at 145 °C, 18 h. Yield was determined by ¹H NMR analysis using 1,1,2,2-tetrachloroethane as an internal standard. ^b N.D. = Not Detected.

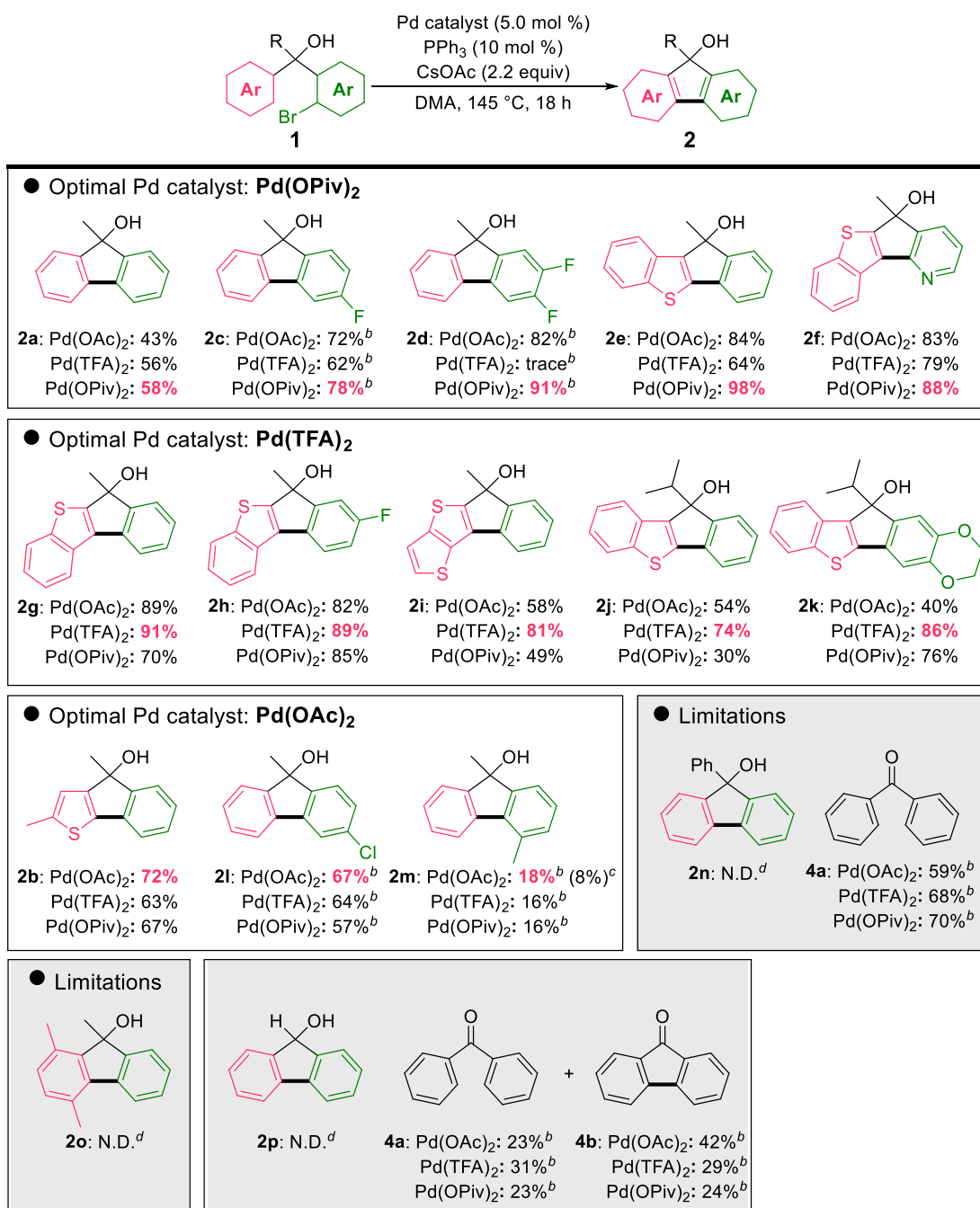
2-4. Substrate Scope

The author next investigated the substrate scope for the selective synthesis of FOLs using various tertiary alcohols **1** by Pd-catalyzed intramolecular cyclization (Scheme 3).

The reaction proceeded on both electron-rich and electron-deficient substrates, and the desired product **2** was obtained with high generality and good yield. Furthermore, this reaction can be applied to the synthesis of various heteroring-fused FOLs. The formation of chromene **3** was not confirmed from any of the substrates. Pd(OPiv)₂ tended to be the optimal catalyst for substrates having electron-withdrawing substituents or aromatic rings. As the number of fluorine atoms increased, the yield of the corresponding FOL also increased (**2a**, **2c** and **2d**). A substrate bearing a pyridine **1f** was also applicable, and **2f** was obtained in a high yield (85%). In the case of substrates having electron-rich substituents or aromatic rings, Pd(TFA)₂ tended to be the optimal catalyst (**2g–k**). Even if substrates had an isopropyl group at the 9-position, the reaction proceeded (**2j** and **2k**). Pd(OAc)₂ was the optimal catalyst with several substrates (**2b**, **2l** and **2m**). This reaction is influenced by the steric hindrance of the substrate. For example, the reaction was strongly inhibited by a methyl group at the 1- or 5,8-positions (**2m** and **2o**). From **1n** bearing a Ph group at the 9-position, the corresponding product **2n** was not observed, and diphenylmethanone **4a** was obtained as a major product. With **1p** having no substituent at the 9-position, the corresponding product **2p** was not obtained, and **4a** and 9-fluorenone **4b** were obtained.⁷

Chapter 2. Synthesis of Heteroring-Fused Fluoreneol via Selective Intramolecular C–H Functionalization

Scheme 3. Substrate scope for the selective synthesis of FOLs^a



^a Reaction conditions: **1a** (0.20 mmol), Pd catalyst (5.0 mol %), PPh₃ (10 mol %), base (2.2 equiv), DMA (0.4 mL) at 145 °C, 18 h. Yield was determined by ¹H NMR analysis using 1,1,2,2-tetrachloroethane as an internal standard. ^b Dppf (5.0 mol %) instead of PPh₃. ^c PPh₃ was used as ligand. ^d N.D. = Not Detected.

2-5. Plausible Reaction Mechanism

A plausible reaction mechanism for the selective synthesis of FOLs is described in Figure 2. The phosphine ligand reduces the Pd^{II} species to Pd⁰ species. Oxidative addition of the C–Br bond of **1** to the Pd⁰ species would generate intermediate **1-Pd**. The aryl C–H is selectively activated to produce the palladacycle **B**. Reductive elimination from the palladacycle **B** forms the target product (FOL) and regenerates Pd⁰ species. Experimental results suggest that **1-Pd** forms Palladacycle **A** when Cs₂CO₃ is used, and Palladacycle **B** is kinetically formed preferentially when CsOAc is used (Table 1, entries 1 and 2). An excessive amount of acetate anion that was supplied to the reaction system should promote intramolecular cyclization. The formation of this palladacycle species is also influenced by the steric and electronic states of the substituents. For example, the formation of the palladacycle **B** is inhibited by substituents with steric hindrance (Scheme 3, **2m** and **2n**). In the case of a substrate bearing a Ph group at the 9-position, diphenylmethanone **4a** was obtained by β-aryl elimination, which means that this equilibrium is biased towards the palladacycle **A**.⁸

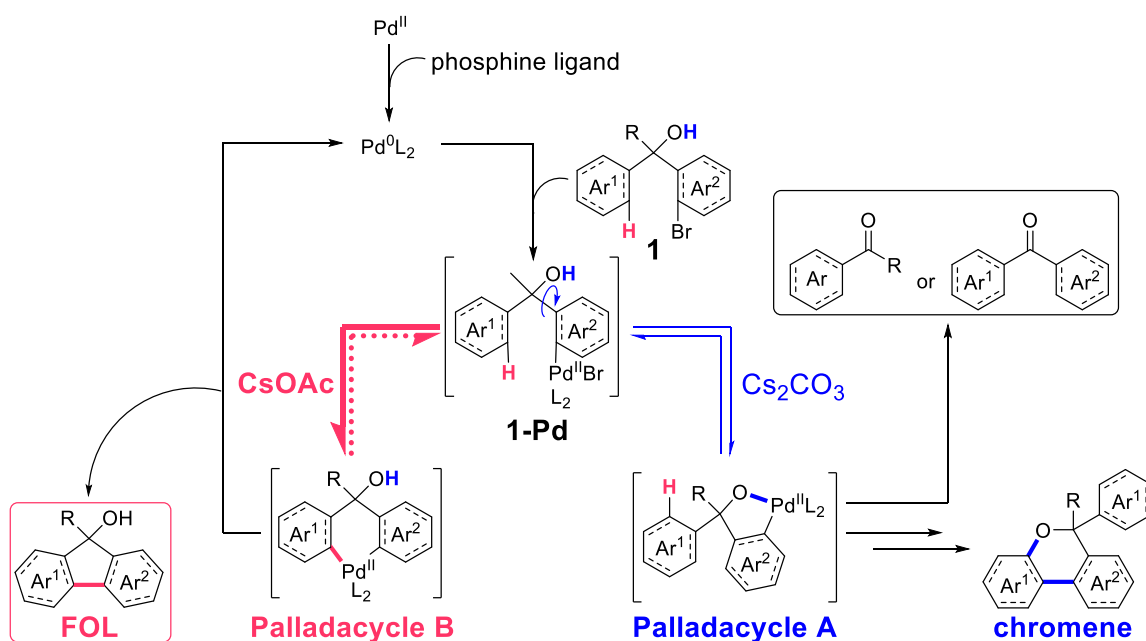
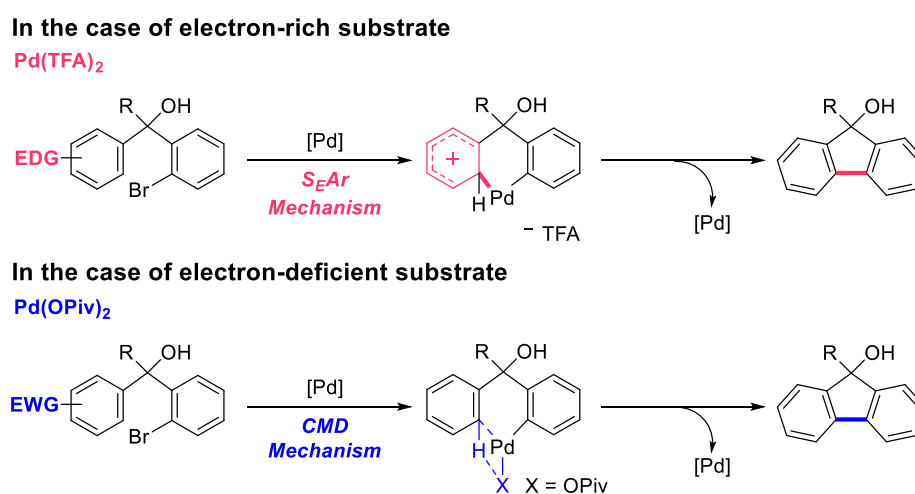


Figure 2. Plausible reaction mechanism

The author describes as shown in Scheme 4 the plausible reason why the optimal catalyst depends on the electronic state of the substrate. In this reaction, two reaction pathways the electrophilic aromatic substitution (S_{EAr}) mechanism and concerted metalation–deprotonation (CMD) mechanism compete. For electron-rich substrates, intramolecular cyclization via the S_{EAr} mechanism would be favored.⁹ Thus, Pd(TFA)₂ with an electron-deficient counter anion is the optimal catalyst for these substrates. Meanwhile, CMD mechanism is favored in electron-deficient substrates.¹⁰ Therefore, Pd(TFA)₂ is not the optimal catalyst, and Pd(OPiv)₂ with a bulky counter anion that promotes reductive elimination, was the optimal catalyst.¹¹

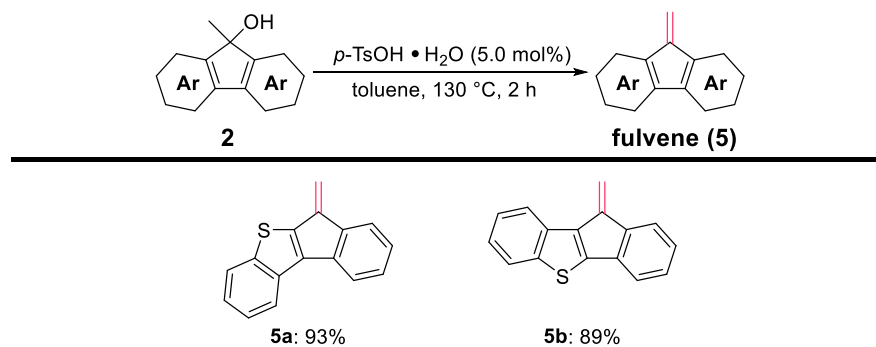
Scheme 4. Plausible reaction pathways



2-6. Application

As for the utility of this method, thus-obtained FOLs were converted to heteroring-fused fulvenes. Treatment of **2** with a catalytic amount of *p*-TsOH facilitated smooth dehydration to produce fulvene **5** (Scheme 5).¹²

Scheme 5. Further transformation of FOLs to fulvenes



^a Reaction conditions: **2** (0.2 mmol), *p*-TsOH·H₂O (5.0 mol %), toluene (10 mL) at 130 °C, 2 h.

2-7. Conclusion

In conclusion, the selective synthesis of FOLs has been developed by the Pd-catalyzed intramolecular cyclization. This reaction is uniquely suited for the synthesis of heteroring-fused FOLs, which are difficult to synthesize by conventional methods. The FOLs also provided rapid access to fulvenes.

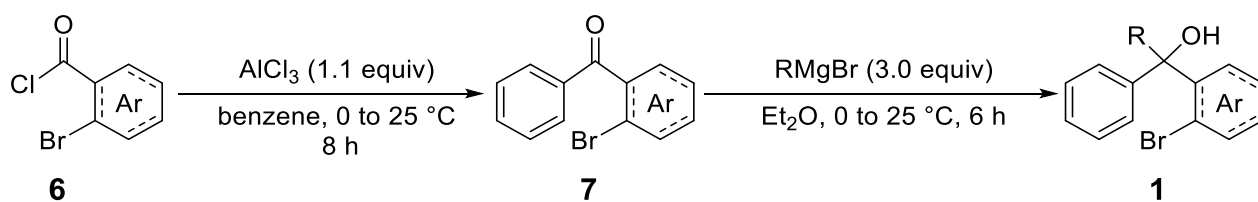
2-8. Experimental Section and Analytical Data

General

Nuclear magnetic resonance (NMR) spectra were recorded on Varian 600 System (^1H 600 MHz, ^{13}C 150 MHz), JEOL JNM-ECZ600R (^1H 600 MHz, ^{13}C 150 MHz), Varian 400-MR (^1H 400 MHz, ^{13}C 100 MHz) and JEOL JNM-ECS400 (^1H 400 MHz, ^{13}C 100 MHz) spectrometers. Chemical shifts for ^1H NMR are expressed in parts per million (ppm) relative to residual CHCl_3 in CDCl_3 (δ 7.26 ppm) or residual C_6HD_5 in C_6D_6 (δ 7.15 ppm). Chemical shifts for ^{13}C NMR are expressed in ppm relative to CDCl_3 (δ 77.0 ppm) or C_6D_6 (δ 128.0 ppm). IR spectra were recorded on a SHIMADZU IRAffinity-1 spectrophotometer. Analytic thin layer chromatography (TLC) was performed on Merck, pre-coated plate silica gel 60 F₂₅₄ (0.25 mm thickness). Column chromatography was performed on KANTO CHEMICAL silica gel 60N (40–50 μm). Unless otherwise noted, all materials were obtained from commercial suppliers and used without further purification. High-resolution mass spectrometry was performed on JEOL JMS-700 MStation (FAB-MS). Dry tetrahydrofuran (THF) and dry diethyl ether (Et_2O) were purchased from Wako pure chemical industries. *N,N*-Dimethylacetamide (DMA), *N,N*-dimethylformamide (DMF), toluene and 1,4-dioxane were dried over MS4A. All reactions were performed under argon atmosphere. 1-(2-Bromophenyl)-1-phenylethan-1-ol (**1a**), (2-bromophenyl)diphenylmethanol (**1n**), and (2-bromophenyl)phenylmethanol (**1p**) were synthesized according to the literatures.^{6b,13}

1. Synthesis of Starting Materials

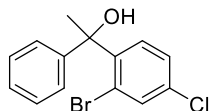
General Procedure A



To a solution of 2-bromobenzoyl chloride derivative **6** (10 mmol) in benzene (20 mL) was added AlCl_3 (1.1 equiv) at 0 °C. After being stirred for a few minutes, the reaction mixture was warmed to 25 °C and stirred for 8 h. Into the resulting mixture were added H_2O (20 mL) and saturated NaCl aq (10 mL), and the mixture was extracted with Et_2O (3×40 mL). The combined organic phase was dried over magnesium sulfate, filtered, and concentrated under reduced pressure. The residue was dissolved into Et_2O (20 mL) and RMgBr (3.0 equiv) was added dropwise to the solution at 0 °C. After being stirred for a few minutes, the reaction mixture was warmed to 25 °C and stirred for 6 h. Into the resulting mixture were added H_2O (20 mL) and HCl aq (1.0 M, 10 mL), and the mixture was extracted with Et_2O (3×40 mL). The combined organic phase was dried over magnesium sulfate,

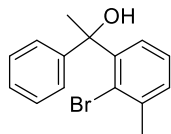
filtered, and concentrated under reduced pressure. The residue was purified by column chromatography on silica gel eluting with *n*-hexane/CHCl₃.

1-(2-Bromo-4-chlorophenyl)-1-phenylethan-1-ol (**1l**)



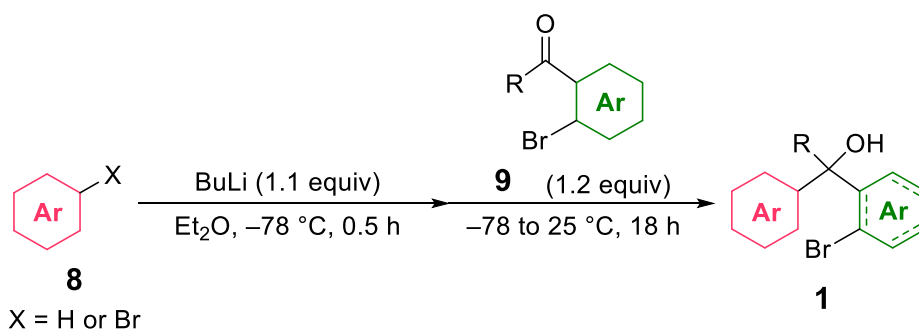
Prepared according to the general procedure A from 2-bromo-4-chlorobenzoyl chloride **6c** (2.54 g, 10 mmol), AlCl₃ (1.47 g, 11 mmol) and MeMgBr (3.0 M in Et₂O, 10 mL, 30 mmol). The product **1l** was purified by chromatography on silica gel eluting with *n*-hexane/CHCl₃ (2/1) and obtained as a colorless liquid (2.65 g, 8.5 mmol, 85%); ¹H NMR (600 MHz, CDCl₃) δ 1.96 (s, 3H), 3.21 (brs, 1H), 7.23–7.33 (m, 5H), 7.38 (d, *J* = 8.4 Hz, 1H), 7.55 (s, 1H), 7.80 (d, *J* = 8.4 Hz, 1H); ¹³C NMR (150 MHz, CDCl₃) δ 29.6, 122.4, 125.6, 127.1, 127.3, 128.1, 128.2, 129.1, 133.8, 134.2, 143.8, 146.7; IR(neat) 3564, 3061, 1601, 1489, 766 cm⁻¹; HRMS (FAB+) *m/z* calcd for C₁₄H₁₃⁷⁹BrClO [M+H]⁺ 310.9832, found 310.9847.

1-(2-Bromo-3-methylphenyl)-1-phenylethan-1-ol (**1m**)



Prepared according to the general procedure A from 2-bromo-3-methylbenzoyl chloride **6d** (2.33 g, 10 mmol), AlCl₃ (1.47 g, 11 mmol) and MeMgBr (3.0 M in Et₂O, 10 mL, 30 mmol). The product **1m** was purified by chromatography on silica gel eluting with *n*-hexane/CHCl₃ (2/1) and obtained as a colorless liquid (2.30 g, 7.9 mmol, 79%); ¹H NMR (600 MHz, CDCl₃) δ 1.95 (s, 3H), 2.37 (s, 3H), 3.78 (brs, 1H), 7.19–7.37 (m, 7H), 7.65 (d, *J* = 7.8 Hz, 1H); ¹³C NMR (150 MHz, CDCl₃) δ 24.2, 30.9, 77.7, 125.0, 125.3, 126.1, 126.5, 126.7, 128.0, 130.2, 139.8, 145.0, 148.0; IR(neat) 3584, 3445, 2980, 1454, 770 cm⁻¹; HRMS (FAB+) *m/z* calcd for C₁₅H₁₅⁷⁹BrO [M]⁺ 290.0300, found 290.0293.

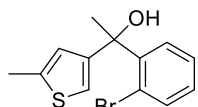
General Procedure B



To a solution of aryl halide or arene **8** (10 mmol) in Et₂O (15 mL) was added dropwise BuLi (11 mmol) at –78 °C. After being stirred for 0.5 h, 2-bromoacetophenone derivative **9** (12 mmol) was added to the solution at the same temperature. After being stirred for a few minutes, the reaction mixture was warmed to 25 °C and stirred for 18 h. Into the resulting mixture were added H₂O (20

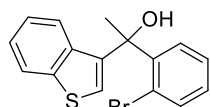
mL) and saturated NH₄Cl aq (10.0 mL), and the mixture was extracted with Et₂O (3 × 40 mL). The combined organic phase was dried over magnesium sulfate, filtered, and concentrated under reduced pressure. The residue was purified by column chromatography on silica gel eluting with *n*-hexane/CHCl₃.

1-(2-Bromo-phenyl)-1-(5-methylthiophene-3-yl)ethan-1-ol (**1b**)



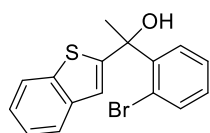
Prepared according to the general procedure B from 4-bromo-2-methylthiophene **8a** (1.77 g, 10 mmol), BuLi (1.58 M, 7.0 mL, 11 mmol) and 2-bromoacetophenone **9a** (2.39 g, 12 mmol). The product **1b** was purified by chromatography on silica gel eluting with *n*-hexane/CHCl₃ (2/1) and obtained as a colorless liquid (2.26 g, 7.6 mmol, 76%); ¹H NMR (400 MHz, CDCl₃) δ 2.00 (s, 3H), 2.43 (s, 3H), 3.26 (brs, 1H), 6.54 (s, 1H), 6.80 (s, 1H), 7.15 (td, *J* = 8.0, 1.2 Hz, 1H), 7.36 (td, *J* = 8.0, 1.2 Hz, 1H), 7.55 (td, *J* = 8.0, 1.2 Hz, 1H), 7.80 (td, *J* = 8.0, 1.2 Hz, 1H); ¹³C NMR (100 MHz, CDCl₃) δ 15.3, 28.9, 75.0, 119.0, 121.9, 124.6, 127.2, 127.77, 127.80, 134.7, 139.9, 144.9, 148.1; IR(neat) 3444, 2978, 2920, 1456, 1018 cm⁻¹; HRMS (FAB⁺) *m/z* calcd for C₁₃H₁₃⁸¹BrOS [M]⁺ 297.9844, found 297.9855.

1-(2-Bromophenyl)-1-(benzo[*b*]thiophene-3-yl)ethan-1-ol (**1e**)



Prepared according to the general procedure B from 3-bromobenzo[*b*]thiophene **8b** (2.13 g, 10 mmol), BuLi (1.58 M, 7.0 mL, 11 mmol) and 2-bromoacetophenone **9a** (2.39 g, 12 mmol). The product **1e** was purified by chromatography on silica gel eluting with *n*-hexane/CHCl₃ (2/1) and obtained as a colorless liquid (3.07 g, 9.2 mmol, 92%); ¹H NMR (400 MHz, CDCl₃) δ 2.15 (s, 3H), 3.70 (brs, 1H), 6.95 (s, 1H), 7.23 (td, *J* = 8.0, 1.4 Hz, 1H), 7.29 (td, *J* = 7.6, 1.2 Hz, 1H), 7.32 (td, *J* = 8.0, 1.4 Hz, 1H), 7.42 (t, *J* = 7.6 Hz, 1H), 7.59 (d, *J* = 8.0 Hz, 1H), 7.65 (d, *J* = 7.6 Hz, 1H), 7.78 (d, *J* = 7.6 Hz, 1H), 7.84 (dd, *J* = 8.0, 1.4 Hz, 1H); ¹³C NMR (100 MHz, CDCl₃) δ 30.1, 75.7, 120.8, 122.2, 122.3, 123.5, 124.1, 124.2, 127.4, 128.0, 129.5, 134.8, 139.5, 139.6, 143.8, 153.1; IR(neat) 3537, 3447, 3057, 2361, 1018 cm⁻¹; HRMS (APCI⁺) *m/z* calcd for C₁₆H₁₃⁷⁹BrOS [M]⁺ 331.9865, found 331.9834.

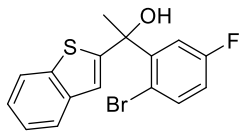
1-(2-Bromophenyl)-1-(benzo[*b*]thiophene-2-yl)ethan-1-ol (**1g**)



Prepared according to the general procedure B from benzo[*b*]thiophene **8c** (1.34 g, 10 mmol), BuLi (1.58 M, 7.0 mL, 11 mmol) and 2-bromoacetophenone **9a** (2.39 g, 12 mmol). The product **1g** was purified by chromatography on silica gel eluting with *n*-hexane/CHCl₃ (2/1) and obtained as a colorless liquid (2.93 g, 8.8 mmol, 88%); ¹H NMR (400 MHz, CDCl₃) δ 2.30 (s, 3H), 4.04 (brs, 1H), 7.12 (s, 1H), 7.29 (t, *J* = 7.6 Hz, 1H), 7.35–7.55 (m, 3H), 7.69 (d, *J* = 7.8 Hz, 1H), 7.76 (d, *J* = 7.6 Hz, 1H), 7.89 (d, *J* = 7.6 Hz, 1H), 7.99 (d, *J* = 7.8 Hz, 1H);

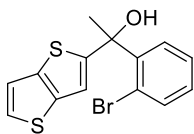
^{13}C NMR (100 MHz, CDCl_3) δ 29.7, 75.3, 120.8, 122.0, 122.1, 123.4, 124.0, 127.2, 127.8, 127.9, 129.2, 134.6, 139.30, 139.32, 143.7, 152.6; IR(neat) 3545, 3443, 3034, 1433, 727 cm^{-1} ; HRMS (FAB+) m/z calcd for $\text{C}_{16}\text{H}_{14}^{81}\text{BrOS}$ $[\text{M}+\text{H}]^+$ 334.9922, found 334.9934.

1-(2-Bromo-5-fluoro-phenyl)-1-(benzo[*b*]thiophene-2-yl)ethan-1-ol (**1h**)



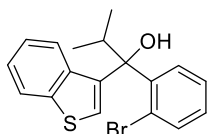
Prepared according to the general procedure B from benzo[*b*]thiophene **8c** (1.34 g, 10 mmol), BuLi (1.58 M, 7.0 mL, 11 mmol) and 2-bromo-5-fluoroacetophenone **9b** (2.85 g, 12 mmol). The product **1h** was purified by chromatography on silica gel eluting with *n*-hexane/ CHCl_3 (2/1) and obtained as a colorless liquid (2.74 g, 7.8 mmol, 78%); ^1H NMR (400 MHz, CDCl_3) δ 2.19 (s, 3H), 3.61 (brs, 1H), 6.96 (ddt, $J = 8.3, 2.7$ Hz, $J_{\text{H-F}} = 8.3$ Hz, 1H), 7.07 (s, 1H), 7.34 (dt, $J = 7.5, 1.5$ Hz, 1H), 7.38 (dt, $J = 7.5, 1.5$ Hz, 1H), 7.53 (dd, $J = 8.3$ Hz, $J_{\text{H-F}} = 5.4$ Hz, 1H), 7.71 (dd, $J = 7.5, 1.5$ Hz, 1H), 7.75 (dd, $J = 3.0$ Hz, $J_{\text{H-F}} = 10.2$ Hz, 1H), 7.82 (dd, $J = 7.5, 1.5$ Hz, 1H); ^{13}C NMR (100 MHz, CDCl_3) δ 29.1, 75.0, 115.4, 115.7, 115.9 (d, $J_{\text{C-F}} = 2.9$ Hz), 116.1, 116.3, 121.2, 122.3, 123.6, 124.3 (d, $J_{\text{C-F}} = 5.7$ Hz), 135.9 (d, $J_{\text{C-F}} = 7.6$ Hz), 139.4 (d, $J_{\text{C-F}} = 10.5$ Hz), 146.4 (d, $J_{\text{C-F}} = 3.7$ Hz), 151.5, 161.7 (d, $J_{\text{C-F}} = 246.3$ Hz); IR(neat) 3537, 3441, 3057, 1458, 746 cm^{-1} ; HRMS (FAB+) m/z calcd for $\text{C}_{16}\text{H}_{13}^{81}\text{BrFOS}$ $[\text{M}+\text{H}]^+$ 352.9828, found 352.9838.

1-(2-Bromophenyl)-1-(thieno[3,2-*b*]thiophene-2-yl)ethan-1-ol (**1i**)



Prepared according to the general procedure B from thieno[3,2-*b*]thiophene **8d** (1.40 g, 10 mmol), BuLi (1.58 M, 7.0 mL, 11 mmol) and 2-bromoacetophenone **9a** (2.39 g, 12 mmol). The product **1i** was purified by chromatography on silica gel eluting with *n*-hexane/ CHCl_3 (2/1) and obtained as a colorless liquid (2.48 g, 7.3 mmol, 73%); ^1H NMR (400 MHz, CDCl_3) δ 2.19 (s, 3H), 3.65 (brs, 1H), 6.97 (s, 1H), 7.206 (d, $J = 8.0$ Hz, 1H), 7.209 (t, $J = 8.0$ Hz, 1H), 7.32 (d, $J = 8.0$ Hz, 1H), 7.40 (td, $J = 8.0, 1.2$ Hz, 1H), 7.61 (dd, $J = 8.0, 1.2$ Hz, 1H), 7.91 (dd, $J = 8.0, 1.2$ Hz, 1H); ^{13}C NMR (100 MHz, CDCl_3) δ 29.8, 75.5, 116.7, 119.4, 122.0, 126.5, 127.2, 127.9, 129.2, 134.7, 138.2, 138.3, 143.8, 154.3; IR(neat) 3554, 3084, 3055, 1464, 760 cm^{-1} ; HRMS (FAB+) m/z calcd for $\text{C}_{14}\text{H}_{11}^{81}\text{BrOS}_2$ $[\text{M}]^+$ 339.9408, found 339.9394.

1-(2-Bromophenyl)-1-(benzo[*b*]thiophene-3-yl)-2-methylpropan-1-ol (**1j**)



Prepared according to the general procedure B from 3-bromobenzo[*b*]thiophene **8b** (2.13 g, 10 mmol), BuLi (1.58 M, 7.0 mL, 11 mmol) and 2'-bromo-2-methylpropiophenone **9c** (2.73 g, 12 mmol). The product **1j** was purified by chromatography on silica gel eluting with *n*-hexane/ CHCl_3 (2/1) and obtained as a colorless liquid (2.57 g, 7.1 mmol, 71%); ^1H NMR (400 MHz, CDCl_3) δ 1.04 (d, $J = 6.8$ Hz, 3H), 1.18 (d, $J = 6.8$ Hz,

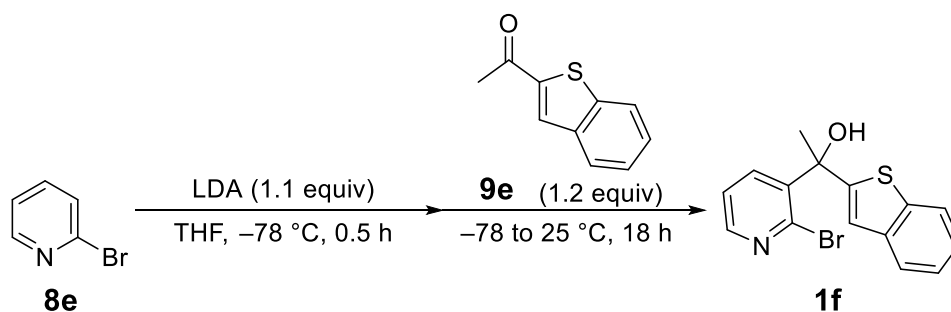
3H), 3.33 (sept, $J = 6.8$ Hz, 1H), 3.60 (s, 1H), 7.18 (td, $J = 7.8, 1.7$ Hz, 1H), 7.298 (td, $J = 7.8, 1.7$ Hz, 1H), 7.304 (s, 1H), 7.35 (td, $J = 7.6, 1.4$ Hz, 1H), 7.43 (td, $J = 7.6, 1.4$ Hz, 1H), 7.57 (dd, $J = 7.8, 1.7$ Hz, 1H), 7.73 (d, $J = 7.6$ Hz, 1H), 7.76 (d, $J = 7.8$ Hz, 1H), 7.95 (dd, $J = 7.6, 1.4$ Hz, 1H); ^{13}C NMR (100 MHz, CDCl_3) δ 18.0, 34.7, 80.4, 121.9, 122.06, 122.08, 123.5, 124.0, 124.1, 127.2, 128.6, 128.9, 135.3, 139.2, 139.6, 143.2, 150.8; IR(neat) 3545, 2972, 2342, 1022, 748 cm^{-1} ; HRMS (FAB+) m/z calcd for $\text{C}_{18}\text{H}_{17}^{81}\text{BrOS}$ $[\text{M}]^+$ 362.0157, found 362.0151.

1-(7-Bromo-2,3-dihydrobenzo[*b*][1,4]dioxin-6-yl)-1-(benzo[*b*]thiophen-3-yl)-2-methylpropan-1-ol (**1k**)



Prepared according to the general procedure B from 3-bromobenzo[*b*]thiophene **8b** (0.64 g, 3 mmol), BuLi (1.58 M, 2.08 mL, 3.3 mmol) and 1-(7-bromo-2,3-dihydrobenzo[*b*][1,4]dioxin-6-yl)-2-methylpropan-1-one **9d** (1.03 g, 3.6 mmol). The product **1k** was purified by chromatography on silica gel eluting with *n*-hexane/ CHCl_3 (1/1) and obtained as a colorless liquid (0.98 g, 2.34 mmol, 78%); ^1H NMR (400 MHz, CDCl_3) δ 0.95 (d, $J = 6.8$ Hz, 3H), 1.15 (d, $J = 6.8$ Hz, 3H), 2.83 (brs, 1H), 3.29 (sept, $J = 6.8$ Hz, 1H), 4.21–4.33 (m, 4H), 6.96 (s, 1H), 7.18 (t, $J = 7.1$ Hz, 1H), 7.23 (t, $J = 7.1$ Hz, 1H), 7.48 (s, 1H), 7.64 (s, 1H), 7.79 (d, $J = 7.1$ Hz, 1H), 7.80 (d, $J = 7.1$ Hz, 1H); ^{13}C NMR (150 MHz, CDCl_3) δ 17.9 and 18.2 (rotamer), 33.4, 64.17, 64.21, 79.5, 111.4, 117.9, 122.53, 123.1, 123.58, 123.61, 124.6, 126.3, 135.5, 137.0, 137.8, 140.3, 142.1, 142.6; IR(KBr) 3545, 2974, 1481, 1069, 673 cm^{-1} ; HRMS (FAB+) m/z calcd for $\text{C}_{20}\text{H}_{20}^{81}\text{BrO}_3\text{S}$ $[\text{M}]^+$ 421.0290, found 421.0283; mp 152.2–152.7 $^\circ\text{C}$.

1-(2-Bromopyridin-3-yl)-1-(benzo[*b*]thiophen-2-yl)-ethan-1-ol (**1f**)



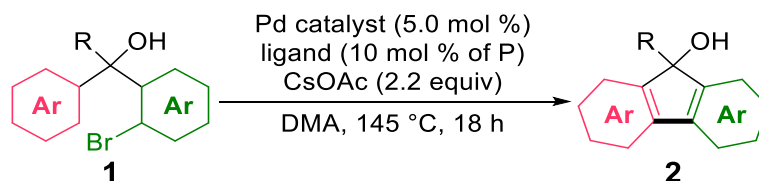
To a solution of *i*-Pr₂NH (1.69 mL, 12 mmol) in THF was added dropwise BuLi (1.58 M, 7.0 mL, 11 mmol) at 0 $^\circ\text{C}$. After being stirred for 0.5 h, 2-bromopyridine **8e** (1.58 g, 10 mmol) was added to the solution at -78 $^\circ\text{C}$. After being stirred for 0.5 h, 1-(benzo[*b*]thiophen-2-yl)ethan-1-one **9e** (2.11 g, 12 mmol) was added to the same temperature. After being stirred for a few minutes, the reaction mixture was warmed to 25 $^\circ\text{C}$ and stirred for 18 h. Into the resulting mixture were added H₂O (20 mL), saturated NH₄Cl aq (10 mL), and the mixture was extracted with Et₂O (3 \times 40 mL). The combined

Chapter 2. Synthesis of Heteroring-Fused Fluorenol via Selective Intramolecular C–H Functionalization

organic phase was dried over magnesium sulfate, filtered, and concentrated under reduced pressure. The residue was purified by column chromatography on silica gel eluting with *n*-hexane/CHCl₃ (1/5) to give 1-(2-bromopyridin-3-yl)-1-(benzo[*b*]thiophen-2-yl)-ethan-1-ol **1f** as colorless oil (2.97g, 8.9 mmol, 89%); ¹H NMR (400 MHz, CDCl₃) δ 2.18 (s, 3H), 3.54 (brs, 1H), 7.04 (s, 1H), 7.30–7.41 (m, 3H), 7.68 (dd, *J* = 7.3, 1.6 Hz, 1H), 7.78 (dd, *J* = 7.3, 1.6 Hz, 1H), 8.18 (dd, *J* = 8.0, 0.8 Hz, 1H), 8.30–8.39 (m, 1H); ¹³C NMR (150 MHz, CDCl₃) δ 29.3, 74.4, 121.4, 122.4, 122.7, 123.7, 124.5, 124.6, 136.5, 139.4, 139.6, 141.6, 141.7, 149.0, 151.4; IR(neat) 3298, 3055, 3034, 1393, 744 cm⁻¹; HRMS (FAB+) *m/z* calcd for C₁₅H₁₂⁷⁹BrNOS [M]⁺ 332.9817, found 332.9819.

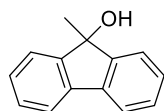
2. Selective Synthesis of FOL

General Procedure



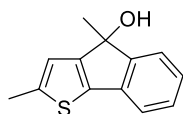
To a solution of tertiary alcohol **1** (1.5 mmol) in DMA (3.0 mL) were added CsOAc (3.3 mmol), ligand (10 mol % of P) and Pd catalyst (0.075 mmol). The mixture was warmed up to 145 °C and stirred for 18 h. After being allowed to cool to 25 °C, Pd catalyst and base was removed by short pass. Then, the residue was concentrated under reduced pressure. The residue was purified by column chromatography on silica gel eluting with *n*-hexane/CHCl₃.

9-Methyl-9H-fluorene-9-ol (**2a**)



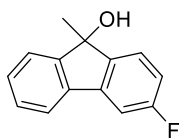
Prepared according to the general procedure from 1-(2-bromophenyl)-1-phenylethan-1-ol **1a** (416 mg, 1.5 mmol), CsOAc (633 mg, 3.3 mmol), dppf (41.6 mg, 0.075 mmol) and Pd(OPiv)₂ (23.3 mg, 0.075 mmol). The product **2a** was purified by chromatography on silica gel eluting with *n*-hexane/CHCl₃ (2/1) and obtained as a colorless solid (200 mg, 1.02 mmol, 68%); ¹H NMR (400 MHz, CDCl₃) δ 1.73 (s, 3H), 2.04 (brs, 1H), 7.31 (td, *J* = 7.6, 1.0 Hz, 2H), 7.36 (td, *J* = 7.6, 1.0 Hz, 2H), 7.48 (d, *J* = 7.6 Hz, 2H), 7.62 (d, *J* = 7.6 Hz, 2H); ¹³C NMR (100 MHz, CDCl₃) δ 26.0, 79.6, 120.0, 123.2, 128.0, 128.9, 138.7, 149.8; IR(KBr) 3308, 3082, 3048, 1092, 673 cm⁻¹; HRMS (FAB+) *m/z* calcd for C₁₄H₁₂O [M]⁺ 196.0882, found 196.0891; mp 173.2–174.0 °C.

2,4-Dimethyl-4H-indeno[1,2-*b*]thiophene-4-ol (**2b**)



Prepared according to the general procedure from 1-(2-bromo-phenyl)-1-(5-methylthiophene-3-yl)ethan-1-ol **1b** (445 mg, 1.5 mmol), CsOAc (633 mg, 3.3 mmol), PPh₃ (39.3 mg, 0.15 mmol) and Pd(Oac)₂ (17.3 mg, 0.075 mmol). The product **2b** was purified by chromatography on silica gel eluting with *n*-hexane/CHCl₃ (2/1) and obtained as a colorless solid (234 mg, 1.08 mmol, 72%); ¹H NMR (400 MHz, CDCl₃) δ 1.70 (s, 3H), 1.77 (brs, 1H), 2.54 (d, *J* = 1.0 Hz, 3H), 6.80 (d, *J* = 1.0 Hz, 1H), 7.16 (dt, *J* = 7.2, 1.8 Hz, 1H), 7.20–7.29 (m, 2H), 7.43 (d, *J* = 7.2 Hz, 1H); ¹³C NMR (150 MHz, C₆D₆) δ 15.9, 25.3, 77.7, 118.5, 120.1, 123.0, 125.8, 128.8, 136.8, 139.2, 143.6, 153.0, 155.5; IR(KBr) 3341, 3333, 2922, 1402, 756 cm⁻¹; HRMS (FAB+) *m/z* calcd for C₁₃H₁₃OS [M+H]⁺ 217.0681, found 217.0680; mp 184.5–185.2 °C.

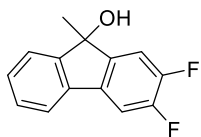
3-Fluoro-9-methyl-9H-fluorene-9-ol (**2c**)



Prepared according to the general procedure from 1-(2-bromo-4-fluorophenyl)-1-phenylethan-1-ol **1c** (443 mg, 1.5 mmol), CsOAc (633 mg, 3.3 mmol), dppf (41.6 mg, 0.075 mmol) and Pd(OPiv)₂ (23.3 mg, 0.075 mmol). The product **2c** was purified

by chromatography on silica gel eluting with *n*-hexane/CHCl₃ (2/1), GPC (toluene) and obtained as a colorless solid (247 mg, 1.16 mmol, 77%); ¹H NMR (400 MHz, CDCl₃) δ 1.69 (s, 3H), 2.02 (brs, 1H), 6.97 (ddt, *J* = 8.8, 1.3 Hz, *J*_{H-F} = 8.8 Hz, 1H), 7.26 (dd, *J* = 1.3 Hz, *J*_{H-F} = 8.8 Hz, 1H), 7.33 (dt, *J* = 6.8, 1.6 Hz, 1H), 7.37 (dt, *J* = 6.8, 1.6 Hz, 1H), 7.45 (dd, *J* = 8.0 Hz, *J*_{H-F} = 5.2 Hz, 1H), 7.52 (d, *J* = 6.8 Hz, 1H), 7.56 (d, *J* = 6.8 Hz, 1H); ¹³C NMR (100 MHz, CDCl₃) δ 26.1, 79.1, 107.2 (d, *J*_{C-F} = 23.9 Hz), 114.5 (d, *J*_{C-F} = 22.9 Hz), 120.2, 123.3, 124.5 (d, *J*_{C-F} = 8.6 Hz), 128.6, 129.0, 137.7 (d, *J*_{C-F} = 2.9 Hz), 141.0 (d, *J*_{C-F} = 8.6 Hz), 145.4 (d, *J*_{C-F} = 2.8 Hz), 150.6, 163.8 (d, *J*_{C-F} = 245.4 Hz); IR(KBr) 3308, 3053, 2978, 1487, 739 cm⁻¹; HRMS (FAB+) *m/z* calcd for C₁₄H₁₂FO [M+H]⁺ 215.0866, found 215.0859; mp 208.7–209.4 °C.

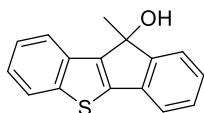
2,3-Difluoro-9-methyl-9H-fluorene-9-ol (2d)



Prepared according to the general procedure from 1-(2-bromo-4,5-difluorophenyl)-1-phenylethan-1-ol **1d** (470 mg, 1.5 mmol), CsOAc (633 mg, 3.3 mmol), dppf (41.6 mg, 0.075 mmol) and Pd(OPiv)₂ (23.3 mg, 0.075 mmol). The product **2d** was

purified by chromatography on silica gel eluting with *n*-hexane/CHCl₃ (2/1) and obtained as a colorless solid (314 mg, 1.35 mmol, 90%); ¹H NMR (400 MHz, CDCl₃) δ 1.70 (s, 3H), 1.85 (brs, 1H), 7.29–7.42 (m, 4H), 7.52 (d, *J* = 5.6 Hz, 1H), 7.54 (d, *J* = 5.6 Hz, 1H); ¹³C NMR (150 MHz, CDCl₃) δ 26.0, 79.2, 108.8 (d, *J*_{C-F} = 18.6 Hz), 112.6 (d, *J*_{C-F} = 18.8 Hz), 119.9, 123.2, 128.2, 129.2, 134.9 (dd, *J*_{C-F} = 7.2, 2.9 Hz), 137.0, 145.9 (d, *J*_{C-F} = 2.9 Hz), 149.8, 150.4 (dd, *J*_{C-F} = 245.6, 11.6 Hz), 151.2 (dd, *J*_{C-F} = 249.2, 16.5 Hz); IR(KBr) 3321, 3048, 2980, 1495, 768 cm⁻¹; HRMS (FAB+) *m/z* calcd for C₁₄H₁₁F₂O [M+H]⁺ 233.0772, found 233.0761; mp 245.3–246.1 °C.

10-Methyl-10H-benzo[*b*]indeno[2,1-*d*]thiophene-10-ol (2e)

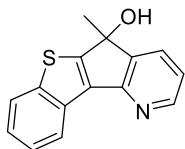


Prepared according to the general procedure from 1-(2-bromophenyl)-1-phenylethan-1-ol **1e** (500 mg, 1.5 mmol), CsOAc (633 mg, 3.3 mmol), PPh₃ (39.3 mg, 0.15 mmol) and Pd(OPiv)₂ (23.3 mg, 0.075 mmol). The

product **2e** was purified by chromatography on silica gel eluting with *n*-hexane/CHCl₃ (2/1) and obtained as a colorless solid (371 mg, 1.47 mmol, 98%); ¹H NMR (400 MHz, CDCl₃) δ 1.71 (brs, 1H), 1.89 (s, 1H), 7.29 (t, *J* = 8.0 Hz, 1H), 7.33 (t, *J* = 8.0 Hz, 1H), 7.35 (t, *J* = 7.2 Hz, 1H), 7.40 (d, *J* = 7.2 Hz, 1H), 7.43 (t, *J* = 7.2 Hz, 1H), 7.55 (d, *J* = 7.2 Hz, 1H), 7.88 (d, *J* = 8.0 Hz, 1H), 7.96 (d, *J* = 8.0 Hz, 1H); ¹³C NMR (100 MHz, CDCl₃) δ 24.4, 78.4, 119.9, 121.8, 122.5, 123.9, 124.1, 125.0,

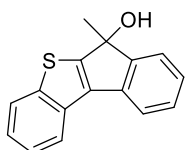
127.0, 128.9, 133.6, 135.9, 142.3, 144.4, 147.0, 153.6; IR(KBr) 3304, 2967, 2924, 1422, 746 cm^{-1} ; HRMS (FAB+) m/z calcd for $\text{C}_{16}\text{H}_{13}\text{OS}$ $[\text{M}+\text{H}]^+$ 253.0681, found 253.0693; mp >300 °C.

5-Methyl-5H-benzo[4',5']thieno[2',3':4,5]cyclopenta[1,2-b]pyridin-5-ol (2f)



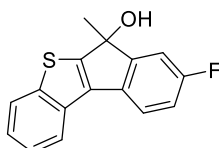
Prepared according to the general procedure from 1-(2-bromopyridin-3-yl)-1-(benzo[*b*]thiophen-2-yl)-ethan-1-ol **1f** (501 mg, 1.5 mmol), CsOAc (633 mg, 3.3 mmol), PPh_3 (39.3 mg, 0.15 mmol) and $\text{Pd}(\text{OPiv})_2$ (23.3 mg, 0.075 mmol). The product **2f** was purified by chromatography on silica gel eluting with *n*-hexane/ CHCl_3 (1/5) and obtained as a colorless solid (324 mg, 1.28 mmol, 85%); ^1H NMR (400 MHz, CDCl_3) δ 1.70 (s, 3H), 4.44 (brs, 1H), 6.33 (dd, $J = 7.2, 4.8$ Hz, 1H), 7.19 (d, $J = 7.2$ Hz, 1H), 7.36 (t, $J = 7.8$ Hz, 1H), 7.45 (t, $J = 7.8$ Hz, 1H), 7.79 (d, $J = 7.8$ Hz, 1H), 7.99 (dd, $J = 7.2, 4.8$ Hz, 1H), 8.20 (d, $J = 7.8$ Hz, 1H); ^{13}C NMR (150 MHz, CDCl_3) δ 25.3, 76.6, 119.1, 123.5, 123.7, 125.0, 125.2, 129.6, 132.1, 137.3, 144.7, 146.7, 148.4, 156.4, 157.9; IR(KBr) 3240, 3061, 2972, 2359, 937 cm^{-1} ; HRMS (FAB+) m/z calcd for $\text{C}_{15}\text{H}_{12}\text{NOS}$ $[\text{M}+\text{H}]^+$ 254.0634, found 254.0625; mp >300 °C.

6-Methyl-6H-benzo[*b*]indeno[1,2-*d*]thiophen-6-ol (2g)



Prepared according to the general procedure from 1-(2-bromophenyl)-1-(benzo[*b*]thiophene-2-yl)ethan-1-ol **1g** (500 mg, 1.5 mmol), CsOAc (633 mg, 3.3 mmol), PPh_3 (39.3 mg, 0.15 mmol) and $\text{Pd}(\text{TFA})_2$ (24.0 mg, 0.075 mmol). The product **2g** was purified by chromatography on silica gel eluting with *n*-hexane/ CHCl_3 (2/1) and obtained as a colorless solid (344 mg, 1.37 mmol, 91%); ^1H NMR (400 MHz, CDCl_3) δ 1.76 (s, 3H), 2.46 (brs, 1H), 7.19 (t, $J = 7.6$ Hz, 1H), 7.33 (t, $J = 8.0$ Hz, 1H), 7.38 (d, $J = 7.6$ Hz, 1H), 7.43 (t, $J = 8.0$ Hz, 1H), 7.47 (t, $J = 7.6$ Hz, 1H), 7.61 (d, $J = 7.6$ Hz, 1H), 7.86 (d, $J = 8.0$ Hz, 1H), 8.04 (d, $J = 8.0$ Hz, 1H); ^{13}C NMR (100 MHz, CDCl_3) δ 26.0, 78.7, 119.2, 122.3, 122.6, 124.0, 124.4, 124.9, 125.7, 128.7, 132.6, 136.6, 137.5, 145.0, 153.17, 153.20; IR(KBr) 3362, 3048, 1483, 1090, 681 cm^{-1} ; HRMS (FAB+) m/z calcd for $\text{C}_{16}\text{H}_{13}\text{OS}$ $[\text{M}+\text{H}]^+$ 254.0681, found 253.0686; mp >300 °C.

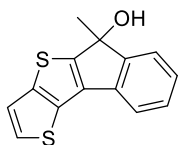
8-Fluoro-6-methyl-6H-benzo[*b*]indeno[1,2-*d*]thiophen-6-ol (2h)



Prepared according to the general procedure from 1-(2-bromo-5-fluorophenyl)-1-(benzo[*b*]thiophene-2-yl)ethan-1-ol **1h** (527 mg, 1.5 mmol), CsOAc (633 mg, 3.3 mmol), PPh_3 (39.3 mg, 0.15 mmol) and $\text{Pd}(\text{TFA})_2$ (24.0 mg, 0.075 mmol). The product **2h** was purified by chromatography on silica gel eluting with *n*-hexane/ CHCl_3 (2/1) and obtained as a colorless solid (464 mg, 1.32 mmol, 88%); ^1H NMR (400 MHz, CDCl_3) δ 1.67 (s, 3H), 2.85 (brs, 1H), 6.99 (t, $J = 8.0$ Hz, 1H), 7.13 (d, $J = 7.2$ Hz, 1H), 7.35 (t, $J = 8.0$ Hz, 1H), 7.40–7.52 (m, 2H), 7.81 (d, $J = 8.0$ Hz, 1H), 7.94 (d, $J = 8.0$ Hz, 1H); ^{13}C NMR (100 MHz, CDCl_3) δ 26.0, 78.4,

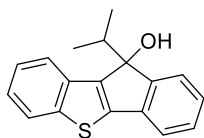
111.1 (d, $J_{C-F} = 23.8$ Hz), 114.8 (d, $J_{C-F} = 22$ Hz), 119.7 (d, $J_{C-F} = 8.6$ Hz), 122.1, 124.0, 124.4, 124.9, 132.2, 132.4 (d, $J_{C-F} = 2.9$ Hz), 136.6, 144.8, 152.3 (d, $J_{C-F} = 2.8$ Hz), 155.5 (d, $J_{C-F} = 6.7$ Hz), 161.6 (d, $J_{C-F} = 244.4$ Hz); IR(KBr) 3356, 3090, 3055, 1260, 673 cm^{-1} ; HRMS (FAB+) m/z calcd for $\text{C}_{16}\text{H}_{12}\text{FOS}$ $[\text{M}+\text{H}]^+$ 271.0587, found 271.0600; mp >300 °C.

5-Methyl-5H-indeno[2,1-b]thieno[2,3-d]thiophen-5-ol (2i)



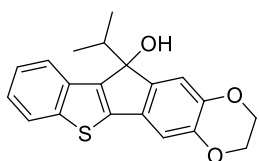
Prepared according to the general procedure from 1-(2-bromophenyl)-1-(thieno[3,2-*b*]thiophene-2-yl)ethan-1-ol **1g** (509 mg, 1.5 mmol), CsOAc (633 mg, 3.3 mmol), PPh_3 (39.3 mg, 0.15 mmol) and $\text{Pd}(\text{TFA})_2$ (24.0 mg, 0.075 mmol). The product **2i** was purified by chromatography on silica gel eluting with *n*-hexane/ CHCl_3 (2/1) and obtained as a colorless solid (312 mg, 1.22 mmol, 81%); ^1H NMR (400 MHz, C_6D_6) δ 1.44 (brs, 1H), 1.64 (s, 3H), 6.83 (d, $J = 5.2$ Hz, 1H), 6.91 (d, $J = 5.2$ Hz, 1H), 6.99 (t, $J = 7.4$ Hz, 1H), 7.10 (t, $J = 7.4$ Hz, 1H), 7.27 (d, $J = 7.4$ Hz, 1H), 7.32 (d, $J = 7.6$ Hz, 1H); ^{13}C NMR (100 MHz, C_6D_6) δ 26.5, 79.3, 119.4, 120.5, 123.0, 126.1, 126.8, 128.8, 131.0, 135.5, 135.6, 144.2, 153.9, 154.9; IR(KBr) 3572, 3406, 3061, 1385, 768 cm^{-1} ; HRMS (FAB+) m/z calcd for $\text{C}_{14}\text{H}_{11}\text{OS}_2$ $[\text{M}+\text{H}]^+$ 252.0245, found 259.0242; mp >300 °C.

10-Isopropyl-10H-benzo[*b*]indeno[2,1-*d*]thiophen-10-ol (2j)



Prepared according to the general procedure from 1-(2-bromophenyl)-1-(benzo[*b*]thiophene-3-yl)-2-methylpropan-1-ol **1e** (542 mg, 1.5 mmol), CsOAc (633 mg, 3.3 mmol), PPh_3 (39.3 mg, 0.15 mmol) and $\text{Pd}(\text{TFA})_2$ (24.0 mg, 0.075 mmol). The product **2j** was purified by chromatography on silica gel eluting with *n*-hexane/ CHCl_3 (2/1), GPC (toluene) and obtained as a colorless solid (299 mg, 1.07 mmol, 71%); ^1H NMR (400 MHz, CDCl_3) δ 0.65 (d, $J = 6.8$ Hz, 3H), 1.22 (d, $J = 6.8$ Hz, 3H), 1.64 (brs, 1H), 2.59 (sept, $J = 6.8$ Hz, 1H), 7.23 (dt, $J = 7.0, 1.2$ Hz, 1H), 7.37 (dt, $J = 7.8, 1.0$ Hz, 1H), 7.38 (dt, $J = 7.8, 1.0$ Hz, 1H), 7.47 (d, $J = 7.0$ Hz, 1H), 7.48 (t, $J = 7.0$ Hz, 1H), 7.69 (d, $J = 7.0$ Hz, 1H), 7.89 (d, $J = 7.8$ Hz, 1H), 8.11 (d, $J = 7.8$ Hz, 1H); ^{13}C NMR (150 MHz, CDCl_3) δ 16.7, 17.1, 85.3, 119.2, 122.3, 122.8, 123.8, 124.4, 124.9, 125.7, 128.7, 132.5, 137.9, 139.4, 145.3, 149.5, 152.3; IR(KBr) 3399, 3048, 2963, 1036, 673 cm^{-1} ; HRMS (FAB+) m/z calcd for $\text{C}_{18}\text{H}_{16}\text{OS}$ $[\text{M}+\text{H}]^+$ 280.0916, found 280.0917; mp >300 °C.

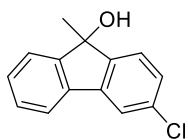
11-Isopropyl-2,3-dihydro-11H-benzo[4',5']thieno[2',3':1,2]indeno[5,6-*b*][1,4]dioxin-11-ol (2k)



Prepared according to the general procedure from 1-(7-bromo-2,3-dihydrobenzo[*b*][1,4]dioxin-6-yl)-1-(benzo[*b*]thiophen-3-yl)-2-methylpropan-1-ol **1e** (629 mg, 1.5 mmol), CsOAc (633 mg, 3.3 mmol), PPh_3 (39.3 mg, 0.15 mmol) and $\text{Pd}(\text{TFA})_2$ (24.0 mg, 0.075 mmol). The product **2k** was purified by

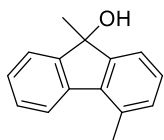
chromatography on silica gel eluting with *n*-hexane/CHCl₃ (1/1) and obtained as a colorless solid (457 mg, 1.35 mmol, 90%); ¹H NMR (400 MHz, CDCl₃) δ 0.70 (d, *J* = 6.8 Hz, 3H), 1.08 (d, *J* = 6.8 Hz, 3H), 2.40 (brs, 1H), 2.67 (sept, *J* = 6.8 Hz, 1H), 4.10–4.29 (m, 4H), 6.82 (s, 1H), 7.01 (s, 1H), 7.25 (t, *J* = 7.7 Hz, 1H), 7.36 (t, *J* = 7.7 Hz, 1H), 7.81 (d, *J* = 7.7 Hz, 1H), 7.91 (t, *J* = 7.7 Hz, 1H); ¹³C NMR (100 MHz, CDCl₃) δ 17.1, 17.8, 36.0, 64.22, 64.25, 84.7, 108.9, 113.9, 122.0, 123.5, 123.7, 124.7, 130.6, 134.0, 142.0, 142.7, 143.4, 143.8, 144.5, 145.8; IR(KBr) 3482, 3036, 2965, 2361, 1065 cm⁻¹; HRMS (FAB+) *m/z* calcd for C₂₀H₁₉O₃S [M+H]⁺ 339.1049, found 339.1040; mp >300 °C.

3-Chloro-9-methyl-9H-fluorene-9-ol (2l)



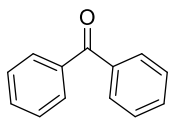
Prepared according to the general procedure from 1-(2-bromo-4-chlorophenyl)-1-phenylethan-1-ol **1l** (467 mg, 1.5 mmol), CsOAc (633 mg, 3.3 mmol), dppf (41.6 mg, 0.075 mmol) and Pd(OAc)₂ (17.3 mg, 0.075 mmol). The product **2l** was purified by chromatography on silica gel eluting with *n*-hexane/CHCl₃ (2/1) and obtained as a colorless solid (235 mg, 1.02 mmol, 68%); ¹H NMR (400 MHz, CDCl₃) δ 1.71 (s, 3H), 2.01 (brs, 1H), 7.27 (dd, *J* = 8.3, 1.8 Hz, 1H), 7.34 (dt, *J* = 7.6, 1.4 Hz, 1H), 7.38 (dt, *J* = 7.6, 1.4 Hz, 1H), 7.46 (d, *J* = 8.3 Hz, 1H), 7.55 (dd, *J* = 7.6, 1.4 Hz, 1H), 7.57 (s, 1H), 7.58 (dd, *J* = 7.6, 1.4 Hz, 1H); ¹³C NMR (100 MHz, CDCl₃) δ 26.0, 79.2, 120.2, 120.3, 123.4, 124.4, 127.9, 128.7, 129.1, 134.8, 137.5, 140.5, 148.0, 150.0; IR(KBr) 3335, 2978, 2922, 1447, 773 cm⁻¹; HRMS (FAB+) *m/z* calcd for C₁₄H₁₂³⁵ClO [M+H]⁺ 231.0571, found 231.0567; mp 244.9–245.6 °C.

4,9-Dimethyl-9H-fluorene-9-ol (2m)



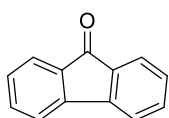
Prepared according to the general procedure from 1-(2-bromo-3-methylphenyl)-1-phenylethan-1-ol **1m** (437 mg, 1.5 mmol), CsOAc (633 mg, 3.3 mmol), dppf (41.6 mg, 0.075 mmol) and Pd(OAc)₂ (17.3 mg, 0.075 mmol). The product **2m** was purified by chromatography on silica gel eluting with *n*-hexane/CHCl₃ (2/1), GPC (toluene) and obtained as a colorless solid (50 mg, 0.24 mmol, 16%); ¹H NMR (600 MHz, CDCl₃) δ 1.73 (s, 3H), 1.94 (brs, 1H), 2.66 (s, 3H), 7.15 (d, *J* = 7.2 Hz, 1H), 7.23 (t, *J* = 7.2 Hz, 1H), 7.33 (t, *J* = 7.2 Hz, 1H), 7.39 (t, *J* = 7.2 Hz, 1H), 7.43 (d, *J* = 7.2 Hz, 1H), 7.60 (d, *J* = 7.2 Hz, 1H), 7.77 (d, *J* = 7.2 Hz, 1H); ¹³C NMR (150 MHz, CDCl₃) δ 20.8, 26.4, 79.1, 120.7, 123.2, 127.4, 127.8, 128.7, 131.2, 133.2, 136.7, 139.7, 150.17, 150.22; IR(neat) 3551, 3412, 2980, 1447, 770 cm⁻¹; HRMS (FAB+) *m/z* calcd for C₁₅H₁₅O [M+H]⁺ 211.1117, found 211.1114; mp 151.1–151.9 °C.

Benzophenone (4a)¹⁴



Prepared according to the general procedure from 9-phenyl-9H-fluorene-9-ol **1n** (273 mg, 1.5 mmol), CsOAc (633 mg, 3.3 mmol), dppf (41.6 mg, 0.075 mmol) and Pd(OAc)₂ (17.3 mg, 0.075 mmol). The product **4a** was purified by chromatography on silica gel eluting with *n*-hexane/CHCl₃ (2/1), GPC (toluene) and obtained as a colorless solid (195 mg, 1.07 mmol, 71%); ¹H NMR (600 MHz, CDCl₃) δ 7.49 (t, *J* = 7.2 Hz, 4H), 7.60 (t, *J* = 7.2 Hz, 1H), 7.81 (d, *J* = 7.2 Hz, 1H); ¹³C NMR (150 MHz, CDCl₃) δ 128.2, 130.0, 132.3, 137.4, 196.6; IR(KBr) 3055, 3030, 1651, 1449, 708 cm⁻¹; HRMS (FAB+) *m/z* calcd for C₁₃H₁₀O [M]⁺ 182.0726, found 182.0722; mp 50.3–51.1 °C.

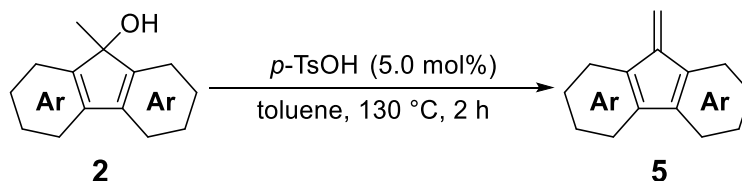
9H-Fluorene-9-one (**4b**)¹⁴



Prepared according to the general procedure from 9H-fluorene-9-ol **1p** (273 mg, 1.5 mmol), CsOAc (633 mg, 3.3 mmol), dppf (41.6 mg, 0.075 mmol) and Pd(OAc)₂ (17.3 mg, 0.075 mmol). The product **4a** and **4b** were purified by chromatography on silica gel eluting with *n*-hexane/CHCl₃ (2/1), GPC (toluene) and obtained as colorless solid **4a** (57.7 mg, 0.32 mmol, 21%) and yellow solid **4b** (114 mg, 0.63 mmol, 42%); ¹H NMR (600 MHz, CDCl₃) δ 7.29 (t, *J* = 7.2 Hz, 2H), 7.49 (t, *J* = 7.2 Hz, 2H), 7.52 (d, *J* = 7.2 Hz, 2H), 7.66 (d, *J* = 7.2 Hz, 2H); ¹³C NMR (150 MHz, CDCl₃) δ 120.4, 124.3, 129.1, 132.1, 134.7, 144.4, 193.9; IR(KBr) 3061, 3013, 1715, 1450, 735 cm⁻¹; HRMS (FAB+) *m/z* calcd for C₁₃H₈O [M]⁺ 180.0569, found 180.0577; mp 78.8–79.5 °C.

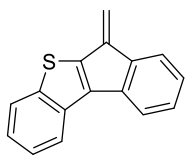
5. Further Transformation of FOLs to Fulvenes

General Procedure



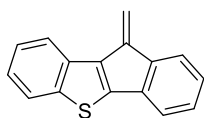
To a solution of FOL **2** (0.2 mmol) in toluene (10 mL) was added *p*-TsOH (0.01 mmol). The mixture was warmed up to 130 °C and stirred for 2 h. After being allowed to cool to 25 °C, the residue was purified by column chromatography on silica gel eluting with *n*-hexane. The target products **4** are slowly decomposed by air or moisture.

6-Methylene-6*H*-benzo[*b*]indeno[1,2-*d*]thiophene (**5a**)



Prepared according to the general procedure from 6-methyl-6*H*-benzo[*b*]indeno[1,2-*d*]thiophen-6-ol **2g** (50.5 mg, 0.2 mmol) and *p*-TsOH·H₂O (1.9 mg, 0.01 mmol). The product **5a** was purified by chromatography on silica gel eluting with *n*-hexane and obtained as a yellow solid (43.6 mg, 0.186 mmol, 93%); ¹H NMR (600 MHz, CDCl₃) δ 5.93 (s, 1H), 6.13 (s, 1H), 7.23 (t, *J* = 8.1 Hz, 1H), 7.370 (t, *J* = 7.2 Hz, 1H), 7.373 (t, *J* = 7.2 Hz, 1H), 7.47 (t, *J* = 8.1 Hz, 1H), 7.66 (d, *J* = 7.2 Hz, 1H), 7.70 (d, *J* = 7.2 Hz, 1H), 7.87 (d, *J* = 8.1 Hz, 1H), 8.10 (d, *J* = 8.1 Hz, 1H); ¹³C NMR (150 MHz, CDCl₃) δ 110.9, 118.9, 120.5, 122.5, 123.9, 124.8, 124.9, 125.0, 128.5, 132.9, 137.9, 140.3, 140.5, 141.3, 141.6, 144.5; IR(KBr) 2926, 2859, 1726, 1287, 770 cm⁻¹; HRMS (FAB+) *m/z* calcd for C₁₆H₁₀S [M]⁺ 234.0497, found 234.0500; mp 105.4–106.1 °C.

10-Methylene-10*H*-benzo[*b*]indeno[2,1-*d*]thiophene (**5b**)



Prepared according to the general procedure from 10-methyl-10*H*-benzo[*b*]indeno[2,1-*d*]thiophen-10-ol **2e** (50.5 mg, 0.2 mmol) and *p*-TsOH·H₂O (1.9 mg, 0.01 mmol). The product **5b** was purified by chromatography on silica gel eluting with *n*-hexane and obtained as a yellow solid (41.7 mg, 0.178 mmol, 89%); ¹H NMR (600 MHz, CDCl₃) δ 6.16 (s, 1H), 6.19 (s, 1H), 7.27 (t, *J* = 7.0 Hz, 1H), 7.31 (t, *J* = 7.5 Hz, 1H), 7.34 (t, *J* = 7.0 Hz, 1H), 7.42 (t, *J* = 7.5 Hz, 1H), 7.44 (d, *J* = 7.5 Hz, 1H), 7.66 (d, *J* = 7.0 Hz, 1H), 7.85 (d, *J* = 7.5 Hz, 1H), 8.02 (d, *J* = 7.0 Hz, 1H); ¹³C NMR (150 MHz, CDCl₃) δ 109.6, 119.3, 120.3, 121.6, 123.97, 124.03, 125.3, 126.3, 128.5, 133.8, 136.4, 136.6, 140.4, 140.8, 144.0, 146.4; IR(KBr) 2928, 2859, 1726, 1462, 746 cm⁻¹; HRMS (FAB+) *m/z* calcd for C₁₆H₁₁S [M+H]⁺ 235.0575, found 235.0577; mp 129.0–129.8 °C.

References

- (1) (a) Kurdyukova, I. V.; Ishchenko, A. A. *Russian Chem. Rev.* **2012**, *81*, 258–290. (b) Fun, H. K.; Yeap, C. S.; Vijesh, A. M.; Isloor, A. M.; Vasudeva, P. K. *Acta Cryst.* **2010**, *E66*, 2624–2625. (c) Ahmed, S. A.; Althagafi, I. I.; Asghar, B. H.; Khairou, K. S.; Muathen, H. A. *J. Photochem. Photobiol.* **2016**, *328*, 163–170. (d) Ahmed, S. A.; El Guesmi, N.; Asghar, B. H.; Maurel, F.; Althagafi, I. I.; Khairou, K. S.; Muathen, H. A. *J. Phys. Org. Chem.* **2017**, *30*, e3614. (e) El Guesmi, N.; Ahmed, S. A.; Althagafi, I. I.; Khairou, K. S. *J. Photochem. Photobiol. A*, **2017**, *346*, 287–295. (f) El Guesmi, N.; Ahmed, S. A.; Maurel, F.; Althagafi, I. I.; Khairou, K. S. *J. Photochem. Photobiol.* **2017**, *348*, 125–133. (g) El Guesmi, N.; Ahmed, S. A.; Maurel, F.; Althagafi, I. I.; Khairou, K. S. *J. Photochem. Photobiol.* **2018**, *360*, 210–223.
- (2) (a) Dunn, D.; Hostetler, G.; Iqbal, M.; Marcy, V. R.; Lin, Y. G.; Jones, B.; Aimone, L. D.; Gruner, J.; Ator, M. A.; Bacon, E. R.; Chatterjee, S. *Bioorg. Med. Chem. Lett.* **2012**, *22*, 3751–3753. (b) Yasser, M. A.; A-G, I. O. B.; Mohamed, M. S.; Yong, S. O. *Asian. J. Plant Sci.* **2009**, *8*, 536–543. (c) Mathur, M.; Ramawat, K. G. *Plant. Biotechnol. Rep.* **2008**, *2*, 133–136. (d) Sun, X.; Xue, Q.; Zhu, Z.; Xiao, Q.; Jiang, K.; Yip, H. L.; Yan, H.; Li, Z. *Chem. Sci.* **2018**, *9*, 2698–2704.
- (3) (a) Upadhayaya, R. S.; Lahore, S. V.; Sayyed, A. Y.; Shinde, P. D.; Chattopadhyaya, J. *Org. Biomol. Chem.* **2010**, *8*, 2180–2197. (b) Upadhayaya, R. S.; Shinde, P. D.; Kadam, S. A.; Bawane, A. N.; Sayyed, A. Y.; Kardile, R. A.; Gitay, P. N.; Lahore, S. V.; Dixit, S. S.; Földesi, A.; Chattopadhyaya, J. *Eur. J. Med. Chem.* **2011**, *46*, 1306–1324. (c) Upadhayaya, R. S.; Dixit, S. S.; Földesi, A.; Chattopadhyaya, J. *Bioorg. Med. Chem. Lett.* **2013**, *23*, 2750–2758. (d) Tseng, C. H.; Tung, C. W.; Wu, C. H.; Tzeng, C. C.; Chen, Y. H.; Hwang, T. L.; Chen, Y. L. *Molecules* **2017**, *22*, 1001. (e) Yamada, H.; Itahana, H.; Morimoto, A.; Matsuzawa, T.; Nozawa, E.; Akuzawa, S.; Harada, K. WO2007018168A1
- (4) (a) Vougioukalakis, G. C.; Roubelakis, M. M.; Orfanopoulos, M. *J. Org. Chem.* **2010**, *75*, 4124–4130. (b) Wei, B.; Li, H.; Zhang, W. X.; Xi, Z. *Organometallics* **2015**, *34*, 1339–1344. (c) Zhao, C. Y.; Li, L. G.; Liu, Q. R.; Pan, C. X.; Su, G. F.; Mo, D. L. *Org. Biomol. Chem.* **2016**, *14*, 6795–6803. (d) Kapoor, M.; Liu, D.; Young, M. C. *J. Am. Chem. Soc.* **2018**, *140*, 6818–6822.
- (5) (a) Chen, Z.; Zeng, M.; Yuan, J.; Yang, Q.; Peng, Y. *Org. Lett.* **2012**, *14*, 3588–3591. (b) Liu, L.; Zhang, J. *Angew. Chem., Int. Ed.* **2009**, *48*, 6093–6096. (c) Liu, L.; Wei, L.; Zhang, J. *Adv. Synth. Catal.* **2010**, *352*, 1920–1924. (d) Zhao, Y. B.; Mariampillai, B.; Candito, D. A.; Laleu, B.; Li, M.; Lautens, M. *Angew. Chem., Int. Ed.* **2009**, *121*, 1881–1884. (e) Casnati, A.; Fontana, M.; Motti, E.; Ca, N. D. *Org. Biomol. Chem.* **2019**, *17*, 6165–6173. (f) Itoh, M.; Hirano, K.; Satoh, T.; Shibata, Y.; Tanaka, K.; Miura, M. *J. Org. Chem.* **2013**, *78*, 1365–1370.
- (6) (a) Mahendar, L.; Krishna, J.; Reddy, A. G. K.; Ramulu, B. V.; Satyanarayana, G. *Org. Lett.* **2012**, *14*, 628–631. (b) Mahendar, L.; Satyanarayana, G. *J. Org. Chem.* **2014**, *79*, 2059–2074.

- (7) Xu and co-workers reported that **4a** and **4b** were obtained under similar reaction conditions; see: Gao, Q.; Xu, S. *Org. Biomol. Chem.* **2018**, *16*, 208–212.
- (8) Bour, J. R.; Green, J. C.; Winton, V. J.; Johnson, J. B. *J. Org. Chem.* **2013**, *78*, 1665–1669.
- (9) Gensch, T.; Hopkinson, M. N.; Glorius, F.; Delord, J. W. *Chem. Soc. Rev.* **2016**, *45*, 2900–2936.
- (10) Cuadrado, D. G.; Braga, A. A. C.; Maseras, F.; Echavarren, A. M. *J. Am. Chem. Soc.* **2006**, *128*, 1066–1067.
- (11) Lafrance, M.; Lapointe D.; Fagnou, K. *Tetrahedron* **2008**, *64*, 6015–6020.
- (12) Mladnova, G.; Chen, L.; Rodriguez, C. F.; Siu, K. W. M.; Johnson, L. J.; Hopkinson, A. C.; Lee-Ruff, E. *J. Org. Chem.* **2001**, *66*, 1109–1114.
- (13) Nickerson, L. A.; Bergstorm, B. D.; Gao, M.; Shiue, Y. S.; Laconsay, C. J.; Culberson, M. R.; Knauss, W. A.; Fetting, J. C.; Tantillo, D. J.; Shaw, J. T. *Chem. Sci.* **2020**, *11*, 494–498.
- (14) Suzuki, Y.; Iinuma, M.; Moriyama, K.; Togo, H. *Synlett* **2012**, *23*, 1250–1256.

Chapter 2. Synthesis of Heteroring-Fused Fluoreneol via Selective Intramolecular C–H Functionalization

**Chapter 3. Synthesis of Benzodithienofuran (BDTF) via Construction of
Oxygen-Bridged Bithiophenes Using
3-Bromobenzo[*b*]thiophene 1,1-Dioxide as a Key Compound**

3-1.	Abstract	52
3-2.	Introduction	52
3-3.	Optimization for the Transition Metal-Catalyzed Synthesis of Dithienyl Ethers	54
3-4.	Optimization for the Synthesis of Dithienyl Ethers Using 3-Bromobenzo[<i>b</i>]thiophene 1,1-Dioxides	56
3-5.	Synthesis of BDTF via Pd-Catalyzed Intramolecular Cyclization	59
3-6.	Transformation of π -Extended BDTF	60
3-7.	Conclusion	61
3-8.	Experimental Section and Analytical Data	62
	References	77

3-1. Abstract

The author developed an efficient synthetic method of [1]benzothieno[3,2-*b*]thieno[2,3-*d*]furan (BDTF) by Pd-catalyzed intramolecular C–H functionalization of 3-benzo[*b*]thienyl 3-thienyl ether. Synthesis of the precursor was achieved by the addition–elimination reaction of 3-bromobenzo[*b*]thiophene 1,1-dioxides as key compounds. The obtained BDTF was easily transformed to π -extended BDTFs by a bromination reaction and subsequent Suzuki–Miyaura cross-coupling.

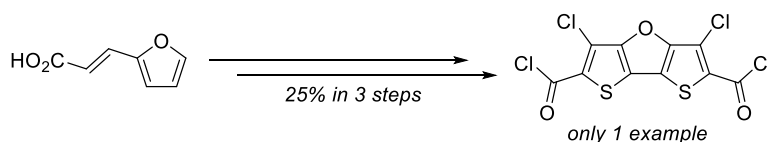
3-2. Introduction

Heteroatom-bridged 2,2'-bithiophenes, such as dithieno[3,2-*b*:2',3'-*d*]pyrroles (DTPs), silolo[3,2-*b*:4,5-*b'*]dithiophene (dithienosiloles, DTSSs), and phospholo[3,2-*b*:4,5'-*b'*]dithiophene, have been attracting interest due to their role in organic functional materials.¹ Among them, oxygen-bridged 2,2'-bithiophenes (dithienofurans, DTFs) are expected to be applied to the active material of organic light emitting transistors due to the high probability of exhibiting excellent fluorescent properties. However, there have been only two reports on the synthesis of DTFs.

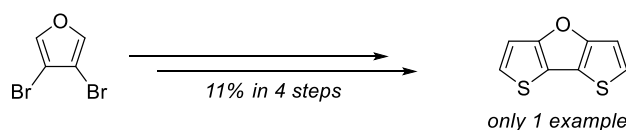
In 1993, Karminski-Zamola and co-workers reported the first synthesis of a DTF derivative (Scheme 1A).^{2a} They converted furylacrylic acid to a DTF derivative through several steps including a Vilsmeier–Haak reaction and Knoevenagel condensation. In 2015, Svoboda and co-workers achieved the second synthesis of a DTF derivative from 3,4-dibromofuran via a Vilsmeier–Haak reaction and subsequent reaction with methyl thioglycolate, and decarboxylation (Scheme 1B).^{2b} In their works, they constructed DTF skeletons by the cyclization reactions near a furan skeleton. However, it is difficult to apply such strategies for the synthesis of more π -expanded ladder-type DTFs. Indeed, to the best of our knowledge, there has been no report on the synthesis of such π -expanded DTFs even for [1]benzothieno[3,2-*b*]thieno[2,3-*d*]furan (benzodithienofuran, BDTF).

Scheme 1. Reported synthetic methods of DTFs

A. Karminski-Zamola's work



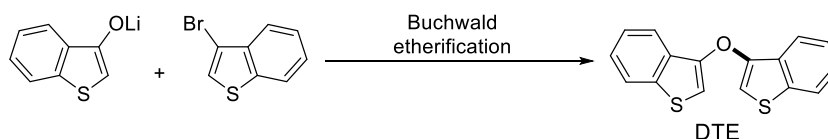
B. Svoboda's work



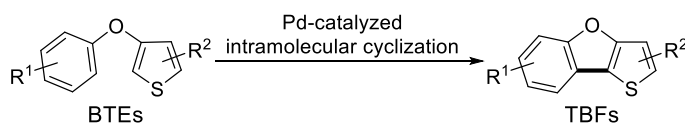
Therefore, the author aimed to develop a straightforward method for the synthesis of BDTFs. The approach for synthesizing BDTFs is envisioned in Scheme 2C. The author considered that BDTFs could be synthesized from the 3,3'-dithienyl ethers (DTEs) by Pd-catalyzed intramolecular cyclization. The reason for thinking as described above is that related studies for the Pd-catalyzed synthesis of thieno[3,2-*b*]benzofurans (TBFs) from benzo[*b*]thienyl ethers (BTEs) have been reported by Miura and Kuninobu (Scheme 2B).³ However, there have been only one report on the synthesis of DTE (Scheme 2A).⁴ Thus, the synthesis of DTEs is challenging, but the author devised that efficient synthesis of DTEs can be achieved by utilizing methods such as Ullmann ether synthesis and Buchwald etherification.

Scheme 2. Previous and This work

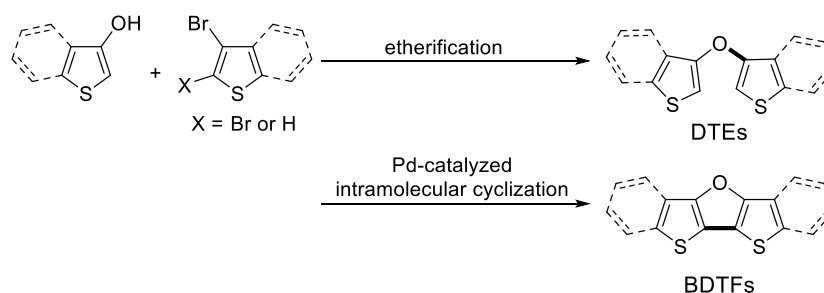
A. Previous Work: Reported synthetic method of DTE (Xueyan)



B. Previous Work: Reported synthetic method of TBFs using BTEs (Miura, Kuninobu)



C. This Work: Development of synthetic method of BDTFs



3-3. Optimization for the Transition Metal-Catalyzed Synthesis of Dithienyl Ethers

Initially, the author attempted to synthesize DTE **3a** with the Buchwald type cross-coupling of 3-hydroxybenzo[*b*]thiophenes **1a** and 3-bromobenzo[*b*]thiophene **2** (Scheme 3).⁴ Unfortunately, the corresponding product **3a** was not obtained at all, and benzo[*b*]thiophene which was caused by debromination of **2** was obtained as the major product. The author next examined the synthesis of **3a** with reference to Buchwald's report (Table 1).⁵ Although various ligands and solvents were examined, **3a** was not obtained, and unreacted **2** was mainly recovered.

Scheme 3. Optimization for the synthesis of DTE **3a** by Buchwald type etherification 1

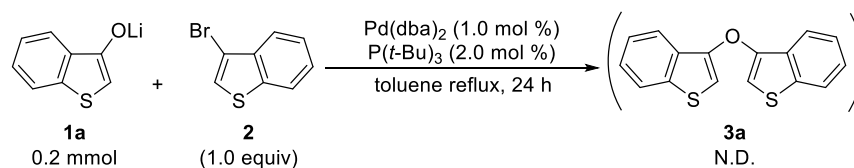
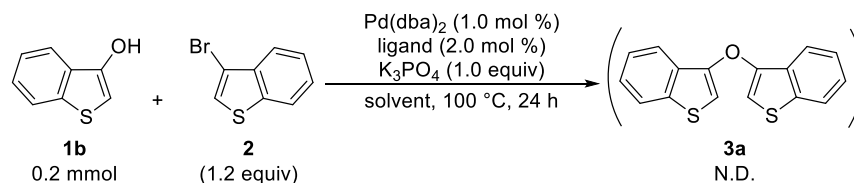


Table 1. Optimization for the synthesis of DTE **3a** by Buchwald etherification 2^a



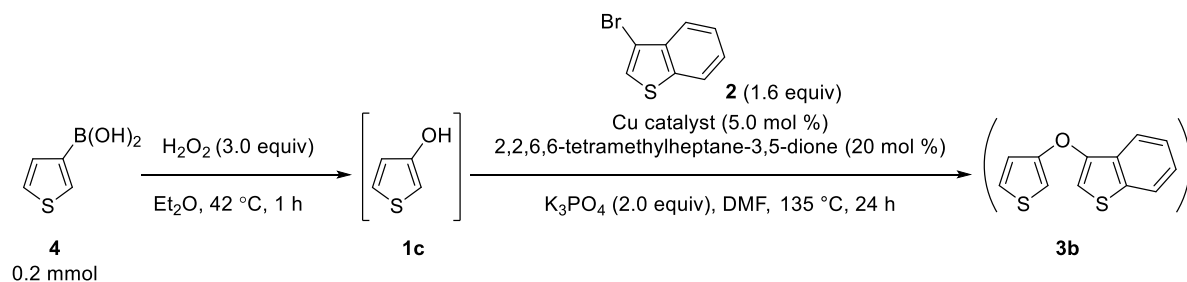
entry	ligand	Solvent	3a (%)
1	Cy-JohnPhos	DMSO	N.D. ^b
2	XPhos	DMSO	N.D. ^b
3	JohnPhos	DMSO	N.D. ^b
4	BrettPhos	DMSO	N.D. ^b
5	<i>t</i> -BuXPhos	DMSO	N.D. ^b
6	<i>t</i> -BuXPhos	Toluene	N.D. ^b
7	<i>t</i> -BuXPhos	DMF	N.D. ^b
8	<i>t</i> -BuXPhos	H ₂ O/1,4-dioxane = 1/1	N.D. ^b
9	<i>t</i> -BuXPhos	DMA	N.D. ^b
10	<i>t</i> -BuXPhos	CPME	N.D. ^b

^a Reaction conditions: **1b** (0.20 mmol), **2** (0.24 mmol), Pd(dba)₂ (1.0 mol %), ligand (2.0 mol %), K₃PO₄ (1.0 equiv), solvent (0.3 mL) at 100 °C, 24 h. ^b

N.D. = Not Detected.

Next, the author examined the synthesis of DTE **3b** by Ullmann ether synthesis. Cross-coupling of 3-hydroxythiophene (**1c**) and **2** was attempted (Table 2).⁶ Various catalysts were examined, but **3b** was not obtained, and unreacted **2** decomposed compound of **1c** was mainly recovered.

Table 2. Optimization for the synthesis of DTE **3b** by Ullmann ether synthesis^a

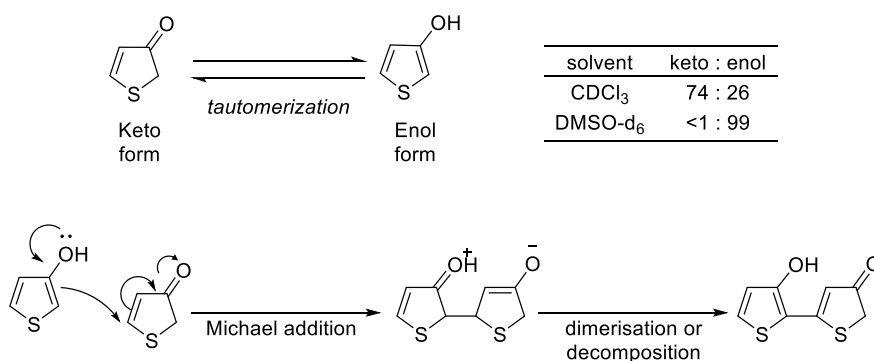


entry	Cu catalyst	3b (%)
1	CuI	N.D. ^b
2	CuBr	N.D. ^b
3	CuTc	N.D. ^b

^a Reaction conditions: **1c** (0.20 mmol), **2** (0.32 mmol), Cu catalyst (5.0 mol %), 2,2,6,6-tetramethylheptane-3,5-dione (20 mol %), K₃PO₄ (2.0 equiv), DMF (0.2 mL) at 135 °C, 24 h. 3-Hydroxythiophene (**4**) was generated by the reaction of 3-thienylboronic acid and H₂O₂ aq, and used without purification.⁷ ^b N.D. = Not Detected.

The author assumed that tautomerization of **1c** would be problematic. The reason for thinking as described above is that McNab and co-workers reported that **1c** is not only unstable compound that undergoes a decomposition, but also shows to tautomerize to a keto tautomer (thiophen-3(2*H*)-one: **1d**). Furthermore, dimerization proceeds between **1c** and **1d** by Michael addition (Scheme 4)⁸.

Scheme 4. Tautomerization of **1c**

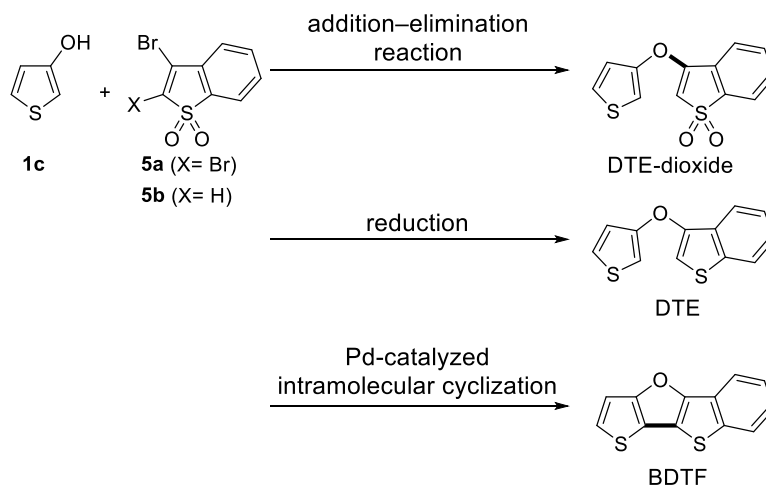


3-4. Optimization for the Synthesis of Dithienyl Ethers Using 3-Bromobenzo[*b*]thiophene 1,1-Dioxides

The author considered etherification should proceed faster than the competing decomposition and dimerization of **1c**. From the viewpoint, the transition metal-catalyzed reaction described above would be slow although it required harsh reaction conditions. Therefore, the author changed synthetic strategy of etherification from transition metal-catalyzed reactions to addition–elimination reactions. A new strategy for synthesizing BDTF is envisioned in Scheme 5. **2** is not an active reactant for addition–elimination reactions due to the aromaticity of the thiophene ring. The author predicted that oxidation of **2** to 3-bromobenzo[*b*]thiophene 1,1-dioxides **5** increases electrophilicity and **5** would be used as an active reactant for addition–elimination reactions. It is known that addition–elimination reactions usually proceed smoothly under milder conditions. Thus, the author planned to construct dithienyl ether dioxide (DTE-dioxide) by an addition–elimination reaction using **5** as a key compound. Thus-obtained DTE-dioxide is converted to DTE by reduction and then converted to BDTF by a subsequent Pd-catalyzed intramolecular cyclization.

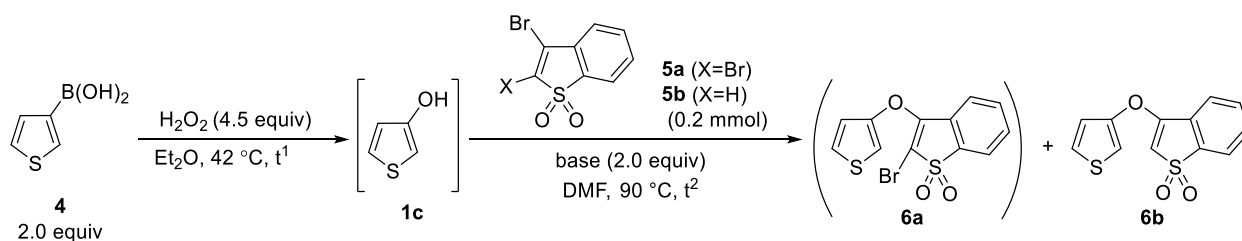
Scheme 5. A new approach for synthesizing BDTF via construction of DTE-dioxide

New approach: Synthesis of **BDTF** via construction of DTE-dioxides



According to the approach described above, the author examined to synthesize DTE-dioxide **6** by addition–elimination reactions (Table 3). In DMF, 2,3-dibromobenzo[b]thiophene 1,1-dioxide **5a** was treated with **1c**, derived from 3-thienylboronic acid by oxidation using H₂O₂, in the presence of DABCO or Et₃N as a base, but the target product is not obtained at all (entries 1 and 2). In contrast, with K₂CO₃, the addition–elimination reaction proceeded smoothly, and the debrominated product **6b** was unexpectedly obtained selectively (entry 3). It is not yet clear why the debromination proceeded. **6b** was also obtained from the addition–elimination reaction of 3-bromobenzo[b]thiophene 1,1-dioxide (**5b**) with **1c** (entry 5). During the course of further optimizations, the author found that the addition–elimination reaction proceeded under mild conditions when using Cs₂CO₃ in THF (Scheme 6, reaction temperature was 42 °C).

Table 3. Optimization for the synthesis of DTE-dioxide **6** by addition–elimination reaction^a

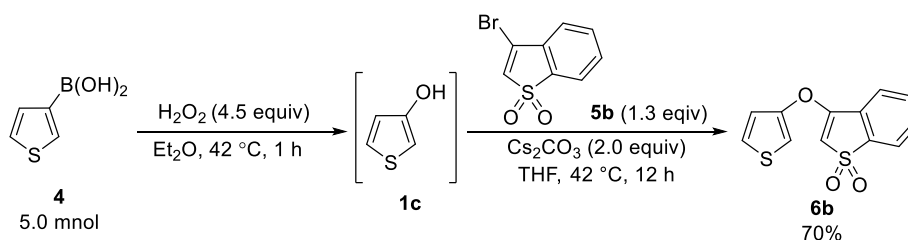


entry	t ¹ (h)	5	base	t ² (h)	yield of 6a (%) ^b	yield of 6b (%) ^b
1	2	5a	DABCO	24	–	N.D. ^b
2	1	5a	Et ₃ N	24	–	N.D. ^b
3	1	5a	K ₂ CO ₃	24	–	79 (75) ^c
4	1	5a	K ₂ CO ₃	12	–	74
5	1	5b	K ₂ CO ₃	12	–	75 (74)

^a Reaction conditions: **5a** or **5b** (0.20 mmol), base (2.0 equiv), DMF (1.0 mL) at 90 °C. 3-Hydroxythiophene (**1c**) was generated by the reaction of 3-thienylboronic acid and H₂O₂ aq, and used without purification.^{7 b}

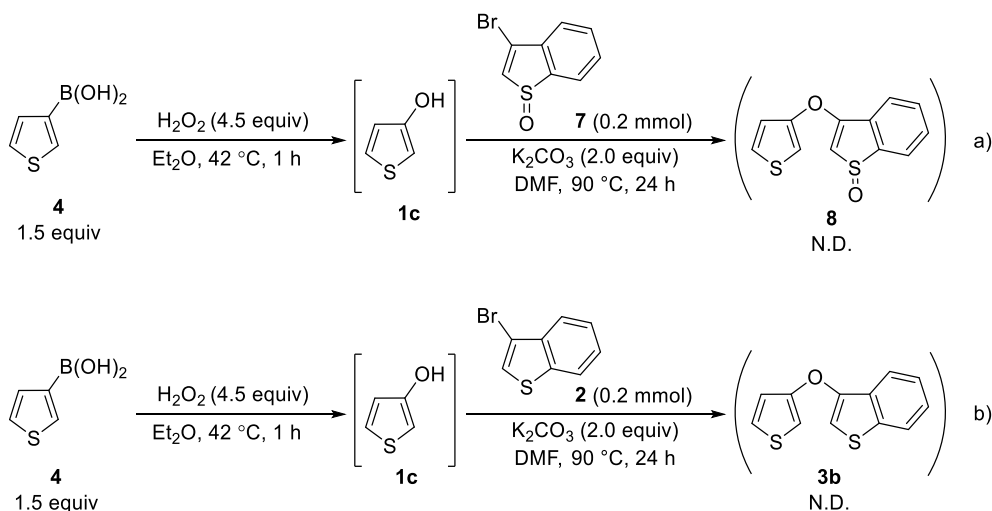
Isolated yield. ^c Not detected. ^d Performed with 5.0 mmol of **5a**. ^e Performed with 15 mmol of **5b**.

Scheme 6. Optimization for the synthesis of **6b** under mild condition



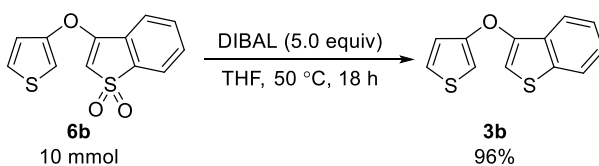
The author continued to screen 3-bromobenzo[*b*]thiophene derivatives (**7** or **2**) to explore more atomically efficient reaction conditions (Scheme 7a and b). However, the corresponding product was not obtained, and decomposed compounds of **1c** were mainly obtained. This result may support that the decomposition of **1c** proceeded faster than an addition–elimination reaction due to the lack of electrophilicity of 3-bromobenzo[*b*]thiophene derivatives.

Scheme 7. Optimization for the synthesis of DTEs using 3-bromobenzo[*b*]thiophene derivatives



The thus-obtained **6b** was readily reduced to DTE **3b** by treatment with DIBAL (Scheme 8).

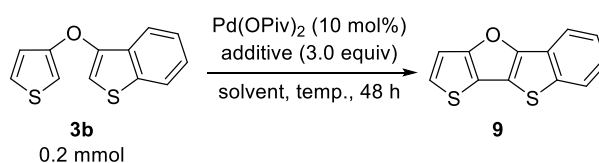
Scheme 8. Synthesis of DTE **3b** by reduction with DIBAL



3-5. Synthesis of BDTF via Pd-catalyzed Intramolecular Cyclization

The author next investigated transformations of **3b** to BDTF **9**. By heating **3b** in the presence of palladium pivalate (Pd(OPiv)₂, 10 mol %), AgOPiv (3.0 equiv) in DMF at 160 °C for 48 h, the desired **9** was obtained in 49% yield (Table 4, entry 1). When pivalic acid (PivOH) was used instead of DMF at 160 °C, the yield of **9** increased to 65% (entry 2). The yield of **9** also increased to 77% when the reaction was performed at 190 °C (entry 3). The efficiency of the reaction on a 2.0 mmol scale was similar to that on a 0.2 mmol scale. The use of a bulkier silver salt such as silver adamantane-1-carboxylate (AgOCOAd) gave a result similar to that with the use of AgOPiv (76%, entry 4). When NaOCOAd was used instead of a silver salt, the yield of **9** drastically decreased to 16% (entry 5). The palladium catalyst and the silver salt play key roles in the reaction,⁹ and only a trace amount of **9** was obtained in the absence of either Pd(OPiv)₂ or AgOPiv (entries 6 and 7).

Table 4. Optimization for the synthesis of BDTF **9** via Pd-catalyzed intramolecular cyclization ^a



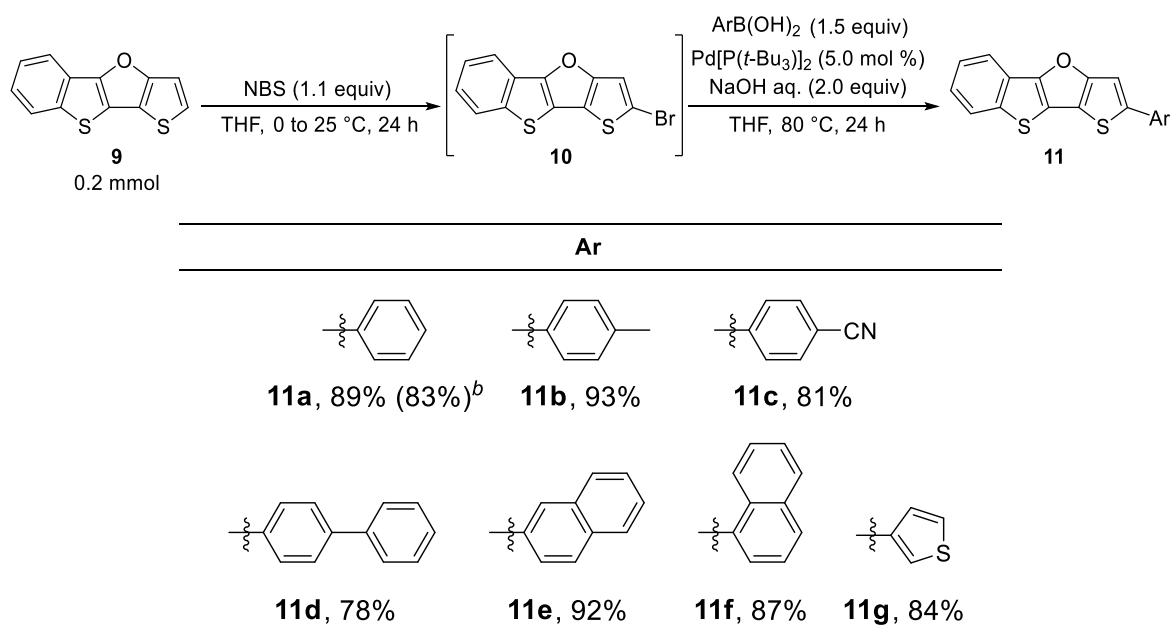
entry	additive	solvent	Temp. (°C)	yield (%)
1	AgOPiv	DMF	160	49
2	AgOPiv	PivOH	160	65
3	AgOPiv	PivOH	190	77 (79) ^b
4	AgOCOAd ^c	PivOH	190	76
5	NaOCOAd ^c	PivOH	190	16
6	none	PivOH	190	<5
7	AgOPiV	PivOH	190	<5 ^d

^a Reaction conditions: **3b** (0.2 mmol), Pd(OPiv)₂ (10 mol %), AgOPiv (3.0 equiv), PivOH (1.0 mL) at 190 °C, 48 h. Isolated yields. ^b The reaction scale was up to 2.0 mmol. ^c Ad = adamantane ^d Pd(OPiv)₂ was not used.

3-6. Transformation of π -Extended BDTF

The synthesized **9** was converted into various π -expanded BDTFs **11** by bromination followed by Suzuki–Miyaura cross-coupling (Table 5). The bromination of **9** with NBS proceeded smoothly at 25 °C to give brominated BDTF **10**. Next, in the presence of Pd[P(*t*-Bu)₃]₂ (5.0 mol %), arylboronic acid (1.5 equiv) and NaOH aq (1.0 M, 2 equiv) in THF at 80 °C for 24 h. The reaction proceeded on both electron-rich and electron-deficient arylboronic acids, and the desired products **11** were obtained with high generality in good yields.

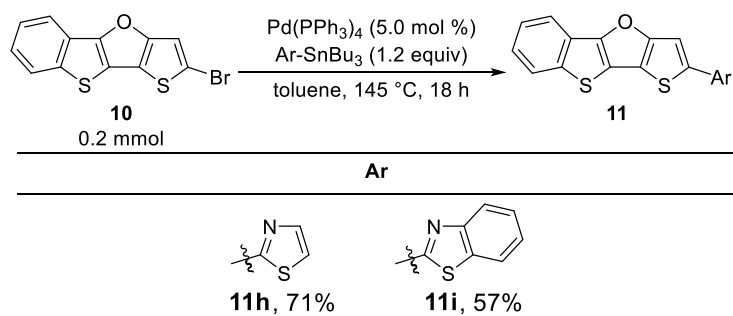
Table 5. Synthesis of π -expanded BDTFs **11** by Suzuki–Miyaura cross-coupling^a



^a Isolated yield. ^b The reaction scale was up to 1.0 mmol.

10 could also be converted by the Migita–Kosugi–Stille coupling (Table 6). By heating **10** in the presence of Pd(PPh₃)₄ (5.0 mol %), ArSnBu₃ (1.2 equiv) in toluene at 145 °C for 18 h, the desired **11** were obtained.

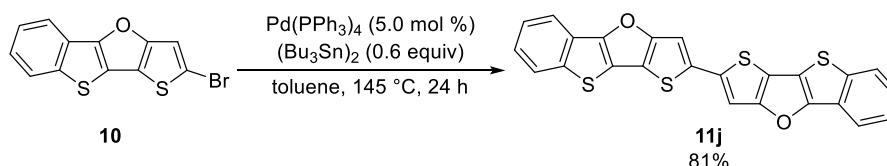
Table 6. Synthesis of π -expanded BDTFs **11** by Migita–Kosugi–Stille coupling^a



^a Isolated yield.

The author also succeeded in synthesizing BDTF dimer **11j** (BBTTF; 2,2'-bis([1]benzothieno[3,2-*b*]thieno[2,3-*d*]furan)) by Stille–Kelly coupling (Scheme 9). In the presence of Pd(PPh₃)₄ (5 mol%), (Bu₃Sn)₂ (0.6 equiv), the coupling reaction proceeded to give the desired **11j** in 81% yield.

Scheme 9. Synthesis of BDTF dimer **11j** by Stille–Kelly coupling



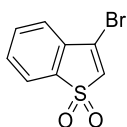
3-7. Conclusion

In conclusion, the author has achieved the syntheses of DTE-dioxides **3b** by an addition–elimination reaction using 3-bromobenzo[*b*]thiophene 1,1-dioxides as key compounds. An efficient transformation from **3b** to BDTF **9** was also developed by reduction following by Pd-catalyzed intramolecular cyclization. Thus-obtained **9** could be readily transformed to π -extended BDTF derivatives **11a–j**.

3-8. Experimental Section and Analytical Data

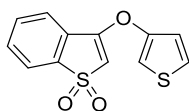
General

Nuclear magnetic resonance (NMR) spectra were recorded on Varian 600 System (^1H 600 MHz, ^{13}C 150 MHz), Varian 400-MR (^1H 400 MHz, ^{13}C 100 MHz), and JEOL JNM-ECS400 (^1H 400 MHz, ^{13}C 100 MHz) spectrometers. Chemical shifts for ^1H NMR are expressed in parts per million (ppm) relative to TMS (δ 0 ppm) or residual CHCl_3 in CDCl_3 (δ 7.26 ppm) or residual CH_2Cl_2 in CD_2Cl_2 (δ 5.32 ppm). Chemical shifts for ^{13}C NMR are expressed in ppm relative to CDCl_3 (δ 77.0 ppm) or CD_2Cl_2 (δ 53.84 ppm). IR spectra were recorded on a JASCO FT/IR-4100 and Varian 7000e FT-IR spectrophotometers. Elemental analysis was obtained with Perkin-Elmer PE 2400 Series II CHNS/O analyzer. Analytic thin layer chromatography (TLC) was performed on Merck, pre-coated plate silica gel 60 F₂₅₄ (0.25 mm thickness). Column chromatography was performed on KANTO CHEMICAL silica gel 60N (40–50 μm). Unless otherwise noted, all materials were obtained from commercial suppliers and used without further purification. High-resolution mass spectrometry was performed on JEOL JMS-700 MStation (FAB-MS). Dry tetrahydrofuran (THF) and dry diethyl ether (Et_2O) were purchased from Wako pure chemical industries. *N,N*-Dimethylformamide (DMF) was dried over MS4A. All reactions were performed under argon atmosphere. 2,3-Dibromobenzo[*b*]thiophene 1,1-dioxide (**5a**),¹⁰ 3-hydroxythiophene (**1c**),¹¹ NaOCOAd ,¹² and AgOCOAd ¹³ were synthesized according to the literatures. ^{13}C NMR of 2-([1,1'-biphenyl]-4-yl)benzo[4,5]thieno[3,2-*b*]thieno[2,3-*d*]furan (**11d**) could not be measured due to its low solubility. ^1H and ^{13}C NMR of 2,2'-bis(benzo[4,5]thieno[3,2-*b*]thieno[2,3-*d*]furan) (**11j**) could not be measured due to its low solubility.



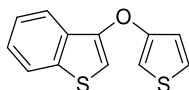
3-Bromobenzo[*b*]thiophene 1,1-dioxide (**5b**)

To a solution of 3-bromobenzo[*b*]thiophene (3.20 g, 15.0 mmol) in Ac_2O (20.3 mL) and AcOH (20.3 mL) was added dropwise H_2O_2 aq. (34.5%, 7.5 mL, 96 mmol) at 0 °C. The mixture was warmed to 110 °C and stirred for 2.5 h. Into the resulting mixture were added H_2O (35 mL), saturated $\text{Na}_2\text{S}_2\text{O}_3$ aq. (20 mL), K_2CO_3 (5.00 g) and the mixture was extracted with Et_2O (3×30 mL). The combined organic phase was dried over magnesium sulfate, filtered and concentrated under reduced pressure. The residue was purified by recrystallization (hexane/ EtOAc) to give 3-bromobenzo[*b*]thiophene 1,1-dioxide as yellow solid (3.57 g, 14.6 mmol, 97%). ^1H NMR (400 MHz, CDCl_3) δ 6.98 (s, 1H), 7.57 (d, $J = 7.4$ Hz, 1H), 7.62 (td, $J = 7.4, 1.1$ Hz, 1H), 7.68 (td, $J = 7.4, 1.1$ Hz, 1H), 7.73 (dd, $J = 7.4, 1.1$ Hz, 1H); ^{13}C NMR (100 MHz, CDCl_3) δ 120.8, 124.6, 129.5, 129.7, 131.1, 131.6, 133.8, 136.9; IR (KBr) 3104, 3075, 1551, 1175, 750 cm^{-1} .



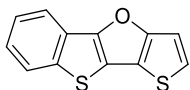
3-(Thiophen-3-yloxy)benzo[*b*]thiophene 1,1-dioxide (6b)

To a solution of thiophen-3-ylboronic acid (2.88 g, 22.5 mmol) in Et₂O (50 mL) was added dropwise H₂O₂ aq (35%, 6.1 mL, 68 mmol) at 0 °C. After complete addition, the reaction mixture was refluxed for 1 h. Into the resulting mixture were added H₂O (25 mL), saturated Na₂S₂O₃ aq (15.0 mL) and the mixture was extracted with Et₂O (3 × 50 mL). The combined organic phase was dried over magnesium sulfate and filtered. Removal of ether by heating to 42 °C gave 3-hydroxythiophene as orangish ethereal solution, and that was used immediately in the next reaction. To a solution of thus obtained thiophen-3-ol in dry DMF (75 mL) was added 3-bromobenzo[*b*]thiophene 1,1-dioxide (3.68 g, 15.0 mmol) and K₂CO₃ (3.11 g, 22.5 mmol), and the mixture was stirred at 100 °C for 12 h. The resulting mixture was directly purified by column chromatography on silica gel (hexane/EtOAc 1:0 → 4:1) to give 3-(thiophen-3-yloxy)benzo[*b*]thiophene 1,1-dioxide as colorless solid (2.93 g, 11.1 mmol, 74%). ¹H NMR (400 MHz, CDCl₃) δ 5.74 (s, 1H), 6.99 (dd, *J* = 5.3, 1.4 Hz, 1H), 7.08 (dd, *J* = 3.3, 1.4 Hz, 1H), 7.38 (dd, *J* = 5.3, 3.3 Hz, 1H), 7.62 (td, *J* = 6.8, 1.5 Hz, 1H), 7.66 (td, *J* = 6.8, 1.7 Hz, 1H), 7.73 (td, *J* = 6.8, 1.5 Hz, 1H), 7.76 (td, *J* = 6.8, 1.7 Hz, 1H); ¹³C NMR (100 MHz, CDCl₃) δ 103.2, 112.0, 120.2, 120.7, 121.3, 126.4, 128.6, 131.5, 133.1, 139.4, 149.8, 160.2; IR (neat) 3111, 1614, 1296, 1157, 770 cm⁻¹; HRMS (FAB+) *m/z* calcd for C₁₂H₉O₃S₂ [M + H]⁺ 264.9987, found 264.9994.



3-(Thiophen-3-yloxy)benzo[*b*]thiophene (3b)

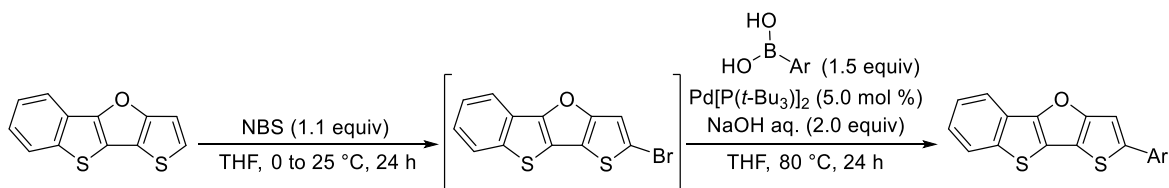
To a solution of 3-(thiophen-3-yloxy)benzo[*b*]thiophene 1,1-dioxide (2.64 g, 10.0 mmol) in THF (25 mL) was added dropwise DIBAL-H (1.00 M in THF, 50.0 mL, 50.0 mmol) at 0 °C. The reaction mixture was warmed to 50 °C and stirred for 18 h. The reaction was quenched by the addition of saturated aq. potassium sodium tartrate (50 mL) at 0 °C and stirred at the same temperature for 1 h. Into the resulting mixture were added H₂O (25 mL), brine (10 mL) and the mixture was extracted with EtOAc (3 × 20 mL). The combined organic phase was dried over magnesium sulfate, filtered, and concentrated under reduced pressure. The residue was purified by column chromatography on silica gel (hexane) to give 3-(thiophen-3-yloxy)benzo[*b*]thiophene as colorless liquid (2.14 g, 9.21 mmol, 92%). ¹H NMR (400 MHz, CDCl₃) δ 6.69 (s, 1H), 6.72 (dd, *J* = 3.2, 1.4 Hz, 1H), 6.99 (dd, *J* = 5.6, 1.4 Hz, 1H), 7.28 (dd, *J* = 5.6, 3.2 Hz, 1H), 7.36–7.42 (m, 2H), 7.79–7.83 (m, 2H); ¹³C NMR (100 MHz, CDCl₃) δ 105.3, 106.5, 120.3, 121.0, 123.0, 124.1, 125.21, 125.24, 131.8, 137.8, 148.9, 154.6; IR (neat) 3111, 3063, 1520, 1163, 756 cm⁻¹; HRMS (FAB+) *m/z* calcd for C₁₂H₉OS₂ [M + H]⁺ 233.0089, found 233.0082.



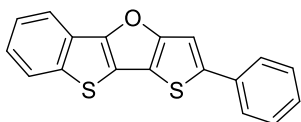
[1]Benzothieno[3,2-*b*]thieno[2,3-*d*]furan (9)

To a solution of 3-(thiophen-3-yloxy)benzo[*b*]thiophene (464.6 mg, 2.0 mmol) in pivalic acid (10 mL) were added Pd(OPiv)₂ (62.0 mg, 0.2 mmol) and AgOPiv (1.25 g, 6.0 mmol). The mixture was warmed up to 190 °C and stirred for 48 h. After being allowed to cool to 25 °C, the resulting mixture was concentrated under reduced pressure. The residue was purified by column chromatography on silica gel (hexane) to give [1]benzothieno[3,2-*b*]thieno[2,3-*d*]furan as colorless solid (363.9 mg 1.58 mmol, 79%). ¹H NMR (400 MHz, CDCl₃) δ 7.22 (d, *J* = 5.4 Hz, 1H), 7.28 (d, *J* = 5.4 Hz, 1H), 7.33 (td, *J* = 7.8 Hz, 0.9 Hz, 1H), 7.45 (td, *J* = 7.8, 1.1 Hz, 1H) 7.84 (d, *J* = 7.8 Hz, 1H), 7.92 (d, *J* = 7.8 Hz, 1H); ¹³C NMR (100 MHz, CDCl₃) δ 111.9, 118.0, 118.7, 119.1, 124.0, 124.2, 124.8, 125.0, 125.6, 139.9, 154.4, 161.0; IR (KBr) 3104, 3050, 2961, 1470, 750 cm⁻¹; HRMS (FAB+) *m/z* calcd for C₁₂H₇OS₂ [M + H]⁺ 230.9932, found 230.9937; mp 148.2–148.4 °C.

General Procedure for the Suzuki–Miyaura Coupling



To a solution of [1]benzothieno[3,2-*b*]thieno[2,3-*d*]furan (46.1 mg, 0.20 mmol) in THF (2.0 mL) was added *N*-bromosuccinimide (35.6 mg, 0.22 mmol) at 0 °C. The reaction mixture was warmed to 25 °C and stirred for 24 h. To the resulting mixture were added bis(*tri-tert*-butylphosphine)palladium (5.1 mg, 0.01 mmol), arylboronic acid (0.30 mmol) and NaOH (aq. 1.0 M, 0.40 mL, 0.40 mmol), and the mixture was stirred at 80 °C for 24 h. After being allowed to cool to 25 °C, the resulting mixture was concentrated under reduced pressure. The residue was purified by column chromatography on silica gel and recrystallization.



2-Phenyl[1]benzothieno[3,2-*b*]thieno[2,3-*d*]furan (11a)

The general procedure for the Suzuki–Miyaura coupling was performed with [1]benzothieno[3,2-*b*]thieno[2,3-*d*]furan (46.1 mg, 0.20 mmol), phenylboronic acid (36.6 mg, 0.30 mmol), bis(*tri-tert*-butylphosphine)palladium (5.1 mg, 0.01 mmol) and THF (2.0 mL). The product was purified by column chromatography on silica gel (hexane) and recrystallization (hexane/2-propanol) to give 2-phenyl[1]benzothieno[3,2-*b*]thieno[2,3-*d*]furan as yellow solid (54.5 mg, 0.178 mmol, 89%). ¹H NMR (400

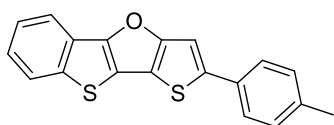
Chapter 3. Synthesis of Benzodithienofuran (BDTF) via Construction of Oxygen-Bridged Bithiophenes Using

3-Bromobenzo[*b*]thiophene 1,1-Dioxide as a Key Compound

MHz, CD₂Cl₂) δ 7.32 (t, *J* = 7.9 Hz, 1H), 7.34 (t, *J* = 7.9 Hz, 1H), 7.42 (t, *J* = 7.4 Hz, 2H), 7.46 (t, *J* = 7.4 Hz, 1H) 7.48 (s, 1H), 7.66 (d, *J* = 7.4 Hz, 2H), 7.86 (d, *J* = 7.9 Hz, 1H), 7.92 (d, *J* = 7.9 Hz, 1H); ¹³C NMR (150 MHz, CD₂Cl₂) δ 108.3, 118.7, 118.8, 119.0, 124.6, 124.7, 125.6, 125.7, 125.8, 128.4, 129.5, 135.1, 140.6, 144.4, 154.4, 161.5; IR (KBr) 3051, 1375, 750, 741, 683 cm⁻¹; HRMS (FAB+) *m/z* calcd for C₁₈H₁₁OS₂ [M + H]⁺ 307.0245, found 307.0236; mp 207.6–207.8 °C.

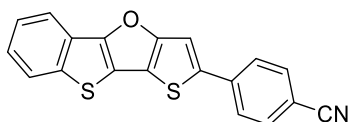
Synthesis of 11a from 9 (1.0 mmol)

The general procedure for the Suzuki–Miyaura coupling was performed with [1]benzothieno[3,2-*b*]thieno[2,3-*d*]furan (230.3 mg, 1.0 mmol), phenylboronic acid (183.0 mg, 1.5 mmol), bis(tri-*tert*-butylphosphine)palladium (25.5 mg, 0.05 mmol) and THF (2.0 mL). The product was purified by column chromatography on silica gel (hexane) and recrystallization (hexane/2-propanol) to give 2-phenyl[1]benzothieno[3,2-*b*]thieno[2,3-*d*]furan as yellow solid (254.2 mg, 0.83 mmol, 83%).



2-(*p*-tolyl)[1]benzothieno[3,2-*b*]thieno[2,3-*d*]furan (11b)

The general procedure for the Suzuki–Miyaura coupling was performed with [1]benzothieno[3,2-*b*]thieno[2,3-*d*]furan (46.1 mg, 0.20 mmol), *p*-tolylboronic acid (40.8 mg, 0.30 mmol), bis(tri-*tert*-butylphosphine)palladium (5.1 mg, 0.01 mmol) and THF (2.0 mL). The product was purified by column chromatography on silica gel (hexane) and recrystallization (hexane/2-propanol) to give 2-(*p*-tolyl)[1]benzothieno[3,2-*b*]thieno[2,3-*d*]furan as yellow solid (60.1 mg, 0.186 mmol, 93%). ¹H NMR (400 MHz, CD₂Cl₂) δ 2.37 (s, 3H), 7.23 (d, *J* = 8.0 Hz, 2H), 7.33 (td, *J* = 7.9, 1.2 Hz, 1H), 7.42 (s, 1H) 7.45 (td, *J* = 7.9, 1.2 Hz, 1H), 7.54 (d, *J* = 8.0 Hz, 2H), 7.85 (d, *J* = 7.9 Hz, 1H), 7.90 (d, *J* = 7.9 Hz, 1H); ¹³C NMR (150 MHz, CD₂Cl₂) δ 21.3, 107.7, 118.2, 118.7, 119.0, 124.5, 124.6, 125.5, 125.6, 125.8, 130.1, 132.2, 138.6, 140.5, 144.6, 154.2, 161.5; IR (KBr) 3096, 3032, 1375, 804, 745 cm⁻¹; HRMS (FAB+) *m/z* calcd for C₁₉H₁₃OS₂ [M + H]⁺ 321.0402, found 321.0401; mp 209.3–210.1 °C.

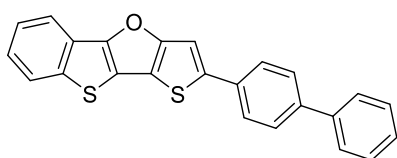


4-([1]benzothieno[3,2-*b*]thieno[2,3-*d*]furan-2-yl)benzonitrile (11c)

The general procedure for the Suzuki–Miyaura coupling was performed with [1]benzothieno[3,2-*b*]thieno[2,3-*d*]furan (46.1 mg, 0.20 mmol), 4-cyanophenylboronic acid (44.1 mg, 0.30 mmol), bis(tri-*tert*-

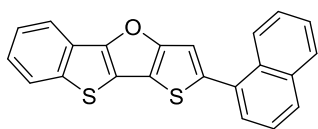
3-Bromobenzo[b]thiophene 1,1-Dioxide as a Key Compound

butylphosphine)palladium (5.1 mg, 0.01 mmol) and THF (2.0 mL). The product was purified by column chromatography on silica gel (hexane) and recrystallization (hexane/2-propanol) to give 4-([1]benzothieno[3,2-*b*]thieno[2,3-*d*]furan-2-yl)benzotrile as yellow solid (53.7 mg, 0.162 mmol, 81%). ¹H NMR (400 MHz, CD₂Cl₂) δ 7.38 (td, *J* = 8.0, 1.2 Hz, 1H), 7.49 (td, *J* = 8.0, 1.2 Hz, 1H), 7.61 (s, 1H), 7.70 (dd, *J* = 6.4, 2.0 Hz, 2H), 7.76 (dd, *J* = 6.4, 2.0 Hz, 2H) 7.88 (d, *J* = 8.0 Hz, 1H), 7.95 (d, *J* = 8.0 Hz, 1H); ¹³C NMR (150 MHz, CD₂Cl₂) δ 110.1, 111.3, 118.6, 119.4, 124.8, 125.1, 125.6, 125.7, 125.9, 133.3, 139.4, 141.0, 141.6, 161.4; IR (KBr) 3390, 2230, 1375, 810, 748 cm⁻¹; HRMS (FAB+) *m/z* calcd for C₁₉H₁₀NOS₂ [M + H]⁺ 332.0198, found 332.0198; mp 281.3–281.9 °C.



2-([1,1'-biphenyl]-4-yl)[1]benzothieno[3,2-*b*]thieno[2,3-*d*]furan (11d)

The general procedure for the Suzuki–Miyaura coupling was performed with [1]benzothieno[3,2-*b*]thieno[2,3-*d*]furan (46.1 mg, 0.20 mmol), 4-biphenylboronic acid (59.4 mg, 0.30 mmol), bis(tri-*tert*-butylphosphine)palladium (5.1 mg, 0.01 mmol) and THF (2.0 mL). The product was purified by column chromatography on silica gel (hexane) and recrystallization (hexane/2-propanol) to give 2-([1,1'-biphenyl]-4-yl)[1]benzothieno[3,2-*b*]thieno[2,3-*d*]furan as yellow solid (59.7 mg, 0.156 mmol, 78%). ¹H NMR (400 MHz, CD₂Cl₂) δ 7.36 (t, *J* = 8.3 Hz 1H), 7.38 (t, *J* = 6.8 Hz, 1H), 7.47 (t, *J* = 6.8 Hz, 2H), 7.48 (t, *J* = 8.0 Hz 1H) 7.55 (s, 1H), 7.66 (d, *J* = 6.8 Hz 1H), 7.67 (d, *J* = 6.8 Hz, 1H), 7.69 (d, *J* = 8.6 Hz, 2H), 7.77 (d, *J* = 8.6 Hz, 2H), 7.88 (d, *J* = 8.0 Hz, 1H), 7.94 (d, *J* = 8.3 Hz, 1H); IR (KBr) 3050, 3032, 1375, 760, 746 cm⁻¹; HRMS (FAB+) *m/z* calcd for C₂₄H₁₅OS₂ [M + H]⁺ 383.0558, found 383.0549; mp > 300 °C.

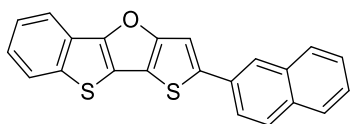


2-(naphthalen-1-yl)[1]benzothieno[3,2-*b*]thieno[2,3-*d*]furan (11e)

The general procedure for the Suzuki–Miyaura coupling was performed with [1]benzothieno[3,2-*b*]thieno[2,3-*d*]furan (46.1 mg, 0.20 mmol), 1-naphthalenboronic acid (51.6 mg, 0.30 mmol), bis(tri-*tert*-butylphosphine)palladium (5.1 mg, 0.01 mmol) and THF (2.0 mL). The product was purified by column chromatography on silica gel (hexane) and recrystallization (hexane/2-propanol) to give 2-(naphthalen-1-yl)[1]benzothieno[3,2-*b*]thieno[2,3-*d*]furan as yellow solid (62.0 mg, 0.174 mmol, 87%). ¹H NMR (400 MHz, CD₂Cl₂) δ 7.36 (td, *J* = 7.7, 0.8 Hz 1H), 7.44 (s, 1H), 7.48 (td, *J* = 7.7, 0.8 Hz, 1H), 7.53 (d, *J* = 4.8 Hz, 1H),

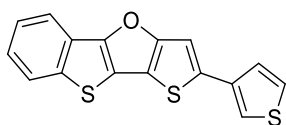
3-Bromobenzo[b]thiophene 1,1-Dioxide as a Key Compound

7.55 (t, $J = 6.7$ Hz, 1H), 7.55 (d, $J = 6.7$ Hz, 1H), 7.66 (dd, $J = 6.7, 1.2$ Hz, 1H), 7.89 (d, $J = 8.4$ Hz, 1H), 7.92 (d, $J = 8.4$ Hz, 1H), 7.91-7.96 (m, 1H), 7.96 (d, $J = 4.8$ Hz, 1H), 8.31-8.36 (m, 1H); ^{13}C NMR (150 MHz, CD_2Cl_2) δ 112.8, 118.7, 119.1, 119.5, 124.6, 124.7, 125.6, 125.7, 125.8, 125.9, 126.6, 127.2, 128.81, 128.83, 129.3, 132.0, 132.9, 134.3, 140.5, 141.8, 154.1, 161.0; IR (KBr) 3090, 3053, 1381, 787, 743 cm^{-1} ; HRMS (FAB+) m/z calcd for $\text{C}_{22}\text{H}_{13}\text{OS}_2$ [$\text{M} + \text{H}$] $^+$ 357.0402, found 357.0388; mp 204.4–204.9 $^\circ\text{C}$.



2-(naphthalen-2-yl)[1]benzothieno[3,2-b]thieno[2,3-d]furan (11f)

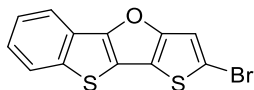
The general procedure for the Suzuki–Miyaura coupling was performed with [1]benzothieno[3,2-*b*]thieno[2,3-*d*]furan (46.1 mg, 0.20 mmol), 2-naphthalenboronic acid (51.6 mg, 0.30 mmol), bis(tri-*tert*-butylphosphine)palladium (5.1 mg, 0.01 mmol) and THF (2.0 mL). The product was purified by column chromatography on silica gel (hexane) and recrystallization (hexane/2-propanol) to give 2-(naphthalen-2-yl)[1]benzothieno[3,2-*b*]thieno[2,3-*d*]furan as yellow solid (65.6 mg, 0.184 mmol, 92%). ^1H NMR (400 MHz, CD_2Cl_2) δ 7.35 (td, $J = 7.6, 1.2$ Hz 1H), 7.46 (td, $J = 7.6, 1.2$ Hz 1H), 7.48 (td, $J = 6.8, 1.2$ Hz 1H), 7.52 (d, $J = 6.8, 1.2$ Hz 1H), 7.61 (s, 1H), 7.79 (dd, $J = 8.6, 1.7$ Hz, 1H), 7.82-7.91 (m, 4H), 7.93 (d, $J = 7.6$ Hz, 1H), 8.11 (d, $J = 1.7$ Hz, 1H); ^{13}C NMR (150 MHz, CD_2Cl_2) δ 108.6, 118.7, 118.9, 119.0, 123.96, 123.97, 124.6, 124.7, 125.6, 125.8, 126.7, 127.2, 128.1, 128.4, 129.2, 132.5, 133.4, 134.0, 140.6, 144.3, 154.5, 161.5; IR (KBr) 3049, 3032, 1375, 804, 741 cm^{-1} ; HRMS (FAB+) m/z calcd for $\text{C}_{22}\text{H}_{13}\text{OS}_2$ [$\text{M} + \text{H}$] $^+$ 357.0402, found 357.0389; mp 232.5–233.2 $^\circ\text{C}$.



2-(thiophen-3-yl)[1]benzothieno[3,2-b]thieno[2,3-d]furan (11g)

The general procedure for the Suzuki–Miyaura coupling was performed with [1]benzothieno[3,2-*b*]thieno[2,3-*d*]furan (46.1 mg, 0.20 mmol), 3-thienylboronic acid (38.4 mg, 0.30 mmol), bis(tri-*tert*-butylphosphine)palladium (5.1 mg, 0.01 mmol) and THF (2.0 mL). The product was purified by column chromatography on silica gel (hexane) and recrystallization (hexane/2-propanol) to give 2-(thiophen-3-yl)[1]benzothieno[3,2-*b*]thieno[2,3-*d*]furan as yellow solid (52.5 mg, 0.168 mmol, 84%). ^1H NMR (400 MHz, CD_2Cl_2) δ 7.34 (td, $J = 7.5, 1.2$ Hz 1H), 7.35 (s, 1H), 7.37 (dd, $J = 5.2, 1.2$ Hz 1H), 7.42 (dd, $J = 5.2, 2.9$ Hz 1H), 7.45 (t, $J = 8.0$ Hz 1H), 7.48 (dd, $J = 2.9, 1.2$ Hz, 1H), 7.85 (d, $J = 8.0$ Hz, 1H), 7.90 (d, $J = 7.5$ Hz, 1H); ^{13}C NMR (150 MHz, CD_2Cl_2) δ 108.3, 118.0, 118.6, 119.0, 120.1, 124.5, 124.7, 125.6, 125.8, 126.0, 127.3,

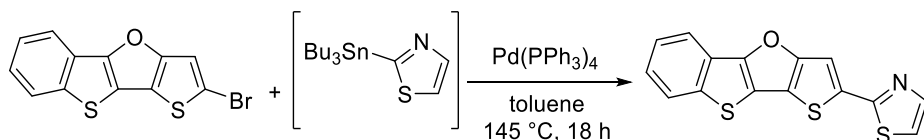
136.4, 139.2, 140.5, 154.3, 161.1; IR (KBr) 3098, 3086, 1379, 770, 745 cm^{-1} ; HRMS (FAB+) m/z calcd for $\text{C}_{18}\text{H}_9\text{OS}_3$ $[\text{M} + \text{H}]^+$ 312.9810, found 312.9804; mp 213.7–214.1 $^\circ\text{C}$



2-Bromobenzo[4,5]thieno[3,2-*b*]thieno[2,3-*d*]furan (10)

To a solution of benzo[4,5]thieno[3,2-*b*]thieno[2,3-*d*]furan (246.4 mg, 1.0 mmol) in THF (4.0 mL) was added *N*-bromosuccinimide (195.78 mg, 1.1 mmol) at 0 $^\circ\text{C}$. The reaction mixture was warmed to 25 $^\circ\text{C}$ and stirred for 18 h. Into the resulting mixture were added H_2O (10 mL) and the mixture was extracted with EtOAc (3×10 mL). The combined organic phase was dried over magnesium sulfate, filtered, and concentrated under reduced pressure. The residue was purified by column chromatography on silica gel (hexane) to give 2-bromobenzo[4,5]thieno[3,2-*b*]thieno[2,3-*d*]furan as colorless solid (284.5 mg, 0.92 mmol, 92%). ^1H NMR (400 MHz, CDCl_3) δ : δ 7.27 (s, 1H), 7.35 (t, $J=7.8$ Hz, 1H), 7.45 (t, $J=7.8$ Hz, 1H), 7.83 (d, $J=7.8$ Hz, 1H), 7.90 (d, $J=7.8$ Hz, 1H); ^{13}C NMR (150 MHz, CDCl_3) δ 112.1, 115.2, 117.8, 118.8, 119.5, 124.2, 124.4, 125.2, 125.3, 140.0, 153.8, 158.1; IR (KBr) 3117, 3044, 2361, 848, 748 cm^{-1} ; HRMS (FAB+) m/z calcd for $\text{C}_{12}\text{H}_5\text{BrOS}_2$ $[\text{M}]^+$ 309.8939, found 309.8920; mp 169.0–169.7 $^\circ\text{C}$.

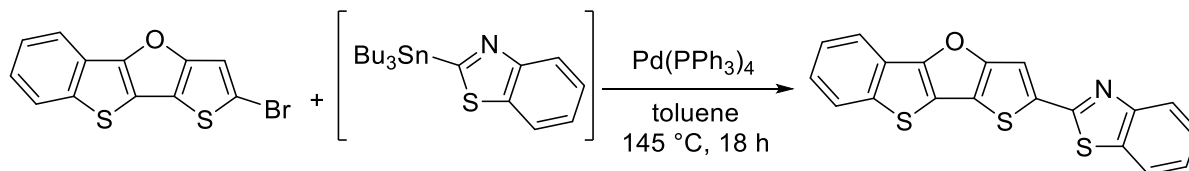
2-(Benzo[4,5]thieno[3,2-*b*]thieno[2,3-*d*]furan-2-yl)thiazole (11h)



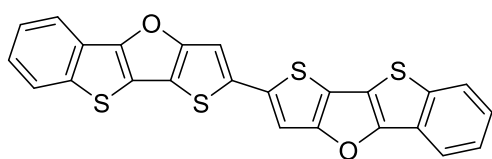
To a solution of 2-bromothiazole (114.8 mg, 0.7 mmol) in THF (4.0 mL) was added dropwise *n*-BuLi (1.55 M, 0.50 mL, 0.77 mmol) at -78 $^\circ\text{C}$. After being stirred for 1 h, tri-*n*-butylstannyl chloride (273.4 mg, 0.84 mmol) was added to the solution at the same temperature. The reaction mixture was warmed to 25 $^\circ\text{C}$ and stirred for 18 h. After filtration, THF was removed under vacuum, and toluene (10.0 mL) was added. To the solution were then added a 2-bromobenzo[4,5]thieno[3,2-*b*]thieno[2,3-*d*]furan (123.7 mg, 0.4 mmol) and tetrakis(triphenylphosphine)palladium (23.1 mg, 0.02 mmol), and the mixture was stirred at 140 $^\circ\text{C}$ for 18 h. After being allowed to cool to 25 $^\circ\text{C}$, the resulting mixture was concentrated under reduced pressure. The residue was purified by column chromatography on silica gel (hexane/EtOAc = 4/1) to give 2-(benzo[4,5]thieno[3,2-*b*]thieno[2,3-*d*]furan-2-yl)thiazole as yellow solid (88.9 mg, 0.28 mmol, 71%). ^1H NMR (400 MHz, CD_2Cl_2) δ 7.34 (d, $J=3.2$ Hz, 1H), 7.38 (td, $J=7.8, 1.3$ Hz, 1H), 7.48 (td, $J=7.8, 1.3$ Hz, 1H), 7.65 (s, 1H), 7.77 (d, $J=3.2$ Hz, 1H), 7.88 (d, $J=7.8$ Hz, 1H), 7.94 (d, $J=7.8$ Hz, 1H); ^{13}C NMR (150 MHz, CDCl_3) δ 111.1, 118.5, 119.0, 119.4, 121.3, 124.7, 125.1, 125.6, 125.7, 136.7, 141.0, 143.7, 155.7, 160.4, 162.3; IR (KBr) 3103, 3057, 2361, 750, 721 cm^{-1} ; HRMS (FAB+) m/z calcd for $\text{C}_{15}\text{H}_8\text{NOS}_3$ $[\text{M}]^+$ 313.9762,

found 313.9769; mp 212.5–213.1 °C.

2-(Benzo[4,5]thieno[3,2-*b*]thieno[2,3-*d*]furan-2-yl)benzo[*d*]thiazole (11i)



To a solution of 2-bromobenzo[*d*]thiazole (149.9 mg, 0.7 mmol) in THF (4.0 mL) was added dropwise *n*-BuLi (1.55 M, 0.50 mL, 0.77 mmol) at -78 °C. After being stirred for 1 h, tri-*n*-butylstannyl chloride (273.4 mg, 0.84 mmol) was added to the solution at the same temperature. The reaction mixture was warmed to 25 °C and stirred for 18 h. After filtration, THF was removed under vacuum, and toluene (10.0 mL) was added. To the solution were then added a 2-bromobenzo[4,5]thieno[3,2-*b*]thieno[2,3-*d*]furan (123.7 mg, 0.4 mmol) and tetrakis(triphenylphosphine)palladium (23.1 mg, 0.02 mmol), and the mixture was stirred at 140 °C for 18 h. After being allowed to cool to 25 °C, the resulting mixture was concentrated under reduced pressure. The residue was purified by column chromatography on silica gel (hexane/CH₂Cl₂ = 2/1) to give 2-(benzo[4,5]thieno[3,2-*b*]thieno[2,3-*d*]furan-2-yl)benzo[*d*]thiazole as yellow solid (82.9 mg, 0.23 mmol, 57%). ¹H NMR (400 MHz, CDCl₃) δ 7.37 (t, *J* = 8.0 Hz, 2H), 7.47 (t, *J* = 7.6 Hz, 1H), 7.49 (t, *J* = 7.6 Hz, 1H), 7.75 (s, 1H), 7.77 (d, *J* = 8.0 Hz, 2H), 7.88 (d, *J* = 7.8 Hz, 1H), 7.96 (d, *J* = 7.6 Hz, 1H), 8.04 (d, *J* = 7.6 Hz, 1H); ¹³C NMR (150 MHz, CDCl₃) δ 112.5, 118.1, 119.3, 121.4, 122.7, 123.1, 124.4, 125.0, 125.28, 125.31, 125.4, 126.6, 134.8, 136.0, 141.0, 153.8, 156.0, 160.1, 161.4; IR (KBr) 3048, 2922, 1431, 750, 721 cm⁻¹; HRMS (FAB+) *m/z* calcd for C₁₉H₁₀NOS₃ [M+H]⁺ 363.9919, found 363.9930; mp 220.2–220.9 °C.



2,2'-bis(benzo[4,5]thieno[3,2-*b*]thieno[2,3-*d*]furan) (11j)

To a solution of 2-bromobenzo[4,5]thieno[3,2-*b*]thieno[2,3-*d*]furan (691.5 mg, 3.0 mmol) in toluene (12.0 mL) were added bis(tributyltin) (1.04 g, 1.8 mmol) and tetrakis(triphenylphosphine)palladium (173.3mg, 0.15 mmol) The mixture was warmed up to 140 °C and stirred for 24 h. After being allowed to cool to 25 °C, the desired product was collected by filtration, washed with hexane, Et₂O, H₂O to give 2,2'-bis(benzo[4,5]thieno[3,2-*b*]thieno[2,3-*d*]furan) as orange solid (559.5 mg, 1.22 mmol, 81%). Further purification by gradient sublimation for OFET characterization (174.3 mg, 0.57 mmol, 38%). This material was insufficiently soluble to obtain useful ¹H and ¹³C NMR spectra. Anal. Calcd for C₂₄H₁₀O₂S₄: C 62.86, H 2.20, Found: C 62.56, H 2.11; IR (KBr) 3075, 2361, 1379, 791, 748 cm⁻¹; HRMS (FAB+) *m/z* calcd for

*Chapter 3. Synthesis of Benzodithienofuran (BDTF) via Construction of Oxygen-Bridged Bithiophenes
Using*

3-Bromobenzo[b]thiophene 1,1-Dioxide as a Key Compound

$C_{24}H_{11}O_2S_4$ [M+H]⁺ 458.9636, found 458.9644; mp > 300 °C.

1. X-ray Crystallography

Details of the crystal data and a summary of the intensity data collection parameters for **9** are listed in Table S1 and Figure S1 **11j** are listed in Table S2 and Figure S2. X-ray single crystal analysis was conducted with a Rigaku VariMax with Saturn. Graphite-monochromated Mo K α radiation ($\lambda = 0.71075 \text{ \AA}$) was used. The structure was solved by direct methods with SIR2014¹⁴ and refined by full-matrix least-squares techniques against F^2 (SHELXL-2014).¹⁵ The non-hydrogen atoms were refined anisotropically. Hydrogen atoms were placed using AFIX instructions. All calculations were performed by using Yadokari-XG¹⁶ and the ORTEP illustration was drawn by ORTEP-3¹⁷ and colored by Adobe Illustrator.

Table S1. Crystal data and structure refinement for **9**

Empirical formula	C ₁₂ H ₆ OS ₂	
Formula weight	230.29	
Temperature	120(2) K	
Wavelength	0.71075 Å	
Crystal system	Orthorhombic	
Space group	Pbca (#61)	
Unit cell dimensions	$a = 5.541(4)$ Å	$\alpha = 90^\circ$.
	$b = 15.387(12)$ Å	$\beta = 90^\circ$.
	$c = 22.574(18)$ Å	$\gamma = 90^\circ$.
Volume	1925(3) Å ³	
Z	8	
Density (calculated)	1.589 Mg/m ³	
Absorption coefficient	0.515 mm ⁻¹	
F(000)	944	
Crystal size	0.170 x 0.070 x 0.010 mm ³	
Theta range for data collection	3.205 to 31.481°.	
Index ranges	-6 ≤ h ≤ 7, -22 ≤ k ≤ 21, -31 ≤ l ≤ 31	
Reflections collected	24401	
Independent reflections	2950 [R(int) = 0.1578]	
Completeness to theta = 25.242°	98.6 %	
Absorption correction	Semi-empirical from equivalents	
Max. and min. transmission	1.000 and 0.817	
Refinement method	Full-matrix least-squares on F ²	
Data / restraints / parameters	2950 / 0 / 136	
Goodness-of-fit on F ²	1.429	
Final R indices [I > 2σ(I)]	$R_1 = 0.1594$, $wR_2 = 0.2392$	
R indices (all data)	$R_1 = 0.1777$, $wR_2 = 0.2467$	
Extinction coefficient	n/a	
Largest diff. peak and hole	0.543 and -0.598 e.Å ⁻³	

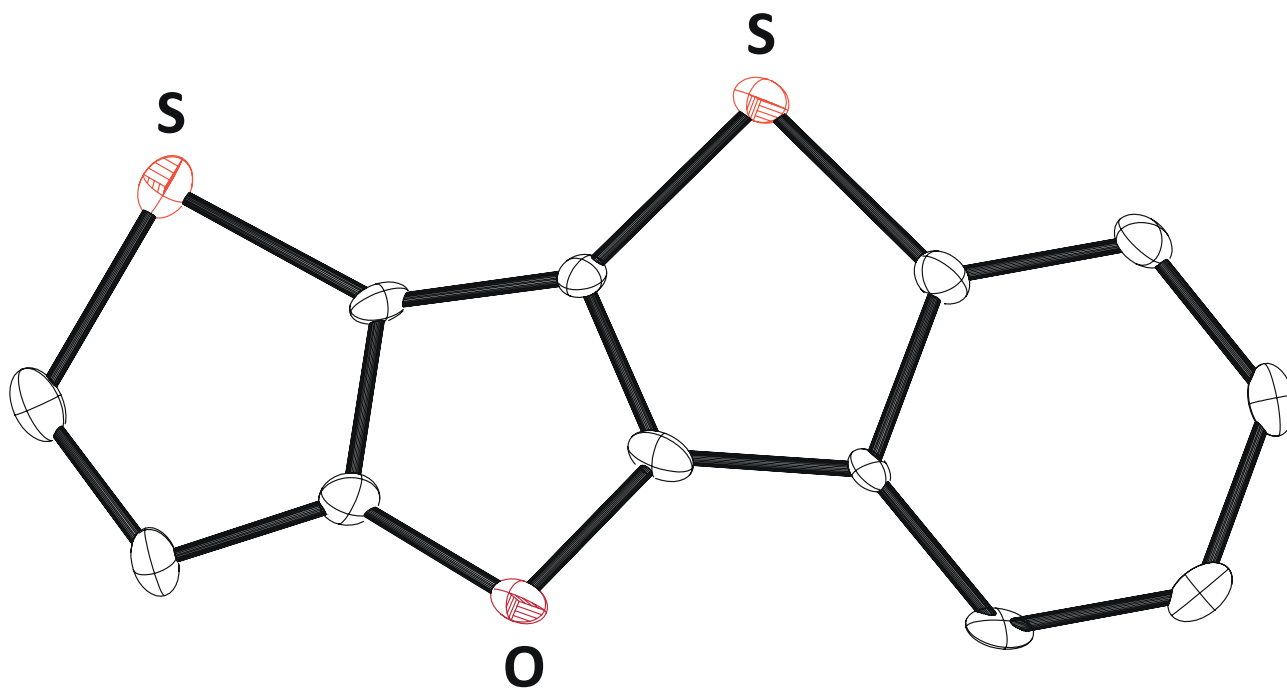


Figure S1. ORTEP drawing of **9** with 50% thermal ellipsoids; hydrogen atoms were omitted for clarity.

Table S2. Crystal data and structure refinement for **11j**

Identification code	CCDC:1577850	
Empirical formula	C ₂₄ H ₁₀ O ₂ S ₄	
Formula weight	458.56	
Temperature	100(2) K	
Wavelength	0.71075 Å	
Crystal system	Orthorhombic	
Space group	P2 ₁ 2 ₁ 2 ₁ (#19)	
Unit cell dimensions	$a = 5.733(5)$ Å	$\alpha = 90^\circ$.
	$b = 11.845(11)$ Å	$\beta = 90^\circ$.
	$c = 27.81(3)$ Å	$\gamma = 90^\circ$.
Volume	1889(3) Å ³	
Z	4	
Density (calculated)	1.613 Mg/m ³	
Absorption coefficient	0.524 mm ⁻¹	
F(000)	936	
Crystal size	0.200 x 0.090 x 0.020 mm ³	
Theta range for data collection	1.464 to 30.775°.	
Index ranges	-8 ≤ h ≤ 8, -16 ≤ k ≤ 16, -37 ≤ l ≤ 39	
Reflections collected	16927	
Independent reflections	5238 [R(int) = 0.1210]	
Completeness to theta = 25.242°	97.9 %	
Absorption correction	Semi-empirical from equivalents	
Max. and min. transmission	1.000 and 0.496	
Refinement method	Full-matrix least-squares on F ²	
Data / restraints / parameters	5238 / 481 / 272	
Goodness-of-fit on F ²	1.025	
Final R indices [I > 2σ(I)]	R ₁ = 0.0925, wR ₂ = 0.2231	
R indices (all data)	R ₁ = 0.1131, wR ₂ = 0.2514	
Absolute structure parameter	0.06(13)	
Extinction coefficient	0.089(11)	
Largest diff. peak and hole	1.488 and -0.909 e.Å ⁻³	

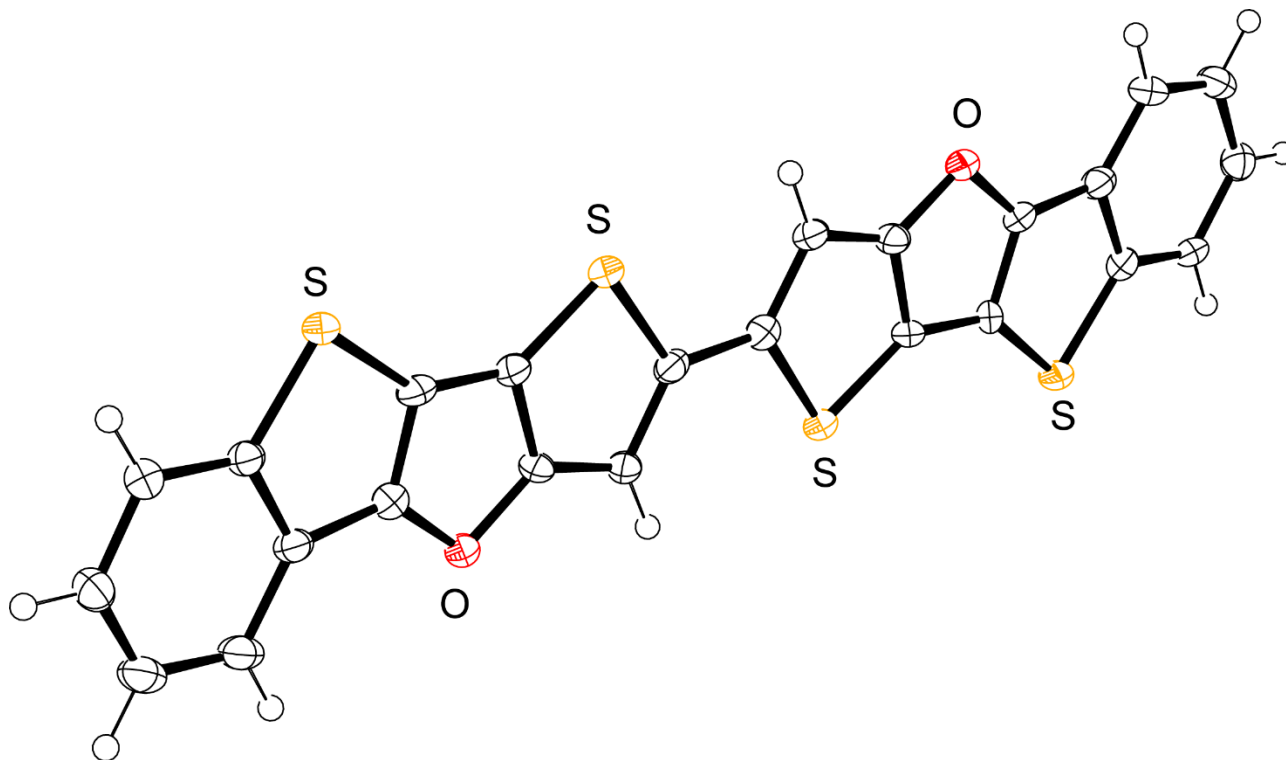


Figure S2. ORTEP drawing of 11j with 50% thermal ellipsoids

References

- (1) For reviews, see: (a) Takimiya, K.; Shinamura, S.; Osaka, I.; Miyazaki, E. *Adv. Mater.* **2011**, *23*, 4347–4370. (b) Rasmussen, S. C.; Evenson, S. J. *Prog. Polym. Sci.* **2013**, *38*, 1773–1804. (c) Ohshita, J. *Macromol. Chem. Phys.* **2009**, *210*, 1360–1370. (d) Romero-Nieto, C.; Baumgartner, T. *Synlett* **2013**, *24*, 920–937.
- (2) (a) Karminski-Zamola, G. M.; Malesevic, M.; Bajic, M.; Golja, G. *Croat. Chem. Acta* **1993**, *65*, 847–849. (b) Kozmik, V.; Poznik, M.; Svoboda, J.; Frere, P. *Tetrahedron Lett.* **2015**, *56*, 6251–6253.
- (3) (a) Kaida, H.; Satoh, T.; Hirano, K.; Miura, M. *Chem. Lett.* **2015**, *44*, 1125–1127. (b) Saito, K.; Chikkade, P. K.; Kanai, M.; Kuninobu, Y. *Chem. Eur. J.* **2015**, *21*, 8365–8368. (c) Kaida, H.; Satoh, T.; Nishii, Y.; Hirano, K. Miura, M. *Chem. Lett.* **2016**, *45*, 1069–1071.
- (4) Youg, Q.; Hongtao, F.; Xing, W.; Lian, D.; Xueyan, R. WO2014075382
- (5) (a) Burgos, C. H.; Barder, T. E.; Huang, X.; Buchwald, S. L. *Angew. Chem., Int. Ed.* **2006**, *45*, 4321–4326. (b) Anderson, K. W.; Ikawa, T.; Tundel, R. E.; Buchwald, S. L. *J. Am. Chem. Soc.* **2016**, *128*, 10694–10695.
- (6) (a) Altman, R. A.; Buchwald, S. L. *Org. Lett.* **2007**, *9*, 643–646. (b) Zhang, J.; Wu, J.; Xiong, Y.; Cao, S. *Chem. Commun.* **2012**, *48*, 8553–8555.
- (7) Itami, K.; Yamaguchi, J.; Yamaguchi, A.; Mandal, D. *J. Am. Chem. Soc.* **2011**, *133*, 19660–19663.
- (8) McNab, H.; Hunter, G. A. *New J. Chem.* **2010**, *34*, 2558–2563.
- (9) (a) Lee, S. Y.; Hartwig, J. F. *J. Am. Chem. Soc.* **2016**, *138*, 15278–15284. (b) Lotz, M. D.; Camasso, N. M.; Canty, A. J.; Sanford, M. S. *Organometallics* **2017**, *36*, 165–171.
- (10) (a) Bordwell, F. G.; Albisetti, C. J., Jr. *J. Am. Chem. Soc.* **1948**, *70*, 1558–1560. (b) Nanson, L.; Blouin, N.; Mitchell, W. *PCT Int. Appl.* **2015**, WO 2015139802 A1 20150924.
- (11) Mandal, D.; Yamaguchi, A.; Yamaguchi, J.; Itami, K. *J. Am. Chem. Soc.* **2011**, *133*, 19660–19663.
- (12) Li, W.; Lu, L.; Qu, J.; Pan, W.; Wu, S.; Yang, J.; Li, Z. *Zhongguo Yaowu Huaxue Zazhi* **2011**, *21*, 345–351.
- (13) (a) Zednik, J.; Sedlacek, J.; Svoboda, J.; Vohlidal, J.; Bondarev, D.; Cisarova, I. *Collect. Czech. Chem. Commun.* **2008**, *73*, 1205–1221. (b) Kostas, I. D.; Vallianatou, K. A.; Kyritsis, P.; Zednik, J.; Vohlidal, J. *Inorg. Chim. Acta* **2004**, *357*, 3084–3088.
- (14) *SIR2014*, Burla, M. C.; Caliandro, R.; Carrozzini, B.; Cascarano, G. L.; Cuocci, C.; Giacovazzo, C.; Mallamo, M.; Mazzone, A.; Polidori, G. *Appl. Cryst.* **2015**, *48*, 306–309.
- (15) *SHELX*, Program for the Solution of Crystal Structures (a) Sheldrick, G. M.; University of Göttingen: Göttingen, Germany, 2014. (b) Sheldrick, G.M. *Acta Cryst.* **2008**, *A64*, 112–122.
- (16) Yadokari-XG, Software for Crystal Structure Analyses, K. Wakita (2001); Release of Software (Yadokari-XG 2009) for Crystal Structure Analyses, Kabuto, C.; Akine, S.; Nemoto, T.; Kwon, E. *J.*

*Chapter 3. Synthesis of Benzodithienofuran (BDTF) via Construction of Oxygen-Bridged Bithiophenes
Using*

3-Bromobenzo[b]thiophene 1,1-Dioxide as a Key Compound

Cryst. Soc. Jpn. **2009**, *51*, 218–224.

(17) Farrugia, L. J. *J. Appl. Cryst.* **2012**, *45*, 849–854.

*Chapter 3. Synthesis of Benzodithienofuran (BDTF) via Construction of Oxygen-Bridged Bithiophenes
Using
3-Bromobenzo[b]thiophene 1,1-Dioxide as a Key Compound*

Chapter 4. Synthesis of Benzodithienothiophene (BDTT) via Construction of Sulfur-Bridged Bithiophenes Using 3-Bromobenzo[*b*]thiophene 1,1-Dioxide as a Key Compound

4-1.	Abstract	80
4-2.	Introduction	80
4-3.	Synthesis of Dithienyl Thioether Dioxides by addition-elimination reaction	82
4-4.	Synthesis of Benzodithienothiophene (BDTT) by Reduction following by Pd-catalyzed Intramolecular Cyclization	84
4-5.	Synthesis of BDTT by Pd-catalyzed Intramolecular Cyclization following by Reduction	85
4-6.	Transformation of π -Extended BDTT	87
4-7.	Conclusion	87
4-8.	Experimental Section and Analytical Data	88
	References	92

4-1. Abstract

The author developed an efficient synthetic method of [1]benzothieno[3,2-*b*]thieno[2,3-*d*]thiophene (BDTT) by addition-elimination reaction using 3-bromobenzo[*b*]thiophene 1,1-dioxides as key compounds following by reduction and Pd-catalyzed intramolecular C–H functionalization. This method has been established by applying the synthetic approach of BDTF was described in Chapter 3. Furthermore, obtained BDTT was easily transformed to π -extended BDTTs by a bromination reaction and subsequent Suzuki–Miyaura cross-coupling.

4-2. Introduction

Recently, conjugated organic materials have been attracting interest due to their role in organic thin film transistors (OFETs) and organic photovoltaics (OPVs).¹ In particular, DTTs (dithienothiophenes) have been used widely to build functional materials such as *p*-type semiconductors for OFETs, due to their planar, electron-rich, rigid, conjugated, and highly thermal- and photostable structures.² For instance, dibenzo[*d,d'*]thieno[3,2-*b*;4,5-*b'*]dithiophene (DBTDT) and bisbenzo[*d,d'*]thieno[3,2-*b*:4',5'-*b'*]dithiophenes) (BBTDT) exhibited hole mobilities of 0.51 and 0.15 cm²V⁻¹s⁻¹, respectively (Figure 1).^{3,4a}

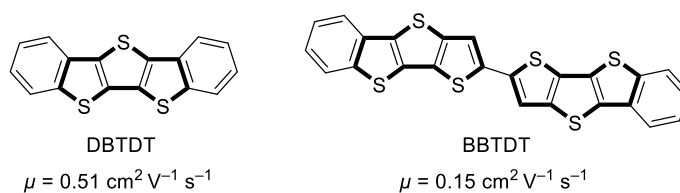
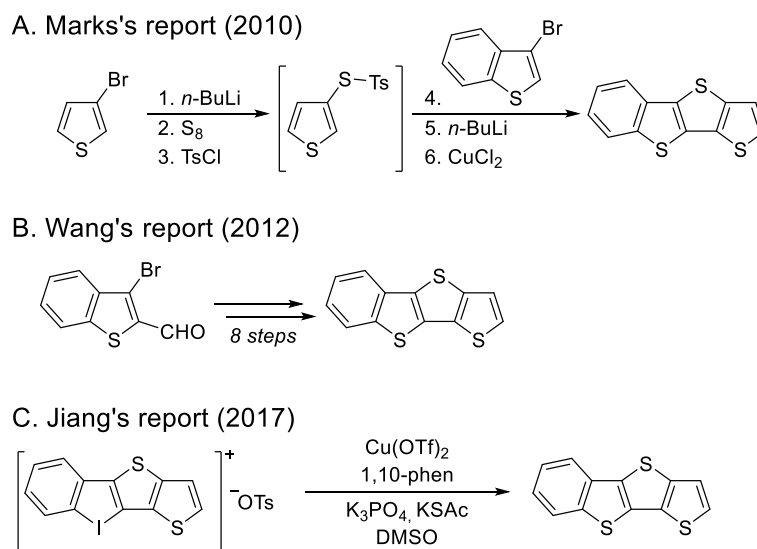


Figure 1. Representative DTTs

Focusing on the synthetic method of BBTDT, BBTDT is synthesized from BDTT by Stille–Kelly coupling. Several methods have been reported for the synthesis of BDTT. Marks and co-workers reported the first synthesis of BDTT.^{4a} They achieved the one-pot synthesis of BDTT via *S*-(thiophen-3-yl) 4-methylbenzenesulfonothioate as a synthetic intermediate (Scheme 1A). Wang and co-workers achieved the synthesis of BDTT from 3-bromobenzo[*b*]thiophene-2-carbaldehyde in 8 steps (Scheme 1B).^{4b} Jiang and co-workers also achieved the synthesis of BDTT from diaryliodonium salt via intramolecular sulfur–iodine exchange (Scheme 1C).^{4c} However, these reported methods are not inefficient method due to problems with the number of steps and yield. Meanwhile, the author recently achieved the synthesis of [1]benzothieno[3,2-*b*]thieno[2,3-*d*]furan (BDTF), which is an analog of BDTT, by addition-elimination reaction using 3-bromobenzo[*b*]thiophene 1,1-dioxides as key compounds following by reduction and Pd-catalyzed intramolecular C–H functionalization (Scheme 2A). An addition–elimination reaction, which is the key reaction of this method, has the potential to apply various nucleophiles other than 3-hydroxythiophene to the substrate. Therefore, the author considered that an addition–elimination reaction could proceed using 3-mercaptothiophene as a substrate. The author also assumed that the dithienyl thioether dioxide (DTT-dioxide)

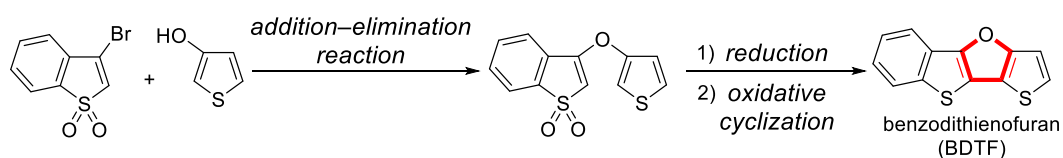
obtained by this reaction can be efficiently converted to BDTT by reduction and Pd-catalyzed intramolecular C–H functionalization (Scheme 2B). Thus, the author aimed to develop an efficient synthetic method of BDTT by applying the synthetic strategy of BDTF.

Scheme 1. Reported synthetic methods of BDTTs

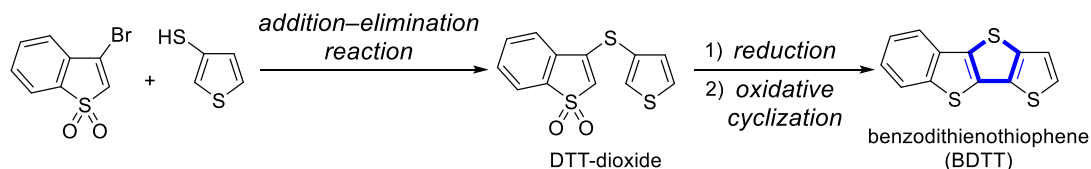


Scheme 2. Previous and This work

A. Previous Work: Synthesis of **BDTF**



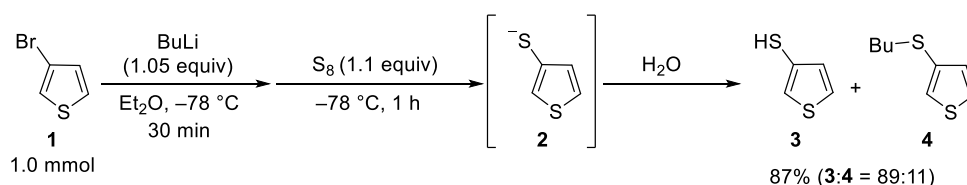
B. This Work: Synthesis of **BDTT**



4-3. Synthesis of Dithienyl Thioether Dioxides by addition-elimination reaction

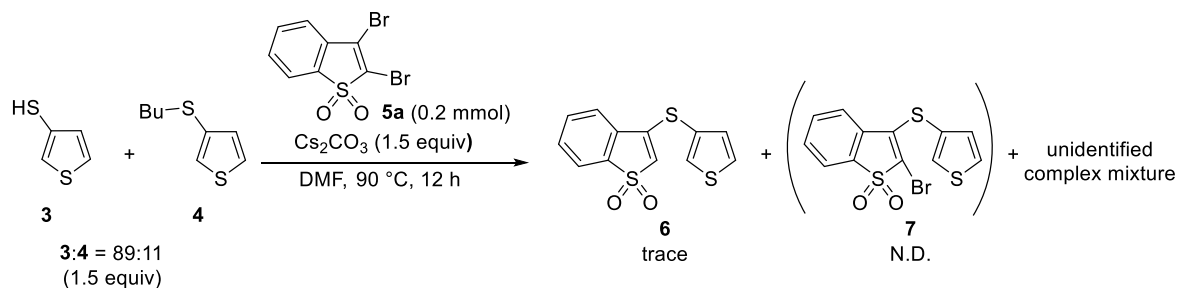
Initially, the author examined to synthesize the substrate 3-mercaptothiophene (**3**) (Scheme 3). BuLi was allowed to act on 3-bromothiophene (**1**) at a reaction temperature of $-78\text{ }^{\circ}\text{C}$ to carry out the lithium-halogen exchange reaction, and then S_8 was allowed to act, and then quenched with H_2O . As a result, the reaction proceeded and the target product **3** was obtained. However, small amounts of byproduct **4** was also produced by the nucleophilic addition of butyl bromide and 3-thienylthiolate (**2**) present in the reaction system. Since it was difficult to isolate **3** and **4**, the author decided to use a mixture with a production ratio of **3**:**4** = 89:11 as a reactant in the addition elimination reaction.

Scheme 3. Synthesis of 3-mercaptothiophene (**3**)



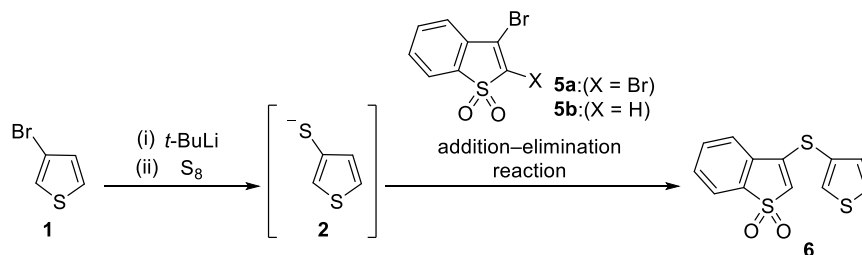
Next, the author attempted to synthesize DTT-dioxides (**6** or **7**) by addition-elimination reaction using the mixture of **3** and **4** (Scheme 4), but only a trace amount of the target compound **6** was obtained, and an unidentifiable mixture was obtained as the major product.

Scheme 4. Synthesis of DTT-dioxides (**6** or **7**) by addition elimination reaction



The problems in the above examinations are shown below. (i) **4** was obtained as a byproduct in the synthesis of **3**. (ii) The addition-elimination reaction using **3** as a substrate did not proceed efficiently. The author assumed that the solution to problem (i) could be solved by using 2 equivalents of *t*-BuLi instead of 1 equivalent of BuLi. One reason of problem (ii) would be dimerization of **3** to give 3,3'-bis(thienyl) disulfide under the conditions. Therefore, the author assumed that by using **2** prepared from **1** as a substrate, unintended side reactions could be suppressed and the addition-elimination reaction could proceed efficiently (Scheme 5). If the reaction proceeds using this methodology, it will lead to the reduction of the synthesis process of **3**.

Scheme 5. Synthetic approach of DTT-dioxide (**6**)



Following the approach described above, the author examined to synthesize DTT-dioxide (**6**) by addition–elimination reaction using **2** as a substrate (Table 1). In Et₂O, *t*-BuLi was allowed to act on **1** at –78 °C to perform lithium-halogen exchange reaction, then S₈ was allowed to act and the mixture was stirred for 1 hour, and then 2,3-dibromobenzo[*b*]thiophene 1,1-dioxides (**5a**) was added, the temperature was raised to room temperature, and the mixture was stirred for 15 hours, **6** was obtained in 72% yield (entry 1). The reaction proceeded even when 3-bromobenzo[*b*]thiophene 1,1-dioxides (**5b**) was used as a substrate, and **6** was obtained in 74% (entry 2). the reaction time could be shortened from 15 hours to 6 hours by raising the reaction temperature after adding **5b** (entry 3). Furthermore, even when the scale-up was performed, the **6** was obtained with a similar yield.

Table 1. Synthesis of DTT-dioxide (**6**) by addition elimination reaction using **2** as a substrate ^a

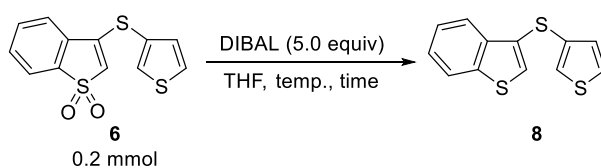
entry	X	temp (°C)	time (h)	yield (%) ^a
1	Br	–78 to 25	15	72
2	H	–78 to 25	15	74
3	H	0 to 45	6.5	78 (76) ^b

^a Reaction conditions: **5a** or **5b** (1.3 equiv), Et₂O (1.0 mL), 3-thienylthiolate (**2**) was generated by allowing S₈ (1.1 equiv) to act after the reaction of 3-bromothiophene (1.0 mmol) and *t*-BuLi (2.1 equiv). Isolated yield. ^b Performed with 15.0 mmol of **1**.

4-4. Synthesis of Benzodithienothiophene (BDTT) by Reduction following by Pd-catalyzed Intramolecular Cyclization

The author next investigated transformations of **6** to dithienyl thioether (DTT, **8**) by reduction with DIBAL (Table 2). When **6** was treated with DIBAL at 50 °C, the desired reaction proceeded to afford **8** in 57% yield and **6** was not recovered. The reproducibility of this reaction was insufficient, and the yield of **8** decreased to 48% when the author performed the same reaction again (entry 1). When the reaction temperature decreased to 40 or 25 °C, the reduction did not proceed completely and the yield was not improved, although the formation of byproducts was suppressed (entries 2 and 3).

Table 2. Optimization for the synthesis of DTT (**8**) by reduction ^a



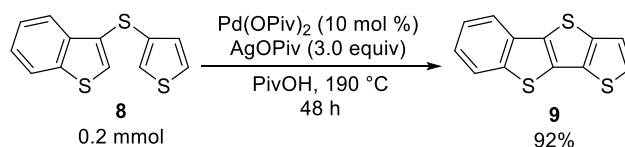
entry	temp (°C)	time (h)	yield (%)	recovery (%)
1	50	9	57 (48) ^b	0 (0) ^b
2	40	18	56 (42) ^b	31 (36) ^b
3	25	18	52 (54) ^b	40 (44) ^b

^a Reaction conditions: **11** (0.2 mmol), DIBAL (5.0 equiv), THF (0.5 mL),.

Isolated yield. ^b Isolated yield in the second run.

The obtained **8** was converted into BDTT (**9**) by Pd-catalyzed intramolecular cyclization (Scheme 6). By heating **8** in the presence of palladium pivalate (Pd(OPiv)₂, 10 mol %), AgOPiv (3.0 equiv) in PivOH at 190 °C for 48 h, the desired **9** was obtained in 92% yield.

Scheme 6. Synthesis of BDTT (**9**) by Pd-catalyzed intramolecular cyclization

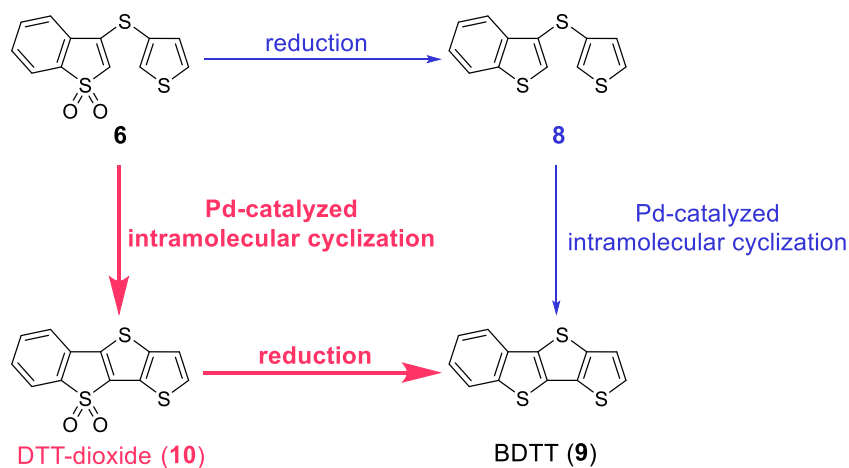


4-5. Synthesis of BDTT by Pd-catalyzed Intramolecular Cyclization following by Reduction

While the author achieved the synthesis of **8** and **9**, poor reproducibility and low yield in the conversion of **6** to **8** were still problematic (Table 2). They are probably because **6** or **8** would be unstable under the reducing conditions, and the decomposed mixture was obtained as byproducts. To overcome the situation, the author changed the synthetic strategy to Pd-catalyzed intramolecular cyclization following by reduction (Scheme 7, red arrow). Compared to **6**, DTT-dioxide (**10**) obtained by converting **6** has a rigid structure with delocalized electrons in the molecule. Therefore, **10** is expected to be a highly stable compound even under reducing conditions. Indeed, many efficient reductions have been reported in **10** analogs.⁵ Thus, **10** is expected to be converted to BDTT (**9**) by reduction.

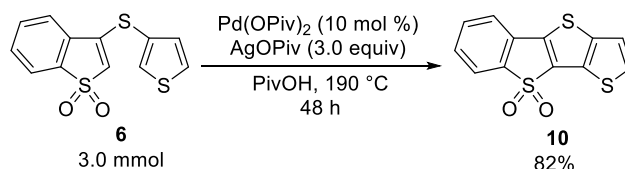
Scheme 7. A new approach for synthesizing BDTT via construction of DTT-dioxide

New approach: Synthesis of BDTT (**9**) via construction of BDTT-dioxide (**10**)



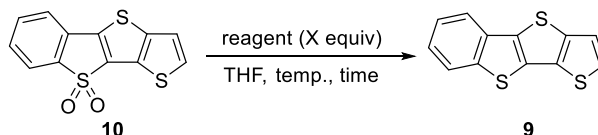
Following the approach described above, the author examined to synthesize DTT-dioxide **10** by Pd-catalyzed intramolecular cyclization (Scheme 8). By heating **6** in the presence of palladium pivalate ($\text{Pd}(\text{OPiv})_2$, 10 mol %), AgOPiv (3.0 equiv) in PivOH at 190 °C for 48 h, the desired **10** was obtained in 82% yield.

Scheme 8. Synthesis of DTT-dioxide (**10**) by Pd-catalyzed intramolecular cyclization



Next, the author examined transformations of **10** to **9** by reduction with DIBAL (Table 3). First, the author carried out reduction using LiAlH_4 , which is commonly used to convert thiophene 1,1-dioxides to thiophenes.^{5b} Reduction was carried out using 10 equiv of LiAlH_4 at 25 °C. After 2 hours, target product **9** was obtained in 74% yield (entry 1). With 5.0 equivalents of LiAlH_4 , **9** was obtained in 77% yield (entry 2). Better yield was attained when DIBAL was used at higher temperature (entry 3). The overall yield of **9** was 92% from 2.0 mmol of **10**.

Table 3. Optimization for synthesis of BDTT (**9**) by reduction^a



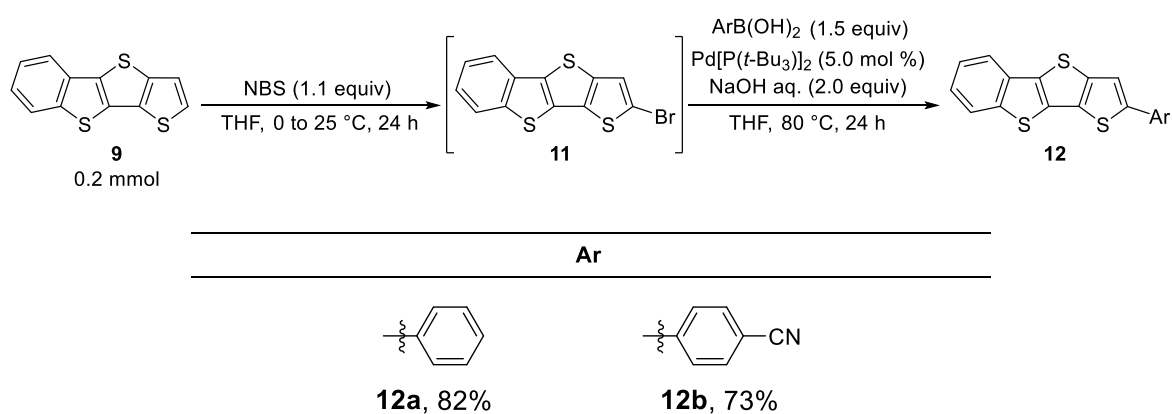
entry	reagent	X (equiv)	temp (°C)	time (h)	yield (%)
1	LiAlH_4	10	25	2	74
2	LiAlH_4	5	25	2	77
3	DIBAL	5	70	15	94 (92) ^b

^a Reaction conditions: **10** (0.2 mmol), LiAlH_4 or DIBAL (5–10 equiv), THF (0.5 mL), Isolated yield. ^b Performed with 2.0 mmol of **10**.

4-6. Transformation of π -Extended BDTT

The synthesized **9** was converted into various π -expanded BDTTs **12** by bromination followed by Suzuki–Miyaura cross-coupling (Table 4). The bromination of **11** with NBS proceeded smoothly at 25 °C to give brominated BDTT **11**. Next, in the presence of Pd[P(*t*-Bu)₃]₂ (5.0 mol %), arylboronic acid (1.5 equiv) and NaOH aq (1.0 M, 2 equiv) in THF at 80 °C for 24 h. The reaction between **11** and phenylboronic acid gave 2-phenyl-BDTT **12a** in 82% yield (over 2 steps, based on **9**). With 4-cyanophenylboronic acid, the corresponding coupling product **12b** was obtained in 73% yield.

Table 4. Synthesis of π -expanded BDTTs **12** by Suzuki–Miyaura cross-coupling^a



^a Isolated yield.

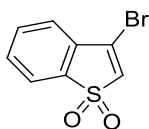
4-7. Conclusion

In conclusion, the author has achieved the efficient syntheses of BDTT (**9**) by addition-elimination reaction using 3-bromobenzo[*b*]thiophene 1,1-dioxides as key compounds following by Pd-catalyzed intramolecular C–H functionalization and reduction. The obtained **9** could be readily transformed to π -extended BDTF derivatives **12a** and **12b**.

4-8. Experimental Section and Analytical Data

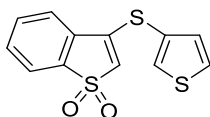
General

Nuclear magnetic resonance (NMR) spectra were recorded on Varian 600 System (^1H 600 MHz, ^{13}C 150 MHz), Varian 400-MR (^1H 400 MHz, ^{13}C 100 MHz), and JEOL JNM-ECS400 (^1H 400 MHz, ^{13}C 100 MHz) spectrometers. Chemical shifts for ^1H NMR are expressed in parts per million (ppm) relative to TMS (δ 0 ppm) or residual CHCl_3 in CDCl_3 (δ 7.26 ppm) or residual CHDCl_2 in CD_2Cl_2 (δ 5.32 ppm). Chemical shifts for ^{13}C NMR are expressed in ppm relative to CDCl_3 (δ 77.0 ppm) or CD_2Cl_2 (δ 53.84 ppm). IR spectra were recorded on a JASCO FT/IR-4100 and Varian 7000e FT-IR spectrophotometers. Elemental analysis was obtained with Perkin-Elmer PE 2400 Series II CHNS/O analyzer. Analytic thin layer chromatography (TLC) was performed on Merck, pre-coated plate silica gel 60 F₂₅₄ (0.25 mm thickness). Column chromatography was performed on KANTO CHEMICAL silica gel 60N (40–50 μm). Unless otherwise noted, all materials were obtained from commercial suppliers and used without further purification. High-resolution mass spectrometry was performed on JEOL JMS-700 MStation (FAB-MS). Dry tetrahydrofuran (THF) and dry diethyl ether (Et_2O) were purchased from Wako pure chemical industries. *N,N*-Dimethylformamide (DMF) was dried over MS4A. All reactions were performed under argon atmosphere. 2,3-Dibromobenzo[*b*]thiophene 1,1-dioxide (**5a**),⁶ was synthesized according to the literature.



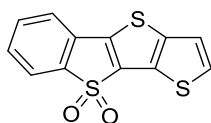
3-Bromobenzo[*b*]thiophene 1,1-dioxide (**5b**)

To a solution of 3-bromobenzo[*b*]thiophene (3.20 g, 15.0 mmol) in Ac_2O (20.3 mL) and AcOH (20.3 mL) was added dropwise H_2O_2 aq. (34.5%, 7.5 mL, 96 mmol) at 0 °C. The mixture was warmed to 110 °C and stirred for 2.5 h. Into the resulting mixture were added H_2O (35 mL), saturated aq. $\text{Na}_2\text{S}_2\text{O}_3$ (20 mL), K_2CO_3 (5.00 g) and the mixture was extracted with Et_2O (3×30 mL). The combined organic phase was dried over magnesium sulfate, filtrated and concentrated under reduced pressure. The residue was purified by recrystallization (hexane/ EtOAc) to give 3-bromobenzo[*b*]thiophene 1,1-dioxide as yellow solid (3.57 g, 14.6 mmol, 97%). ^1H NMR (400 MHz, CDCl_3) δ 6.98 (s, 1H), 7.57 (d, $J = 7.4$ Hz, 1H), 7.62 (td, $J = 7.4, 1.1$ Hz, 1H), 7.68 (td, $J = 7.4, 1.1$ Hz, 1H), 7.73 (dd, $J = 7.4, 1.1$ Hz, 1H); ^{13}C NMR (100 MHz, CDCl_3) δ 120.8, 124.6, 129.5, 129.7, 131.1, 131.6, 133.8, 136.9; IR (KBr) 3104, 3075, 1551, 1175, 750 cm^{-1} .



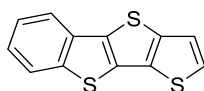
3-(Thiophene-3ylthio)benzo[*b*]thiophene 1,1-dioxide (6)

To a solution of 3-bromothiophene (2.45 g, 15.0 mmol) in Et₂O (60 mL) was added dropwise *t*-BuLi (1.77 M, 17.8 mL, 31.5 mmol) at -78 °C. After being stirred for 0.5 h, sulfur powder (0.53 g, 16.5 mmol) was added to the solution at the same temperature. After being stirred for 1 h, 3-bromobenzo[*b*]thiophene 1,1-dioxide (4.78 g, 19.5 mmol) was added to the solution at the 0 °C. After being stirred for a few minutes, the reaction mixture was warmed to 45 °C and stirred for 6.5 h. Into the resulting mixture were added H₂O (25 mL), saturated NH₄Cl aq (10.0 mL), and the mixture was extracted with CHCl₃ (3 × 80 mL). The combined organic phase was dried over magnesium sulfate, filtrated, and concentrated under reduced pressure. The residue was purified by column chromatography on silica gel (hexane/EtOAc 4/1) to give 3-(thiophene-3ylthio)benzo[*b*]thiophene 1,1-dioxide as yellow solid (3.21 g, 11.4 mmol, 76%). ¹H NMR (400 MHz, CDCl₃) δ 5.83 (s, 1H), 7.21 (d, *J* = 4.2 Hz, 1H), 7.50–7.65 (m, 4H), 7.71 (d, *J* = 4.2 Hz, 1H), 7.72 (d, *J* = 8.4 Hz, 1H); ¹³C NMR (100 MHz, CDCl₃) δ 118.9, 120.9, 121.4, 122.0, 128.3, 130.5, 131.1, 131.4, 133.1, 133.3, 137.8, 148.9; IR (KBr) 3096, 2361, 1296, 1171, 718 cm⁻¹; HRMS (FAB+) *m/z* calcd for C₁₂H₉O₂S₃ [M + H]⁺ 280.9759, found 280.9768; mp 116.7–117.4 °C.



Benzo[4,5]thieno[3,2-*b*]thieno[2,3-*d*]thiophene 9,9-dioxide (10)

To a solution of 3-(thiophene-3ylthio)benzo[*b*]thiophene 1,1-dioxide (841.2 mg, 3.0 mmol) in pivalic acid (10 mL) were added AgOPiv (1.88 g, 9.0 mmol) and Pd(OPiv)₂ (93.0 mg, 0.3 mmol). The mixture was warmed up to 190 °C and stirred for 48 h. After being allowed to cool to 25 °C, the resulting mixture was concentrated under reduced pressure. The residue was purified by column chromatography on silica gel (hexane/EtOAc = 4/1) to give benzo[4,5]thieno[3,2-*b*]thieno[2,3-*d*]thiophene 9,9-dioxide as yellow solid (684.9 mg, 2.46 mmol, 82%). ¹H NMR (400 MHz, CDCl₃) δ 7.33 (d, *J* = 5.2 Hz, 1H), 7.43 (d, *J* = 7.8 Hz, 1H), 7.45 (t, *J* = 7.8 Hz, 1H), 7.55 (d, *J* = 5.2 Hz, 1H), 7.56 (t, *J* = 7.8 Hz, 1H), 7.74 (d, *J* = 7.8 Hz, 1H); ¹³C NMR (100 MHz, CDCl₃) δ 119.9, 121.1, 122.1, 129.1, 129.5, 130.1, 130.2, 131.8, 133.7, 141.6, 143.5, 144.3; IR (KBr) 3117, 3088, 1296, 1148, 762 cm⁻¹; HRMS (FAB+) *m/z* calcd for C₁₂H₇O₂S₃ [M + H]⁺ 278.9602, found 278.9596; mp 258.2–258.7 °C.

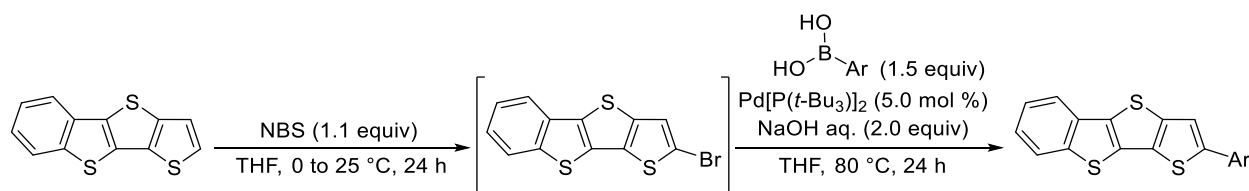


Benzo[4,5]thieno[3,2-*b*]thieno[2,3-*d*]thiophene (9)

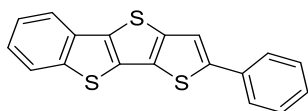
To a solution of benzo[4,5]thieno[3,2-*b*]thieno[2,3-*d*]thiophene 9,9-dioxide (556.8 mg, 2.0 mmol)

in THF (10 mL) was added dropwise DIBAL (1.00 M in THF, 10.0 mL, 10.0 mmol) at 0 °C. The reaction mixture was warmed to 70 °C and stirred for 15 h. The reaction was quenched by the addition of saturated aq. potassium sodium tartrate (50 mL) at 0 °C and stirred at the same temperature for 1 h. Into the resulting mixture were added H₂O (25 mL) and brine (10 mL), and the mixture was extracted with EtOAc (3 × 20 mL). The combined organic phase was dried over magnesium sulfate, filtrated, and concentrated under reduced pressure. The residue was purified by column chromatography on silica gel (hexane) to give benzo[4,5]thieno[3,2-*b*]thieno[2,3-*d*]thiophene as colorless solid (453.4 mg, 1.84 mmol, 92%). ¹H NMR (400 MHz, CDCl₃) δ 7.35–7.40 (m, 2H), 7.41–7.47 (m, 2H), 7.83 (d, *J* = 7.6 Hz, 1H), 7.87 (d, *J* = 8.0 Hz, 1H); ¹³C NMR (100 MHz, CDCl₃) δ 120.8, 120.9, 124.1, 124.7, 125.1, 127.2, 129.7, 131.7, 133.7, 136.7, 141.7, 141.8; IR (KBr) 3076, 2924, 2852, 1458, 748 cm⁻¹; HRMS (FAB+) *m/z* calcd for C₁₂H₆S₃ [M]⁺ 246.9626, found 246.9619; mp 138.1–138.7 °C.

General Procedure for the Suzuki–Miyaura Coupling



To a solution of benzo[4,5]thieno[3,2-*b*]thieno[2,3-*d*]thiophene (98.6 mg, 0.4 mmol) in THF (4.0 mL) was added *N*-bromosuccinimide (71.2 mg, 0.44 mmol) at 0 °C. The reaction mixture was warmed to 25 °C and stirred for 24 h. To the resulting mixture were added bis(*tri-tert*-butylphosphine)palladium (10.2 mg, 0.02 mmol), arylboronic acid (0.6 mmol) and NaOH (aq. 1.0 M, 0.8 mL, 0.8 mmol), and the mixture was stirred at 80 °C for 24 h. After being allowed to cool to 25 °C, the resulting mixture was concentrated under reduced pressure. The residue was washed with hexane, Et₂O and H₂O, followed by recrystallization.

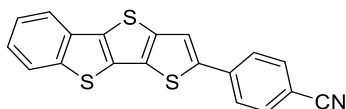


2-Phenylbenzo[4,5]thieno[3,2-*b*]thieno[2,3-*d*]thiophene (12a)

The general procedure for the Suzuki–Miyaura coupling was performed with benzo[4,5]thieno[3,2-*b*]thieno[2,3-*d*]thiophene (98.6 mg, 0.40 mmol), phenylboronic acid (73.2 mg, 0.60 mmol), bis(*tri-tert*-butylphosphine)palladium (10.2 mg, 0.02 mmol) and THF (4.0 mL). The residue was washed with hexane, Et₂O and H₂O, followed by recrystallization (hexane) to give 2-phenylbenzothieno[3,2-*b*]thieno[2,3-*d*]thiophene as yellow solid (105.8 mg, 0.328 mmol, 82%). ¹H NMR (400 MHz, CD₂Cl₂) δ 7.35 (t, *J* = 7.8 Hz, 1H), 7.39 (t, *J* = 7.8 Hz, 1H), 7.45 (t, *J* = 7.4 Hz, 2H), 7.47 (t, *J* = 7.4 Hz, 1H), 7.63 (s, 1H), 7.70 (d, *J* = 7.4 Hz,

Chapter 4. Synthesis of Benzodithienothiophene (BDTT) via Construction of Sulfur-Bridged Bithiophenes Using 3-Bromobenzo[*b*]thiophene 1,1-Dioxide as a Key Compound

2H), 7.86 (d, $J = 7.8$ Hz, 1H), 7.91 (d, $J = 7.8$ Hz, 1H); ^{13}C NMR (150 MHz, CDCl_3) δ 116.7, 120.7, 124.0, 124.6, 125.0, 125.9, 128.1, 129.1, 130.0, 130.8, 133.6, 134.6, 136.1, 141.8, 142.3, 146.3; IR (KBr) 3057, 3016, 2361, 743, 687 cm^{-1} ; HRMS (FAB+) m/z calcd for $\text{C}_{18}\text{H}_{11}\text{S}_3$ [$\text{M} + \text{H}$] $^+$ 323.0017, found 323.0011; mp 258.3–258.9 °C.



4-(Benzo[4,5]thieno[3,2-*b*]thieno[2,3-*d*]thiophene-2-yl)benzonitrile (12b)

The general procedure for the Suzuki–Miyaura coupling was performed with benzo[4,5]thieno[3,2-*b*]thieno[2,3-*d*]thiophene (98.6 mg, 0.40 mmol), 4-cyanophenylboronic acid (88.2 mg, 0.60 mmol), bis(*tert*-butylphosphine)palladium (10.2 mg, 0.02 mmol) and THF (4.0 mL). The residue was washed with hexane, Et_2O and H_2O , followed by recrystallization (hexane) to give 4-(benzothieno[3,2-*b*]thieno[2,3-*d*]thiophene-2-yl)benzonitrile as yellow solid (101.5 mg, 0.292 mmol, 73%). ^1H NMR (400 MHz, CDCl_3) δ 7.39 (t, $J = 7.5$ Hz, 1H), 7.46 (t, $J = 7.5$ Hz, 1H), 7.67 (s, 1H), 7.68 (dd, $J = 9.0, 2.4$ Hz, 2H), 7.74 (dd, $J = 9.0, 2.4$ Hz, 2H), 7.84 (d, $J = 7.5$ Hz, 1H), 7.89 (d, $J = 7.5$ Hz, 1H); ^{13}C NMR (150 MHz, CDCl_3) δ 111.2, 118.6, 118.7, 121.0, 124.1, 125.1, 125.2, 125.9, 129.7, 132.4, 132.9, 133.4, 137.5, 138.8, 142.0, 142.4, 143.4; IR (KBr) 3098, 3065, 2230, 813, 746 cm^{-1} ; HRMS (FAB+) m/z calcd for $\text{C}_{19}\text{H}_{10}\text{NS}_3$ [M] $^+$ 346.9891, found 346.9879; mp > 300 °C.

References

- (1) (a) Katz, H. E.; Bao, Z.; Gilat, S. L. *Acc. Chem. Res.* **2001**, *34*, 359–369. (b) Wang, C.; Dong, H.; Hu, W.; Liu, Y.; Zhu, D. *Chem. Rev.* **2012**, *112*, 2208–2267. (c) Kang, B.; Lee, W. H.; Cho, K. *ACS Appl. Mater. Interfaces* **2013**, *5*, 2302–2315. (d) Cheng, Y.-J.; Yang, S.-H.; Hsu, C.-S. *Chem. Rev.* **2009**, *109*, 5868–5923. (e) Mishra, A.; Bäuerle, P. *Angew. Chem., Int. Ed.* **2012**, *51*, 2020–2067.
- (2) (a) Mishra, A.; Ma, C.-Q.; Bäuerle, P. *Chem. Rev.* **2009**, *109*, 1141–1276. (b) Wu, W.; Liu, Y.; Zhu, D. *Chem. Soc. Rev.* **2010**, *39*, 1489–1502. (c) Coropceanu, V.; Cornil, J.; da Silva Filho, D. A.; Olivier, Y.; Silbey, R.; Bre´das, J. L. *Chem. Rev.* **2007**, *107*, 926–952. (d) Jørgensen, M.; Norrman, K.; Gevorgyan, S. A.; Tromholt, T.; Andreasen, B.; Krebs, F. C. *Adv. Mater.* **2012**, *24*, 580–612.
- (3) (a) Gao, J.; Li, R.; Li, L.; Meng, Q.; Jiang, H.; Li, H.; Hu, W. *Adv. Mater.* **2007**, *19*, 3008–3011. (b) Li, R.; Jiang, L.; Meng, Q.; Gao, J.; Li, H.; Tang, Q.; He, M.; Hu, W.; Liu, Y.; Zhu, D. *Adv. Mater.* **2009**, *21*, 4492–4495.
- (4) (a) Youn, J.; Chen, M. C.; Liang, Y. J.; Huang, H.; Ortiz, R. P.; Kim, C.; Stern, C.; Hu, T. S.; Chen, L. H.; Yan, J. Y.; Facchetti, A.; Marks, T. J. *Chem. Mater.* **2010**, *22*, 5031–5041. (b) Tian, H.; Han, Y.; Bao, C.; Yan, D.; Geng, Y.; Wang, F. *Chem. Commun.* **2012**, *48*, 3557–3559. (c) Wang, M.; Wei, J.; Fan, Q.; Jiang, X. *Chem. Commun.* **2016**, *53*, 2918–2921.
- (5) (a) Klemm, L. H.; Hall, E.; Cousins, L.; Klofenstein, C. E.; *J. Heterocycl. Chem.* **1987**, *24*, 1749–1755. (b) Zander, M. *Zeitschrift Für Naturforschung* **1989**, *44*, 1116–1118. (c) Nandakumar, M.; Karunakaran, J.; Mohanakrishnan, A. K. *Org. Lett.* **2014**, *16*, 3068–3071. (d) Vasu, D.; Hausmann, J. N.; Saito, H.; Yanagi, T.; Yorimitsu, H.; Osuka, A. *Asian J. Org. Chem.* **2017**, *6*, 1390–1393.
- (6) (a) Bordwell, F. G.; Albisetti, C. J., Jr. *J. Am. Chem. Soc.* **1948**, *70*, 1558–1560. (b) Nanson, L.; Blouin, N.; Mitchell, W. *PCT Int. Appl.* **2015**, WO 2015139802 A1 20150924.

Chapter 5. Physical Properties of BDTF, BDTT and Their Derivatives

5-1.	Abstract	94
5-2.	Introduction	94
5-3.	Photophysical Properties of BDTFs and BDTTs	95
5-4.	Electrochemical Properties of BDTFs and BDTTs	99
5-5.	X-ray Crystal Structure Analysis of BBTDF and Comparison with BBTDT	105
5-6.	OFET Properties of BBTDF and Comparison with BBTDT	106
5-7.	Conclusion	108
5-8.	Experimental Section and Analytical Data	109
	References	128

5-1. Abstract

The author investigated physical properties of [1]benzothieno[3,2-*b*]thieno[2,3-*d*]furans (BDTFs) and [1]benzothieno[3,2-*b*]thieno[2,3-*d*]thiophenes (BDTTs). Cyclic voltammograms (CV), UV-vis absorption, fluorescence emission, and quantum yields of BDTFs and BDTTs were measured. Fluorescence properties of BDTFs were better than those of BDTTs. In particular, BDTF derivative bearing a 4-cyano-C₆H₄ group exhibited the strongest fluorescence ($\Phi_{\text{PL}} = 0.85$).

Among synthesized BDTFs, X-ray single-crystal analysis and thermogravimetric analysis (TGA) of 2,2'-bis([1]benzothieno[3,2-*b*]thieno[2,3-*d*]furan (BBTDF) was carried out. Molecules with a highly oriented packing structure such as BBTDF are expected to be a suitable packing form for organic field-effect transistor (OFET). Therefore, the author investigated its OFET properties and clarified that BBTDF has the similar hole mobility as 2,2'-bis([1]benzothieno[3,2-*b*]thieno[2,3-*d*]thiophene (BBTDT).

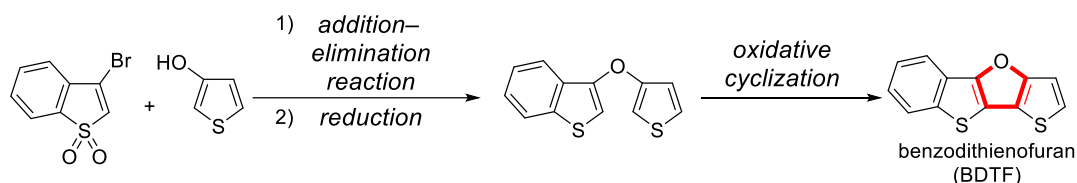
5-2. Introduction

Thienoacenes have been attracting interest due to their role in organic functional materials.¹ In particular, oxygen-bridged 2,2'-bithiophenes (dithienofurans, DTFs) are expected to be applied to the active material of organic light emitting transistors due to the high probability of exhibiting excellent fluorescent properties. However, these properties have not yet been clarified, and only two synthetic methods have been reported.²

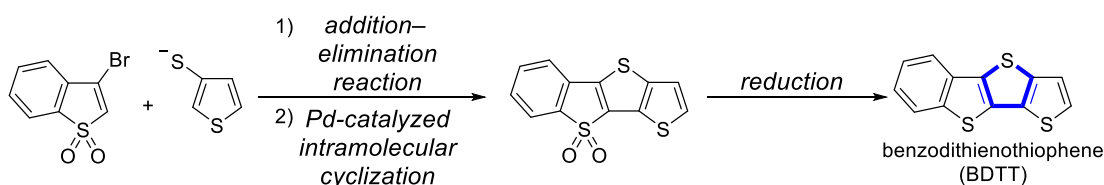
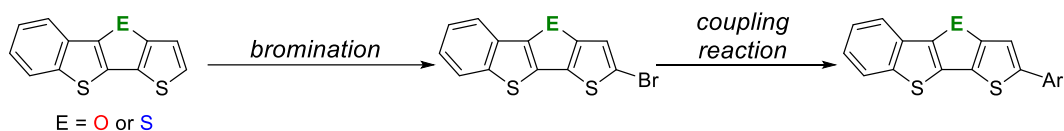
As mentioned in Chapter 3, the authors have achieved efficient syntheses of novel π -expanded DTFs (BDTF) by the combination of an addition–elimination reaction using 3-bromobenzo[*b*]thiophene 1,1-dioxides as key compounds following by reduction and Pd-catalyzed intramolecular C–H functionalization (Scheme 1A). The author is motivated to compare them with those of analogs such as BDTT, which has been known as its π -extended derivatives exhibited semiconductor properties.³ In contrast to BDTF, several methods have been reported for the synthesis of BDTT.⁴ However, these methods required several reaction steps and yield was insufficient. As described in Chapter 4, the author found that BDTT could be synthesized by applying the synthetic strategy of BDTF (Scheme 1B). The synthesis of π -extended BDTF and BDTTs by coupling reactions were also achieved (Scheme 1C). Therefore, the author investigated physical properties of BDTFs, and compared them with those of BDTTs. The author is especially interested in the fluorescence properties. BDTFs are expected to show superior fluorescence properties compared to BDTTs due to the absence of the heavy atom effect.⁵ In addition, an X-ray crystal structure analysis of a dimer of BDTF (BBTDF) was performed and its OFET properties was examined.

Scheme 1. Efficient synthesis of BDTFs and BDTTs

A. Synthesis of BDTF (Chapter 3)



B. Synthesis of BDTT (Chapter 4)

C. Synthesis of π -extended BDTFs and BDTTs (Chapters 3 and 4)

5-3. Photophysical Properties of BDTFs and BDTTs

Initially, the photophysical measurements of BDTFs were conducted. After preparing the o -C₆H₄Cl₂ solution (1.0×10^{-5} M), the author performed ultraviolet-visible absorption spectroscopy (UV-vis) measurement, fluorescence emission (FL) measurement, and fluorescence quantum yield measurement (Figures 1–3). UV-vis spectra are indicated by the dotted lines and fluorescence spectra are indicated by the solid lines. The absorption wavelength (λ_{abs}) and fluorescence wavelength (λ_{PL}) of BDTF **1** were observed at 311 nm and 349 nm, respectively. The introduction of an aryl group highly influenced the photophysical properties. For example, the introduction of a phenyl group to BDTF resulted in a 45 nm red-shift of λ_{abs} and a 63 nm red-shift of λ_{PL} (**1** vs. **2a**). The photoluminescence quantum yield improved drastically, from almost 0 to 0.35. This trend was also confirmed for other π -extended BDTFs except **2f** and **2j** ($\Phi_{\text{PL}} = 0.12$ and 0.20, respectively). Furthermore, BDTF derivatives having an acceptor unit such as a 4-cyano-C₆H₄ group (**2c**) or 2-benzothiazolyl group (**2i**) have λ_{PL} values that are closer to the visible light region with a higher quantum yield than those having a donor unit (**2a–2b**, **2d–2g**, **2j**). This should be due to intramolecular charge transfer from the BDTF unit to an electron-accepting unit.⁶ In particular, **2c** exhibited the strongest fluorescence among them ($\Phi_{\text{PL}} = 0.85$). More detailed optical data are summarized in Tables 1–3.

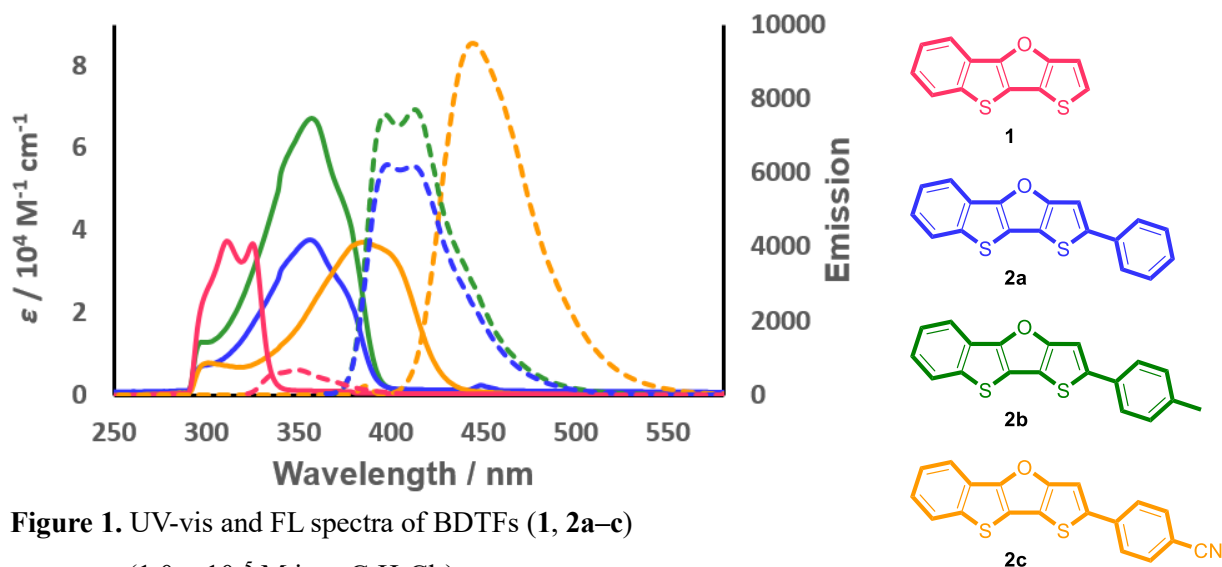


Figure 1. UV-vis and FL spectra of BDTFs (**1**, **2a–c**)

(1.0×10^{-5} M in *o*-C₆H₄Cl₂)

Table 1. Photophysical properties of BDTFs (**1**, **2a–c**)^a

compd.	λ_{abs} [nm]	$\log \varepsilon$	λ_{onset} [nm]	λ_{PL} [nm]	λ_{ex} [nm] for Φ_{PL}	Φ_{PL}
1	311	4.57	335	349	-	0
2a	356	4.58	391	412	350	0.35
2b	357	4.83	392	413	350	0.36
2c	385	4.57	427	445	370	0.85

^a Recorded in *o*-dichlorobenzene (1.0×10^{-5} M).



1 **2a** **2b** **2c**

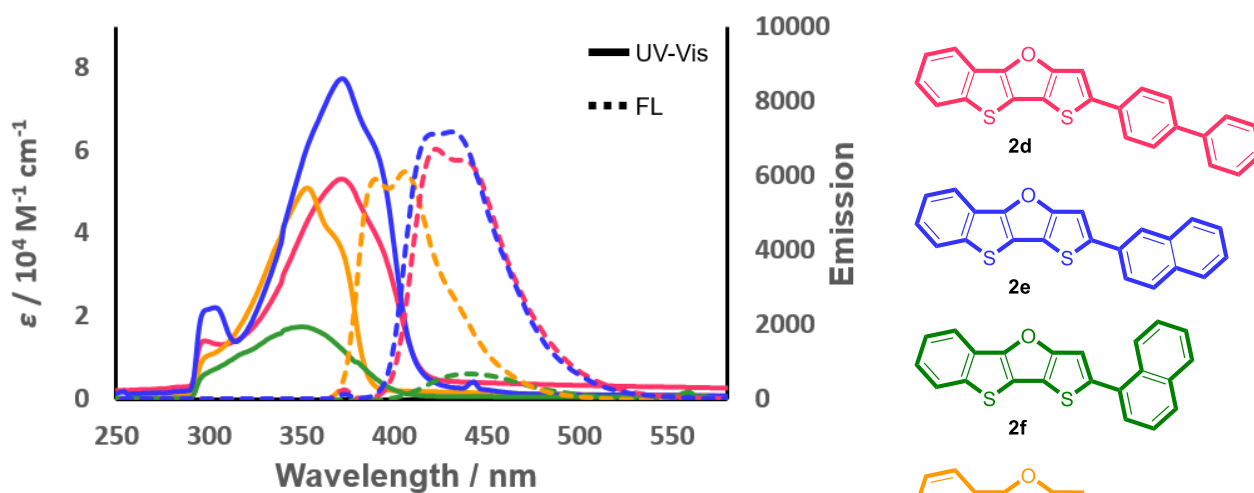


Figure 2. UV-vis and FL spectra of BDTFs (**2d–g**)

(1.0×10^{-5} M in *o*-C₆H₄Cl₂)

Table 2. Photophysical properties of BDTFs (**2d–g**)^a

compd.	λ_{abs} [nm]	$\log \varepsilon$	λ_{onset} [nm]	λ_{PL} [nm]	λ_{ex} [nm] for Φ_{PL}	Φ_{PL}
2d	372	4.73	412	422	370	0.48
2e	303, 372	4.35, 4.89	409	431	370	0.44
2f	350	4.24	401	440	360	0.12
2g	353	4.71	385	406	340	0.20

^a Recorded in *o*-dichlorobenzene (1.0×10^{-5} M).



2d **2e** **2f** **2g**

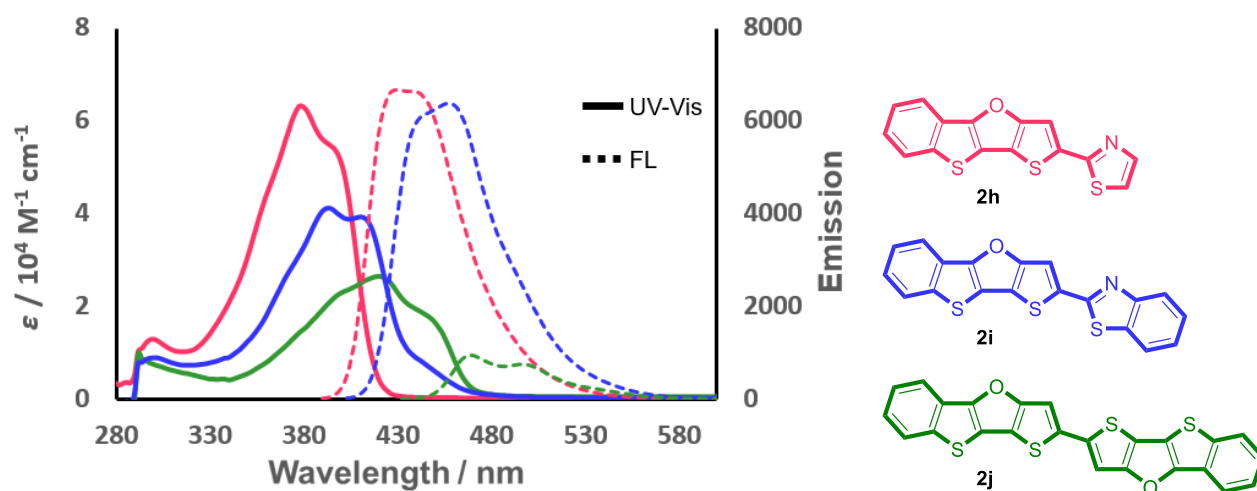


Figure 3. UV-vis and FL spectra of BDTFs (**2h–j**)

(1.0×10^{-5} M in *o*-C₆H₄Cl₂)

Table 3. Photophysical properties of BDTFs (**2h–j**)^a

compd.	λ_{abs} [nm]	$\log \varepsilon$	λ_{onset} [nm]	λ_{PL} [nm]	λ_{ex} [nm] for Φ_{PL}	Φ_{PL}
2h	379	4.80	418	429	370	0.45
2i	394	4.61	439	457	370	0.72
2j	420	4.42	469	469, 496	400	0.20

^a Recorded in *o*-dichlorobenzene (1.0×10^{-5} M).



2h 2i 2j

Next, the author compared the photophysical properties of BDTFs and BDTTs. Their fluorescence properties were clearly different. First, UV-vis absorption spectra and fluorescence spectra were measured (Figure 4 and Table 4). UV-vis spectra are indicated by the dotted lines and fluorescence spectra are indicated by the solid lines. As is evident in Figure 4, BDTFs show a slight red-shift of the maximum wavelengths of absorption and emission compared to those of BDTTs. For example, BDTF **2c** has bathochromic shifts of 9 nm (λ_{abs}) and 13 nm (λ_{PL}) compared to those of BDTT **3b**. Furthermore, BDTFs exhibited stronger fluorescence than BDTTs. For example, the quantum yield of the derivatives with a 4-cyano- C_6H_4 group are $\Phi_{\text{PL}} = 0.85$ (BDTF **2c**) and $\Phi_{\text{PL}} = 0.42$ (BDTT **3b**), respectively. The reason that BDTFs exhibited a strong fluorescence are considered to be a result of absence of the heavy atom effect.

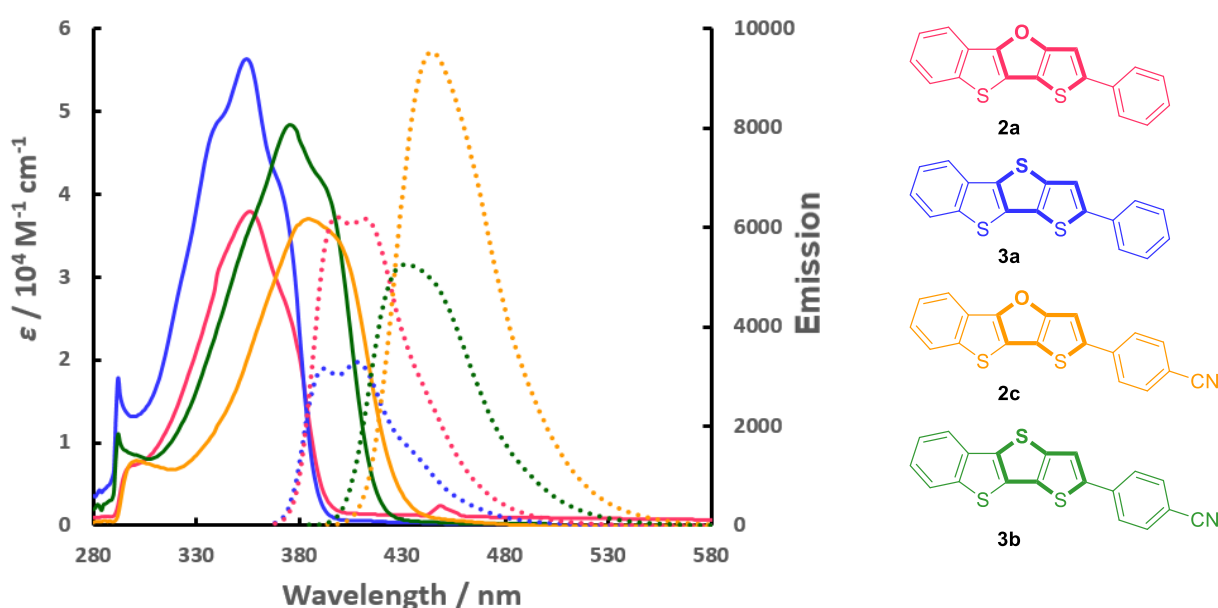


Figure 4. UV-vis and FL spectra of BDTFs (**2a** and **2c**) and BDTTs (**3a** and **3b**) (1.0×10^{-5} M in *o*- $\text{C}_6\text{H}_4\text{Cl}_2$)

Table 4. Photophysical properties of BDTFs BDTFs (**2a** and **2c**) and BDTTs (**3a** and **3b**)^a

compd.	λ_{abs} [nm]	$\log \varepsilon$	λ_{onset} [nm]	λ_{PL} [nm]	λ_{ex} [nm] for Φ_{PL}	Φ_{PL}
2a	356	4.58	391	412	350	0.35
3a	355	4.75	388	408	340	0.15
2c	385	4.57	427	445	370	0.85
3b	376	4.68	416	432	370	0.42

^a Recorded in *o*-dichlorobenzene (1.0×10^{-5} M).



2a **3a** **2c** **3b**

5-4. Electrochemical Properties of BDTFs and BDTTs

Next, the author performed cyclic voltammetry (CV) measurements to estimated E_{HOMO} values. In the cyclic voltammograms of BDTFs, an irreversible oxidation peak was confirmed in **1**. However, reversible oxidation peaks were confirmed in all BDTFs bearing an aryl group except for **2a–2j** (Figures 5–8 and Tables 5–8). These difference in the oxidation peaks suggest that the cationic species generated from **1** under electro-oxidative conditions would react or decompose at the a-position of the thiophene unit and BDTFs.

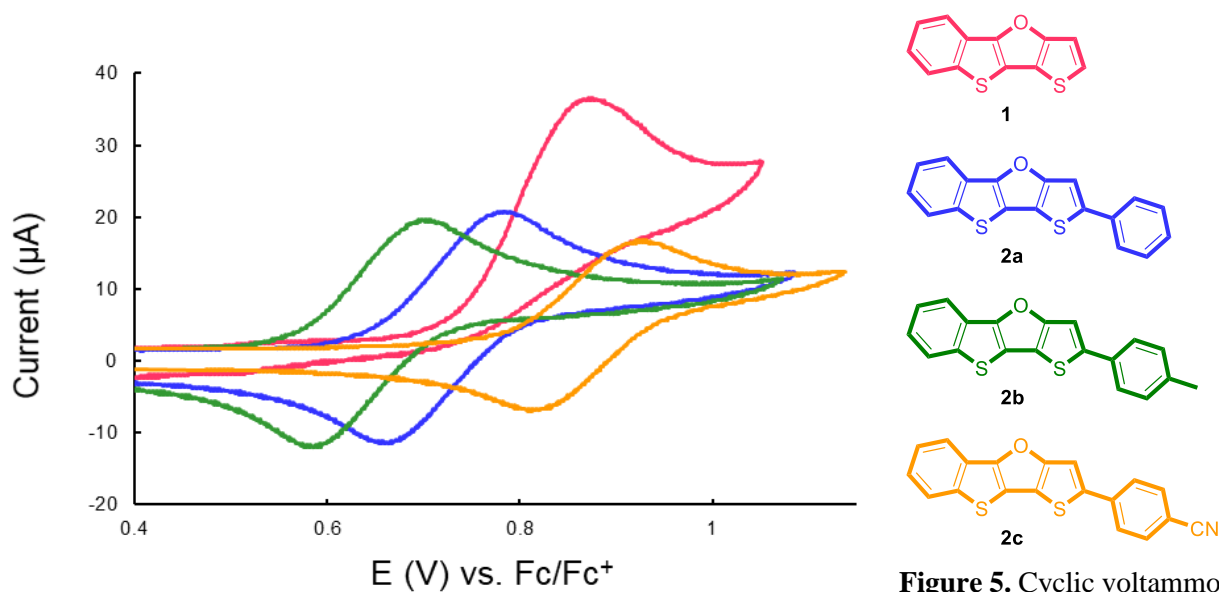


Figure 5. Cyclic voltammograms

of BDTFs (**1**, **2a–c**)

Table 5. Electrochemical properties of BDTFs (**1**, **2a–c**)^a

compd.	E_{onset} (eV)
1	0.74
2a	0.64
2b	0.57
2c	0.78

^a Supporting electrolyte solvent : 0.1 M $\text{Bu}_4\text{NPF}_6/\text{CH}_2\text{Cl}_2$ substrate concentration : 1 mM

working electrode : Pt counter electrode : Pt coil reference electrode : $\text{Ag}/\text{Ag}^+/\text{CH}_2\text{Cl}_2$

reference : Fc/Fc^+ scan rate : 100 mV/s

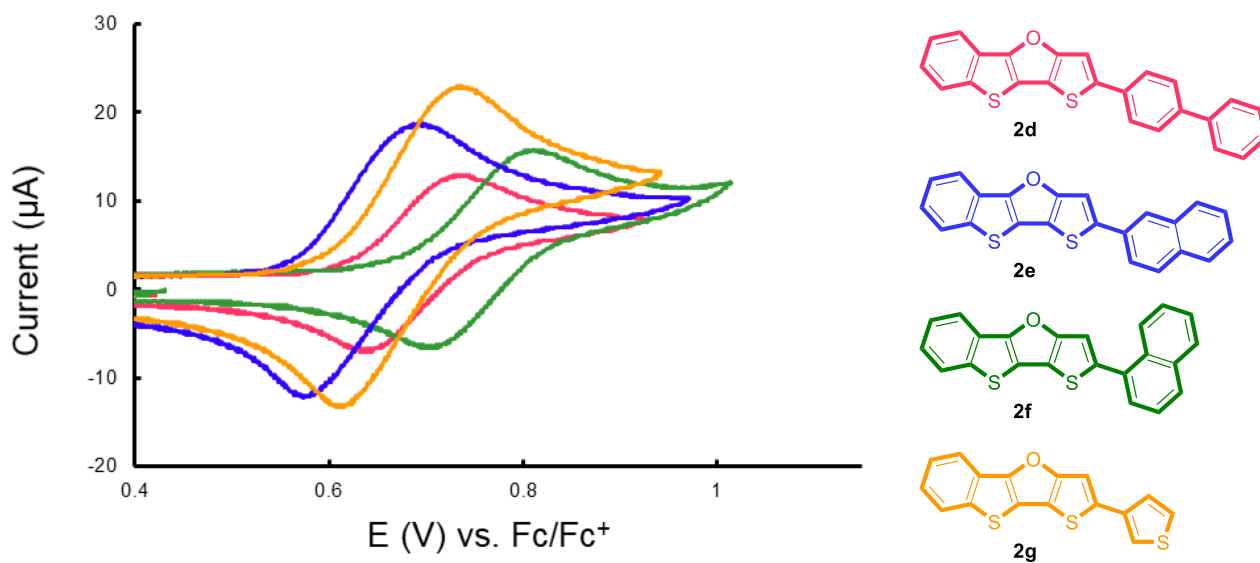


Figure 6. Cyclic voltammograms of BDTFs (**2d–g**)

Table 6. Electrochemical properties of BDTFs (**2d–g**)^a

compd.	E_{onset} (eV)
2d	0.62
2e	0.56
2f	0.68
2g	0.60

^a Supporting electrolyte solvent : 0.1 M Bu₄NPF₆/CH₂Cl₂ substrate concentration : 1 mM

working electrode : Pt counter electrode : Pt coil reference electrode : Ag/Ag⁺/CH₂Cl₂

reference : Fc/Fc⁺ scan rate : 100 mV/s

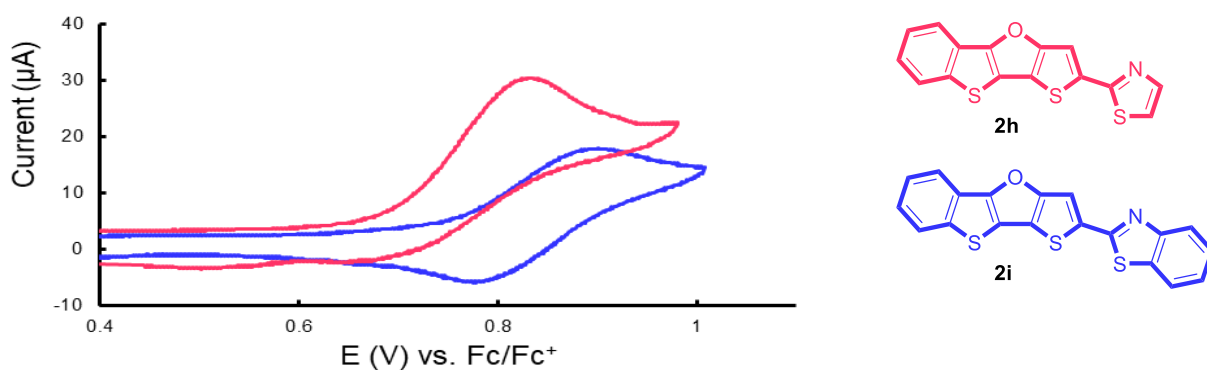


Figure 7. Cyclic voltammograms of BDTFs (**2h** and **2i**)

Table 7. Electrochemical properties of BDTFs (**2h** and **2i**)^a

compd.	E_{onset} (eV)
2h	0.69
2i	0.75

^a Supporting electrolyte solvent : 0.1 M Bu₄NPF₆/CH₂Cl₂ substrate concentration : 1 mM
 working electrode : Pt counter electrode : Pt coil reference electrode : Ag/Ag⁺/CH₂Cl₂
 reference : Fc/Fc⁺ scan rate : 100 mV/s

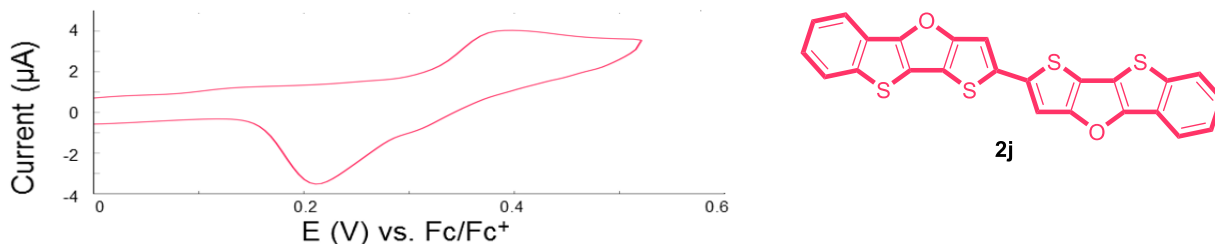


Figure 8. Cyclic voltammograms of BDTFs (**2j**)

Table 8. Electrochemical properties of BDTFs (**2j**)^a

compd.	E_{onset} (eV)
2j	0.32

^a Supporting electrolyte solvent : 0.1 M Bu₄NPF₆/C₆H₄Cl₂ substrate concentration : 1 mM
 working electrode : Pt counter electrode : Pt coil reference electrode : Ag/Ag⁺/CH₂Cl₂
 reference : Fc/Fc⁺ scan rate : 100 mV/s

In the cyclic voltammograms of BDTTs, an irreversible oxidation peak was confirmed in **4**. Reversible oxidation peaks were confirmed in BDTTs bearing an aryl group (**3a** and **3b**). The similar trends as BDTTs were confirmed (Figure 9 and Table 9).

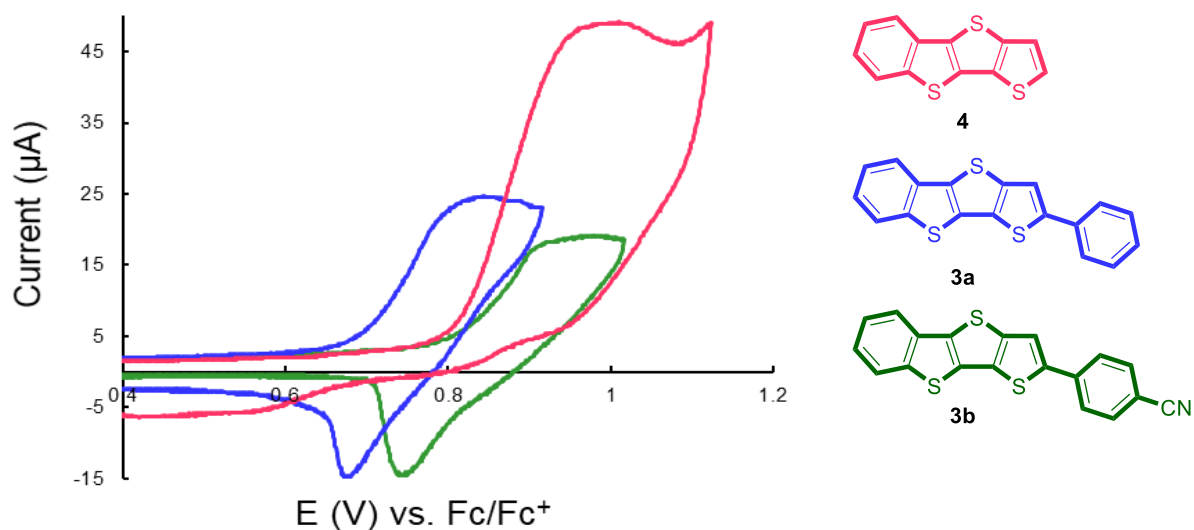


Figure 9. Cyclic voltammograms of BDTTs (**4**, **3a** and **3b**)

Table 9. Electrochemical properties of BDTTs (**4**, **3a** and **3b**)^a

compd.	E_{onset} (eV)
4	0.82
3a	0.69
3b	0.81

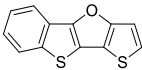
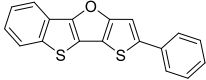
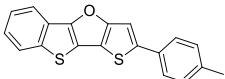
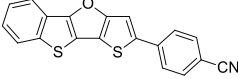
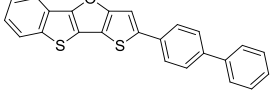
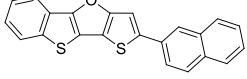
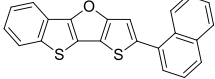
^a Supporting electrolyte solvent : 0.1 M Bu₄NPF₆/CH₂Cl₂ substrate concentration : 1 mM

working electrode : Pt counter electrode : Pt coil reference electrode : Ag/Ag⁺/CH₂Cl₂

reference : Fc/Fc⁺ scan rate : 100 mV/s

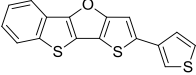
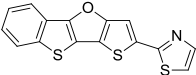
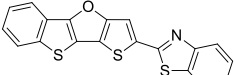
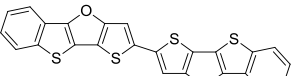
Next, the author estimated E_{HOMO} values and E_{LUMO} values of BDTFs and BDTTs (Tables 10–12). E_{HOMO} was estimated based on the onset value of the oxidation peak (λ_{onset}) and E_{LUMO} was estimated based on the energy band gap (ΔE). Both BDTF and BDTT derivatives are expected to have low E_{LUMO} values and tend to have a narrow energy band gap as the π -conjugated system expand. Totally, the estimate E_{HOMO} values of BDTFs and BDTTs are similar, even when aryl group was introduced (**1** vs **4**, **2a** vs **3a** and **2c** vs **3b**). These values showed a reasonable correlation with the values obtained by the DFT calculations (Figure S1).

Table 10. The energy levels of BDTFs (**1**, **2a–2f**)^a

compd.	E_{HOMO} (eV) ^a	E_{LUMO} (eV) ^b	ΔE (eV) ^c
 1	-5.54	-1.84	3.70
 2a	-5.44	-2.27	3.17
 2b	-5.37	-2.21	3.16
 2c	-5.58	-2.68	2.90
 2d	-5.42	-2.41	3.01
 2e	-5.36	-2.33	3.09
 2f	-5.47	-2.38	3.03

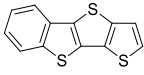
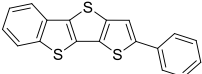
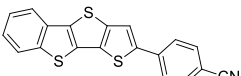
^a $E_{\text{HOMO}} = -(E_{[\text{onset, ox vs. Fc/Fc}^+]} + 4.8)$ (eV). ^b $E_{\text{LUMO}} = E_{\text{HOMO}} + \Delta E$ (eV). ^c $\Delta E = (hc/\lambda_{\text{onset}})$ (eV)

Table 11. The energy levels of BDTFs (**2h–2j**)^a

compd.	E_{HOMO} (eV) ^a	E_{LUMO} (eV) ^b	ΔE (eV) ^c
 2g	-5.40	-2.18	3.22
 2h	-5.49	-2.53	2.96
 2i	-5.55	-2.73	2.82
 2j	-5.12	-2.48	2.64

a $E_{\text{HOMO}} = - (E_{[\text{onset, ox vs. Fc/Fc}^+]} + 4.8)$ (eV). b $E_{\text{LUMO}} = E_{\text{HOMO}} + \Delta E$ (eV). c $\Delta E = (hc/\lambda_{\text{onset}})$ (eV)

Table 12. The energy levels of BDTFs (**4**, **3a** and **3b**)^a

compd.	E_{HOMO} (eV) ^a	E_{LUMO} (eV) ^b	ΔE (eV) ^c
 4	-5.62	-1.99	3.63
 3a	-5.49	-2.30	3.19
 3b	-5.61	-2.63	2.98

a $E_{\text{HOMO}} = - (E_{[\text{onset, ox vs. Fc/Fc}^+]} + 4.8)$ (eV). b $E_{\text{LUMO}} = E_{\text{HOMO}} + \Delta E$ (eV). c $\Delta E = (hc/\lambda_{\text{onset}})$ (eV)

5-5. X-ray Crystal Structure Analysis of BBDTF and Comparison with BBDTT

The author next compared crystal structures of BBDTF (**2j**) and BBDTT (**3c**) (Figure 10). Our analysis revealed that these packing structures were clearly different. First, the author investigated the crystal structure of **2j**. **2j** crystallized in an orthorhombic lattice (space group $P2_12_12_1$ (#19)) and the crystals exhibited a packing structure in the face-to-face π - π -stacking arrangement. The transfer integral of **2j** in each laminating direction was calculated by Amsterdam density functional software (ADF),⁷ which showed that a pair of **2j** has a large integral value for holes (307 meV) in the laminating direction and a small integral value (12 and 3 meV) in the orthogonal (*c*-axis) and lateral direction (Figure 10a). This result suggests that **2j** has strong π - π interaction, and hole transfer along the laminating direction would be favorable. The results also suggested that the packing structure of **2j** was highly influenced by intermolecular S-S interaction between sulfur atoms of the thiophene rings (Figure 10b). These two factors, π - π and S-S interaction, should significantly influence the directions of adjacent molecular chains.

The crystal structure of **3c** has been reported by Marks and co-workers.³ **3c** crystallizes in a monocyclic lattice (space group $P2_1/c$) and exhibits a packing structure in the face-to-face π - π -stacking arrangement. **3c** exhibits stronger S-S interaction than **2j**, since it has a thiophene ring instead of a furan ring. This strong S-S interaction may explain, at least in part, why it has a different crystal lattice from **2j**, and why adjacent molecular chains are arranged in parallel.

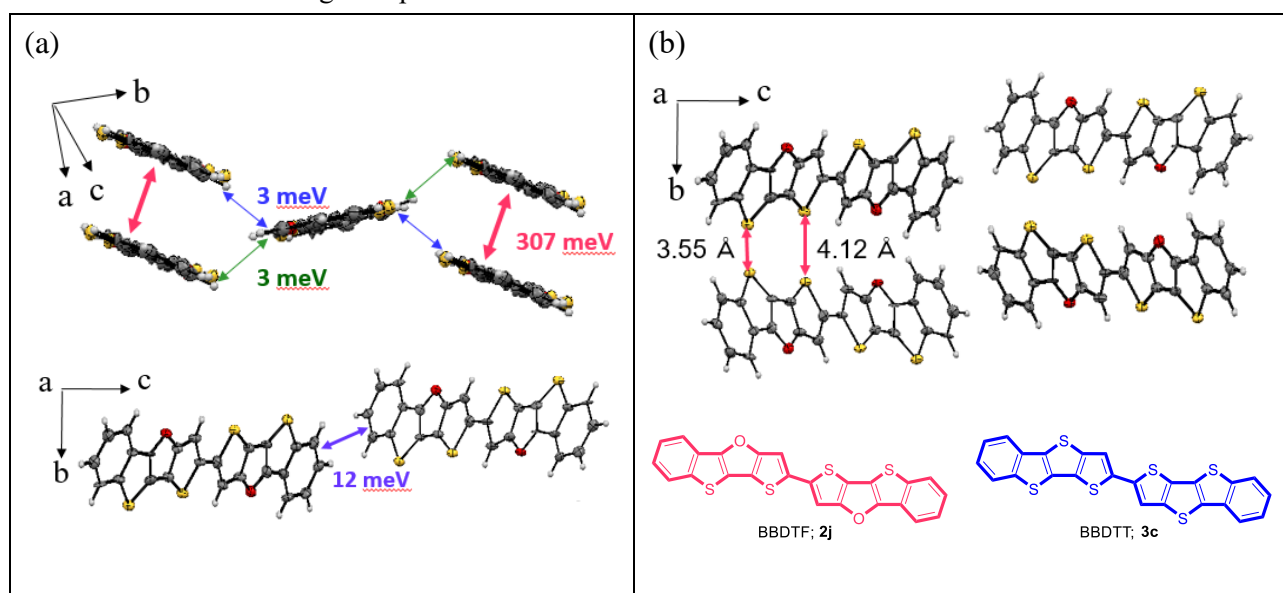


Figure 10. Crystal structures of **2j**: (a) Transfer integral: Red arrow indicates integral value for holes in the laminating direction. Blue and green arrows indicate integral value for holes in the lateral direction. Purple arrows indicate integral value for holes in the orthogonal (*c*-axis) direction. Calculated at the PW91/TZP of theory. (b) *c*-axis projection: yellow, red, black and white colors indicate sulfur, oxygen, carbon, and hydrogen atoms, respectively. Red arrows indicate the closest S-S contact distances.

5-6. OFET Properties of BBTF and Comparison with BBTDT

Molecules with a highly oriented packing structure such as BBTF **2j** are expected to be a suitable packing form for OFET. Therefore, we were also interested in the OFET properties of **2j**. Initially, The author performed a thermogravimetric analysis (TGA) to evaluate the thermal stability of **2j**. The temperature that gave 5% weight loss was 382 °C, suggesting that **2j** has high thermal stability (Figure S2). E_{HOMO} and E_{LUMO} for **2j** were estimated to be -5.12 eV and -2.48 eV, respectively (Table 8). These values are almost similar to those of BBTDT **3c** which were already reported by Marks and co-workers ($E_{\text{HOMO}} = -5.34$ eV and $E_{\text{LUMO}} = -2.45$ eV).³ The low E_{HOMO} and large energy bandgap of **2j** suggest that **2j** is an environmentally stable organic semiconductor material. Indeed, it has been reported that BBTDT **3c**, having the almost similar E_{HOMO} and E_{LUMO} value as **2j**, exhibited OFET properties.

The author evaluated the OFET properties using **2j**. OFET devices based on **2j** were fabricated by vapor deposition with a top-contact/bottom-gate configuration on octyltrichlorosilane (OTS)- or octadecyltrichlorosilane (ODTS)-treated n⁺-Si/SiO₂ substrate. The fabricated thin films were thermally annealed at 50 and 100 °C in a glove box for 30 min. The gold source and drain electrodes were deposited through a shadow mask by vapor deposition, which gave a channel length (L) and channel width of 100 nm and 2 μm, respectively. The measurements were carried out under ambient conditions. All OFET characterization data including carrier mobility (μ), current on/off ratio ($I_{\text{on}}/I_{\text{off}}$), and threshold voltage (V_{th}) are summarized in Table 13. The transfer and output plots are shown in Figure 11. OFET devices based on as-deposited thin films exhibited the typical p-channel behavior with highest hole mobility of $0.13 \text{ cm}^2 \text{ V}^{-1} \text{ s}^{-1}$. This value is similar to the value for BBTDT (**3c**) ($0.15 \text{ cm}^2 \text{ V}^{-1} \text{ s}^{-1}$).³

However, **3c** showed better values of $I_{\text{on}}/I_{\text{off}}$ and V_{th} than **2j**. This result is consistent with the notion that **2j** has a packing structure with weaker intermolecular interaction than **3c**.

Table 13. OFET characterization of **2j**^a

Sub	T_{anneal} (°C)	μ_{max} (cm ² /Vs)	$I_{\text{on}}/I_{\text{off}}$	V_{th} (V)
OTS	(as depo.)	1.2×10^{-2}	3.1×10^5	2.1
OTS	50	7.2×10^{-3}	2.5×10^3	1.8
OTS	100	1.1×10^{-2}	5.9×10^4	0.8
ODTS	(as depo.)	0.13	5.6×10^2	-0.1
ODTS	50	0.12	2.8×10^1	3.6
ODTS	100	2.2×10^{-2}	1.0×10^6	3.8

^a Method : vacuum deposition, Deposition rate : 1.0 Å/s, Thickness : 300 Å, Gold film : 80 Å, Device structure : bottom-gate, top-contact, Channel length : 100 μm, Channel width : 2.0 mm

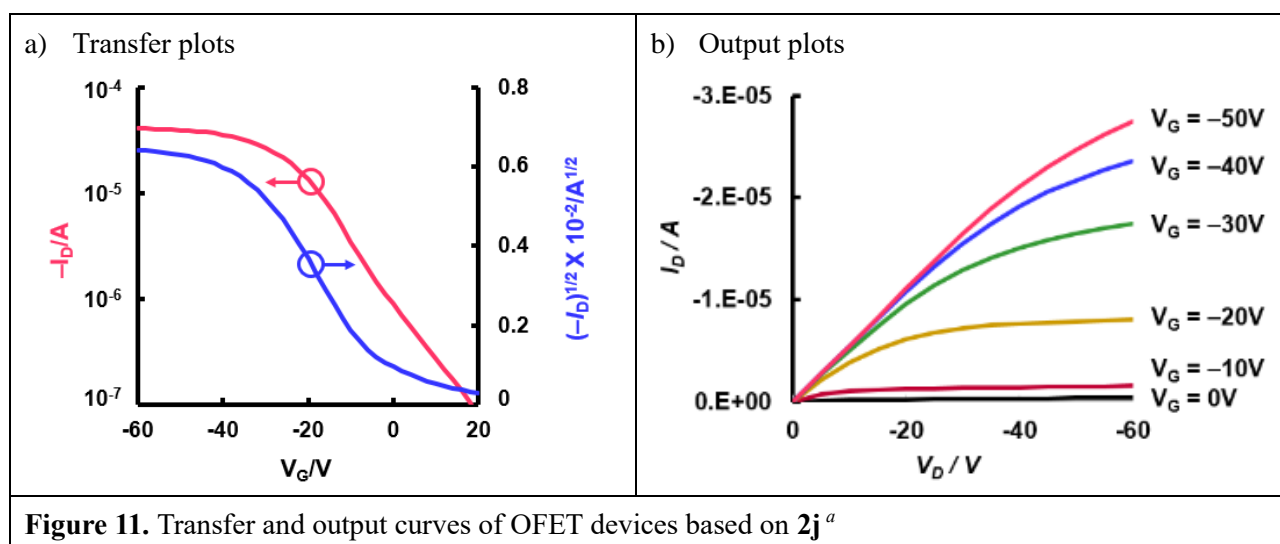


Figure 11. Transfer and output curves of OFET devices based on **2j**^a

^a These plots of **2j** based OFET devices in as-deposited thin films.

5-7. Conclusion

In conclusion, the author investigated the physical properties of BDTFs and BDTTs, respectively. While their fluorescence properties and packing structures were clearly different, E_{HOMO} , E_{LUMO} and hole mobility were similar. BDTFs have better fluorescence properties than BDTTs. In particular, BDTFs with a 4-cyano- C_6H_4 group exhibited the strongest fluorescence ($\Phi_{\text{PL}}=0.85$). Furthermore, the OFET properties of 2,2'-bis([1]benzothieno[3,2-b]thieno[2,3-d]furan) were confirmed. As far as I know, this is the first report showing that thienoacenes containing DTF have OFET and fluorescence properties.

5-8. Experimental Section and Analytical Data

1. UV–Vis Absorption

UV-visible spectra were measured with HITACHI U-1900 UV–Vis Ratio Beam spectrophotometer. Dilute solution (**1**, **2a–2j**, **3a** and **3b**, **4**: 1.0×10^{-5} M) in degassed spectral grade *o*-C₆H₄Cl₂ in a 1 cm square quartz cell was used for measurements. The UV–vis absorption measurement was performed at a scan speed of 100 nm/min from 600 to 220 nm. FL spectra were measured with HITACHI F-2700 spectrophotometer. Dilute solution of **1**, **2a–2j**, **3a** and **3b**, **4** (1.0×10^{-5} M) in degassed spectral grade *o*-C₆H₄Cl₂ in a 1 cm square quartz cell was used for measurements. The FL absorption measurement was performed at a scan speed of 60 nm/min from 682 to 220 nm. Quantum yields of **1**, **2a–2j**, **3a** and **3b**, **4** were measured with a Hamamatsu Photonics Quantaurus QY C11347 with calibrated integrating sphere system.

2. Cyclic Voltammetry

Cyclic voltammograms (CVs) were recorded on Electrochemical Analyzer CHI-600B. A Pt electrode (surface area: $A = 0.071$ cm², BAS), a Ag/Ag⁺ (Ag wire in 0.01 M AgNO₃/0.1 M Bu₄NPF₆/CH₂Cl₂), and a Pt wire electrode were used as working, reference, and counter electrodes, respectively. The working electrode was polished with 5 μm diamond slurry and then with 0.5 μm alumina slurry. After polishing, it was washed with deionized water and acetone, and dried in an oven. A CH₂Cl₂ solution of sample including 1 mM of each sample and 0.1 M of Bu₄NPF₆ was prepared as an electrochemical solution. Using the electrodes and the solutions, beaker-typed three electrode electrochemical cells were constructed, and were connected with the potentiostat to perform cyclic voltammetry. The redox potentials were calibrated with ferrocene as an international standard.

3. DFT Calculations

Density functional theory (DFT) calculations were performed using Gaussian 09 program.⁸ Geometries were optimized at the B3LYP/6-31G(d) level of theory.⁹ TD-DFT calculations were carried out at the same level of theory. The data were summarized in Figure S1.

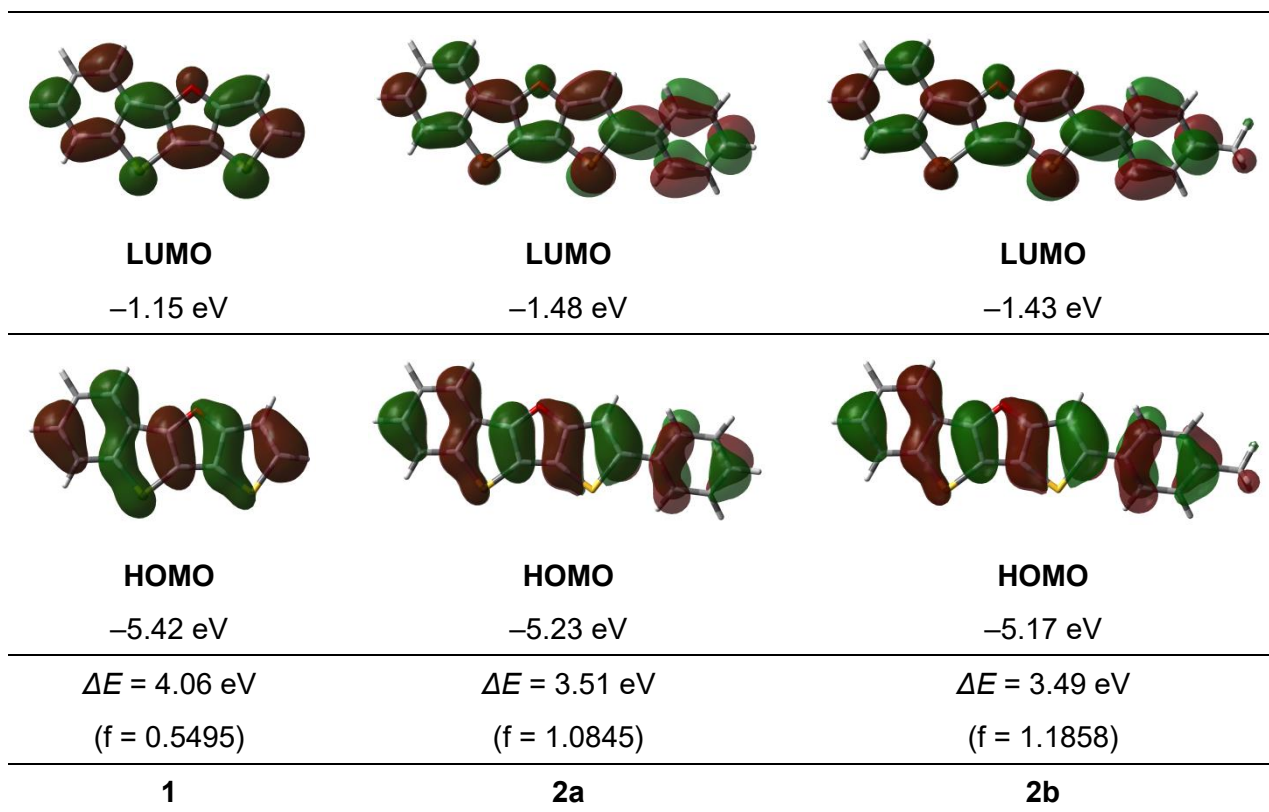


Figure S1. Kohn–Sham HOMO–LUMO orbitals of **1**, **2a–2j**, **3a** and **3b** (continued)

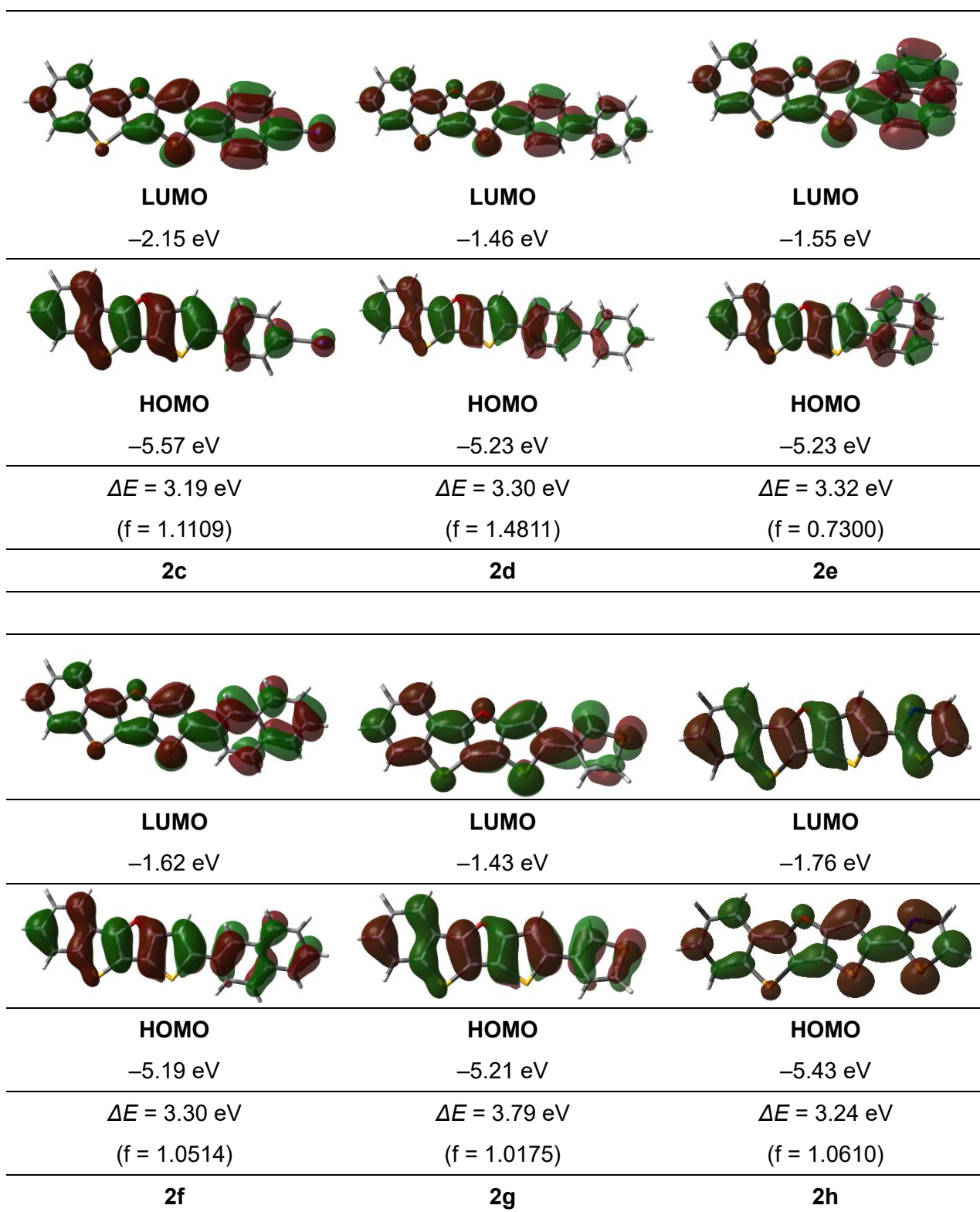


Figure S1. Kohn–Sham HOMO–LUMO orbitals of **1**, **2a–2j**, **3a** and **3b** (continued)

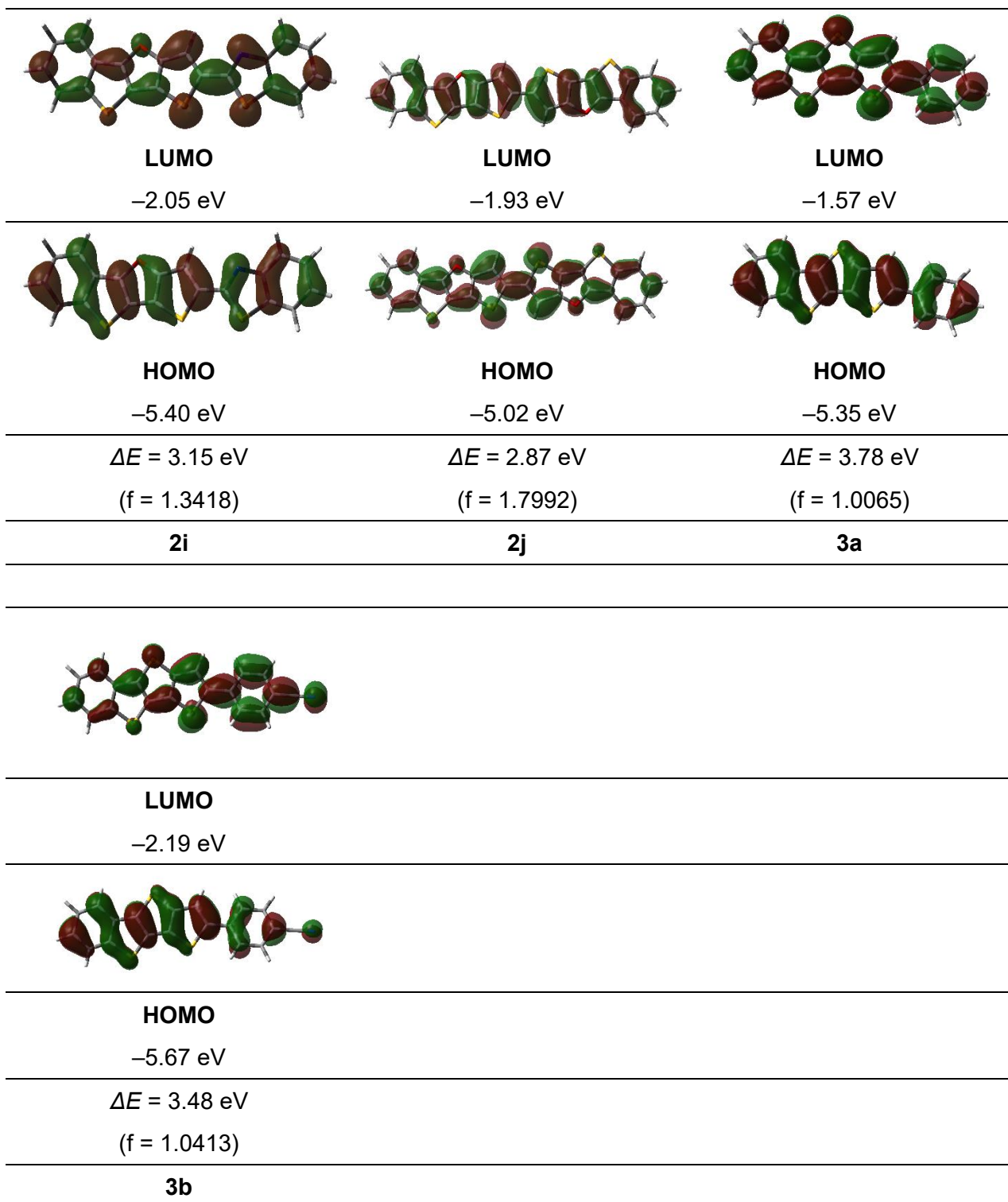


Figure S1. Kohn–Sham HOMO–LUMO orbitals of **1**, **2a–2j**, **3a** and **3b**

4. Computed Geometries

1

C	-1.321506669779	3.937530516127	0.000000000000
C	-1.642935230066	2.586373937713	0.000000000000
C	-0.608777803794	1.635117265778	0.000000000000
C	0.744946515024	2.074367016306	0.000000000000
C	1.059307273506	3.433081847249	0.000000000000
C	0.018702789996	4.359815540495	0.000000000000
C	-0.630657021769	0.209140095369	0.000000000000
C	0.600263253469	-0.417271208929	0.000000000000
S	1.917794519419	0.733374750868	0.000000000000
O	-1.672009908759	-0.683688533873	0.000000000000
C	-1.066601529328	-1.913361480501	0.000000000000
C	0.319153413850	-1.812092504294	0.000000000000
C	-1.584480946462	-3.231914370330	0.000000000000
C	-0.553936402121	-4.135168327752	0.000000000000
S	1.038638437388	-3.391883344673	0.000000000000
H	-2.116528766446	4.677643745945	0.000000000000
H	-2.677902117852	2.257813147349	0.000000000000
H	2.094136150764	3.763240768826	0.000000000000
H	0.249758236187	5.421087521769	0.000000000000
H	-2.633967784900	-3.498686137366	0.000000000000
H	-0.624544208327	-5.214192246077	0.000000000000

2a

C	-3.293417367963	2.514902168734	-0.001481643165
C	-1.910834353634	2.381675042611	-0.000323889746
C	-1.346050688731	1.095041046314	0.001804262701
C	-2.200461519706	-0.043406117491	0.002568148715
C	-3.587534496882	0.099030217532	0.001243880400
C	-4.127189610595	1.383975472235	-0.000554184713
C	0.009463056869	0.654237933506	0.003404159059
C	0.203704205640	-0.714460673279	0.005220241673
S	-1.311857855714	-1.587798786568	0.004780559981
O	1.192047229365	1.350045007788	0.004953437374

Chapter 5. Physical Properties of BDTF, BDTT and Their Derivatives

C	2.158481076250	0.377489749152	0.010633868430
C	1.612239612619	-0.900590809331	0.009355076245
C	3.567637743260	0.443290600440	0.003577991849
C	4.118798996327	-0.822054141935	-0.001189007560
S	2.871381802740	-2.092835450176	0.011764852130
H	-3.736121089563	3.506908158483	-0.003031700202
H	-1.265064686143	3.254653467224	-0.001022057837
H	-4.234792008437	-0.773413187701	0.001616714371
H	-5.206091229056	1.509497679360	-0.001459146318
H	4.149160419766	1.355900444852	-0.029546313633
C	5.538862832303	-1.185544563834	-0.002057935958
C	5.989478966152	-2.398882394394	-0.553996424450
C	6.493927016339	-0.312417055125	0.553402595083
C	7.343575480423	-2.725870954732	-0.550221967418
H	5.275690208721	-3.080135803138	-1.009362291584
C	7.847828039542	-0.636430769981	0.543117685043
H	6.165623141149	0.614162498395	1.015178341043
C	8.280639496018	-1.845710350751	-0.006129192242
H	7.667678078121	-3.667922104068	-0.984259192425
H	8.566480552698	0.052659922943	0.978776525814
H	9.336812642123	-2.100181177065	-0.007093692660

2b

C	5.643156590987	1.563117035872	0.144408591790
C	4.270570877250	1.775460849676	0.161806474242
C	3.404794570744	0.673224349882	0.061824394947
C	3.951089834818	-0.636059461644	-0.054841750099
C	5.330226593608	-0.840627338679	-0.071310549272
C	6.171218249431	0.266251622323	0.028685565974
C	1.982416946002	0.582056340472	0.052195453578
C	1.455387081449	-0.690800283983	-0.062184936358
S	2.707814431999	-1.907261059737	-0.169717791697
O	1.008515889727	1.545210698997	0.135026183375
C	-0.168491485464	0.845182216066	0.066761563428
C	0.044584209251	-0.522940066658	-0.052918159636

Chapter 5. Physical Properties of BDTF, BDTT and Their Derivatives

C	-1.517672783310	1.255593482596	0.112120211266
C	-2.365243288861	0.170019105304	0.021918884444
S	-1.470917571430	-1.363027996623	-0.128368947851
H	6.317533701082	2.411299526240	0.221275203678
H	3.860977873908	2.777141216981	0.251246136746
H	5.741384597210	-1.842209499419	-0.160304419422
H	7.247629060864	0.121321203234	0.016967168744
H	-1.855022034333	2.276819943137	0.236312451411
C	-3.830290253512	0.167855123829	0.023326544220
C	-4.570697250268	-0.937592103346	0.477900105848
C	-4.545890716616	1.292909605404	-0.428162102025
C	-5.962650275136	-0.916098367922	0.478536352860
H	-4.052243458069	-1.813128535721	0.859708153940
C	-5.936325800152	1.310112112793	-0.411692359596
H	-4.004597802826	2.152959396428	-0.811763299778
C	-6.675011911306	0.205509434140	0.035834702226
H	-6.506089614305	-1.785109875532	0.842572881316
H	-6.460153078996	2.195404922957	-0.765666782817
C	-8.184898018788	0.216567457781	0.014264585905
H	-8.582406363340	1.214312046593	0.230297508469
H	-8.571724057380	-0.079397527306	-0.970335476700
H	-8.601182704234	-0.480121154133	0.749365196843
2c			
C	5.627503324606	1.567829270324	0.119613674363
C	4.255113390544	1.779697256485	0.130923305848
C	3.391294393487	0.673911441124	0.057681160838
C	3.937295175123	-0.637634879948	-0.026131186755
C	5.316790807261	-0.841722849573	-0.036835397973
C	6.155863682719	0.268344273450	0.036285917804
C	1.968939918245	0.581577929394	0.048866308936
C	1.443480586789	-0.695075463917	-0.034432478588
S	2.695993452609	-1.913044861595	-0.110255793997
O	0.996033658072	1.546429659929	0.107905766041
C	-0.180460249473	0.845438938425	0.057184449915

Chapter 5. Physical Properties of BDTF, BDTT and Their Derivatives

C	0.033577557603	-0.526728033217	-0.027570017110
C	-1.527304583479	1.254728540184	0.084143115079
C	-2.374479067742	0.164261452109	0.018046371940
S	-1.477818182106	-1.371000094941	-0.085574617948
H	6.301625625384	2.417633391282	0.175827176294
H	3.844439295267	2.782786208086	0.195223643118
H	5.729223092571	-1.844554017940	-0.100783264387
H	7.232335950745	0.124126276356	0.028814808195
H	-1.863042214691	2.279627446209	0.178552033921
C	-3.835878060878	0.165100483554	0.018995153284
C	-4.576728321649	-0.965577683078	0.417555973258
C	-4.548045881100	1.314831947726	-0.381838396956
C	-5.964623346641	-0.952574497955	0.418009277365
H	-4.058785293706	-1.859631000359	0.752109783418
C	-5.934720568461	1.340278703796	-0.372457576274
H	-4.005168990124	2.189531803667	-0.725292193389
C	-6.660243983271	0.203681502770	0.026393161650
H	-6.518496958088	-1.831643543434	0.731190645538
H	-6.466575862044	2.232791917944	-0.686033969868
C	-8.091974987443	0.224026876653	0.030456130227
N	-9.255686400131	0.241376046489	0.034135606215

2d

C	-7.574989777737	1.620399298259	-0.052078471653
C	-6.199592013186	1.813925280753	-0.045117807193
C	-5.349846847100	0.694828179081	-0.037626105904
C	-5.914665195947	-0.611770410652	-0.037192530568
C	-7.296586005402	-0.797363028204	-0.044545216585
C	-8.121474030441	0.325951925126	-0.051835056806
C	-3.928988769039	0.582939045519	-0.029908639133
C	-3.420262914432	-0.702605230372	-0.023394946329
S	-4.689879668581	-1.905880483306	-0.026982848419
O	-2.941707035361	1.535794518962	-0.026733465723
C	-1.774821318369	0.816002329846	-0.015153965787
C	-2.007496208914	-0.554510152354	-0.014036009982

Chapter 5. Physical Properties of BDTF, BDTT and Their Derivatives

C	-0.420610397894	1.209277842086	-0.019508559988
C	0.411958424815	0.107477221280	-0.019085596143
S	-0.504935295579	-1.419809699864	-0.004599267687
H	-8.237220456614	2.481493732732	-0.057739626225
H	-5.775711580477	2.813636110520	-0.045336340976
H	-7.722057150555	-1.796895134807	-0.044496675223
H	-9.199827835575	0.195958071238	-0.057451867817
H	-0.069371835982	2.232756990135	-0.053925132153
C	1.875208670121	0.085207043603	-0.016457637891
C	2.603530137527	-1.006678097085	-0.523452292212
C	2.606425915217	1.173518382879	0.497307307674
C	3.993471756537	-1.009092740878	-0.516468872568
H	2.075390463550	-1.851429882950	-0.957582158077
C	3.995518983906	1.172112114512	0.490654666861
H	2.077525430011	2.014732382278	0.935557149088
C	4.724634562520	0.080469767379	-0.013547106330
H	4.522455486327	-1.856401844383	-0.943306907651
H	4.526982791828	2.015939916648	0.921536829792
C	6.207808822693	0.078268126181	-0.011689548707
C	6.932815326907	1.256618869035	-0.260415344501
C	6.928871090290	-1.102181617846	0.238594214411
C	8.326654175840	1.254932582827	-0.258653076579
H	6.397849786778	2.175452280448	-0.483998482334
C	8.322687370519	-1.104554640959	0.239383124108
H	6.390824508122	-2.019366460484	0.461409653573
C	9.028479413451	0.074146076376	-0.009016595818
H	8.865449548912	2.176754282115	-0.461843424266
H	8.858355286657	-2.027944053359	0.443678122900
H	10.115078434658	0.072538397684	-0.007983061181

2e

C	5.686424126244	1.470799898147	0.366930307577
C	4.318126539686	1.709666624342	0.374140226486
C	3.434641585462	0.642920021986	0.137919007762
C	3.958448471688	-0.658321922977	-0.103484976828

Chapter 5. Physical Properties of BDTF, BDTT and Their Derivatives

C	5.333541023249	-0.889641415792	-0.109119411884
C	6.192412200027	0.182121290565	0.127380096386
C	2.011266566480	0.584074449913	0.085143812384
C	1.463459275453	-0.657855564884	-0.174611861042
S	2.694596958784	-1.883208252735	-0.381092721639
O	1.054397504705	1.553594979655	0.249076093374
C	-0.133941744395	0.889426653138	0.083858032460
C	0.055341210987	-0.463012023764	-0.174359169501
C	-1.476332364518	1.324886235021	0.135830324513
C	-2.342372934715	0.274576161424	-0.088799985808
S	-1.474449782700	-1.254236602348	-0.373515015397
H	6.374574794554	2.291375000775	0.549044489373
H	3.925405084330	2.704987351834	0.559189317746
H	5.728016965706	-1.884802856288	-0.293798155956
H	7.265807748555	0.015925137797	0.125979369458
H	-1.798731804519	2.333520456807	0.360928621723
C	-3.814545959259	0.262696102396	-0.068526529791
C	-4.592842019876	1.248874054458	-0.775440119594
C	-4.472020579572	-0.722443123843	0.656667295204
C	-6.023789237605	1.211679512459	-0.655637333425
C	-4.020352392789	2.242417185505	-1.616082992731
C	-5.879208327858	-0.764686698175	0.745616844992
H	-3.885601843952	-1.459102370863	1.198016961057
C	-6.803146811649	2.190117819139	-1.330064047776
C	-6.640073675022	0.191904656461	0.116165701194
C	-4.806234121987	3.169651260314	-2.264992428853
H	-2.946572852006	2.254041962664	-1.762317704875
H	-6.352721311593	-1.546885406346	1.332278631999
C	-6.211874700174	3.154728170693	-2.112172209436
H	-7.884571029522	2.154924629643	-1.220824507151
H	-7.724438445229	0.178393326539	0.194706596983
H	-4.342131064602	3.913529019037	-2.906968895320
H	-6.820743972368	3.895026217303	-2.623893773660

Chapter 5. Physical Properties of BDTF, BDTT and Their Derivatives

C	-7.569305391223	1.623312716447	-0.074525377308
C	-6.193564073660	1.814628939412	-0.069043637232
C	-5.345584765426	0.694524587758	-0.039314187977
C	-5.912555268378	-0.610898548654	-0.015744996298
C	-7.294782921121	-0.794253141180	-0.021482107825
C	-8.117871184368	0.330010022462	-0.050947064853
C	-3.924845829546	0.580351304672	-0.027653112536
C	-3.418598869396	-0.705728294208	0.002827135253
S	-4.690193939562	-1.906686493223	0.019756131076
O	-2.935651533561	1.531263437643	-0.041922039706
C	-1.770014356113	0.809717226038	-0.016358367341
C	-2.005484735976	-0.560196284502	0.009976744282
C	-0.414921479425	1.199895208252	-0.032637805342
C	0.414836230906	0.096584166116	-0.012271613034
S	-0.505166214930	-1.428498427842	0.029008095510
H	-8.230033667368	2.485263330588	-0.097370369496
H	-5.768036634981	2.813482051810	-0.087400743378
H	-7.722078368504	-1.792846188115	-0.003375628726
H	-9.196415852150	0.201546802540	-0.055705317450
H	-0.059655879280	2.221006066915	-0.089561447431
C	1.879298293826	0.070796982138	-0.003897585810
C	2.602006531493	1.128592405313	0.530843476848
C	2.598190150349	-1.035721465947	-0.549662570577
C	4.018370660311	1.140907065458	0.528974217250
H	2.077984606747	1.964728489033	0.986445749149
C	3.970882471572	-1.056919316444	-0.553446189557
H	2.047116870834	-1.862065535634	-0.989956811619
C	4.765076976009	2.223707586405	1.070216675613
C	4.725849953302	0.023255676996	-0.022468667057
H	4.499386687934	-1.906742465014	-0.978893913810
C	6.141290971777	2.204665907232	1.060851372568
H	4.228455346284	3.070381922744	1.491983208225
C	6.144926651667	0.034693787099	-0.017188937016
C	6.838969711369	1.100517906991	0.511348958463
H	6.699659463889	3.039221763443	1.476282441118

Chapter 5. Physical Properties of BDTF, BDTT and Their Derivatives

H	6.676817019392	-0.815177926299	-0.438621891003
H	7.925532387306	1.098203013559	0.510252457028
2g			
C	5.622917325966	1.540933084348	0.271095644905
C	4.250773133296	1.753163553296	0.310224023340
C	3.382920106623	0.669128356761	0.095476421618
C	3.926560873269	-0.621794745528	-0.157661102542
C	5.305287691377	-0.826395075293	-0.195314942913
C	6.148378713767	0.262145108995	0.020683156585
C	1.960333135951	0.582295320819	0.075670881765
C	1.430883256863	-0.670358502989	-0.171717661127
S	2.680765555574	-1.871300782456	-0.406412432196
O	0.988076694024	1.532889956743	0.261935845932
C	-0.190185999480	0.845332346991	0.128331286843
C	0.020354273101	-0.502684742147	-0.137580267109
C	-1.538579438232	1.257275734020	0.189392634850
C	-2.385655433985	0.190366970360	-0.027907407003
S	-1.496750246568	-1.325982957430	-0.307362635134
H	6.298992070193	2.374997937370	0.436423514092
H	3.843200442342	2.740891124878	0.503593581047
H	5.714480392061	-1.813901666171	-0.388974759327
H	7.224492016361	0.117017962591	-0.005728519144
H	-1.876912456226	2.273147997085	0.350768943127
C	-3.845000086936	0.182359276892	-0.028683928557
C	-4.620137678558	1.084468539001	0.667907388193
C	-4.657771151964	-0.755046308300	-0.759356868176
S	-6.311834145023	0.812817290897	0.433098344487
H	-4.283426915943	1.871400590397	1.328529788803
C	-5.995646323543	-0.540985389658	-0.605787172764
H	-4.248701643499	-1.537084416719	-1.389915393361
H	-6.815079880814	-1.086950534754	-1.053184766236
2h			
C	-3.250701786728	2.529360886444	-0.031835001783

Chapter 5. Physical Properties of BDTF, BDTT and Their Derivatives

C	-1.869890702325	2.381097209757	-0.037486761452
C	-1.320075293193	1.088283864111	-0.008361909767
C	-2.186055993635	-0.040599520126	0.026227674722
C	-3.571551222415	0.117060490266	0.031668075159
C	-4.096402519959	1.407639289217	0.002447858839
C	0.030564396397	0.633267434787	-0.006049983620
C	0.209229664221	-0.738332999953	0.027633277531
S	-1.315368225494	-1.594791601199	0.059755132089
O	1.218403448440	1.316621851638	-0.031489575431
C	2.176451083075	0.336109107659	-0.013050264779
C	1.613793408888	-0.937888435061	0.023172330910
C	3.581538408242	0.386196430602	-0.023896592618
C	4.106939407832	-0.892316521322	0.004990960119
S	2.853081455022	-2.149802526979	0.045534900244
H	-3.682884757996	3.525639292258	-0.054212695612
H	-1.214268414028	3.246209673297	-0.063962031937
H	-4.228556308927	-0.747554711612	0.058118639386
H	-5.173792275588	1.545190845741	0.006301129598
H	4.199040548411	1.274039104469	-0.050722396990
C	5.517894186592	-1.217930187705	0.003694426845
S	6.128125266982	-2.879229031032	0.041017499294
C	7.705317188697	-0.882661749215	-0.020371677256
C	7.743200079329	-2.247992722930	0.014458912351
H	8.580366887586	-0.242641783745	-0.042860935641
H	8.602358533662	-2.903718054217	0.025333142967
N	6.462792816912	-0.307978475152	-0.025524223169

2i

C	-3.170099621583	2.605578986809	0.320323284431
C	-1.797482833178	2.397813043398	0.352473410228
C	-1.293592515281	1.112716880358	0.089572358907
C	-2.196071627619	0.052061583344	-0.203641689318
C	-3.573243391707	0.269282986109	-0.233910938367
C	-4.052324629156	1.550992861361	0.029654214261
C	0.038576263261	0.607788408370	0.051844164547

Chapter 5. Physical Properties of BDTF, BDTT and Their Derivatives

C	0.169974023395	-0.737062005094	-0.246183873300
S	-1.380498098160	-1.502153338523	-0.509705702129
O	1.246458999247	1.220185633897	0.260881988478
C	2.169510096804	0.221307613081	0.087320450176
C	1.564691534751	-0.995562461823	-0.224244908717
C	3.571818127360	0.205855627821	0.164828461863
C	4.052310722336	-1.065169129009	-0.096288858798
S	2.758038634606	-2.232817083941	-0.436542514861
H	-3.567323088510	3.596105001899	0.522452803381
H	-1.113500791226	3.210705361466	0.576760316084
H	-4.258640967231	-0.543009371601	-0.458138262397
H	-5.122676901326	1.734392764590	0.009438529998
H	4.219087645528	1.042251981417	0.392401598212
C	5.448014353956	-1.447160978560	-0.102406110940
C	7.626304458975	-2.606042544137	-0.240060359090
C	7.647190913723	-1.223581333544	0.076134190846
C	8.802479449971	-3.350282178908	-0.341608801281
C	8.879125331960	-0.585840172765	0.292826505034
C	10.013141912303	-2.696442206693	-0.122543259193
H	8.778870765559	-4.408325585336	-0.584077296592
C	10.049728456484	-1.326659752109	0.191749464248
H	8.892182502133	0.472156449420	0.534693657583
H	10.941129572224	-3.256285447990	-0.196469710603
H	11.007710678137	-0.842133873342	0.357643683042
N	6.414077669561	-0.608972737805	0.144680868943
S	5.965727692701	-3.124073892160	-0.454411224677

2j

C	-8.692985096369	1.565182556526	-0.315875039529
C	-7.316457342880	1.747635318661	-0.343184121282
C	-6.474448705207	0.640480941697	-0.143337874024
C	-7.047610952910	-0.642730526142	0.082588521225
C	-8.430703975025	-0.817310637020	0.108070214700
C	-9.247855941059	0.293790473894	-0.092132237629
C	-5.054729570340	0.521883800517	-0.117525217952

Chapter 5. Physical Properties of BDTF, BDTT and Their Derivatives

C	-4.554271516351	-0.747460392411	0.109745323933
S	-5.831639110924	-1.924461464018	0.315117765589
O	-4.061210563408	1.454528567085	-0.277090547552
C	-2.899538463993	0.740794427663	-0.141451766877
C	-3.141910531439	-0.608349779628	0.096688747424
C	-1.545157715384	1.119015105240	-0.220421431331
C	-0.720754545712	0.024120962709	-0.029460185804
S	-1.646149470711	-1.472458119421	0.260688695228
H	-9.349550841849	2.416801591842	-0.469504570651
H	-6.885713025249	2.729305347864	-0.515861378471
H	-8.863127586900	-1.798791728153	0.280434851084
H	-10.327026683118	0.172138224257	-0.074531226754
H	-1.185370030534	2.118906904071	-0.429847496384
C	0.720754545712	-0.024120962709	-0.029460185804
C	1.545157715384	-1.119015105240	-0.220421431331
S	1.646149470711	1.472458119421	0.260688695228
C	2.899538463993	-0.740794427663	-0.141451766877
H	1.185370030534	-2.118906904071	-0.429847496384
C	3.141910531439	0.608349779628	0.096688747424
O	4.061210563408	-1.454528567085	-0.277090547552
C	4.554271516351	0.747460392411	0.109745323933
C	5.054729570340	-0.521883800517	-0.117525217952
S	5.831639110924	1.924461464018	0.315117765589
C	6.474448705207	-0.640480941697	-0.143337874024
C	7.047610952910	0.642730526142	0.082588521225
C	7.316457342880	-1.747635318661	-0.343184121282
C	8.430703975025	0.817310637020	0.108070214700
C	8.692985096369	-1.565182556526	-0.315875039529
H	6.885713025249	-2.729305347864	-0.515861378471
C	9.247855941059	-0.293790473894	-0.092132237629
H	8.863127586900	1.798791728153	0.280434851084
H	9.349550841849	-2.416801591842	-0.469504570651
H	10.327026683118	-0.172138224257	-0.074531226754

Chapter 5. Physical Properties of BDTF, BDTT and Their Derivatives

C	-0.990764501363	5.884257979402	-0.067538796995
C	-1.426792246312	4.567205476723	-0.135630306930
C	-0.501883008182	3.521101265717	0.026272613185
C	0.863617075758	3.840891729908	0.257252985002
C	1.298400053385	5.164886388935	0.324895509395
C	0.362547802249	6.183430850874	0.160920907932
C	-0.684285921384	2.098406044124	0.000649873128
C	0.478630286563	1.370755648086	0.201957617097
S	1.880210914365	2.399151829227	0.437217295393
C	-1.079084884110	-0.356876558725	-0.054722445082
C	0.256980836825	-0.030048916320	0.170522496128
C	-1.332588810585	-1.751617451583	-0.101612223436
C	-0.191416991864	-2.498861196899	0.089756043420
S	1.226059761495	-1.464573418958	0.341214586463
H	-1.705311070878	6.692840512910	-0.192532995989
H	-2.475057335172	4.341963208152	-0.312705062359
H	2.344625933626	5.397173311587	0.501958432246
H	0.685613857473	7.219271934770	0.210875146172
H	-2.302058151516	-2.193699043845	-0.298941144705
S	-2.089541697710	1.070264895515	-0.236173095157
C	-0.061569417461	-3.959759784144	0.112184275514
C	-1.152327679590	-4.761964418548	0.498155451524
C	1.138365612755	-4.598475880554	-0.250303777451
H	1.988455802598	-4.002841086801	-0.572003282800
C	-1.048886154239	-6.150358157307	0.505706159257
C	1.242323722139	-5.987585001136	-0.229221926281
H	2.178703198782	-6.458642234141	-0.515786069167
C	0.149133901045	-6.771156360141	0.144367715450
H	0.230333961146	-7.854437794920	0.157454962113
H	-2.077079720418	-4.289345252614	0.815742378065
H	-1.903487209423	-6.749381479298	0.808809358869
3b			
C	-0.958810466457	6.488292299921	0.010782428129
C	-1.406825406531	5.175914128155	-0.063166593478

Chapter 5. Physical Properties of BDTF, BDTT and Their Derivatives

C	-0.485646690379	4.121488155480	0.061934070645
C	0.887694447958	4.427106784261	0.262290047108
C	1.334619673502	5.746894050444	0.336050208346
C	0.402475037818	6.773740613850	0.208836225052
C	-0.679995078927	2.700681808491	0.023142342822
C	0.482854390545	1.962276377115	0.185710656284
S	1.897838391274	2.976168564404	0.398025806971
C	-1.097732689918	0.251965466429	-0.054285680507
C	0.247815256471	0.564699023087	0.140457368051
C	-1.363480474775	-1.137908226514	-0.107919206750
C	-0.222317434620	-1.897192390197	0.045636290455
S	1.210172111802	-0.876898630829	0.268556176464
H	-1.669466425451	7.304008130678	-0.085652607415
H	-2.460883181230	4.960775999301	-0.216496069956
H	2.386589271324	5.969381372095	0.489453234750
H	0.734646805470	7.806364681180	0.263828028612
H	-2.342764318169	-1.567306682135	-0.283395786921
S	-2.100039942042	1.689200709152	-0.191407000576
C	-0.106693891284	-3.355391446679	0.043429575354
C	-1.220437452450	-4.158943575594	0.363199329491
C	1.104438935023	-4.000044202713	-0.276745979872
H	1.975050088520	-3.409506192067	-0.546569622102
C	-1.134169432109	-5.543344383782	0.349882788843
C	1.202649053891	-5.384755769586	-0.280973090621
H	2.142604399419	-5.864696744208	-0.533404232785
C	0.081478826493	-6.172689892202	0.028723422994
H	-2.156835639679	-3.689721104190	0.647215760658
H	-2.000372782274	-6.147085214158	0.600755374651
C	0.175946839270	-7.601598730289	0.020877053103
N	0.251895387515	-8.762878548898	0.013973072200

Charge transfer integrals calculated by the Amsterdam density functional (ADF) theory program^{7a} which has been employed for calculating the electronic coupling.¹⁰ The TZP basis set in ADF was used and the local density functional VWN¹¹ was employed in conjunction with the PW91 gradient corrections.¹²

5. OFET Device Fabrication

Typical bottom-gate top-contact OFET devices were fabricated as follows. All processes, except for a substrate cleaning, were performed under a nitrogen atmosphere. A heavily doped *n*-Si wafer with 200 nm thick thermally grown SiO₂ ($C_i = 17.3 \text{ nF cm}^{-2}$) as the dielectric layer was used as the substrate. The Si/SiO₂ substrates were carefully cleaned using ultrasonication with acetone and isopropanol for 10 min, respectively. After being dried, the substrates were irradiated by UV-O₃ for 20 min, and then treated with the solution of 0.1 M *n*-octyltrichlorosilane (OTS) in anhydrous toluene to form a self-assembled monolayer (SAM). The active layers were deposited on the treated substrate by vapor deposition at the rate of 0.1 Å/s. Thermal annealing was performed at 50 and 100 °C for 30 minutes on the hotplate in glove box. After treatment, gold electrodes (50 nm thick) was deposited through a shadow mask on the top of the active layer under reduced pressure ($5 \times 10^{-5} \text{ Pa}$). The current-voltage characteristics of the OFET devices were measured at room temperature in air on a Keithley 6430 sub-femto ampere remote source meter combined with Keithley 2400 measure-source unit. Field-effect mobilities were calculated in the saturation regime of the I_D using following equation,

$$I_D = (WC_i/2L) \mu (V_G - V_{th})^2$$

Where C_i is the capacitance of the SiO₂ insulator. I_D is the source-drain current, and V_D , V_G , and V_{th} are the source-drain, gate, and threshold voltages, respectively. Current on/off ratio ($I_{on/off}$) was determined from a minimum I_D at around $V_G = -60 \text{ V}$. The parameters of all devices were collected from more than five different devices.

TGA measurements of 2j

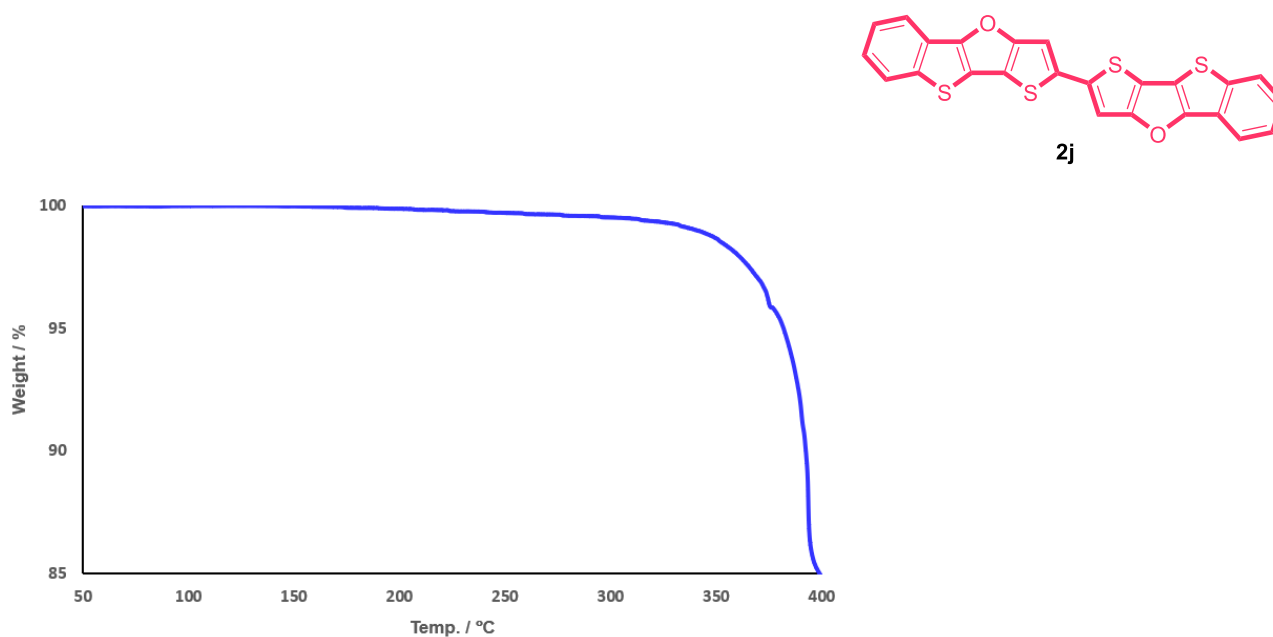


Figure S2. TGA curves of 2j

References

- (1) (a) Takimiya, K.; Shinamura, S.; Osaka, I.; Miyazaki, E. *Adv. Mater.* **2011**, *23*, 4347–4370. (b) Cinar, M. E.; Ozturk, T. *Chem. Rev.* **2015**, *115*, 3036–3140. (c) Cernovská, K.; Košata, B.; Svoboda, J.; Novotná, V.; Glogarová, M. *Liquid Cryst.* **2006**, *33*, 987–996. (d) Ding, Y.; Jiang, Y.; Zhang, W.; Zhang, L.; Lu, X.; Wang, Q.; Zhou, G.; Liu, J.-M.; Kempa, K.; Gao, J. *J. Phys. Chem. C* **2017**, *121*, 16731–16738. (e) Yang, Y.; Yasuda, T.; Adachi, C. *Bull. Chem. Soc. Jpn.* **2012**, *85*, 1186–1191. (f) Sugiyama, H.; Yoshida, M.; Mori, K.; Kawamoto, T.; Sogabe, S.; Takagi, T.; Oki, H.; Tanaka, T.; Kimura, H.; Ikeura, Y. *Chem. Pharm. Bull.* **2007**, *55*, 613–624.
- (2) (a) Karminski-Zamola, G. M.; Malesevic, M.; Bajic, M.; Golja, G. *Croat. Chem. Acta* **1993**, *65*, 847–849. (b) Kozmik, V.; Poznik, M.; Svoboda, J.; Frere, P. *Tetrahedron Lett.* **2015**, *56*, 6251–6253.
- (3) Youn, J.; Chen, M. C.; Liang, Y.; Huang, H.; Ortiz, R.; Kim, C.; Stern, C.; Hu, T. S.; Chen, L. H.; Yan, J. Y.; Facchetti, A.; Marks, T. *Chem. Mater.* **2010**, *22*, 5031–5041.
- (4) (a) Tian, H.; Han, Y.; Bao, C.; Yan, D.; Geng, Y.; Wang, F. *Chem. Commun.* **2012**, *48*, 3557–3559 (b) Wang, M.; Wei, J.; Fan, Q.; Jiang, X. *Chem. Commun.* **2017**, *53*, 2918–2921.
- (5) (a) Zander, M. *Z. Naturforsch. A* **1989**, *44*, 1116–1118 (b) Zander, M.; Kirsch, G. *Z. Naturforsch. A* **1989**, *44*, 205–209.
- (6) Yamaguchi, Y.; Ochi, T.; Matsubara, Y.; Yoshida, Z. *J. Phys. Chem.* **2015**, *119*, 8630–8642.
- (7) (a) te Velde, G.; Bickelhaupt, F. M.; Baerends, E. J.; Fonseca Guerra, C.; van Gisbergen, S. J. A.; Snijders, J. G.; Ziegler, T. *J. Comput. Chem.* **2001**, *22*, 931–967. (b) Guerra, C. F.; Snijders, J. G.; te Velde, G.; Baerends, E. J.; *Theor. Chem. Acc.* **1998**, *99*, 391–403. (c) ADF2017, SCM, Theoretical Chemistry, Vrije Universiteit, Amsterdam, Baerends, E. J.; Ziegler, T.; Atkins, A. J.; Autschbach, J.; Basoggio, O.; Bashford, D.; Bérces, A.; Bickelhaupt, F. M.; Bo, C.; Boerrigter, P. M.; Cavallo, L.; Daul, C.; Chong, D. P.; Chulhai, D. V.; Deng, L.; Dickson, R. M.; Dieterich, J. M.; Ellis, D. E.; van Faassen, M.; Fan, L.; Fischer, T. H.; Fonseca Guerra, C.; Franchini, M.; Ghysels, A.; Giammona, A.; van Gisbergen, S. J. A.; Goez, A.; Götz, A. W.; Groeneveld, J. A.; Gritsenko, O. V.; Grening, M.; Gusarov, S.; Harris, F. E.; van den Hoek, P.; Hu, Z.; Jacob, C. R.; Jacobsen, H.; Jensen, L.; Joubert, L.; Kaminski, J. W.; van Kessel, G.; König, C.; Kootstra, F.; Kovalenko, A.; Krykunov, M. V.; van Lenthe, E.; McCormack, D. A.; Michalak, A.; Mitoraj, M.; Morton, S. M.; Neugebauer, J.; Nicu, V. P.; Noodleman, L.; Osinga, V. P.; Patchkovskii, S.; Pavanello, M.; Peebles, C. A.; Philipsen, P. H. T.; Post, D.; Pye, C. C.; Ramanantoanina, H.; Ramos, P.; Ravenek, W.; Rodríguez, J. I.; Ros, P.; Rüger, R.; Schipper, P. R. T.; Schlüns, D.; van Schoot, H.; Schreckenbach, G.; Seldenthuis, J. S.; Seth, M.; Snijders, J. G.; Solà, M.; Stener, M.; Swart, M.; Swerhone, D.; Tognetti, V.; te Velde, G.; Vernooijs, P.; Versluis, L.; Visscher, L.; Visser, O.; Wang, F.; Wesolowski, T. A.; van Wezenbeek, E. M.; Wiesenekker, G.; Wolff, S. K.; Woo, T. K.; Yakovlev, A. L.
- (8) *Gaussian 09, Revision E.01*, Frisch, M. J.; Trucks, G. W.; Schlegel, H. B.; Scuseria, G. E.; Robb, M. A.; Cheeseman, J. R.; Scalmani, G.; Barone, V.; Mennucci, B.; Petersson, G. A.; Nakatsuji, H.; Caricato, M.; Li,

X.; Hratchian, H. P.; Izmaylov, A. F.; Bloino, J.; Zheng, G.; Sonnenberg, J. L.; Hada, M.; Ehara, M.; Toyota, K.; Fukuda, R.; Hasegawa, J.; Ishida, M.; Nakajima, T.; Honda, Y.; Kitao, O.; Nakai, H.; Vreven, T.; Montgomery, J. A., Jr.; Peralta, J. E.; Ogliaro, F.; Bearpark, M.; Heyd, J. J.; Brothers, E.; Kudin, K. N.; Staroverov, V. N.; Kobayashi, R.; Normand, J.; Raghavachari, K.; Rendell, A.; Burant, J. C.; Iyengar, S. S.; Tomasi, J.; Cossi, M.; Rega, N.; Millam, N. J.; Klene, M.; Knox, J. E.; Cross, J. B.; Bakken, V.; Adamo, C.; Jaramillo, J.; Gomperts, R.; Stratmann, R. E.; Yazyev, O.; Austin, A. J.; Cammi, R.; Pomelli, C.; Ochterski, J. W.; Martin, R. L.; Morokuma, K.; Zakrzewski, V. G.; Voth, G. A.; Salvador, P.; Dannenberg, J. J.; Dapprich, S.; Daniels, A. D.; Farkas, Ö.; Foresman, J. B.; Ortiz, J. V.; Cioslowski, J.; Fox, D. J. Gaussian, Inc., Wallingford CT, 2009.

(9) (a) Becke, A. D. *J. Chem. Phys.* **1993**, *98*, 5648–5652. (b) Lee, C.; Yang, W.; Parr, R. G. *Phys. Rev. B* **1988**, *37*, 785–789. (c) Becke, A. D. *J. Chem. Phys.* **1993**, *98*, 1372–1377. (d) Stephens, P. J.; Devlin, F. J.; Chabalowski, C. F.; Frisch, M. J. *J. Phys. Chem.* **1994**, *98*, 11623–11627.

(10) (a) Senthilkumar, K.; Grozema, F. C.; Bickelhaupt, F. M.; Siebbeles, L. D. A. *J. Chem. Phys.* **2003**, *119*, 9809–9817. (b) Prins, P.; Senthilkumar, K.; Grozema, F. C.; Jonkheijm, P.; Schenning, A. P. H. J.; Meijer, E. W.; Siebbeles, L. D. A. *J. Phys. Chem. B.* **2005**, *109*, 18267–18274. (c) Valiyev, F.; Hu, W. S.; Chen, H. Y.; Kuo, M. Y.; Chao, I.; Tao, Y. T. *Chem. Mater.* **2007**, *19*, 3018–3026.

(11) Vosko, S. H.; Wilk, L.; Nusair, M. *Can. J. Phys.* **1980**, *58*, 1200–1211.

(12) Perdew, J. P.; Wang, Y. *Phys. Rev. B.* **1992**, *45*, 13244–13249.

Chapter 6. Synthesis of Diarylphosphole Oxide via Electrochemical Cyclization

6-1.	Abstract	132
6-2.	Introduction	132
6-3.	Optimization for the Synthesis of Diarylphosphole Oxide via Electrochemical Cyclization	134
6-4.	Substrate Scope	136
6-5.	Cyclic Voltammograms of Related Compounds	138
6-6.	Control Experiments	139
6-7.	Plausible Reaction Mechanism	140
6-8.	Conclusion	140
6-9.	Experimental Section and Analytical Data	141
	References	153

6-1. Abstract

The author achieved that the first electrochemical synthesis of diarylphosphole oxides (DPOs) from biarylphosphine oxides (BPOs) under mild conditions. The practical protocol employs commercially available and cheap DABCO as a hydrogen atom transfer (HAT) mediator, leading to various DPOs in moderate to good yields. Furthermore, this synthetic method can also be applied to the synthesis of six-membered phosphacycles such as phenophosphazine derivatives. The control experiments suggested that the reaction proceeds via the electrogenerated phosphinyl radical.

6-2. Introduction

Phosphole oxide-containing π -conjugated molecules have been attracting attention because they have high electron acceptability, thermal stability and chemical stability, and have been used as basic skeletons for organic functional materials^{1,2,3} Among them, diarylphosphole oxide (DPO) is a key motif in the design of phosphole-containing organic functional materials.⁴ For instance, dibenzophosphole analogue is known as an organic light-emitting diodes (OLED) emitter with TADF ability.^{4g} thienobenzophosphole analogue is also known as an active material for an organic photovoltaic (OPV) (Figure 1).^{4d}

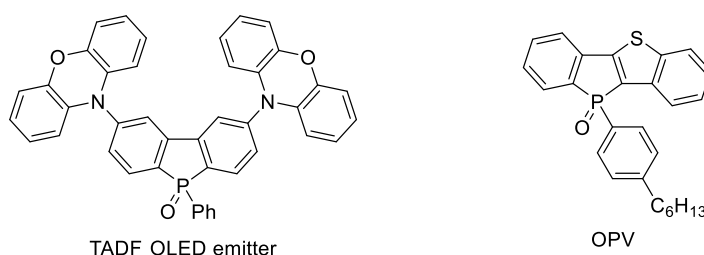
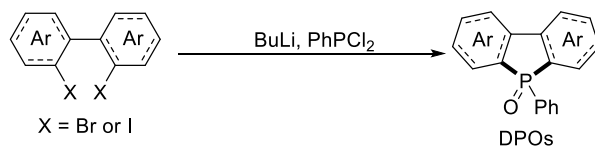


Figure 1. Representative DPOs

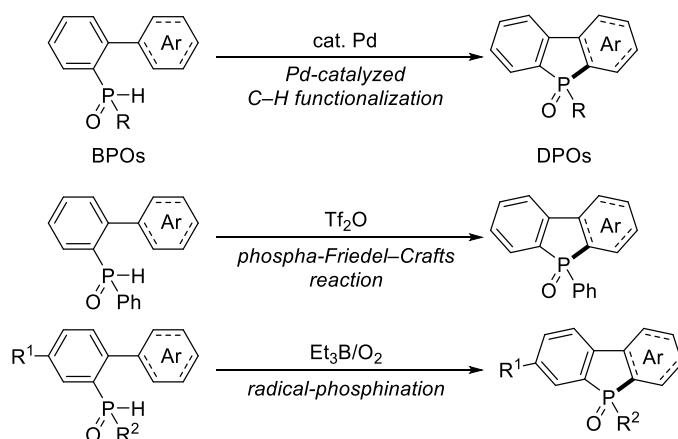
DPOs are generally synthesized by bislithiation of 2,2'-dihalobiaryl derivatives followed by trapping with PhPCl_2 (Scheme 1A),⁵ but this conventional synthetic procedure required tedious and multistep sequences with complicated and unstable starting substrates and/or reagents. As a method for the direct synthesis of DPOs, intramolecular cyclization of biarylphosphine oxides (BPOs) has received attention. Several efficient methods have been reported for synthesizing DPOs with this protocol (Scheme 1B).⁶ However, these methods require the use of transition metal catalyst or excess amounts of acid. Therefore, development of a transition metal-free and environmentally benign synthetic methodology is highly desirable.

Scheme 1. Representative synthetic methods of DPOs

A. Conventional Method: Bislithiation strategy



B. Representative Reported Method: Intramolecular cyclization strategy

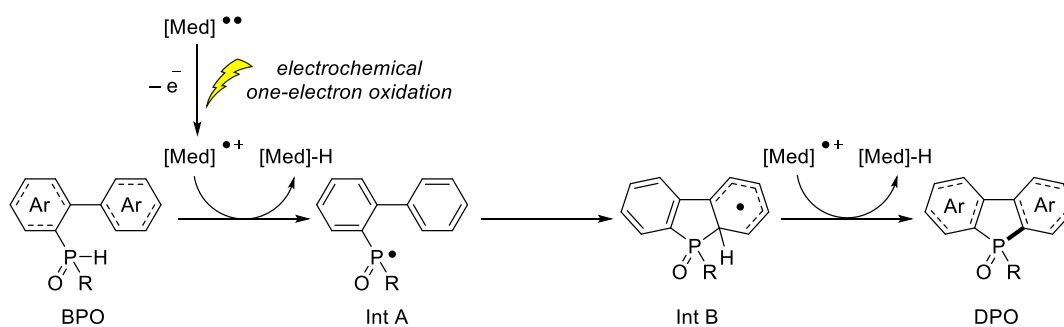


Electrochemistry offers a green and efficient alternative to conventional chemical approaches.⁷ By solely employing electric current as inexpensive and sustainable reducing or oxidizing agents, amounts of waste are tremendously diminished and thus toxic reagents can be superseded.

To the best of the author's knowledge, the synthesis of DPOs from BPOs via the electrochemical method has never been reported. As a related study, electrochemical dehydrogenative C–H/P–H cross-coupling using biphenylphosphine oxide as a substrate has been reported.^{8,9} In these methods, target products were synthesized by direct electrolysis⁸ or mediated electrolysis⁹ using transition metal mediator such as Cu,^{9a} Rh,^{9b} Ag,^{9c} Mn^{9d,9e} and Ni.^{9f} Mediated electrolysis is a practical methodology because it is applicable for a wider range of substrates than direct electrolysis and facilitates the reaction under mild conditions. Furthermore, a mediated electrolysis using a nonmetallic mediator is useful as a more attractive methodology from a green chemistry perspective. Thus, the author aimed to develop a synthetic method of DPOs from BPOs by a mediated electrolysis.

The author's approach for synthesizing DPOs is envisioned in Scheme 2. Initially, reactive radical cation species ($[\text{Med}]^{\bullet+}$) would be generated by one-electron oxidation of mediator ($[\text{Med}]^{\bullet\bullet}$). Next, $[\text{Med}]^{\bullet+}$ acts as a hydrogen atom transfer (HAT) mediator, transferring the hydrogen atom on the phosphorus atom of BPO to produce radical intermediate A (**Int A**). Subsequent intramolecular addition of the phosphinyl radical species to unsaturated bond produces intermediate B (**Int B**). Finally, DPO is obtained by abstracting a hydrogen atom of **Int B** by $[\text{Med}]^{\bullet+}$.¹⁰

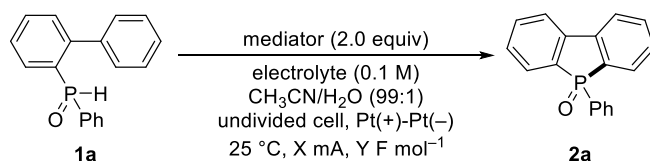
Scheme 2. Working hypothesis (Electrochemical synthetic approach)



Meanwhile, Baran and co-workers reported a practical electrochemical oxidation of unactivated C–H bonds using tertiary amine as a HAT mediator.¹¹ Tertiary amines such as quinuclidine are highly efficient mediators that allow the transfer of hydrogen atom to unsaturated hydrocarbons with high redox potentials. Thus, the authors considered that an efficient synthetic method of DPO was feasible if **Int A** could be prepared from BPO with a tertiary amine as a HAT mediator.

6-3. Optimization for the Synthesis of Diarylphosphole Oxide via Electrochemical Cyclization

According to the designed synthetic approach described above, BPO (biphenylphenylphosphine oxide: **1a**) was selected as a model substrate to optimize the reaction conditions (Table 1). The electrolysis was first conducted under a constant current of 2.5 mA in an undivided cell equipped with a platinum (Pt) anode and a Pt cathode using Bu_4NBF_4 as a supporting electrolyte in a mixed solvent of $\text{CH}_3\text{CN}/\text{H}_2\text{O}$ (99:1) at room temperature. By direct electrolysis, the corresponding product **2a** was obtained in 8% yield, and the starting material **1a** was mainly recovered (entry 1). The author next examined mediated electrolysis using tertiary amine as a mediator. Running the reaction with DABCO furnished **2a** in 71% yield (entry 2). The use of quinuclidine and Et_3N resulted in inferior efficiency (entries 3 and 4). Replacing Bu_4NBF_4 with other supporting electrolytes, such as LiBF_4 and Bu_4NClO_4 , was found to be inappropriate for this reaction (entries 5 and 6). Reducing or increasing the electric current resulted in poor results (entries 7 and 8). Increasing the amount of charge decreased the yield (entries 9 and 10). Changing the amount of DABCO and the amount of H_2O negatively affected the yield (entries 11–15). Moreover, without electric current, this electrochemical progression was mostly suppressed (entries 16 and 17). These results suggested that both electric current and DABCO are essential for the progress of this reaction.

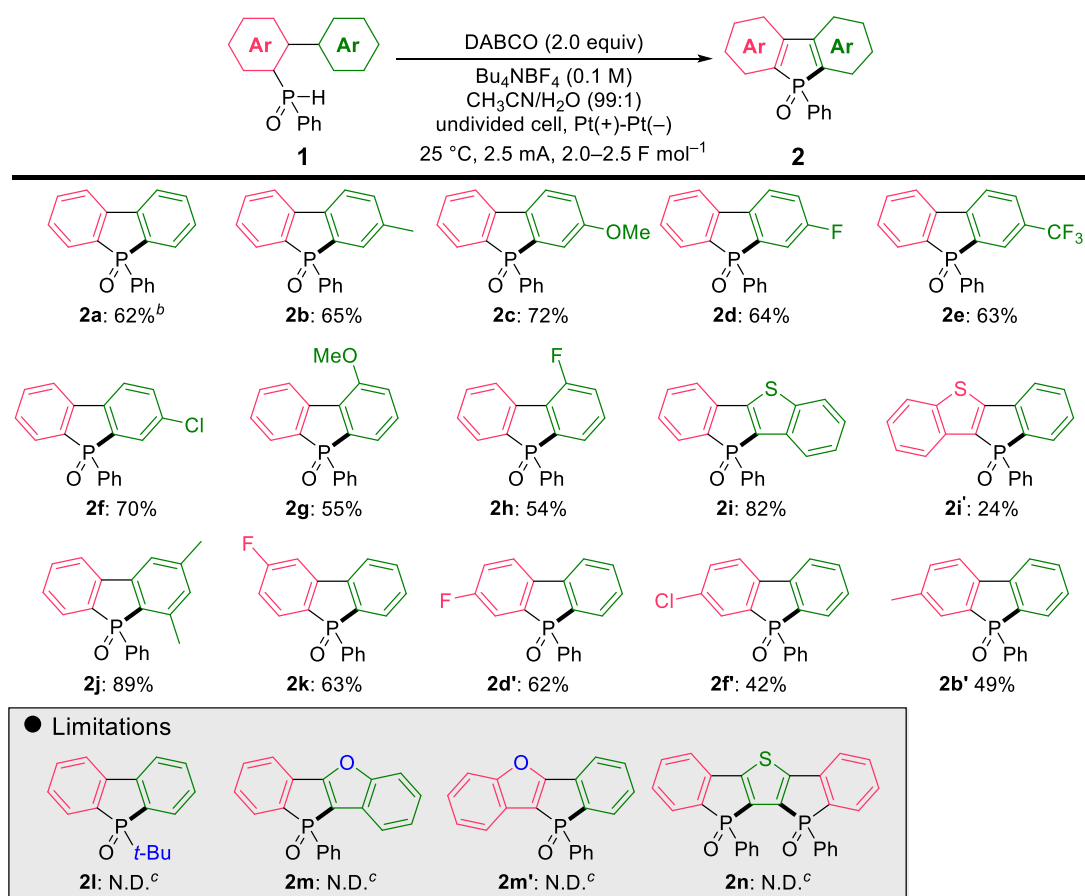
Table 1. Optimization for the synthesis of DPO **2a**^a

entry	mediator	electrolyte	X (mA)	Y (F mol ⁻¹)	yield (%)
1	–	Bu ₄ NBF ₄	2.5	2.0	8
2	DABCO	Bu ₄ NBF ₄	2.5	2.0	71
3	quinuclidine	Bu ₄ NBF ₄	2.5	2.0	27
4	Et ₃ N	Bu ₄ NBF ₄	2.5	2.0	16
5	DABCO	LiBF ₄	2.5	2.0	61
6	DABCO	Bu ₄ NClO ₄	2.5	2.0	49
7	DABCO	Bu ₄ NBF ₄	2.0	2.0	64
8	DABCO	Bu ₄ NBF ₄	3.0	2.0	54
9	DABCO	Bu ₄ NBF ₄	2.5	2.5	62
10	DABCO	Bu ₄ NBF ₄	2.5	3.0	59
11 ^b	DABCO	Bu ₄ NBF ₄	2.5	2.0	43
12 ^c	DABCO	Bu ₄ NBF ₄	2.5	2.0	58
13 ^d	DABCO	Bu ₄ NBF ₄	2.5	2.0	67
14 ^e	DABCO	Bu ₄ NBF ₄	2.5	2.0	66
15 ^f	DABCO	Bu ₄ NBF ₄	2.5	2.0	50
16 ^g	DABCO	Bu ₄ NBF ₄	–	–	11
17 ^g	–	Bu ₄ NBF ₄	–	–	N.D.

^a Reaction conditions: **1a** (0.4 mmol) and mediator (0.8 mmol) in CH₃CN/H₂O (3.96/0.04 mL) with 0.1 M supporting electrolyte were electrolyzed. Yield was determined by ¹H NMR analysis using 1,1,2,2-tetrachloroethane as an internal standard. ^b 1.0 equivalent of DABCO ^c 2.5 equivalent of DABCO ^d Performed in CH₃CN/H₂O (99.5/0.5). ^e Performed in CH₃CN/H₂O (98/2). ^f Performed in CH₃CN. ^g Performed for 8.58 h without electrolysis

6-4. Substrate Scope

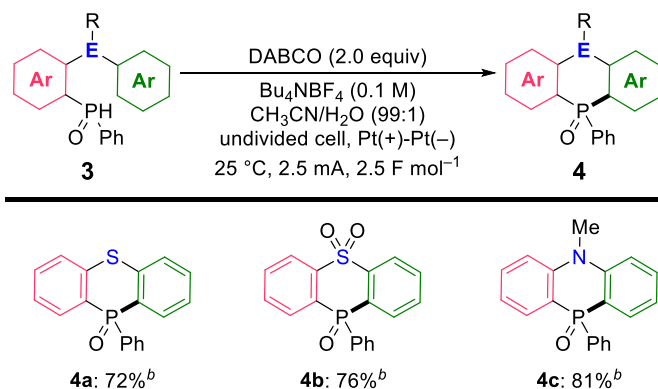
The author next investigated the substrate scope for the synthesis of DPOs **2** via electrochemical cyclization (Scheme 3). BPOs bearing several substituents including Me, OMe, F, CF₃, and Cl on the benzene ring were applicable, and the corresponding products **2b–n** were obtained in moderate to high yields. Furthermore, this reaction can be applied to the synthesis of heteroring-fused DPOs **2i** and **2i'**. The reactions were slightly inhibited by a substituent at the ortho position, and the corresponding DPOs **2g** and **2h** were isolated in respective yields of 55% and 54%. Unfortunately, the reaction of substrates (**1l–n**) did not give the desired product under the standard conditions (**2l–n**).

Scheme 3. Substrate scope for the synthesis of DPOs **2**^a

^a Reaction conditions: **1** (0.4 mmol) and DABCO (0.8 mmol) in CH₃CN/H₂O (99/1) with 0.1 M Bu₄NBF₄ as a supporting electrolyte were electrolyzed with 2.5 F mol⁻¹ under a constant current of 2.5 mA. Isolated yield. ^b Performed with 2.0 F mol⁻¹ ^c N.D. = Not Detected.

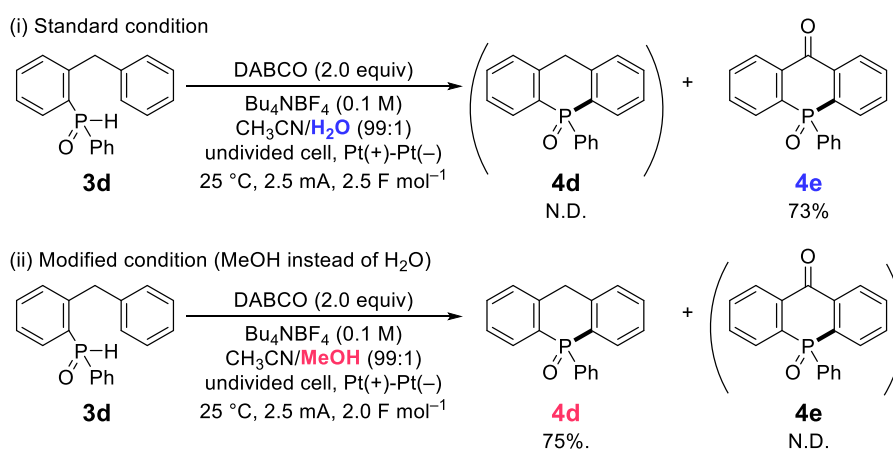
This synthetic method can also be applied to the synthesis of six-membered phosphacycles **4a–4c** (Scheme 4). To the best of our knowledge, this is the first electrochemical synthesis of **4** from **3**.¹² In the case of substrate **3d**, the corresponding product **4d** was not observed under the standard conditions, and oxidized six-membered phosphacycle **4e** was selectively obtained (Scheme 5(i)).^{11a} After further investigation, we were delighted to find that **4d** was selectively obtained when MeOH was used instead of H₂O (Scheme 5(ii)). These results suggest that the oxygen source for **4e** would be H₂O.^{11b}

Scheme 4. Application for the synthesis of six-membered phosphacycles **4**^a



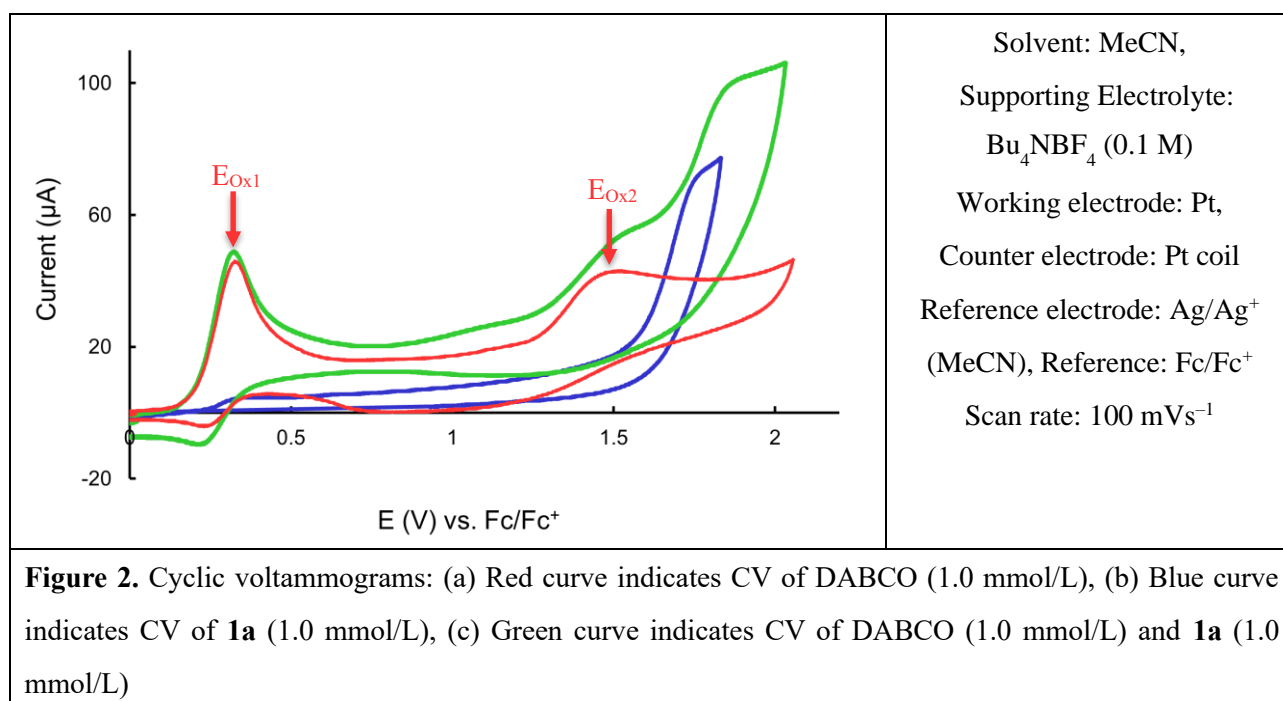
^a Reaction conditions: **3** (0.4 mmol) and DABCO (0.8 mmol) in CH₃CN/H₂O (99/1) with 0.1 M Bu₄NBF₄ as a supporting electrolyte were electrolyzed with 2.5 F mol⁻¹ under a constant current of 2.5 mA. Isolated yield.

Scheme 5. Switching synthesis of six-membered phosphacycles



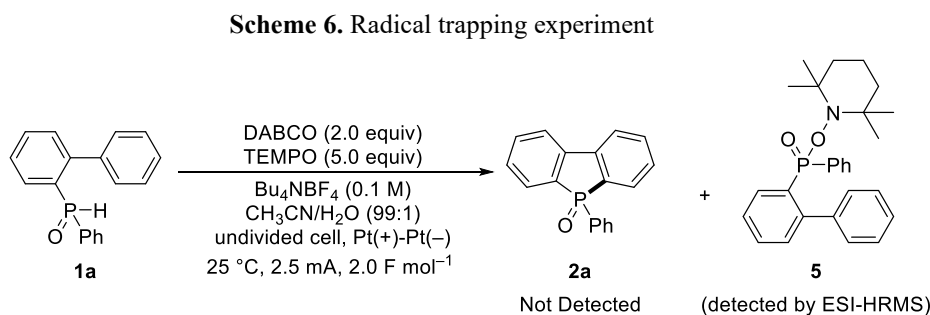
6-5. Cyclic Voltammograms of Related Compounds

To get further insight into the reaction mechanism, cyclic voltammograms (CV) were measured (Figure 2). CV of DABCO exhibits a quasi-reversible redox couple ($E_{\text{Ox1}} = 0.32$ V vs. Fc/Fc^+) and an irreversible wave ($E_{\text{Ox2}} = 1.50$ V), corresponding to the oxidation of DABCO to form $\text{DABCO}^{\bullet+}$ and DABCO biradical cation to DABCO^{*+} , respectively (red curve). Model substrate **1a** showed an irreversible oxidation wave around 1.83 V vs. Fc/Fc^+ (blue curve). A catalytic current was not observed in the mixture of **1a** and DABCO. We next examined constant potential electrolysis (Scheme S1). The electrolysis was first conducted under a constant potential at 0.9 V vs. Ag/Ag^+ (22.8 h), and target product **2a** was obtained in 28% yield. Similarly, **2a** was obtained in 14% yield by the constant potential electrolysis at 1.5 V (3.6 h). From these results, $\text{DABCO}^{\bullet+}$ generated by electro-oxidation of DABCO should serve as a key reactive intermediate.



6-6. Control Experiments

Control experiments were carried out to gain additional insights. When 5.0 equivalents of 2,2,6,6-tetramethyl-1-piperidinyloxy (TEMPO) was added to the system, target product **2a** was not obtained, and TEMPO-trapped product **5** was detected by ESI-HRMS (Scheme 6, Figure S2). This result strongly suggests that a phosphinyl radical was generated in situ by the reaction of **1a** with DABCO⁺, and the reaction should proceed via a radical pathway.



6-7. Plausible Reaction Mechanism

On the basis of CVs and the control experiments described above as well as related references,^{8,10} a plausible mechanism for electrochemical synthesis of DPO is suggested in Figure 3.

First, DABCO is oxidized into DABCO⁺ by anodic oxidation. Subsequently, DABCO⁺ abstracts a hydrogen atom from the P-H bond of BPO to generate intermediate **A** and DABCOH⁺. Finally, intramolecular cyclization of the intermediate **A** followed by hydrogen elimination would then give DPO.¹² Two reaction pathways can be considered in this hydrogen elimination step. One possibility is that DABCO⁺ generated by anodic oxidation acts as a HAT mediator and abstracts hydrogen atom from intermediate **B** (path A). The other possibility is that DPO is produced by anodic oxidation of intermediate **B** (path B). Generated DABCOH⁺ or H₂O would be reduced at the cathode.

The experimental results shown in Scheme 6 support the formation of this intermediate **A**. As mentioned above, no catalytic current was observed in the CV measurement of the mixture of **1a** and DABCO. This is probably due to the slow reaction rate between **1a** and DABCO⁺. CV measurement also revealed the instability of DABCO⁺, which could be why a stoichiometric amount of DABCO was required for the reaction.

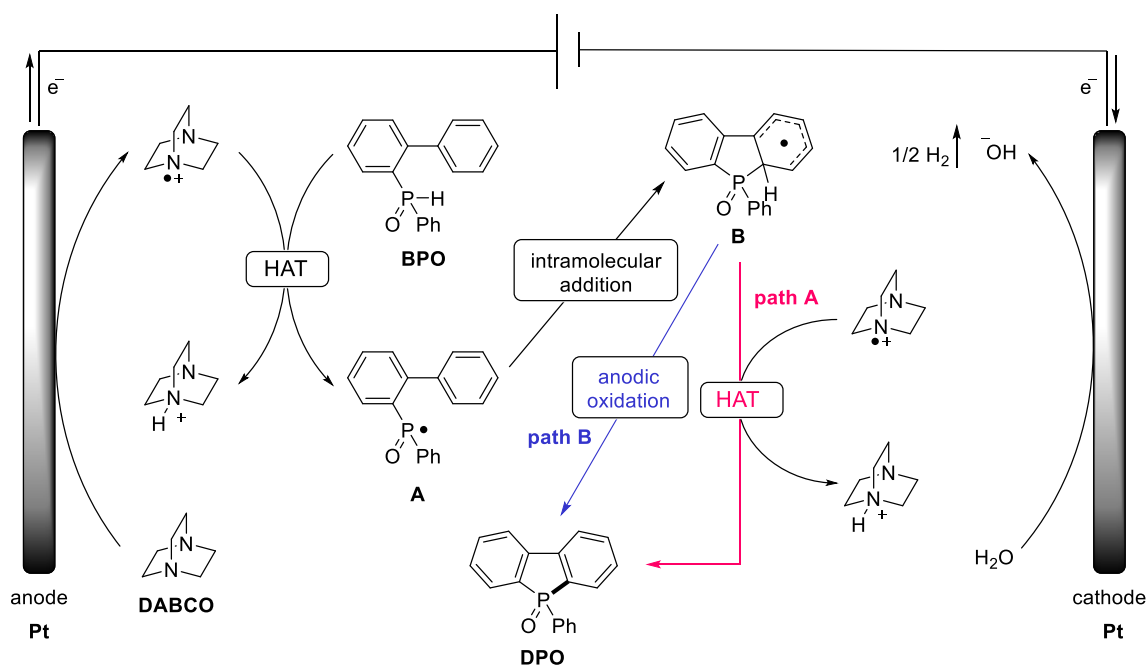


Figure 3. Plausible reaction mechanism

6-8. Conclusion

In conclusion, the author achieved the first electrochemical synthesis of diarylphosphole oxides (DPOs) from biarylphosphine oxides (BPOs) under mild conditions. The protocol does not use a transition metal mediator and instead uses readily available and inexpensive DABCO as a HAT mediator. A variety of BPOs could be obtained by the electrochemical method. This method can also be applied to the synthesis of six-membered phosphacycles. The control experiments suggested that a phosphinoyl radical was generated in situ and the reaction would proceed via a radical pathway.

6-9. Experimental Section and Analytical Data

General

Nuclear magnetic resonance (NMR) spectra were recorded on JEOL JNM-ECZ600R (^1H 600 MHz, ^{13}C 150 MHz) and JEOL JNM-ECS400 (^1H 400 MHz, ^{13}C 100 MHz) spectrometers. Chemical shifts for ^1H NMR are expressed in parts per million (ppm) relative to TMS (δ 0 ppm) or residual CHCl_3 in CDCl_3 (δ 7.26 ppm). Chemical shifts for ^{13}C NMR are expressed in ppm relative to CDCl_3 (δ 77.16 ppm). IR spectra were recorded on a SHIMADZU IRAffinity-1 spectrophotometer. Elemental analysis was obtained with Perkin-Elmer PE 2400 Series II CHNS/O analyzer. Analytic thin layer chromatography (TLC) was performed on Merck, pre-coated plate silica gel 60 F_{254} (0.25 mm thickness). Column chromatography was performed on KANTO CHEMICAL silica gel 60N (40–50 μm). Unless otherwise noted, all materials were obtained from commercial suppliers and used without further purification. High-resolution mass spectrometry was performed on JEOL JMS-700MStation (FAB-MS). Dry tetrahydrofuran (THF) and dry diethyl ether (Et_2O) were purchased from FUJIFILM Wako pure chemical corporation. Acetonitrile (CH_3CN) was dried over MS3A . All secondary phosphine oxides **1** or **3** were synthesized from the corresponding aryl halides and PhPCl_2 according to the literature method.^{1,3a,3b} All reactions were performed under argon atmosphere.

General for Electrochemical Reaction

Electrochemical cyclization was carried out using Pt plate electrodes ($1.0 \times 1.5 \text{ cm}^2$) connected to Pt wire (Figure S1a). The electrochemical reactions were performed in a 10 mL two-necked flask equipped with a three-way cock and two Pt electrodes (Figure S1b). The two electrodes are connected to DC power supply (KIKUSUI PMX350-0.2A) and an ammeter (YOKOGAWA 2051 03) (Figure S1c).

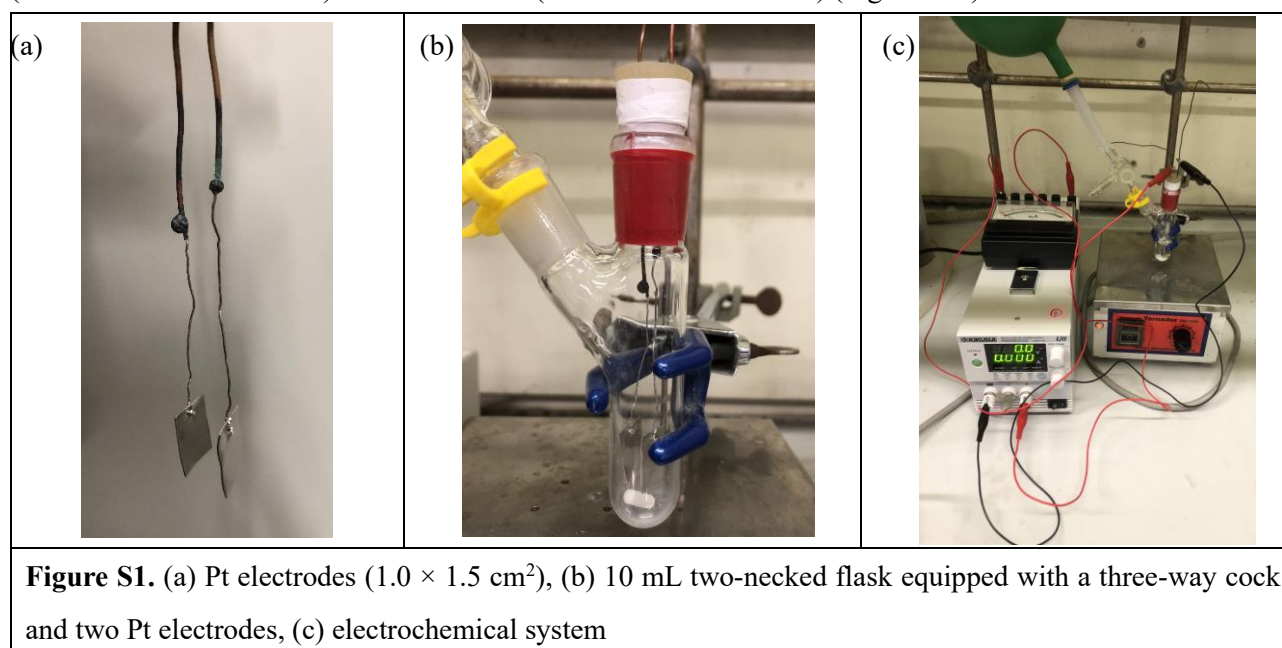
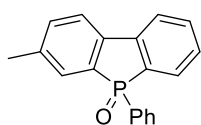


Figure S1. (a) Pt electrodes ($1.0 \times 1.5 \text{ cm}^2$), (b) 10 mL two-necked flask equipped with a three-way cock and two Pt electrodes, (c) electrochemical system

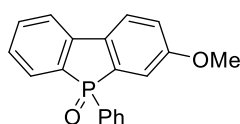
133.4, 132.9 (d, $J_{C-P} = 106.9$ Hz), 132.7 (d, $J_{C-P} = 106.9$ Hz), 132.2, 131.08 (d, $J_{C-P} = 11.6$ Hz), 131.02 (d, $J_{C-P} = 104.0$ Hz), 130.4 (d, $J_{C-P} = 10.1$ Hz), 129.9 (d, $J_{C-P} = 10.1$ Hz), 129.0 (d, $J_{C-P} = 10.1$ Hz), 128.8 (d, $J_{C-P} = 13.0$ Hz), 121.1 (d, $J_{C-P} = 10.1$ Hz), 121.0 (d, $J_{C-P} = 10.1$ Hz), 21.4; IR(KBr) 3044, 1437, 1196, 1109, 729 cm^{-1} ; HRMS (FAB+) m/z calcd for $\text{C}_{19}\text{H}_{16}\text{OP}$ $[\text{M}+\text{H}]^+$ 291.0933, found 291.0921; mp 144.2–144.9 $^{\circ}\text{C}$

3-Methyl-5-phenyl-5H-dibenzophosphole 5-oxide (**2b'**)



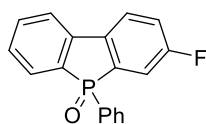
Prepared according to the general procedure from (4-methylbiphenyl)phenylphosphine oxide (**1b'**, 117 mg, 0.4 mmol), DABCO (90 mg, 0.8 mmol) and Bu_4NBF_4 (132 mg, 0.4 mmol). A constant current (2.5 mA, 2.0 F mol^{-1} , 8.58 h) was supplied. The product **2b'** was purified by chromatography on silica gel eluting with $\text{CHCl}_3/\text{EtOAc}$ (5:1) and obtained as a colorless solid (56.9 mg, 0.196 mmol, 49%).

3-Methoxy-5-phenyl-5H-dibenzophosphole 5-oxide (**2c**)



Prepared according to the general procedure from (4'-methoxybiphenyl)phenylphosphine oxide (**1c**, 123 mg, 0.4 mmol), DABCO (90 mg, 0.8 mmol) and Bu_4NBF_4 (132 mg, 0.4 mmol). A constant current (2.5 mA, 2.5 F mol^{-1} , 10.73 h) was supplied. The product **2c** was purified by chromatography on silica gel eluting with $\text{CHCl}_3/\text{EtOAc}$ (3:1) and obtained as a colorless solid (88.2 mg, 0.288 mmol, 72%). ^1H NMR (600 MHz, CDCl_3) δ 7.74–7.70 (m, 2H), 7.69–7.63 (m, 3H), 7.54 (t, $J = 7.8$ Hz, 1H), 7.50 (dd, $J = 7.8, 1.4$ Hz, 1H), 7.40 (td, $J = 7.8$ Hz, $J_{\text{H-P}} = 3.0$ Hz, 2H), 7.30 (td, $J = 7.2$ Hz, $J_{\text{H-P}} = 3.2$ Hz, 1H), 7.21 (dd, $J = 2.7$ Hz, $J_{\text{H-P}} = 11.1$ Hz, 1H), 7.09 (dd, $J = 8.7$ Hz, $J_{\text{H-P}} = 2.1$ Hz, 1H), 3.81 (s, 3H); ^{13}C NMR (150 MHz, CDCl_3) δ 160.8 (d, $J_{C-P} = 14.5$ Hz), 142.0 (d, $J_{C-P} = 21.7$ Hz), 134.6 (d, $J_{C-P} = 105.5$ Hz), 134.4 (d, $J_{C-P} = 21.7$ Hz), 133.5, 132.4 (d, $J_{C-P} = 106.9$ Hz), 132.2 (d, $J_{C-P} = 2.9$ Hz), 131.1 (d, $J_{C-P} = 11.4$ Hz), 130.9 (d, $J_{C-P} = 102.6$ Hz), 129.8 (d, $J_{C-P} = 10.1$ Hz), 128.8 (d, $J_{C-P} = 13.0$ Hz), 128.3 (d, $J_{C-P} = 11.6$ Hz), 122.5 (d, $J_{C-P} = 13.0$ Hz), 120.5 (d, $J_{C-P} = 11.6$ Hz), 119.9, 113.9 (d, $J_{C-P} = 11.6$ Hz), 56.7; IR(KBr) 2965, 1454, 1279, 1134, 729 cm^{-1} ; HRMS (FAB+) m/z calcd for $\text{C}_{19}\text{H}_{15}\text{O}_2\text{P}$ $[\text{M}]^+$ 306.0804, found 306.0815; mp 155.3–155.9 $^{\circ}\text{C}$

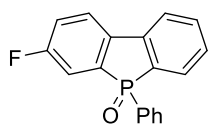
3-Fluoro-5-phenyl-5H-dibenzophosphole 5-oxide (**2d**)



Prepared according to the general procedure from (4'-fluorobiphenyl)phenylphosphine oxide (**1d**, 119 mg, 0.4 mmol), DABCO (90 mg, 0.8 mmol) and Bu_4NBF_4 (132 mg, 0.4 mmol). A constant current (2.5 mA, 2.5 F mol^{-1} , 10.73 h) was supplied. The product **2d** was purified by chromatography on silica gel eluting with $\text{CHCl}_3/\text{EtOAc}$ (4:1) and obtained as a colorless solid (75.3 mg, 0.256 mmol, 64%). ^1H NMR (600 MHz, CDCl_3) δ 7.83–7.75 (m, 2H), 7.71 (dd, $J = 7.2$ Hz, $J_{\text{H-F}} = 8.7$ Hz, 1H), 7.65 (d, $J = 7.2$ Hz, 1H), 7.63 (d, $J = 7.2$ Hz, 1H), 7.60 (td, $J = 7.2, 1.8$ Hz, 1H), 7.52 (td, $J = 7.2, 1.8$ Hz, 1H), 7.45–7.35 (m, 4H), 7.27 (td, $J = 8.4$ Hz, $J_{\text{H-P}} = 2.1$ Hz, 1H); ^{13}C NMR (150 MHz, CDCl_3) δ 163.5

(dd, $J_{C-P} = 15.9$ Hz, $J_{C-F} = 252.9$ Hz), 141.1 (d, $J_{C-P} = 20.2$ Hz), 137.8 (dd, $J_{C-P} = 21.7$ Hz, $J_{C-F} = 2.8$ Hz), 135.6 (dd, $J_{C-P} = 105.5$ Hz, $J_{C-F} = 7.2$ Hz), 133.8, 132.7 (d, $J_{C-P} = 108.4$ Hz), 132.6 (d, $J_{C-P} = 2.9$ Hz), 131.1 (d, $J_{C-P} = 11.6$ Hz), 130.18 (d, $J_{C-P} = 104.0$ Hz), 130.15 (d, $J_{C-P} = 10.1$ Hz), 129.3 (d, $J_{C-P} = 11.6$ Hz), 129.0 (d, $J_{C-P} = 13.0$ Hz), 123.0 (dd, $J_{C-P} = 11.6$ Hz, $J_{C-F} = 7.2$ Hz), 121.1 (d, $J_{C-P} = 10.1$ Hz), 120.6 (d, $J_{C-F} = 23.1$ Hz), 117.0 (dd, $J_{C-P} = 10.1$ Hz, $J_{C-F} = 23.1$ Hz); IR(KBr) 3051, 1437, 1260, 1200, 729 cm^{-1} ; HRMS (FAB+) m/z calcd for $\text{C}_{18}\text{H}_{13}\text{FOP}$ $[\text{M}+\text{H}]^+$ 295.0682, found 295.0687; mp 177.7–178.4 $^{\circ}\text{C}$

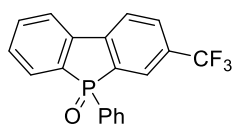
3-Fluoro-5-phenyl-5H-dibenzophosphole 5-oxide (2d')



Prepared according to the general procedure from (4-fluorobiphenyl)phenylphosphine oxide (**1d'**, 119 mg, 0.4 mmol), DABCO (90 mg, 0.8 mmol) and Bu_4NBF_4 (132 mg, 0.4 mmol). A constant current (2.5 mA, 2.0 F mol^{-1} , 8.58 h) was supplied. The product **2d'**

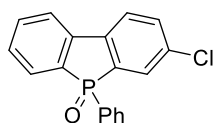
was purified by chromatography on silica gel eluting with $\text{CHCl}_3/\text{EtOAc}$ (4:1) and obtained as a colorless solid (73.0 mg, 0.248 mmol, 62%).

3-(Trifluoromethyl)-5-phenyl-5H-dibenzophosphole 5-oxide (2e)



Prepared according to the general procedure from [4'-(trifluoromethyl)biphenyl]phenylphosphine oxide (**1e**, 139 mg, 0.4 mmol), DABCO (90 mg, 0.8 mmol) and Bu_4NBF_4 (132 mg, 0.4 mmol). A constant current (2.5 mA, 2.5 F mol^{-1} , 10.73 h) was supplied. The product **2e** was purified by chromatography on silica gel eluting with $\text{CHCl}_3/\text{EtOAc}$ (4:1) and obtained as a colorless solid (86.8 mg, 0.252 mmol, 63%). ^1H NMR (400 MHz, CDCl_3) δ 7.99–7.91 (m, 2H), 7.90 (dd, $J = 7.5$ Hz, $J_{\text{H-P}} = 2.7$ Hz, 1H), 7.83 (d, $J = 8.2$ Hz, 1H), 7.76 (dd, $J = 7.5$ Hz, $J_{\text{H-P}} = 8.8$ Hz, 1H), 7.70–7.60 (m, 3H), 7.54 (td, $J = 7.3$, 1.0 Hz, 1H), 7.48 (td, $J = 7.5$ Hz, $J_{\text{H-P}} = 3.7$ Hz, 1H), 7.43 (td, $J = 7.3$ Hz, $J_{\text{H-P}} = 3.2$ Hz, 2H); ^{13}C NMR (150 MHz, CDCl_3) δ 145.1 (d, $J_{C-P} = 21.7$ Hz), 140.5 (d, $J_{C-P} = 21.7$ Hz), 134.2 (d, $J_{C-P} = 105.5$ Hz), 133.9, 133.4 (d, $J_{C-P} = 108.4$ Hz), 132.8, 131.6 (dq, $J_{C-P} = 11.6$ Hz, $J_{C-F} = 31.8$ Hz), 131.2 (d, $J_{C-P} = 11.6$ Hz), 130.8 (d, $J_{C-P} = 11.6$ Hz), 130.6, 130.3 (d, $J_{C-P} = 8.7$ Hz), 129.7 (d, $J_{C-P} = 104.0$ Hz), 129.1 (d, $J_{C-P} = 13.0$ Hz), 127.0 (dq, $J_{C-P} = 4.3$ Hz, $J_{C-F} = 4.3$ Hz), 123.7 (q, $J_{C-F} = 271.7$ Hz), 122.1 (d, $J_{C-P} = 10.1$ Hz), 121.7 (d, $J_{C-P} = 10.1$ Hz); IR(KBr) 3055, 1441, 1323, 1194, 731 cm^{-1} ; HRMS (FAB+) m/z calcd for $\text{C}_{19}\text{H}_{13}\text{F}_3\text{OP}$ $[\text{M}+\text{H}]^+$ 345.0650, found 345.0664; mp 179.6–180.4 $^{\circ}\text{C}$

3-Chloro-5-phenyl-5H-dibenzophosphole 5-oxide (2f)

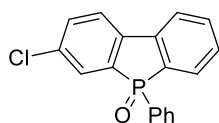


Prepared according to the general procedure from (4'-chlorobiphenyl)phenylphosphine oxide (**1f**, 139 mg, 0.4 mmol), DABCO (90 mg, 0.8 mmol) and Bu_4NBF_4 (132 mg, 0.4 mmol). A constant current (2.5 mA, 2.5 F mol^{-1} , 10.73 h) was supplied. The product **2f**

was purified by chromatography on silica gel eluting with $\text{CHCl}_3/\text{EtOAc}$ (5:1) and obtained as a colorless solid (87.0 mg, 0.28 mmol, 70%). ^1H NMR (600 MHz, CDCl_3) δ 7.80 (dd, $J = 7.3$ Hz, $J_{\text{H-P}} = 3.7$ Hz, 1H), 7.76 (dd,

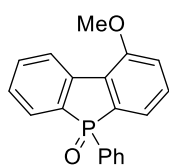
$J = 8.3$ Hz, $J_{\text{H-P}} = 2.8$ Hz, 1H), 7.71 (d, $J = 8.3$ Hz, $J_{\text{H-P}} = 9.6$ Hz, 1H), 7.68–7.59 (m, 4H), 7.56–7.52 (m, 1H), 7.53 (td, $J = 7.2$, 1.8 Hz, 1H), 7.44–7.38 (m, 3H); ^{13}C NMR (150 MHz, CDCl_3) δ 141.0 (d, $J_{\text{C-P}} = 21.7$ Hz), 140.1 (d, $J_{\text{C-P}} = 21.7$ Hz), 135.6 (d, $J_{\text{C-P}} = 14.5$ Hz), 135.2 (d, $J_{\text{C-P}} = 105.5$ Hz), 133.8, 133.5, 132.598 (d, $J_{\text{C-P}} = 106.7$ Hz), 132.598 (d, $J_{\text{C-P}} = 2.9$ Hz), 131.1 (d, $J_{\text{C-P}} = 10.1$ Hz), 130.13 (d, $J_{\text{C-P}} = 10.1$ Hz), 130.05 (d, $J_{\text{C-P}} = 104.0$ Hz), 129.9 (d, $J_{\text{C-P}} = 10.1$ Hz), 129.8 (d, $J_{\text{C-P}} = 11.6$ Hz), 129.0 (d, $J_{\text{C-P}} = 11.6$ Hz), 122.5 (d, $J_{\text{C-P}} = 11.6$ Hz), 121.4 (d, $J_{\text{C-P}} = 10.1$ Hz); IR(KBr) 2924, 1435, 1202, 1134, 727 cm^{-1} ; HRMS (FAB+) m/z calcd for $\text{C}_{18}\text{H}_{12}^{37}\text{ClOP} [\text{M}]^+$ 312.0279, found 312.0268; mp 183.3–183.8 $^\circ\text{C}$

3-Chloro-5-phenyl-5H-dibenzophosphole 5-oxide (2f')



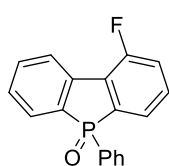
Prepared according to the general procedure from (4-chlorobiphenyl)phenylphosphine oxide (**1f'**, 139 mg, 0.4 mmol), DABCO (90 mg, 0.8 mmol) and Bu_4NBF_4 (132 mg, 0.4 mmol). A constant current (2.5 mA, 2.0 F mol^{-1} , 8.58 h) was supplied. The product **2f'** was purified by chromatography on silica gel eluting with $\text{CHCl}_3/\text{EtOAc}$ (5:1) and obtained as a colorless solid (52.2 mg, 0.168 mmol, 42%).

1-Methoxy-5-phenyl-5H-dibenzophosphole 5-oxide (2g)



Prepared according to the general procedure from (2'-methoxybiphenyl)phenylphosphine oxide (**1g**, 123 mg, 0.4 mmol), DABCO (90 mg, 0.8 mmol) and Bu_4NBF_4 (132 mg, 0.4 mmol). A constant current (2.5 mA, 2.5 F mol^{-1} , 10.73 h) was supplied. The product **2g** was purified by chromatography on silica gel eluting with $\text{CHCl}_3/\text{EtOAc}$ (3:1) and obtained as a colorless solid (67.4 mg, 0.22 mmol, 55%). ^1H NMR (600 MHz, CDCl_3) δ 8.40 (dd, $J = 8.3$ Hz, $J_{\text{H-P}} = 3.7$ Hz, 1H), 7.69 (dd, $J = 7.2$ Hz, $J_{\text{H-P}} = 10.0$ Hz, 1H), 7.66 (dd, $J = 7.8$, 1.8 Hz, 1H), 7.63 (dd, $J = 7.8$, 1.8 Hz, 1H), 7.56 (t, $J = 7.8$ Hz, 1H), 7.47 (t, 7.2 Hz, 1H), 7.40–7.29 (m, 5H), 7.12 (d, $J = 8.3$ Hz, 1H), 4.03 (s, 3H); ^{13}C NMR (150 MHz, CDCl_3) δ 156.8 (d, $J_{\text{C-P}} = 14.5$ Hz), 141.3 (d, $J_{\text{C-P}} = 21.7$ Hz), 134.7 (d, $J_{\text{C-P}} = 105.5$ Hz), 133.4, 132.2 (d, $J_{\text{C-P}} = 105.5$ Hz), 132.1 (d, $J_{\text{C-P}} = 2.9$ Hz), 130.946 (d, $J_{\text{C-P}} = 104.0$ Hz), 130.946 (d, $J_{\text{C-P}} = 10.1$ Hz), 130.7 (d, $J_{\text{C-P}} = 13.0$ Hz), 129.3 (d, $J_{\text{C-P}} = 8.7$ Hz), 129.1 (d, $J_{\text{C-P}} = 23.1$ Hz), 128.6 (d, $J_{\text{C-P}} = 13.0$ Hz), 128.3 (d, $J_{\text{C-P}} = 11.6$ Hz), 126.5 (d, $J_{\text{C-P}} = 10.1$ Hz), 121.5 (d, $J_{\text{C-P}} = 10.1$ Hz), 115.9, 55.5; IR(KBr) 3059, 1437, 1265, 1192, 723 cm^{-1} ; HRMS (FAB+) m/z calcd for $\text{C}_{19}\text{H}_{15}\text{O}_2\text{P} [\text{M}]^+$ 306.0804, found 306.0815; mp 149.5–149.9 $^\circ\text{C}$

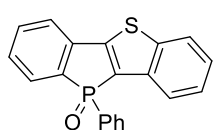
1-Fluoro-5-phenyl-5H-dibenzophosphole 5-oxide (2h)



Prepared according to the general procedure from (2'-fluorobiphenyl)phenylphosphine oxide (**1h**, 119 mg, 0.4 mmol), DABCO (90 mg, 0.8 mmol) and Bu_4NBF_4 (132 mg, 0.4 mmol). A constant current (2.5 mA, 2.5 F mol^{-1} , 10.73 h) was supplied. The product **2h** was purified by chromatography on silica gel eluting with $\text{CHCl}_3/\text{EtOAc}$ (4:1) and obtained as a colorless solid (63.6 mg, 0.216 mmol, 54%), ^1H NMR (400 MHz, CDCl_3) δ 8.12 (dd, $J = 7.8$ Hz, $J_{\text{H-P}} = 3.7$ Hz, 1H),

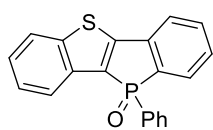
7.74 (dd, $J = 7.8$ Hz, $J_{\text{H-P}} = 10.1$ Hz, 1H), 7.69–7.59 (m, 3H), 7.51 (dd, $J = 7.3$ Hz, 1.6 Hz, 2H), 7.46–7.33 (m, 4H), 7.29 (dd, $J = 8.2$ Hz, $J_{\text{H-P}} = 10.5$ Hz, 1H); ^{13}C NMR (150 MHz, CDCl_3) δ 159.3 (dd, $J_{\text{C-P}} = 14.5$ Hz, $J_{\text{C-F}} = 255.8$ Hz), 139.0 (dd, $J_{\text{C-P}} = 21.7$ Hz, $J_{\text{C-F}} = 4.3$ Hz), 136.0 (d, $J_{\text{C-P}} = 104.0$ Hz), 133.9, 132.6 (d, $J_{\text{C-P}} = 106.9$ Hz), 132.5 (d, $J_{\text{C-P}} = 2.9$ Hz), 131.2 (dd, $J_{\text{C-P}} = 13.0$ Hz, $J_{\text{C-F}} = 7.2$ Hz), 131.0 (d, $J_{\text{C-P}} = 11.6$ Hz), 130.4 (d, $J_{\text{C-P}} = 105.5$ Hz), 129.9 (d, $J_{\text{C-P}} = 10.1$ Hz), 129.6 (d, $J_{\text{C-P}} = 11.6$ Hz), 128.9 (d, $J = 13.0$ Hz), 128.6 (dd, $J_{\text{C-P}} = 13.0$ Hz, $J_{\text{C-F}} = 23.1$ Hz), 125.9 (d, $J_{\text{C-P}} = 10.1$ Hz, $J_{\text{C-F}} = 10.1$ Hz), 125.7 (dd, $J_{\text{C-P}} = 8.7$ Hz, $J_{\text{C-F}} = 2.9$ Hz), 121.2 (d, $J_{\text{C-P}} = 21.7$ Hz); IR(KBr) 3063, 1443, 1204, 1130, 762 cm^{-1} ; HRMS (FAB+) m/z calcd for $\text{C}_{18}\text{H}_{13}\text{FOP}$ $[\text{M}+\text{H}]^+$ 295.0682, found 295.0687; mp 166.4–167.1 $^{\circ}\text{C}$

10-Phenylbenzo[*b*]phosphindolo[2,3-*d*]thiophene 10-oxide (**2i**)



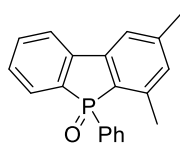
Prepared according to the general procedure from (2-(benzo[*b*]thiophen-2-yl)phenyl)phenylphosphine oxide (**1i**, 134 mg, 0.4 mmol), DABCO (90 mg, 0.8 mmol) and Bu_4NBF_4 (132 mg, 0.4 mmol). A constant current (2.5 mA, 2.5 F mol^{-1} , 10.73 h) was supplied. The product **2i** was purified by chromatography on silica gel eluting with $\text{CHCl}_3/\text{EtOAc}$ (5:1) and obtained as a colorless solid (109.0 mg, 0.328 mmol, 82%). ^1H NMR (600 MHz, CDCl_3) δ 7.88 (dd, $J = 7.2$, 1.8 Hz, 1H), 7.82–7.73 (m, 3H), 7.68 (dd, $J = 7.2$ Hz, $J_{\text{H-P}} = 10.2$ Hz, 1H), 7.57–7.53 (m, 2H), 7.52 (t, $J = 7.5$ Hz, 1H), 7.41 (td, $J = 7.5$, $J_{\text{H-P}} = 2.8$ Hz, 2H), 7.41–7.32 (m, 3H); ^{13}C NMR (150 MHz, CDCl_3) δ 154.7 (d, $J_{\text{C-P}} = 27.3$ Hz), 143.3 (d, $J_{\text{C-P}} = 11.6$ Hz), 137.5 (d, $J_{\text{C-P}} = 18.8$ Hz), 136.6 (d, $J_{\text{C-P}} = 107.7$ Hz), 136.2 (d, $J_{\text{C-P}} = 12.9$ Hz), 133.2, 132.6 (d, $J_{\text{C-P}} = 2.9$ Hz), 131.0 (d, $J_{\text{C-P}} = 11.4$ Hz), 130.6 (d, $J_{\text{C-P}} = 106.2$ Hz), 129.8 (d, $J_{\text{C-P}} = 106.2$ Hz), 129.62 (d, $J_{\text{C-P}} = 8.7$ Hz), 129.58 (d, $J_{\text{C-P}} = 11.4$ Hz), 129.0 (d, $J_{\text{C-P}} = 12.9$ Hz), 126.1, 125.6, 123.5 (d, $J_{\text{C-P}} = 12.9$ Hz), 122.1 (d, $J_{\text{C-P}} = 8.7$ Hz); IR(KBr) 3053, 1460, 1315, 1200, 750 cm^{-1} ; HRMS (FAB+) m/z calcd for $\text{C}_{20}\text{H}_{13}\text{OPS}$ $[\text{M}]^+$ 332.0419, found 332.0408; mp 174.9–175.6 $^{\circ}\text{C}$

10-Phenylbenzo[*b*]phosphindolo[2,3-*d*]thiophene 10-oxide (**2i'**)



Prepared according to the general procedure from (2-phenylbenzo[*b*]thiophen-3-yl)phenylphosphine oxide (**1i'**, 134 mg, 0.4 mmol), DABCO (90 mg, 0.8 mmol) and Bu_4NBF_4 (132 mg, 0.4 mmol). A constant current (2.5 mA, 2.5 F mol^{-1} , 10.73 h) was supplied. The product **2i'** was purified by chromatography on silica gel eluting with $\text{CHCl}_3/\text{EtOAc}$ (5:1) and obtained as a colorless solid (31.9 mg, 0.096 mmol, 24%).

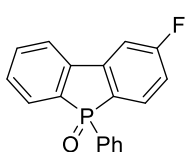
2,4-Dimethyl-5-phenyl-5*H*-dibenzophosphole 5-oxide (**2j**)



Prepared according to the general procedure from (3',5'-dimethylbiphenyl)phenylphosphine oxide (**1j**, 123 mg, 0.4 mmol), DABCO (90 mg, 0.8 mmol) and Bu_4NBF_4 (132 mg, 0.4 mmol). A constant current (2.5 mA, 2.5 F mol^{-1} , 10.73 h) was supplied. The product **2j** was purified by chromatography on silica gel eluting with $\text{CHCl}_3/\text{EtOAc}$ (4:1) and obtained as a colorless

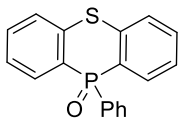
solid (108.3 mg, 0.356 mmol, 89%). ^1H NMR (600 MHz, CDCl_3) δ 7.78 (dd, $J = 7.4$ Hz, $J_{\text{H-P}} = 2.8$ Hz, 1H), 7.69–7.62 (m, 3H), 7.55 (td, $J = 7.4$, 1.8 Hz, 1H), 7.48 (t, $J = 7.8$ Hz, 1H), 7.46 (s, 1H), 7.38 (td, $J = 7.8$ Hz, $J_{\text{H-P}} = 3.2$ Hz, 2H), 7.34 (td, $J = 7.4$ Hz, $J_{\text{H-P}} = 3.8$ Hz, 1H), 6.95 (d, $J_{\text{H-P}} = 3.7$ Hz, 1H), 2.42 (s, 3H), 2.35 (s, 3H); ^{13}C NMR (150 MHz, CDCl_3) δ 144.3, 142.4 (d, $J_{\text{C-P}} = 21.7$ Hz), 142.0, 141.9 (d, $J_{\text{C-P}} = 11.6$ Hz), 133.7 (d, $J_{\text{C-P}} = 106.9$ Hz), 133.2, 132.0, 131.8 (d, $J_{\text{C-P}} = 10.1$ Hz), 131.2 (d, $J_{\text{C-P}} = 11.6$ Hz), 131.0 (d, $J_{\text{C-P}} = 102.6$ Hz), 129.7 (d, $J_{\text{C-P}} = 10.1$ Hz), 129.3 (d, $J_{\text{C-P}} = 11.6$ Hz), 128.7 (d, $J_{\text{C-P}} = 13.0$ Hz), 128.1 (d, $J_{\text{C-P}} = 108.4$ Hz), 121.1 (d, $J_{\text{C-P}} = 10.1$ Hz), 119.5 (d, $J_{\text{C-P}} = 10.1$ Hz), 21.9, 19.5 (d, $J_{\text{C-P}} = 4.3$ Hz); IR(KBr) 2918, 1437, 1202, 1109, 731 cm^{-1} ; HRMS (FAB+) m/z calcd for $\text{C}_{20}\text{H}_{17}\text{OP}$ $[\text{M}]^+$ 304.1011, found 304.1013; mp 171.7–172.6 $^\circ\text{C}$

2-Fluoro-5-phenyl-5H-dibenzophosphole 5-oxide (2k)

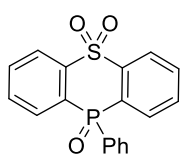


Prepared according to the general procedure from (3'-fluorobiphenyl)phenylphosphine oxide (**1k**, 119 mg, 0.4 mmol), DABCO (90 mg, 0.8 mmol) and Bu_4NBF_4 (132 mg, 0.4 mmol). A constant current (2.5 mA, 2.5 F mol^{-1} , 10.73 h) was supplied. The product **2k** was purified by chromatography on silica gel eluting with $\text{CHCl}_3/\text{EtOAc}$ (4:1) and obtained as a colorless solid (74.2 mg, 0.252 mmol, 63%). ^1H NMR (600 MHz, CDCl_3) δ 7.78 (dd, $J = 7.6$, 2.8 Hz, 1H), 7.74–7.67 (m, 2H), 7.67–7.59 (m, 3H), 7.53–7.47 (m, 2H), 7.46–7.37 (m, 3H), 7.27 (tdd, $J = 6.2$ Hz, $J_{\text{H-P}} = 2.1$ Hz, $J_{\text{H-F}} = 2.1$ Hz, 1H); ^{13}C NMR (150 MHz, CDCl_3) δ 166.7 (d, $J_{\text{C-F}} = 252.9$ Hz), 145.1 (dd, $J_{\text{C-P}} = 23.1$ Hz, $J_{\text{C-F}} = 8.7$ Hz), 140.6 (dd, $J_{\text{C-P}} = 23.1$ Hz, $J_{\text{C-F}} = 2.9$ Hz), 133.9 (d, $J_{\text{C-P}} = 106.9$ Hz), 133.7, 132.5 (d, $J_{\text{C-P}} = 2.9$ Hz), 132.1 (dd, $J_{\text{C-P}} = 10.1$ Hz, $J_{\text{C-F}} = 10.1$ Hz), 131.1 (d, $J_{\text{C-P}} = 11.6$ Hz), 130.5 (d, $J_{\text{C-P}} = 105.5$ Hz), 130.3 (d, $J_{\text{C-P}} = 11.6$ Hz), 130.1 (d, $J_{\text{C-P}} = 10.1$ Hz), 128.9 (d, $J_{\text{C-P}} = 13.0$ Hz), 128.7 (dd, $J_{\text{C-P}} = 106.9$ Hz, $J_{\text{C-F}} = 2.9$ Hz), 121.5 (d, $J_{\text{C-P}} = 10.1$ Hz), 116.7 (dd, $J_{\text{C-P}} = 11.6$ Hz, $J_{\text{C-F}} = 23.1$ Hz), 109.0 (dd, $J_{\text{C-P}} = 11.6$ Hz, $J_{\text{C-F}} = 23.1$ Hz); IR(KBr) 3049, 1597, 1437, 1202, 727 cm^{-1} ; HRMS (FAB+) m/z calcd for $\text{C}_{18}\text{H}_{13}\text{FOP}$ $[\text{M}+\text{H}]^+$ 295.0682, found 295.0687.; mp. 185.2–185.7 $^\circ\text{C}$

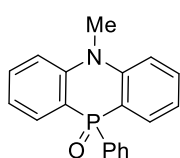
10-Phenyldibenzo[*b,e*][1,4]thiaphosphinine 10-oxide (4a)



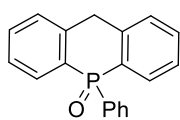
Prepared according to the general procedure from [2-(phenylthio)phenyl]phenylphosphine oxide (**3a**, 124 mg, 0.4 mmol), DABCO (90 mg, 0.8 mmol) and Bu_4NBF_4 (132 mg, 0.4 mmol). A constant current (2.5 mA, 2.5 F mol^{-1} , 10.73 h) was supplied. The product **4a** was purified by chromatography on silica gel eluting with $\text{CHCl}_3/\text{EtOAc}$ (4:1) and obtained as a colorless solid (88.8 mg, 0.288 mmol, 72%). ^1H NMR (600 MHz, CDCl_3) δ 8.29–8.22 (m, 2H), 7.56–7.48 (m, 6H), 7.44–7.36 (m, 3H) 7.31 (t, $J = 7.7$ Hz, $J_{\text{H-P}} = 3.6$, 2H); ^{13}C NMR (150 MHz, CDCl_3) δ 137.3 (d, $J_{\text{C-P}} = 8.6$ Hz), 132.3 (d, $J_{\text{C-P}} = 106.1$ Hz), 132.2 (d, $J_{\text{C-P}} = 7.2$ Hz), 131.9 (d, $J_{\text{C-P}} = 1.5$ Hz), 131.7, 130.8 (d, $J_{\text{C-P}} = 10.1$ Hz), 128.5 (d, $J_{\text{C-P}} = 12.9$ Hz), 127.6 (d, $J_{\text{C-P}} = 7.2$ Hz), 127.29 (d, $J_{\text{C-P}} = 106.1$ Hz), 127.27 (d, $J_{\text{C-P}} = 11.6$ Hz); IR(KBr) 3067, 1431, 1202, 1144, 750 cm^{-1} ; HRMS (ESI+) m/z calcd for $\text{C}_{18}\text{H}_{13}\text{OPSNa}$ $[\text{M}+\text{Na}]^+$ 331.0317, found 331.0315; mp 165.3–166.1 $^\circ\text{C}$

10-Phenyldibenzo[*b,e*][1,4]thiaphosphinine 5,5,10-trioxide (4b)

Prepared according to the general procedure from [2-(phenylsulfonyl)phenyl]phenylphosphine oxide (**3b**, 137 mg, 0.4 mmol), DABCO (90 mg, 0.8 mmol) and Bu₄NBF₄ (132 mg, 0.4 mmol). A constant current (2.5 mA, 2.5 F mol⁻¹, 10.73 h) was supplied. The product **4b** was purified by chromatography on silica gel eluting with CHCl₃/EtOAc (3:1) and obtained as a colorless solid (103.5 mg, 0.304 mmol, 76%). ¹H NMR (600 MHz, CDCl₃) δ 8.44 (ddd, *J* = 7.6, 1.8 Hz, *J*_{H-P} = 11.9 Hz, 2H), 8.27 (td, *J* = 7.6 Hz, *J*_{H-P} = 2.8 Hz, 2H), 7.87–7.80 (m, 4H), 7.64 (dd, *J* = 7.6 Hz, *J*_{H-P} = 13.8, 2H), 7.51 (td, *J* = 7.6, 1.8 Hz, 1H), 7.41 (td, *J* = 7.6 Hz, *J*_{H-P} = 2.8 Hz, 2H); ¹³C NMR (150 MHz, CDCl₃) δ 141.8 (d, *J*_{C-P} = 7.2 Hz), 133.2 (d, *J*_{C-P} = 10.1 Hz), 133.1, 133.0 (d, *J*_{C-P} = 5.8 Hz), 132.7 (d, *J*_{C-P} = 2.9 Hz), 132.1 (d, *J*_{C-P} = 114.2 Hz), 131.5 (d, *J*_{C-P} = 98.3 Hz), 131.4 (d, *J*_{C-P} = 11.6 Hz), 128.7 (d, *J*_{C-P} = 14.5 Hz), 125.2 (d, *J*_{C-P} = 7.2 Hz); IR(KBr) 3090, 1439, 1312, 1128, 748 cm⁻¹; HRMS (ESI+) *m/z* calcd for C₁₈H₁₃O₃PSNa [M+Na]⁺ 363.0215, found 363.0215; mp 253.4–254.0 °C

5-Methyl-10-phenyl-5*H*-phenophosphazinine 10-oxide (4c)

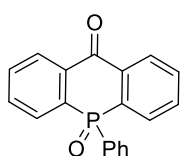
Prepared according to the general procedure from [2-(methylphenylamino)phenyl]phenylphosphine oxide (**3c**, 123 mg, 0.4 mmol), DABCO (90 mg, 0.8 mmol) and Bu₄NBF₄ (132 mg, 0.4 mmol). A constant current (2.5 mA, 2.5 F mol⁻¹, 10.73 h) was supplied. The product **4c** was purified by chromatography on silica gel eluting with CHCl₃/EtOAc (4:1) and obtained as a colorless solid (98.9 mg, 0.324 mmol, 81%). ¹H NMR (600 MHz, CDCl₃) δ 7.77 (ddd, *J* = 7.5, 2.1 Hz, *J*_{H-P} = 13.8, 2H), 7.62 (dd, *J* = 7.6 Hz, *J*_{H-P} = 8.4, 2H), 7.57 (t, *J* = 7.6 Hz, 2H), 7.47 (t, *J* = 7.6 Hz, 1H), 7.40 (dd, *J* = 7.5, 2.1 Hz, 2H), 7.26 (dd, *J* = 7.5 Hz, *J*_{H-P} = 8.4, 2H), 7.14 (t, *J* = 7.5 Hz, 2H), 3.67 (s, 3H); ¹³C NMR (150 MHz, CDCl₃) δ 145.9 (d, *J*_{C-P} = 4.2 Hz), 133.8 (d, *J*_{C-P} = 113.4 Hz), 132.8, 131.65 (d, *J*_{C-P} = 10.1 Hz), 131.61, 131.5 (d, *J*_{C-P} = 5.9 Hz), 128.4 (d, *J*_{C-P} = 12.9 Hz), 121.4 (d, *J*_{C-P} = 10.1 Hz), 116.5 (d, *J*_{C-P} = 102.0 Hz), 115.3 (d, *J*_{C-P} = 7.2 Hz), 37.0; IR(KBr) 3055, 1437, 1200, 1184, 772 cm⁻¹; HRMS (FAB+) *m/z* calcd for C₁₉H₁₇NOP [M+H]⁺ 306.1042, found 306.1044; mp 161.3–162.1 °C

5-Phenyl-10*H*-acridophosphin 5-oxide (4d)

The electro-oxidation was carried out in a 10 mL two-necked flask equipped with a three-way cock and a Pt anode (1.0 × 1.5 cm²), and a Pt cathode (1.0 × 1.5 cm²). [2-(phenylmethyl)phenyl]phenylphosphine oxide (**3d**, 117 mg, 0.4 mmol), DABCO (90 mg, 0.8 mmol) and Bu₄NBF₄ (132 mg, 0.4 mmol) were placed in the flask equipped with a stirring bar. Then CH₃CN (3.96 mL) and MeOH (0.04 mL) were added with a syringe. A constant current (2.5 mA, 2.0 F mol⁻¹, 8.58 h) was supplied. The product **4d** was purified by chromatography on silica gel eluting with CHCl₃/EtOAc (4:1) and obtained as a colorless solid (87.1 mg, 0.30 mmol, 75%). ¹H NMR (600 MHz, CDCl₃) δ 8.12 (ddd, *J* = 7.6, 1.2 Hz, *J*_{H-P} = 11.7 Hz, 2H), 7.51 (tdd, *J* = 7.6, 1.2 Hz, *J*_{H-P} = 1.2 Hz, 2H), 7.50–7.38 (m, 7H), 7.41 (td, *J*

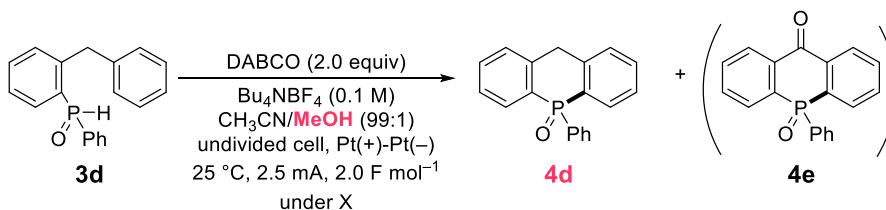
= 7.6 Hz, $J_{\text{H-P}} = 2.8$ Hz, 2H), 4.13 (dd, $J = 18.6, 1.8$ Hz, 1H), 3.91 (dd, $J = 18.6, 3.6$ Hz, 1H); ^{13}C NMR (150 MHz, CDCl_3) δ 141.0 (d, $J_{\text{C-P}} = 8.7$ Hz), 133.5 (d, $J_{\text{C-P}} = 106.9$ Hz), 131.8, 131.7 (d, $J_{\text{C-P}} = 18.8$ Hz), 131.0 (d, $J_{\text{C-P}} = 7.2$ Hz), 130.9 (d, $J_{\text{C-P}} = 10.1$ Hz), 129.3 (d, $J_{\text{C-P}} = 101.2$ Hz), 128.6 (d, $J_{\text{C-P}} = 13.0$ Hz), 128.3 (d, $J_{\text{C-P}} = 10.1$ Hz), 127.1 (d, $J_{\text{C-P}} = 10.1$ Hz), 37.5 (d, $J = 10.1$ Hz); IR(KBr) 3059, 1437, 1202, 1186, 716 cm^{-1} ; HRMS (FAB+) m/z calcd for $\text{C}_{19}\text{H}_{16}\text{OP}$ $[\text{M}+\text{H}]^+$ 291.0933, found 291.0921; mp 165.5–166.2 $^{\circ}\text{C}$

5-Phenyl-10H-acridophosphin-10-one 5-oxide (4e)



Prepared according to the general procedure from [2-(phenylmethyl)phenyl]phenylphosphine oxide (**3d**, 117 mg, 0.4 mmol), DABCO (90 mg, 0.8 mmol) and Bu_4NBF_4 (132 mg, 0.4 mmol). A constant current (2.5 mA, 2.5 F mol^{-1} , 10.73 h) was supplied. The corresponding product **4d** was not obtained, and the oxidized product **4e** was selectively obtained as a colorless solid (88.8 mg, 0.292 mmol, 73%). **4e** was purified by chromatography on silica gel eluting with $\text{CHCl}_3/\text{EtOAc}$ (4:1). ^1H NMR (600 MHz, CDCl_3) δ 8.50–8.40 (m, 2H), 8.06–7.98 (m, 2H), 7.80–7.70 (m, 4H), 7.59 (ddd, $J = 8.4, 1.2$ Hz, $J_{\text{H-P}} = 13.2$, 2H), 7.46 (td, $J = 7.5, 2.2$ Hz, 1H), 7.38 (td, $J = 7.5$ Hz, $J_{\text{H-P}} = 3.2$ Hz, 2H); ^{13}C NMR (150 MHz, CDCl_3) δ 182.9 (d, $J_{\text{C-P}} = 10.1$ Hz), 135.9 (d, $J_{\text{C-P}} = 5.7$ Hz), 133.9 (d, $J_{\text{C-P}} = 11.4$ Hz), 133.5 (d, $J_{\text{C-P}} = 97.7$ Hz), 133.1 (d, $J_{\text{C-P}} = 107.7$ Hz), 132.8, 132.1 (d, $J_{\text{C-P}} = 2.9$ Hz), 131.4 (d, $J_{\text{C-P}} = 5.7$ Hz), 131.0 (d, $J_{\text{C-P}} = 10.1$ Hz), 129.3 (d, $J_{\text{C-P}} = 8.6$ Hz), 129.0 (d, $J_{\text{C-P}} = 11.4$ Hz); IR(KBr) 3057, 1667, 1302, 1202, 741 cm^{-1} ; HRMS (ESI+) m/z calcd for $\text{C}_{19}\text{H}_{13}\text{O}_2\text{PNa}$ $[\text{M}+\text{Na}]^+$ 327.0545, found 327.0549; mp 219.4–220.0 $^{\circ}\text{C}$

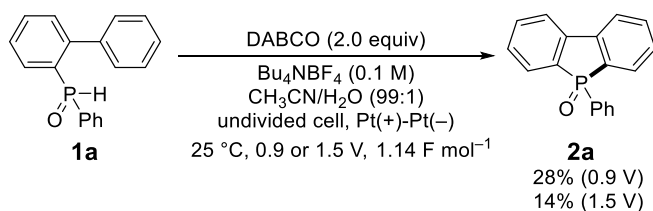
2. Control Experiments

Table S1. Synthesis of Six-Membered Phosphacycle **4d** and **4e**

entry	X	yield of 4d (%)	yield of 4e (%)
1	Ar	75	N.D.
2	O ₂	16	2

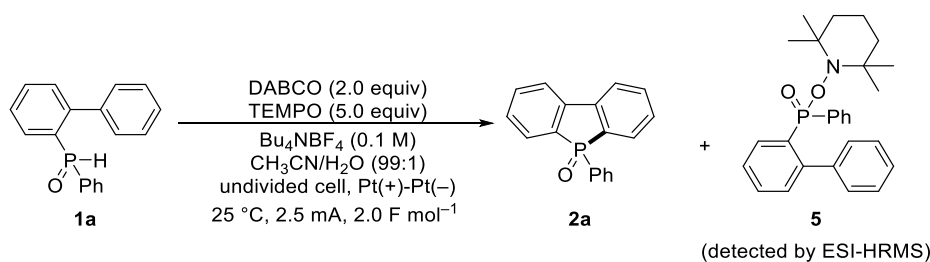
The electro-oxidation was carried out in a 10 mL two-necked flask equipped with a three-way cock and a Pt anode ($1.0 \times 1.5\text{ cm}^2$), and a Pt cathode ($1.0 \times 1.5\text{ cm}^2$). Substrate **3d** (0.4 mmol), DABCO (0.8 mmol), and Bu_4NBF_4 (0.4 mmol) were placed in the flask equipped with a stirring bar. Then CH_3CN (3.96 mL) and MeOH (0.04 mL) were added with a syringe. A constant current ($2.5\text{ mA, } 2.0\text{ F mol}^{-1}$, 8.58 h) was supplied at $25\text{ }^\circ\text{C}$. Under Ar, the corresponding product **4d** was selectively obtained in 75 % and oxidized product **4e** was not obtained. Meanwhile, under O₂, the mass balance is decreased and **4d** was obtained in 16% and **4e** was obtained in 2 %. These results suggest that O₂ significantly inhibits the progress of this reaction and the oxygen source for **4e** is likely to be H₂O.

Scheme S1. Constant Potential Electrolysis



Electrochemical cyclization was carried out in a 20 mL vial equipped with a Pt anode ($1.0 \times 1.5\text{ cm}^2$), and a Pt cathode ($1.0 \times 1.5\text{ cm}^2$), and Ag/Ag⁺ (Ag wire in 0.01 M AgNO₃/0.1 M $\text{Bu}_4\text{NPF}_6/\text{CH}_3\text{CN}$). Substrate **1a** (0.4 mmol), DABCO (0.8 mmol), and Bu_4NBF_4 (0.4 mmol) were placed in a vial equipped with a stirring bar. Then CH_3CN (3.96 mL) and H₂O (0.04 mL) were added with a syringe. A constant potential (0.9 V vs. Ag/Ag⁺, 2.0 F mol^{-1} , 22.8 h) was supplied at $25\text{ }^\circ\text{C}$. Bu_4NBF_4 was removed by short pass. Then, the residue was concentrated under reduced pressure. The yield of **2a** was analyzed by ¹H NMR using 1,1,2,2-tetrachloroethane (33.4 mg, 0.20 mmol) as an internal standard (28% yield). Similarly, **2a** was obtained in 14% yield by the constant potential electrolysis at 1.5 V (3.6 h). The yield of constant potential electrolysis was not good as the constant current electrolysis (49%).

Radical Trapping Experiment



The electro-oxidation was carried out in a 10 mL two-necked flask equipped with a three-way cock and a Pt anode (1.0 × 1.5 cm²), and a Pt cathode (1.0 × 1.5 cm²). Biphenylphenylphosphine oxide **1a** (0.4 mmol), DABCO (0.8 mmol), 2,2,6,6-tetramethyl-1-piperidinyloxy (TEMPO) (2.0 mmol), and Bu₄NBF₄ (0.4 mmol) were placed in the flask equipped with a stirring bar. Then CH₃CN (3.96 mL) and H₂O (0.04 mL) were added with a syringe. A constant current (2.5 mA, 2.0 F mol⁻¹, 8.58 h) was supplied at 25 °C. The corresponding product **2a** was not obtained, and the starting material **1a** was mainly recovered. Moreover, high-resolution mass spectra analysis of this reaction mixture showed that TEMPO-trapped product **5** was formed. This result strongly suggests that a phosphinyl radical was generated in situ and the reaction would proceed via radical pathway.

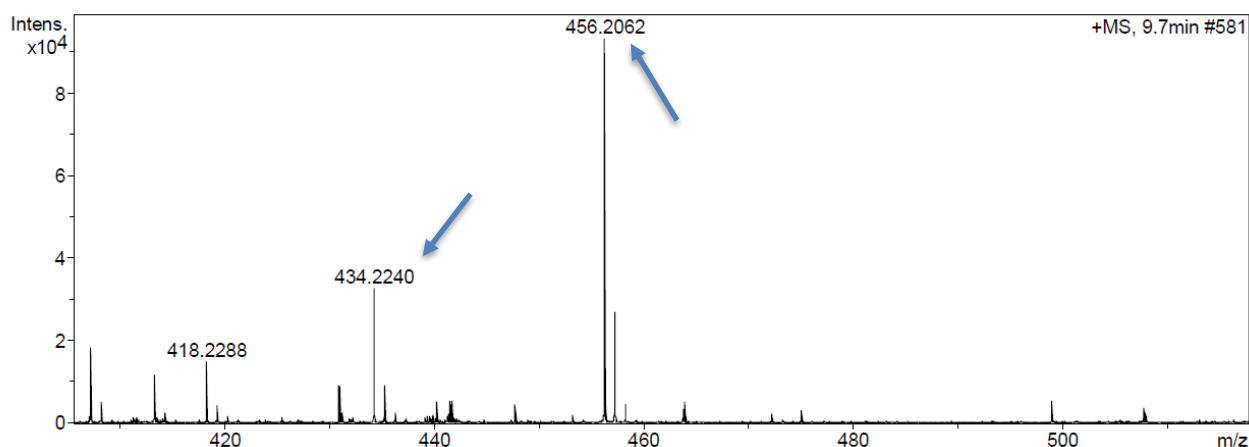
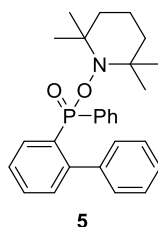


Figure S2. Radical trapping experiment and the ESI-HRMS spectrum for **5**



HRMS m/z calcd for C₂₇H₃₂NO₂PNa [M+Na]⁺

calcd: 456.2063

found: 456.2062

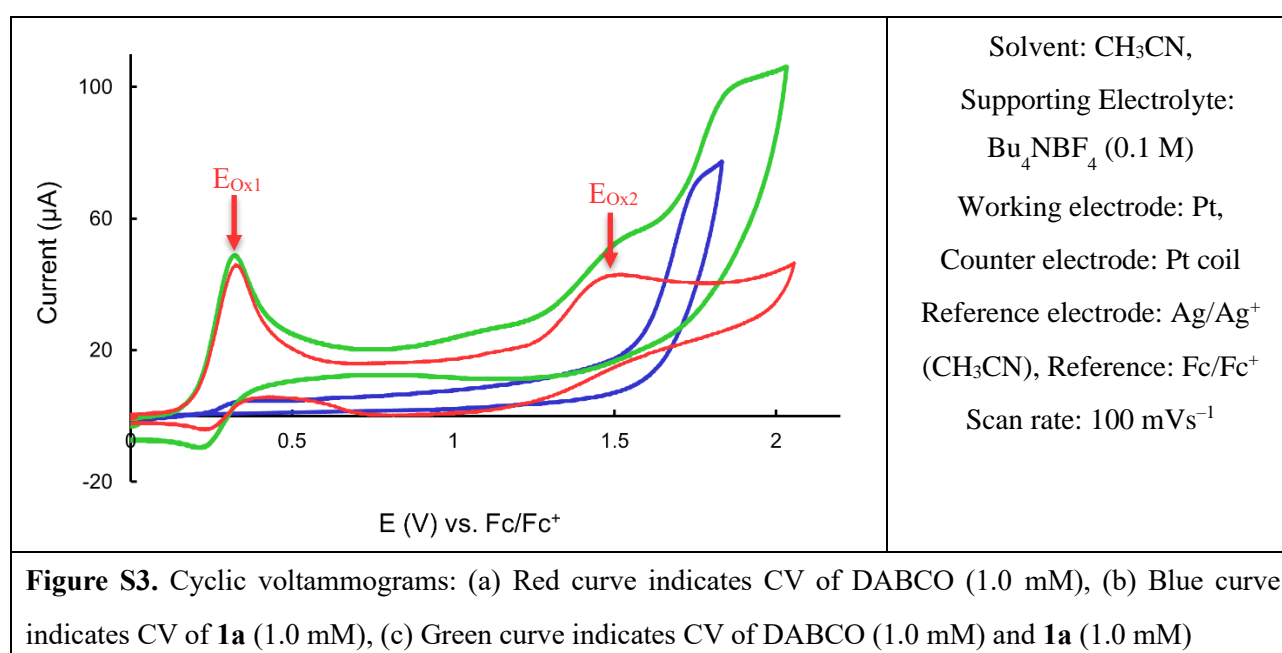
HRMS m/z calcd for C₂₇H₃₂NO₂P [M+H]⁺

calcd: 434.2243

found: 434.2240

3. Cyclic Voltammetry

Cyclic voltammograms (CVs) were recorded on Electrochemical Analyzer CHI-600B. A Pt electrode (surface area: $A = 0.071 \text{ cm}^2$, BAS), a Ag/Ag⁺ (Ag wire in 0.01 M AgNO₃/0.1 M Bu₄NBF₄/CH₃CN), and a Pt wire electrode were used as working, reference, and counter electrodes, respectively. The working electrode was polished with 5 μm diamond slurry and then with 0.5 μm alumina slurry. After polishing, it was washed with deionized water and acetone, and dried in an oven. A CH₃CN solution of sample including 1 mM of each sample and 0.1 M of Bu₄NBF₄ was prepared as an electrochemical solution. Using the electrodes and the solutions, beaker-typed three electrode electrochemical cells were constructed, and were connected with the potentiostat to perform cyclic voltammetry. The redox potentials were calibrated with ferrocene.



References

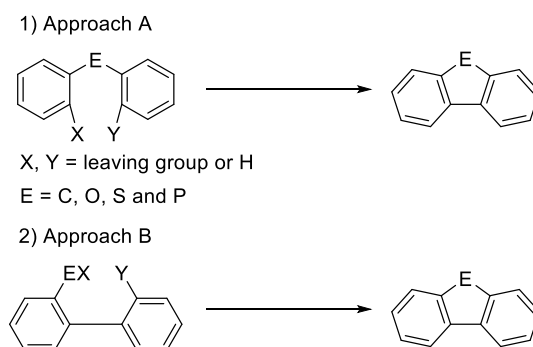
- (1) (a) Baumgartner, T.; Bergmans, W.; Kárpáti, T.; Neumann, T.; Nieger, M.; Nyulászi, L. *Chem. Eur. J.* **2005**, *11*, 4687–4699. (b) Dienes, Y.; Durben, S.; Kárpáti, T.; Neumann, T.; Englert, U.; Nyulászi, L.; Baumgartner, T. *Chem. Eur. J.* **2007**, *13*, 7487–7500. (c) Zhang, S.; Chen, R.; Yin, Y.; Liu, F.; Jiang, H.; Shi, N.; An, Z.; Ma, C.; Liu, B.; Huang, W. *Org. Lett.* **2010**, *12*, 3438–3441. (d) Zhou, Y.; Yang, S.; Li, J.; He, G.; Duan, Z.; Mathey, F. *Dalton Trans.* **2016**, *45*, 18308–18312. (e) Zhuang, Z.; Bu, F.; Luo, W.; Peng, H.; Chen, S.; Hu, R.; Qin, A.; Zhao, Z.; Tang, B. *Z. J. Mater. Chem. C*, **2017**, *5*, 1836–1842. (f) Mousawi, A. A.; Garra, P.; Sallenave, X.; Dumur, F.; Toufaily, J.; Hamieh, T.; Graff, B.; Gigmès, D.; Fouassier, J. P.; Lalevée, J. *Macromolecules* **2018**, *51*, 1811–1821.
- (2) (a) Geramita, K.; Mcbee, J.; Tao, Y.; Segalman, R. A.; Tilley, T. D. *Chem. Commun.* **2008**, *41*, 5107–5109. (b) Tsuji, H.; Sato, K.; Sato, Y.; Nakamura, E. *Chem. Asian J.* **2010**, *5*, 1294–1297. (c) Matano, Y.; Ohkubo, H.; Miyata, T.; Watanabe, Y.; Hayashi, Y.; Umeyama, T.; Imahori, H. *Eur. J. Inorg. Chem.* **2014**, 1620–1624. (d) Welsh, T. A.; Laventure, A.; Baumgartner, T.; Welch, G. C. *J. Mater. Chem. C*, **2018**, *6*, 2148–2154. (e) Welsh, T. A.; Laventure, A.; Alahmadi, A. F.; Zhang, G.; Baumgartner, T.; Zou, Y.; Jäkle, F.; Welch, G. C. *ACS Appl. Energy Mater.* **2019**, *2*, 1229–1240.
- (3) (a) Wang, C.; Fukazawa, A.; Taki, M.; Sato, Y.; Higashiyama, T.; Yamaguchi, S. *Angew. Chem, Int., Ed.* **2015**, *54*, 15213–15217. (b) Wang, C.; Taki, M.; Sato, Y.; Fukazawa, A.; Higashiyama, T.; Yamaguchi, S. *J. Am. Chem. Soc.* **2017**, *139*, 10374–10381. (c) Wang, C.; Fukazawa, A.; Tanabe, Y.; Inai, N.; Yokogawa, D.; Yamaguchi, S. *Chem. Asian J.* **2018**, *13*, 1616–1624. (d) Wang, C.; Taki, M.; Sato, Y.; Tamura, Y.; Yaginuma, H.; Okada, Y.; Yamaguchi, S. *Proc. Natl. Acad. Sci.* **2019**, *116*, 15817–15822.
- (4) (a) Makioka, Y.; Hayashi, T.; Tanaka, M. *Chem. Lett.* **2004**, *33*, 44–45. (b) Zhang, Z.; Li, J.; Huang, B.; Qin, J. *Chem. Lett.* **2006**, *35*, 958–959. (c) Chen, R.-F.; Zhu, R.; Fan, Q.-L.; Huang, W. *Org. Lett.* **2008**, *10*, 2913–2916. (d) Yasukawa, N.; Okubo, Y.; Hattori, T. JP2011049204 (e) Nakano, K.; Oyama, H.; Nishimura, Y.; Nakasako, S.; Nozaki, K. *Angew. Chem, Int., Ed.* **2012**, *51*, 695–699. (f) Riobé, F.; Szűcs, R.; Bouit, P. A.; Tondelier, D.; Geffroy, B.; Aparicio, F.; Buendía, J.; Sánchez, L.; Réau, R.; Nyulászi, L.; Hissler, M. *Chem. Eur. J.* **2015**, *21*, 6547–6556. (g) Zhong, D.; Yu, Y.; Song, D.; Yang, X.; Zhang, Y.; Chen, X.; Zhou, G.; Wu, Z. *ACS Appl. Mater. Interfaces* **2019**, *11*, 27112–27124.
- (5) (a) Bedford, A. F.; Heinekey, D. M.; Millar, I. T.; Mortimer, C. T. *J. Chem. Soc.* **1962**, 2932–2936. (b) Gladiali, S.; Dore, A.; Fabbri, D.; De Lucchi, O.; Valle, G. *J. Org. Chem.* **1994**, *59*, 6363–6371. (c) Baumgartner, T.; Neumann, T.; Wirges, B. *Angew. Chem., Int. Ed.* **2004**, *43*, 6197–6201. (d) Chen, R.-F.; Fan, Q.-L.; Zheng, C.; Huang, W. *Org. Lett.* **2006**, *8*, 203–205.
- (6) (a) Kuninobu, Y.; Yoshida, T.; Takai, K. *J. Org. Chem.* **2011**, *76*, 7370–7376. (b) Nishimura, K.; Hirano, K.; Miura, M. *Org. Lett.* **2019**, *21*, 1467–1470. (c) Furukawa, S.; Haga, S.; Kobayashi, J.; Kawashima, T. *Org. Lett.* **2014**, *16*, 3228–3231.
- (7) (a) Yoshida, J.; Kataoka, K.; Horcajada, R.; Nagaki, A. *Chem. Rev.* **2008**, *108*, 2265–2299. (b) Yan, M.;

- Kawamata, Y.; Baran, P. S. *Chem. Rev.* **2017**, *117*, 13230–13319. (c) Jiang, Y.; Xu, K.; Zeng, C. *Chem. Rev.* **2018**, *118*, 4485–4540. (d) Tang, S.; Liu, Y.; Lei, A. *Chem.* **2018**, *4*, 27–45. (e) Wiebe, A.; Gieshoff, T.; Mochle, S.; Rodrigo, E.; Zirbes, M.; Waldvogel, S. R. *Angew. Chem., Int. Ed.* **2018**, *57*, 5594–5619.
- (8) (a) Cruz, H.; Gallardo, I.; Guirado, G. *Eur. J. Org. Chem.* **2011**, *36*, 7378–7389. (b) Hu, C.; Hong, G.; Zhou, C.; Tang, Z. -C.; Han, J. -W.; Wang, L. -M. *Asian J. Org. Chem.* **2019**, *8*, 2092–2096. (c) Li, K. -J.; Jiang, Y. -Y.; Xu, K.; Zeng, C. -C.; Sun, B. -G. *Green Chem.*, **2019**, *21*, 4412–4421.
- (9) (a) Fu, N.; Song, L.; Liu, J.; Shen, Y.; Siu, J. C.; Lin, S. *J. Am. Chem. Soc.* **2019**, *141*, 14480–14485. (b) Wu, Z. -J.; Su, F.; Lin, W.; Song, J.; Wen, T. -B.; Zhang, H. -J.; Xu, H. -C. *Angew. Chem. Int., Ed.* **2019**, *58*, 16770–16774. (c) Khrizanforova, V. V.; Khrizanforov, M. N.; Gryaznova, T. V.; Budnikova, Y. H. *Phosphorus Sulfur Silicon Relat. Elem.* **2016**, *191*, 1602–1603. (d) Lu, L.; Fu, N.; Lin, S. *Synlett* **2019**, *30*, 1199–1203. (e) Xu, Z.; Li, Y.; Mo, G.; Zheng, Y.; Zeng, S.; Sun, P. -H.; Ruan, Z. *Org. Lett.* **2020**, *22*, 4016–4020. (f) Bai, Y.; Liu, N.; Wang, S.; Wang, S.; Ning, S.; Shi, L.; Cui, L.; Zhang, Z.; Xiang, J. *Org. Lett.* **2019**, *21*, 6835–6838.
- (10) (a) Pudovik, A. N.; Konovalova, I. V. *Zh. Obshch. Khim.* **1959**, *29*, 3342–3346. (b) Pudovik, A. N.; Konovalova, I. V. *Synthesis* **1979**, 81–96. (c) Rey, P.; Taillades, J.; Rossi, J. C.; Gros, G. *Tetrahedron Lett.* **2003**, *44*, 6169–6171. (d) Kagayama, T.; Nakano, A.; Sakaguchi, S.; Ishii, Y. *Org. Lett.* **2006**, *8*, 407–409.
- (11) (a) Electrochemical benzylic oxidation using tertiary amine as a mediator. Kawamata, Y.; Yan, M.; Liu, Z.; Bao, D. -H.; Chen, J.; Starr, J. T.; Baran, P. S. *J. Am. Chem. Soc.* **2017**, *139*, 7448–7451. (b) A trace amount of **4e** was obtained under O₂. For details, see Table S1 in the Supporting Information (SI)
- (12) Tian and co-workers reported that **4a** cannot be synthesized from **3a** by intramolecular radical cyclization. Ye, W.; Li, X.; Ding, B.; Wang, C.; Shrestha, M.; Ma, X.; Chen, Y.; Tian, H. *J. Org. Chem.* **2020**, *85*, 3879–3886.
- (13) (a) Quan, H. -F.; Li, C. -K.; Zhou, Z. -H.; Tao, Z. -K.; Shoiberu, A.; Zou, J. -P. *Org. Lett.* **2018**, *20*, 5947–5951. (b) Baba, K.; Tobisu, M.; Chatani, N. *Angew. Chem. Int., Ed.* **2013**, *52*, 11892–11895. (c) Cui, Y.; Fu, L.; Cao, J.; Deng, Y.; Jiang, J. *Adv. Synth. Catal.* **2014**, *356*, 1217–1222. (d) Si, E.; Zhao, P.; Wang, L.; Duan, Z.; Mathey, F. *Eur. J. Org. Chem.* **2020**, *6*, 697–701. (e) Schaub, T. A.; Brülls, S. M.; Dral, P. O.; Hampel, F.; Maid, H.; Kivala, M. *Chem. Eur. J.* **2017**, *23*, 6988–6992.

Chapter 7. Grand Summary

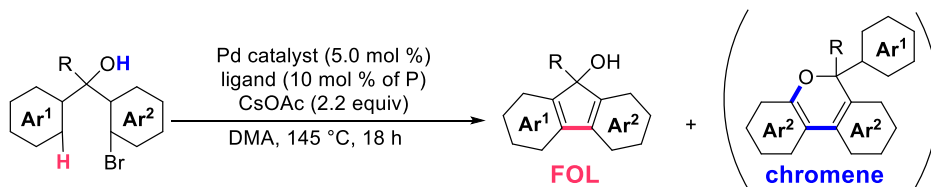
This thesis describes the “Synthesis of Heterocyclic Aromatic Compounds” by “Intramolecular Cyclization” as a key reaction. As far as synthetic strategies toward heterocyclic aromatic compounds scaffold are concerned, two synthetic approaches can be envisioned (Scheme 1). Intramolecular cyclization of the corresponding **E** (C, O, S and P atoms) atom bridged biaryl precursors via C–X and C–Y formation (Approach A) or **E**–X containing 2-biphenyl precursors via **E**–X and C–Y formation (Approach B) are ideal approaches to produce target compounds. In general, these approaches are versatile and allow us to synthesize a wider range of potential structures containing **E**.

Scheme 1. Synthetic strategies of heterocyclic aromatic compounds by intramolecular cyclization



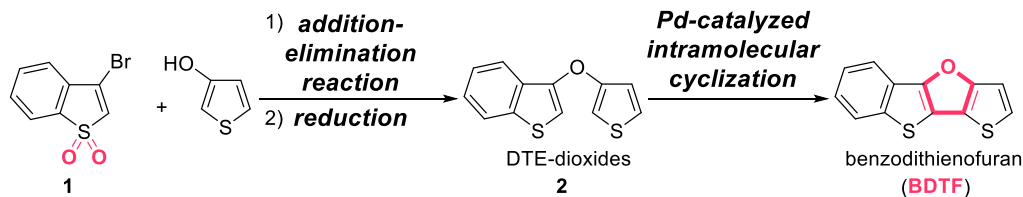
According to the approach mentioned above, the author achieved the selective synthesis of FOLs by the Pd-catalyzed intramolecular cyclization (Scheme 2). This reaction is suited for the synthesis of heteroring-fused FOLs, which are difficult to synthesize by conventional methods. These results were described in Chapter 2.

Scheme 2. Summary of Chapter 2



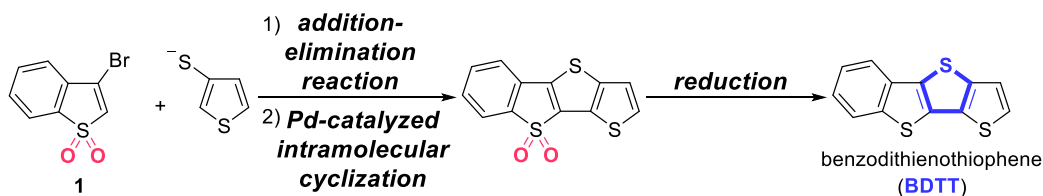
The author achieved the syntheses of DTE-dioxides **2** by an addition–elimination reaction using 3-bromobenzo[*b*]thiophene 1,1-dioxide (**1**) as a key compound. An efficient transformation from **2** to BDTF was also developed by reduction following by Pd-catalyzed intramolecular cyclization (Scheme 3). These results were described in Chapter 3.

Scheme 3. Summary of Chapter 3



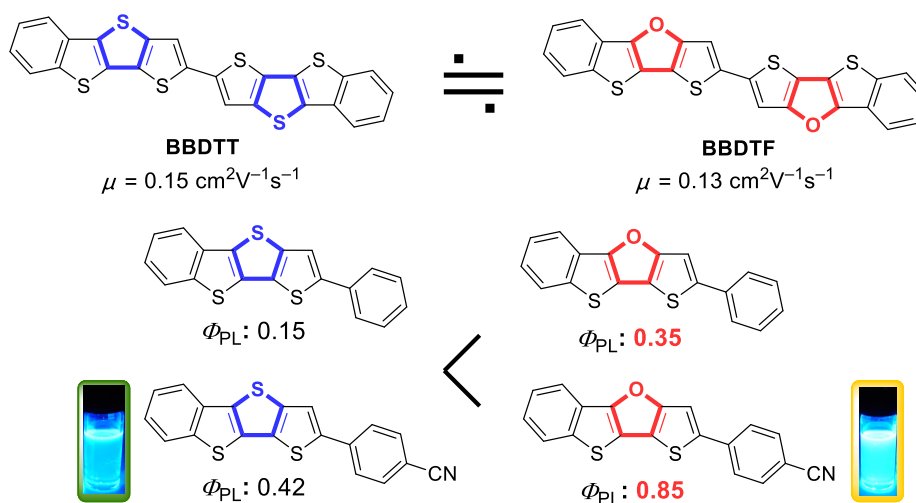
The author also achieved the efficient syntheses of BDTT by addition-elimination reaction using 3-bromobenzo[*b*]thiophene 1,1-dioxide as a key compound following by Pd-catalyzed intramolecular cyclization and reduction (Scheme 4). These results were described in Chapter 4.

Scheme 4. Summary of Chapter 4

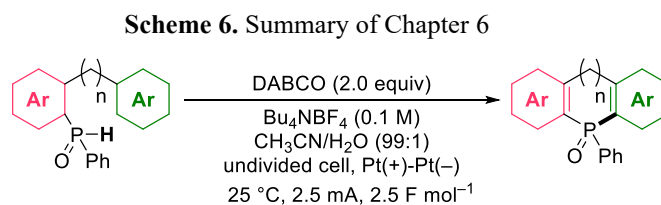


The physical properties of BDTFs and BDTTs were investigated, respectively. While their fluorescence properties and packing structures were clearly different, E_{HOMO} , E_{LUMO} and hole mobility were similar. BDTFs have better fluorescence properties than BDTTs. In particular, BDTFs with a 4-cyano- C_6H_4 group exhibited the strongest fluorescence ($\Phi_{\text{PL}}=0.85$). Furthermore, the OFET properties of BBDTF were confirmed. This is the first report showing that thienoacenes containing DTF have OFET and fluorescence properties (Scheme 5). These results were described in Chapter 5.

Scheme 5. Summary of Chapter 5



The author achieved the first electrochemical synthesis of diarylphosphole oxides from biarylphosphine oxides under mild conditions (Scheme 6). The protocol uses a readily available and inexpensive DABCO as a HAT mediator. A variety of BPOs were available by the present electrochemical method. The method can also be applied to the synthesis of six-membered phosphacycles. These results were described in Chapter 6.



In conclusion, the author achieved the synthesis of various heterocyclic aromatic compounds by intramolecular cyclization as a key reaction. The developed methodologies will contribute to easy access to enable a variety of novel aromatic compounds.

List of Publications

1. Synthesis of 3-Benzo[*b*]thienyl 3-Thienyl Ether via an Addition Elimination Reaction and Its Transformation to an Oxygen-Fused Dithiophene Skeleton: Synthesis and Properties of Benzodithienofuran and Its π -Extended Derivatives
Mitsudo, K.; Kurimoto, Y.; Mandai, H.; Suga, S. *Org. Lett.* **2017**, *19*, 2821-2824.
2. Efficient Synthesis and Properties of [1]Benzothieno[3,2-*b*]thieno[2,3-*d*]furans and [1]Benzothieno[3,2-*b*]thieno[2,3-*d*]thiophenes
Kurimoto, Y.; Mitsudo, K.; Mandai, H.; Wakamiya, A.; Murata, Y.; Mori, H.; Nishihara, Y Suga, S. *Asian J. Org. Chem.* **2018**, *7*, 1635–1641.
3. Synthesis of 9-Substituted Fluorenols and Heteroring-fused Analogues by Intramolecular C–H Functionalization
Kurimoto, Y.; Mitsudo, K.; Suga, S. *Chem. Lett.* **2020**, *50*, 378–381.

Other Publications

1. Cu/Fe/O=PPh₃-Catalyzed Etherification for the Synthesis of Aryl 3-Benzo[*b*]thienyl Ethers
Mistudo, K.; Asada, T.; Inada, T.; Kurimoto, Y.; Mandai, H.; Suga, S. *Chem. Lett.* **2018**, *47*, 1044–1047.
2. Miniaturization and Combinatorial Approach in Organic Electrochemistry
Mistudo, K.; Kurimoto, Y.; Yoshioka, K.; Suga, S. *Chem. Rev.* **2018**, *118*, 5985–5999.
3. Combinatorial Electrochemistry for Organic Synthesis
Mistudo, K.; Kurimoto, Y.; Yoshioka, K.; Suga, S. *Curr. Opin. Electrochem.* **2018**, *8*, 8–13.
4. Metal-free electrochemical fluorodecarboxylation of aryloxyacetic acids to fluoromethyl aryl ethers
Berger, M.; Herszman, J. D.; Kurimoto, Y.; de Kruijff, G. H. M.; Schüll, A.; Ruf, S.; Waldvogel, S. *R. Chem. Sci.* **2020**, *11*, 6053–6057.
5. Integrated Synthesis of Thienyl Thioethers and Thieno[3,2-*b*]thiophenes via 1-Benzothiophen-3(2*H*)-Ones
Mistudo, K.; Habara, N.; Kobashi, Y.; Kurimoto, Y.; Mandai, H.; Suga, S. *Synlett* **2020**, *31*, 1947–1952.